國立交通大學

電控工程研究所

博 士 論 文

應用於時滯系統之輸出回授積分型順滑模態控制

Output Feedback Integral Sliding Mode Control Applied to Time-Delay Systems

研 究 生：丁桓展

指導教授：陳永平 博士

張浚林 博士

中 華 民 國 一 百 年 五 月

應用於時滯系統之輸出回授積分型順滑模態控制

Output Feedback Integral Sliding Mode Control Applied to Time-Delay Systems

研 究 生：丁桓展　　Student：Huan-Chan Ting

指導教授：陳永平 教授　　Advisors：Prof. Yon-Ping Chen

張淺林 教授　　Prof. Jeang-Lin Chang

國 立 交 通 大 學

電 控 工 程 研 究 所

博 士 論 文

A Dissertation

Submitted to Institute of Electrical Control Engineering

College of Electrical and Computer Engineering

National Chiao Tung University

in partial Fulfillment of the Requirements

for the Degree of

Doctor of Philosophy

in

Electrical Control Engineering

May 2011

Hsinchu, Taiwan, Republic of China

中華民國一百年五月

應 用 於 時 滯 系 統 之 輸 出 回 授 積 分 型 順 滑 模 態 控 制

學生：丁桓展　　　　　　　　　　　　　　　　指導教授：陳永平教授

張浚林教授

國立交通大學電控工程研究所博士班

摘　　　要

基於線性多輸入多輸出系統，在部分參數不確定且受到外界未知干擾之環境，本論文提出一動態輸出回授積分型順滑模態控制法則，使受控系統穩定並抑制非匹配干擾之影響。順滑模態控制為一強健非線性的控制方法，先設計一穩定之順滑平面，再設計控制輸入使系統在有限時間內進入該平面，具有設計簡單、可消除匹配性雜訊等優點。當系統只有部分狀態或是輸出訊號可量測，應用於此類系統之傳統輸出回授順滑模態控制器存在著受限於系統結構的控制器合成問題，且只能滿足區域性的逼近與順滑條件。本論文採用積分型順滑平面，可保留順滑模態控制原有之優點，並解決控制器合成問題，當系統進入順滑平面後也可提供一自由度去抑制非匹配型干擾之影響。另外為了滿足全域逼近與順滑條件，在控制輸入中設計了一個適應性法則，計算部份未知量的範數上限。此動態輸出回授積分型順滑模態控制法則，經過修正後亦可應用於參數不確定且受到外界未知干擾之時滯系統。針對於固定但未知延遲時間之狀態延遲時滯系統，沿用輸出回授積分型順滑平面之結構，並加入一全階補償器以完成動態控制器之設計。當系統進入順滑平面，利用一強健干擾抑制分析技術可以推理出一線性矩陣不等式作為穩定性與保證干擾抑制效能的充分條件；若修正補償器結構，則該線性矩陣不等式可分解為兩個維度較小之代數 Riccati 不等式以利計算，兩種不等式之解皆可用來決定順滑平面、補償器、控制器之參數。當延遲時間未知且時變，讓系統在某些延遲時間造成不穩定，使得控制難度大幅提升。利用上述動態輸出回授積分型順滑模態控制器架構，本論文亦針對此複雜系統完成穩定性充分條件分析與控制器設計。

Output Feedback Integral Sliding Mode Control Applied to Time-Delay Systems

student：Huan-Chan Ting　　Advisors：Dr. Yon-Ping Chen
Dr. Jeang-Lin Chang

Institute of Electrical Control Engineering
National Chiao Tung University

ABSTRACT

For linear multi-input multi-output uncertain systems with external unknown disturbances, this thesis proposed a dynamic output feedback integral sliding mode control method to stabilize the system and suppress the effect of mismatched disturbances. The advantages of sliding mode control are its simple design procedure, great robustness against matched disturbances, etc. As part of system states or outputs are only measurable, conventional output feedback sliding mode controllers involved a synthesis problem by a structural constraint and ensured the approaching and sliding condition locally. The thesis adopted an integral sliding surface to improve the controller synthesis problem, reserved inherent benefits of sliding mode control, and offered an extra degree of freedom to suppress the effect of mismatched disturbances when the system is in the sliding mode, simultaneously. For satisfying the approaching and sliding condition globally, an adaption law was added in the controller to estimate the bound of part of unknown terms. The proposed control method can be modified to apply to uncertain time-delay systems with disturbances. For state delays with a fixed and unknown delay time, combined the output feedback integral sliding mode technique with a full-order compensator can complete the dynamic controller design. Since the system is in the sliding mode, using the property of robust disturbance attenuation can derive a linear matrix inequality as a sufficient condition for the stability; this linear matrix inequality can be decomposed into two smaller algebraic Riccati inequalities by modifying the structure of compensator. Solutions to two types of inequalities can both determine parameters of sliding surface, compensator, and controller. In the case of time-varying and unknown delay time, some delay times caused the instability of system and worsened the difficulty designing the controller. The proposed structure of dynamic sliding mode control can also complete the stability analysis and control law design for systems with time-varying delay.

誌　　謝

首先感謝指導教授 陳永平老師、 張浚林老師於學生多年來碩博士修業期間的細心指導，在治學方法、求學態度和待人處世多所啟迪，惠我良多，謹向兩位老師獻上最誠摯的謝意。同時感謝口試委員 徐國鎧老師、 蘇武昌老師、 鄭志強老師、 楊谷洋老師、 徐保羅老師及 梁耀文老師寶貴的意見與指正，使本論文更臻完整。

親愛的家人是我最大的支柱，父母給予我全力的栽培，讓我能無後顧之憂地專心於課業，若我能有所成就，皆歸功於您們；成長與學習的過程中還有妻子及可愛的兒子彥智的支持與陪伴，讓我擁有富足的心靈寄託；兩位弟弟以及五專同學 SB 們也在生活中陪伴我、給予我鼓勵，謝謝你們。

最後也要感謝實驗室的伙伴們，世宏學長與現役學弟們，文俊、文榜、澤翰、榮哲、孫齊、崇賢、振方、咨偉，以及過去相知相惜的已畢業眾學長姊、學弟妹，感謝大家於學業和生活上的互相照顧，共同度過甘苦的研究所歲月，更豐富了我的求學時光。

丁桓展
100 年 5 月

Table of Contents

List of Figures

Symbols

$\mathbb{R}$	: Collection of real numbers
$\mathbb{C}$	: Collection of complex numbers
L_2	: Hilbert space of matrix-valued (or scalar-valued) function
$\boldsymbol{I}_n$	: Identity matrix of size $n \times n$
$\boldsymbol{0}$	: Zero matrix with appropriate dimension
$\boldsymbol{A}^T$	: Transpose of the matrix $\boldsymbol{A}$
$\boldsymbol{A}^{-1}$	: Inverse of the matrix $\boldsymbol{A}$
$\boldsymbol{A}^{+}$	: Pseudo inverse of the matrix $\boldsymbol{A}$
$\lambda(\boldsymbol{A})$	: Eigenvalues of the square matrix $\boldsymbol{A}$
$\lambda_{\min}(\boldsymbol{A})$	: Minimum eigenvalue of the square matrix $\boldsymbol{A}$
$\lambda_{\max}(\boldsymbol{A})$	: Maximum eigenvalue of the square matrix $\boldsymbol{A}$
$\lvert x \rvert$	: Absolute value of the scalar x
$\lVert \boldsymbol{x}(t) \rVert$	: 2-norm of the vector $\boldsymbol{x}$ at time t
$\lVert \boldsymbol{A} \rVert$	: 2-norm of the matrix $\boldsymbol{A}$ defined as max $\dfrac{\lVert \boldsymbol{Ax} \rVert^2}{\lVert \boldsymbol{x} \rVert^2}$
$\triangleq$	: Equal to by definition
$\dot{\boldsymbol{x}}(t)$	: Time derivative of the vector $\boldsymbol{x}(t)$, i.e. $\dot{\boldsymbol{x}}(t) = d\boldsymbol{x}(t)/dt$
$\operatorname{diag}(\bullet)$	: Diagonal matrix with the element $\bullet$
$\Re(\boldsymbol{A})$	: Range space of $\boldsymbol{A}$
$\cup$	: Union between two sets
$\cap$	: Intersection between two sets
$\varnothing$	: Empty set
LMI	: Linear Matrix Inequality
LTI	: Linear Time-Invariant
MIMO	: Multi-Input, Multi-Output

I. INTRODUCTION

In practice, most of system state signals cannot be measured fully to complete a state feedback control scheme. For the same system suffering uncertainties and external disturbances, output feedback sliding mode control method can reserve the original advantages to regulate the system behavior and avoid the design complexity of other robust output feedback control approaches. In contrast with other complex stability criteria, the approaching and sliding condition is simpler as a sufficient condition ensuring the stability while the system enters the stable sliding surface in a finite time.

Time-delay phenomenon means that parts of system states, inputs, or outputs affect the system after a fixed time, or random but finite period. There exists this phenomenon in several various practical systems, such as chemical processes, electrical networks, nuclear reactors, biological reactions, economic models, etc. Therefore controller designs for continuous-time time-delay systems are important and necessary.

1.1 Sliding Mode Control

Sliding mode control [1-28] is one of efficient robust control approaches to stabilize systems in the presence of external disturbances and interior uncertainties. It is well known for the complete invariance to matched disturbances and uncertainties. The design procedure normally follows the rule: 1) choose a stable manifold so-called sliding surface; 2) design a nonlinear switching controller satisfying the approaching and sliding condition such that the system enters the sliding surface in a finite time. The simple and explicit design procedure is another advantage of sliding mode control. Based on Utkin's research [1], the relative papers are continuing presented over a couple of decade. Edwards and Spurgeon [2] contributed the analysis and complete introduction of sliding mode methods, state and output feedback controllers, observers, and other applications. Since the system states are all available, researchers have proposed many significant reports [3-6]. For instance, Chiang and Chiu [5] presented a sliding mode control method based on a TS recurrent fuzzy neural network to stabilize the time-delay systems and compensate system uncertainties effectively. In the field of output feedback sliding mode control methods [7-14], previous researches have designed the output feedback controllers via sliding mode technique to stabilize multivariable plants with matched uncertainties. Early on, Zak and Hui [7] developed an algorithm for output-dependent sliding surface design of uncertain systems, using the eigenstructure method. Yallapragada *et al*. [8] addressed the reaching problem for the static output feedback sliding mode controller design. Thereafter, Kwan [9] presented an adapted dynamic output feedback controller to remove two major limits from the scheme in [7]. Yan *et al*. [14] applied an effective sliding mode design technique using output only to control the systems with disturbances.

However, the abovementioned papers considered the matched uncertainty and disturbance only. Unlike the matched case, any mismatched uncertainty and external disturbance always affect the system performance even if the plant is in the sliding mode. As a result, the existence condition and robust stability for using an output feedback sliding mode controller to tackle a system with the mismatched uncertainty and disturbance are worth further investigation. Choi [15] proposed a static output-dependent sliding surface design developed from LMI technique [29], in which a class of system considered both matched and mismatched uncertainties. Further, Park *et al*. [16] extended Choi's method and proposed a dynamical output feedback variable structure control law to deal with the same problem. Since the dynamics of the sliding surface is always related to the unmeasured system states, the high gain control in [15] was introduced to maintain the global convergence. Upon examining the static output feedback control, Xiang *et al*. [17] applied an iterative LMI technique to avoid the high gain problem. To prepare for obtaining a bounded L_2 gain performance, Juang and Lee [18] developed an observer-based output feedback sliding mode controller which can guarantee the system stability with robust performance. Lewis [19] used the eigenvalue perturbation analysis for an uncertain matrix to guarantee the closed-loop stability. Pai and Sinha [20] used the small gain theorem to analyze the behavior of closed-loop system with parameter uncertainties. Although the advantages of applying LMI technique to output feedback sliding mode control for uncertain systems have been addressed explicitly in these aforementioned papers, the solutions including the constrained LMIs [15-16] or a set of LMIs [18, 21] are difficult to obtain.

Recent researches [22-26] have studied a control scheme called integral sliding mode control, in which an integral controller is added to a sliding mode controller. The main advantages of integral sliding mode controller are to offer the robustness of system stability and the elimination of steady state error within step inputs. Based on the integral sliding mode control structure, several researchers [23-25] developed different observer design methods to accomplish the estimation. In observer-based approaches, the proper observer gain selection which gives reasonable estimation both in steady state and transient state is a difficult task. Since the controlled systems usually involve parameter uncertainties and external unknown disturbances, the use of state observers may reduce robustness. Consequently, it is important to study the integral sliding mode control using output information only for uncertain systems.

1.2 Time-Delay Systems

For the stability analysis of time-delay systems, two kinds of conditions can be adopted — delay-independent and delay-dependent conditions. When delayed states with an unknown but bounded constant delay time are independent of the original stability of systems, the systems satisfy the so-called delay-independent condition within a simple rule assuring the stability of closed-loop systems. If the system belongs to the delay-dependent condition, delayed states with part or all of delay times will cause the instability of system whether the delay time is fixed or time-varying. This condition also brings the complexity and difficulty deriving a sufficient condition of the stability of closed-loop systems. Since time-delay terms frequently induce the system instability and bad performance, the analysis and control of time-delay systems have been an interesting topic over the past decades whether state, input, or output delays.

Focusing on the state delay systems, researchers [3-5, 12-14, 27-28, 30-52] had presented many effective state feedback control methods to various system models. Xia and Jia [3] carried out a robust control method comprising of the sliding mode control and LMI technique for uncertain time-delay systems with matched disturbances. Lee *et al.* [32] developed a control method based on the receding horizon concept to stabilize the closed-loop system and to assure the H_∞ norm bound from the disturbances to the controlled outputs. For a continuous linear state-delay system involving a class of integral term, Santos and Mondié [33] proposed an iterative procedure to complete their state feedback controller design. Wang *et al*. [34] designed a state feedback control law of time-delay systems with system uncertainties and matched unknown nonlinear terms. They combined the LMI technique and adaptive parameter searching law to the controller design ensuring the stability of the closed-loop system. Chen and Chen [35] presented an LMI-based state feedback controller and a disturbance observer to stabilize linear state-delay systems with uncertainties and matched disturbances.

Providing the obtainable system states partly, state observers [36-40] and output feedback controllers [12-14, 28, 41-43, 48-52] are both feasible schemes to regulate time-delay systems. In the field of state observers, Darouach [39-40] have recently developed an observer methodology to estimate states of linear time-delay systems with noises and mismatch disturbances. On the other hand, in the field of output feedback control methods, Niu *et al.* [12] extended an observer-based sliding mode control using LMI technique to regulate uncertain time-delay systems. Pai [28] proposed a Luenberger observer-based output feedback controller for a class of nonlinear uncertain state-delayed systems with matched uncertainties and disturbances. The controller was comprised of integral sliding mode technique and solutions to an LMI, which switching gain parameters were calculated by adaptation laws. Fridman and Shaked [41] described explicitly a significant H_∞ control method using the descriptor system transformation for time-delay systems with mismatched external disturbances and measurement noises. The descriptor system transformation can simplify the analysis of time-delay systems and effectively perform the disturbance attenuation. As a result, the stability analysis [44-47] and various controller designs [48-52] of time-delay systems are still interesting topics so far.

1.3 Motivation

There exists two difficulties in the design of output feedback sliding mode control. The first difficulty is a synthesis problem. Synthesizing a control law using the outputs only is significant since the derivative of the sliding surface is always involved with the unmeasured system states. For resolving the synthesis problem, a normal strategy is to add an extra constraint on the controller parameters. The existence of controller parameters is constrained by the extra constraint simultaneously. The local stability is another problem. In the conventional output feedback sliding mode control, the dynamics of sliding surface always involves unknown state function as an obstacle to complete the controller using output information only. Common strategies dealing with this problem adopted the assumption in which the system trajectories are close to the origin or high-gain control forces covering the effect of unknown states. Unfortunately, these strategies have no ability to complete the global stability and increase the conservation.

Focusing on the case of state-delay, the state delayed for a fixed or varying time usually worsened the performance even caused the instability. In frequency domain the delay term can be transformed into an exponential function with delay time. As a result, the corresponding controller can be designed easily in the frequency domain but very difficult to implement in the time domain. On the other hand, since a time-delay system is subject to uncertainties and disturbances, the robust controller design will become more complex and the related stability condition will be more difficult to fulfill. A sliding mode control method which has improved the previous two problems, within such features as uncomplicated design procedure and strong robustness against the matched unknown terms, is a proper and feasible candidate to complete the controller design of time-delay systems with less design difficulty in the time domain.

1.4 Contribution

For modifying two problems mentioned above in output feedback sliding mode control, this thesis develops a dynamic output feedback integral sliding mode control method with the robust stability guaranteed for linear MIMO systems within mismatched norm-bounded uncertainties along with disturbances and matched nonlinear perturbation. The main advantages of using the integral sliding surface are that, once the system is in the sliding mode, the effect of matched perturbation can be completely eliminated and the robust stability problem of the closed-loop system becomes a standard output feedback controller design problem for a system with mismatched uncertainty and disturbance. Applying H_∞ control for the stability analysis, the proposed method can guarantee robust stability where the existence condition is determined by solving an algebraic Riccati equation involving with the original system parameters. When the number of outputs is equal to the number of inputs and the mismatched disturbance is slowly time-varying, the system outputs are proved to finally approach zero because of the integral action. Without requiring any coordinate transformation, the proposed method is a straightforward design scheme and the controller parameters can be easily solved by the algorithm proposed by Gadewadikar *et al*. [53-54] or the LMI technique [29]. If the mismatched disturbance is defined in L_2-norm space, the proposed control algorithm can satisfy the robust disturbance attenuation and guarantee robust stability as the consistent algebraic Riccati equation has a solution. Introducing an additional dynamics into the control law using output information only, the proposed controller can satisfy the global reaching and sliding condition and obtain the closed-loop stability. Although the dynamic output feedback controller raises control complexity, the magnitude of control input in the proposed method is more effectively reduced in comparison with that in the other papers [15-17].

Based on the proposed integral sliding mode control technique, the related controller design for uncertain time-delay systems with mismatched disturbances is presented. An auxiliary integration function is used to increase a degree of freedom of the system in the sliding mode and to suppress the effect of mismatched disturbances. Moreover, the controller design combined with a full-order compensator for time-delay systems also improves the synthesis problem in traditional output feedback sliding mode control methods. Since mismatched disturbances cannot be eliminated completely even the system is in the sliding mode, the disturbance attenuation technique [55-57] can reduce the effect from mismatched disturbances to the controlled outputs acting on a system to an acceptable level over all frequencies. Consequently, an LMI is derived as a sufficient condition of robust stability and its solutions are used to determine parameters of compensator and controller simultaneously. Modifying the structure of compensator can obtain a set of algebraic Riccaiti inequalities as another stability condition. Solutions to the Ricccati inequalities can also obtain the controller parameters.

The controller design for time-delay systems with a time-varying state delay has been derived within the delay-dependent condition. In the delay-dependent condition, the system is stable for part of unknown delay time and vice versa, i.e. the system stability depends on delay times. For such time-delay systems with mismatched disturbances and uncertainties, an output feedback integral sliding mode control law combined with a compensator is completed in this thesis. An LMI as a sufficient condition of robust disturbance attenuation is derived successfully.

1.5 Organization of Thesis

The sliding mode controller using output information only [2] is introduced in Chapter II. Edwards and Spurgeon [2] contributed a complete analysis for an output feedback sliding mode control and related applications in their book. Chapter III proposed the dynamic output feedback integral sliding mode controller of uncertain systems with matched and mismatched disturbances. Based on the research of integral sliding mode control technique, the output feedback controller with a compensator is applied to time-delay systems with mismatched uncertainties and disturbances in Chapter IV. This chapter discusses two kinds of sufficient conditions guaranteed the property of robust disturbance attenuation. For the case of time-varying delay within delay-dependent condition, the same chapter derived the dynamic output feedback integral sliding mode control algorithm for such disturbed time-delay systems correspondingly. The final chapter comments the overall concluding remarks and some future works.

II. OUTPUT FEEDBACK SLIDING MODE CONTROL

In practice, state variables of most systems are not fully observable. As part of state variables is only measurable, the corresponding controller design is more difficult than the conventional state feedback controller design. Since output variables are only available, referring to [2], this chapter describes the output feedback sliding mode controller and analyzes its merits/demerits. After introducing the target system and some assumptions, section 2.2 presents the sliding mode controller using output variables directly and the corresponding sliding vector.

2.1 Problem Formulation

Consider a continuous-time LTI system as

$$\begin{aligned}\dot{\boldsymbol{x}}(t) &= \boldsymbol{A}\boldsymbol{x}(t) + \boldsymbol{B}\left(\boldsymbol{u}(t) + \boldsymbol{f}(\boldsymbol{x},\boldsymbol{u},t)\right) \\ \boldsymbol{y}(t) &= \boldsymbol{C}\boldsymbol{x}(t)\end{aligned} \tag{2.1}$$

where $\boldsymbol{x} \in \mathbb{R}^n$ is the unmeasurable system state vector, $\boldsymbol{u} \in \mathbb{R}^m$ is the control input vector, $\boldsymbol{y} \in \mathbb{R}^p$ is the measurable output vector, and $\boldsymbol{f}(\boldsymbol{x},\boldsymbol{u},t) \in \mathbb{R}^m$ is consisted of the matched uncertainties and disturbances. The real constant matrices $\boldsymbol{A}$, $\boldsymbol{B}$, and $\boldsymbol{C}$ are known and with appropriate dimensions. Since the outputs are the only available signals, next section will present an output-dependent sliding vector design method and then the control algorithm involving the information of outputs is designed to satisfy the stability condition and to force the controlled system (2.1) to enter the sliding mode. Before introducing main results, the following four assumptions are fulfilled throughout this chapter.

Assumption 2.1: The matched term $\boldsymbol{f}(\boldsymbol{x},\boldsymbol{u},t)$ is norm-bounded as

$$\left\|\boldsymbol{f}(\boldsymbol{x},\boldsymbol{u},t)\right\| < k_1 \left\|\boldsymbol{u}(t)\right\| + \eta(\boldsymbol{y},t) \tag{2.2}$$

where $\eta(\boldsymbol{y},t)$ is a known function $\eta : \mathbb{R}_+ \times \mathbb{R}^p \to \mathbb{R}_+$ and $0 \le k_1 < 1$.

Assumption 2.2: There is no finite zero in the system (2.1), or exists finite zeros all on the open left-half complex plane, i.e., the triple $(\boldsymbol{A},\boldsymbol{B},\boldsymbol{C})$ is minimum phase.

Assumption 2.3: The pairs $(\boldsymbol{A},\boldsymbol{B})$ and $(\boldsymbol{C},\boldsymbol{A})$ are controllable and observable, respectively. Matrices $\boldsymbol{B}$ and $\boldsymbol{C}$ are full rank, $\operatorname{rank}(\boldsymbol{B}) = m$ and $\operatorname{rank}(\boldsymbol{C}) = p$.

Assumption 2.4: The number of output variables is not smaller than input variables, $p \geq m$. Moreover, the relative degree of system (2.1) is one, i.e. $\operatorname{rank}(\boldsymbol{CB}) = m$.

2.2 Output Feedback Sliding Mode Controller Design

2.2.1 System decomposition and analysis

Define a transformation matrix as

$$\boldsymbol{T}_c = \begin{bmatrix} \boldsymbol{N}_c^T \\ \boldsymbol{C} \end{bmatrix} \tag{2.3}$$

where $\boldsymbol{N}_c \in \mathbb{R}^{n\times(n-p)}$ whose columns span the null space of $\boldsymbol{C}$. Changing the coordinates $\boldsymbol{x} \mapsto \boldsymbol{T}_c\boldsymbol{x}$, the output matrix is transformed into $\boldsymbol{C} = \begin{bmatrix} \boldsymbol{0} & \boldsymbol{I}_p \end{bmatrix}$. The input matrix in the transformed system is given by $\boldsymbol{B} = \begin{bmatrix} \boldsymbol{B}_{c1} \\ \boldsymbol{B}_{c2} \end{bmatrix}$ where $\boldsymbol{B}_{c1} \in \mathbb{R}^{(n-p)\times m}$. Since matrix $\boldsymbol{B}_{c2} \in \mathbb{R}^{p\times m}$ is full row rank due to $\boldsymbol{CB} = \boldsymbol{B}_{c2}$ and Assumption 2.4, the left pseudo inverse of $\boldsymbol{B}_{c2}$ is defined as $\boldsymbol{B}_{c2}^{\dagger} = \left(\boldsymbol{B}_{c2}^T\boldsymbol{B}_{c2}\right)^{-1}\boldsymbol{B}_{c2}^T$ and there exists an orthogonal matrix $\boldsymbol{T} \in \mathbb{R}^{p\times p}$ such that

$$\boldsymbol{T}^T\boldsymbol{B}_{c2} = \begin{bmatrix} \boldsymbol{0} \\ \boldsymbol{B}_2 \end{bmatrix} \tag{2.4}$$

where $\boldsymbol{B}_2 \in \mathbb{R}^{m\times m}$ is invertible and $\boldsymbol{T}$ is full rank. Further the second transformation matrix is defined as

$$\boldsymbol{T}_b = \begin{bmatrix} \boldsymbol{I}_{n-p} & -\boldsymbol{B}_{c1}\boldsymbol{B}_{c2}^{\dagger} \\ \boldsymbol{0} & \boldsymbol{T}^T \end{bmatrix}. \tag{2.5}$$

Provided $\boldsymbol{T}_b$ is nonsingular, transforming the coordinate $\boldsymbol{x} \mapsto \boldsymbol{T}_b\boldsymbol{x}$ can attain the following system matrices,

$$\boldsymbol{A}=\begin{bmatrix}\boldsymbol{A}_{11} & \boldsymbol{A}_{12}\\ \boldsymbol{A}_{21} & \boldsymbol{A}_{22}\end{bmatrix},\ \ \boldsymbol{B}=\begin{bmatrix}\boldsymbol{0}\\ \boldsymbol{B}_2\end{bmatrix}, \text{ and } \ \boldsymbol{C}=\begin{bmatrix}\boldsymbol{0} & \boldsymbol{T}\end{bmatrix} \tag{2.6}$$

where $\boldsymbol{A}_{11}\in\mathbb{R}^{(n-m)\times(n-m)}$ and remaining matrices in $\boldsymbol{A}$ are partitioned to appropriate dimensions. Defining a matrix $\boldsymbol{F}\in\mathbb{R}^{m\times p}$ with full rank and multiplying it to $\boldsymbol{C}$ can obtain

$$\boldsymbol{FC}=\begin{bmatrix}\boldsymbol{0} & \boldsymbol{FT}\end{bmatrix}=\begin{bmatrix}\boldsymbol{F}_1\boldsymbol{C}_1 & \boldsymbol{F}_2\end{bmatrix} \tag{2.7}$$

where $\begin{bmatrix}\boldsymbol{F}_1 & \boldsymbol{F}_2\end{bmatrix}=\boldsymbol{FT}$, $\boldsymbol{F}_1\in\mathbb{R}^{m\times(p-m)}$, $\boldsymbol{F}_2\in\mathbb{R}^{m\times m}$, and

$$\boldsymbol{C}_1\triangleq\begin{bmatrix}\boldsymbol{0} & \boldsymbol{I}_{p-m}\end{bmatrix}. \tag{2.8}$$

As a result, $\boldsymbol{FCB}=\boldsymbol{F}_2\boldsymbol{B}_2$ and $\boldsymbol{F}_2$ is invertible because of $\operatorname{rank}(\boldsymbol{CB})=\operatorname{rank}(\boldsymbol{F})=m$. Notice that the pair $(\boldsymbol{A},\boldsymbol{B},\boldsymbol{C})$ in (2.6) can be viewed as a system used in sliding mode controller design [2], and the reduced-order sliding mode motion is dominated by the stable system matrix $\boldsymbol{A}_{11}^s$,

$$\begin{aligned}\boldsymbol{A}_{11}^s &\triangleq \boldsymbol{A}_{11}-\boldsymbol{A}_{12}\boldsymbol{F}_2^{-1}\boldsymbol{F}_1\boldsymbol{C}_1\\ &=\boldsymbol{A}_{11}-\boldsymbol{A}_{12}\boldsymbol{K}\boldsymbol{C}_1\end{aligned} \tag{2.9}$$

where $\boldsymbol{K}=\boldsymbol{F}_2^{-1}\boldsymbol{F}_1$. From (2.9) it is a static output feedback problem to design $\boldsymbol{K}$ stabilizing $\boldsymbol{A}_{11}-\boldsymbol{A}_{12}\boldsymbol{K}\boldsymbol{C}_1$. For checking the controllability of the pair $(\boldsymbol{A}_{11},\boldsymbol{A}_{12})$, the following relationship within (2.6) is established,

$$\begin{aligned}\operatorname{rank}\left(\begin{bmatrix}s\boldsymbol{I}-\boldsymbol{A} & \boldsymbol{B}\end{bmatrix}\right)&=\operatorname{rank}\left(\begin{bmatrix}s\boldsymbol{I}-\boldsymbol{A}_{11} & -\boldsymbol{A}_{12} & \boldsymbol{0}\\ -\boldsymbol{A}_{21} & s\boldsymbol{I}-\boldsymbol{A}_{22} & \boldsymbol{B}_2\end{bmatrix}\right)\\ &=\operatorname{rank}\left(\begin{bmatrix}s\boldsymbol{I}-\boldsymbol{A}_{11} & \boldsymbol{A}_{12}\end{bmatrix}\right)+m\\ &=n\end{aligned} \tag{2.10}$$

for all $s\in\mathbb{C}$. It can conclude that $\operatorname{rank}\left(\begin{bmatrix}s\boldsymbol{I}-\boldsymbol{A}_{11} & \boldsymbol{A}_{12}\end{bmatrix}\right)=n-m$ and $(\boldsymbol{A}_{11},\boldsymbol{A}_{12})$ is controllable. On the other hand, for ensuring the observability of $(\boldsymbol{C}_1,\boldsymbol{A}_{11})$, the detail of $\boldsymbol{A}_{11}$ can be expresses as

$$\boldsymbol{A}_{11}=\begin{bmatrix}\boldsymbol{A}_{1111} & \boldsymbol{A}_{1112}\\ \boldsymbol{A}_{1121} & \boldsymbol{A}_{1122}\end{bmatrix} \tag{2.11}$$

where $\boldsymbol{A}_{1111}\in\mathbb{R}^{(n-p)\times(n-p)}$ and the other matrices in $\boldsymbol{A}_{11}$ are partitioned accordingly. Hence the rank test can be written as

$$\begin{aligned}\operatorname{rank}\left(\begin{bmatrix}s\boldsymbol{I}-\boldsymbol{A}_{11}\\ \boldsymbol{C}_1\end{bmatrix}\right)&=\operatorname{rank}\left(\begin{bmatrix}s\boldsymbol{I}-\boldsymbol{A}_{1111} & -\boldsymbol{A}_{1112}\\ -\boldsymbol{A}_{1121} & s\boldsymbol{I}-\boldsymbol{A}_{1122}\\ \boldsymbol{0} & \boldsymbol{I}_{p-m}\end{bmatrix}\right)\\ &=\operatorname{rank}\left(\begin{bmatrix}s\boldsymbol{I}-\boldsymbol{A}_{1111}\\ \boldsymbol{A}_{1121}\end{bmatrix}\right)+p-m\end{aligned} \tag{2.12}$$

for all $s\in\mathbb{C}$. Consequently, the observable pair $(\boldsymbol{A}_{1121},\boldsymbol{A}_{1111})$ is a sufficient condition of the observability of the pair $(\boldsymbol{C}_1,\boldsymbol{A}_{11})$. If the pair $(\boldsymbol{A}_{1121},\boldsymbol{A}_{1111})$ is not observable, there exists a matrix $\boldsymbol{T}_{obs}\in\mathbb{R}^{(n-p)\times(n-p)}$ putting this pair into the following observability canonical form [58],

$$\boldsymbol{T}_{obs}\boldsymbol{A}_{1111}\boldsymbol{T}_{obs}^{-1}=\begin{bmatrix}\boldsymbol{A}_{11}^{o} & \boldsymbol{A}_{12}^{o}\\ \boldsymbol{0} & \boldsymbol{A}_{22}^{o}\end{bmatrix}\ \text{and}\ \boldsymbol{A}_{1121}\boldsymbol{T}_{obs}^{-1}=\begin{bmatrix}\boldsymbol{0} & \boldsymbol{A}_{21}^{o}\end{bmatrix} \tag{2.13}$$

where $\boldsymbol{A}_{11}^{o}\in\mathbb{R}^{r\times r}$, $\boldsymbol{A}_{22}^{o}\in\mathbb{R}^{(n-p-r)\times(n-p-r)}$, $\boldsymbol{A}_{21}^{o}\in\mathbb{R}^{(p-m)\times(n-p-r)}$, the pair $(\boldsymbol{A}_{21}^{o},\boldsymbol{A}_{22}^{o})$ is completely observable, and $r\ge 0$ represents the number of unobservable nodes of $(\boldsymbol{A}_{1121},\boldsymbol{A}_{1111})$. Define the third transformation matrix as

$$\boldsymbol{T}_a=\begin{bmatrix}\boldsymbol{T}_{obs} & \boldsymbol{0}\\ \boldsymbol{0} & \boldsymbol{I}_p\end{bmatrix} \tag{2.14}$$

and then the transformed system matrices are similar as (2.6) with different $\boldsymbol{A}_{11}$,

$$\boldsymbol{A}_{11}=\left[\begin{array}{cc|c}\boldsymbol{A}_{11}^{o} & \boldsymbol{A}_{12}^{o} & \multirow{2}{*}{$\boldsymbol{A}_{12}^{m}$}\\ \boldsymbol{0} & \boldsymbol{A}_{22}^{o} & \\ \hline \boldsymbol{0} & \boldsymbol{A}_{21}^{o} & \boldsymbol{A}_{22}^{m}\end{array}\right]. \tag{2.15}$$

Furthermore, decompose $\boldsymbol{A}_{12}$ and $\boldsymbol{A}_{12}^{m}$ as

$$\boldsymbol{A}_{12} = \begin{bmatrix} \boldsymbol{A}_{121} \\ \boldsymbol{A}_{122} \end{bmatrix} \text{ and } \boldsymbol{A}_{12}^{m} = \begin{bmatrix} \boldsymbol{A}_{121}^{m} \\ \boldsymbol{A}_{122}^{m} \end{bmatrix} \tag{2.16}$$

where $\boldsymbol{A}_{122} \in \mathbb{R}^{(n-m-r)\times m}$ and $\boldsymbol{A}_{122}^{m} \in \mathbb{R}^{(n-p-r)\times(p-m)}$ forming a subsystem represented by the triple $\left(\tilde{\boldsymbol{A}}_{11}, \boldsymbol{A}_{122}, \tilde{\boldsymbol{C}}_{1}\right)$, where

$$\tilde{\boldsymbol{A}}_{11} \triangleq \begin{bmatrix} \boldsymbol{A}_{22}^{o} & \boldsymbol{A}_{122}^{m} \\ \boldsymbol{A}_{21}^{o} & \boldsymbol{A}_{22}^{m} \end{bmatrix} \text{ and } \tilde{\boldsymbol{C}}_{1} \triangleq \begin{bmatrix} \boldsymbol{0} & \boldsymbol{I}_{p-m} \end{bmatrix}. \tag{2.17}$$

Before discussing the stability of (2.9), three lemmas are introduced below.

Lemma 2.1 [2] The spectrum of $\boldsymbol{A}_{11}^{s}$ decomposes as

$$\lambda\left(\boldsymbol{A}_{11} - \boldsymbol{A}_{12}\boldsymbol{K}\boldsymbol{C}_{1}\right) = \lambda\left(\boldsymbol{A}_{11}^{o}\right) \cup \lambda\left(\tilde{\boldsymbol{A}}_{11} - \boldsymbol{A}_{122}\boldsymbol{K}\tilde{\boldsymbol{C}}_{1}\right) \qquad \square$$

Lemma 2.2 [2] The spectrum of $\boldsymbol{A}_{11}^{o}$ represents the invariant zeros of $\left(\boldsymbol{A}, \boldsymbol{B}, \boldsymbol{C}\right)$. □

Since Assumption 2.2 held, the present target is to design $\boldsymbol{K}$ stabilizing $\tilde{\boldsymbol{A}}_{11} - \boldsymbol{A}_{122}\boldsymbol{K}\tilde{\boldsymbol{C}}_{1}$ such that $\boldsymbol{A}_{11} - \boldsymbol{A}_{12}\boldsymbol{K}\boldsymbol{C}_{1}$ is stable. Suppose that $\operatorname{rank}\left(\boldsymbol{A}_{122}\right) = m'$ and the following equation is given,

$$\boldsymbol{A}_{122}\boldsymbol{T}_{m'} = \begin{bmatrix} \tilde{\boldsymbol{B}}_{1} & \boldsymbol{0} \end{bmatrix} \tag{2.18}$$

where $\boldsymbol{T}_{m'} \in \mathbb{R}^{m\times m}$ is of full rank and constructed such that $\tilde{\boldsymbol{B}}_{1} \in \mathbb{R}^{(n-m-r)\times m'}$. Defining a matrix $\boldsymbol{K}_{m'} = \boldsymbol{T}_{m'}^{-1}\boldsymbol{K} = \begin{bmatrix} \boldsymbol{K}_{1} \\ \boldsymbol{K}_{2} \end{bmatrix}$ where $\boldsymbol{K}_{1} \in \mathbb{R}^{m'\times(p-m)}$ and $\boldsymbol{K}_{2} \in \mathbb{R}^{(m-m')\times(p-m)}$ can attain that

$$\tilde{\boldsymbol{A}}_{11} - \boldsymbol{A}_{122}\boldsymbol{K}\tilde{\boldsymbol{C}}_{1} = \tilde{\boldsymbol{A}}_{11} - \begin{bmatrix} \tilde{\boldsymbol{B}}_{1} & \boldsymbol{0} \end{bmatrix}\boldsymbol{K}_{m'}\tilde{\boldsymbol{C}}_{1} = \tilde{\boldsymbol{A}}_{11} - \tilde{\boldsymbol{B}}_{1}\boldsymbol{K}_{1}\tilde{\boldsymbol{C}}_{1}. \tag{2.19}$$

As a result, the problem stabilizing $\tilde{\boldsymbol{A}}_{11} - \boldsymbol{A}_{122}\boldsymbol{K}\tilde{\boldsymbol{C}}_{1}$ is transferred to stabilize $\tilde{\boldsymbol{A}}_{11} - \tilde{\boldsymbol{B}}_{1}\boldsymbol{K}_{1}\tilde{\boldsymbol{C}}_{1}$. Next lemma presents the controllability of $\left(\tilde{\boldsymbol{A}}_{11}, \tilde{\boldsymbol{B}}_{1}\right)$ and observability of $\left(\tilde{\boldsymbol{C}}_{1}, \tilde{\boldsymbol{A}}_{11}\right)$ respectively.

Lemma 2.3 [2] The pair $\left(\tilde{\boldsymbol{A}}_{11}, \tilde{\boldsymbol{B}}_{1}\right)$ is completely controllable and $\left(\tilde{\boldsymbol{C}}_{1}, \tilde{\boldsymbol{A}}_{11}\right)$ is completely observable. □

Remark 2.1 The reason replacing the system pair $(\tilde{A}_{11},\tilde{B}_1,\tilde{C}_1)$ with $(\tilde{A}_{11},A_{122},\tilde{C}_1)$ is for utilizing the standard output feedback results. Consequently, the triple $(\tilde{A}_{11},\tilde{B}_1,\tilde{C}_1)$ must be controllable, observable, and fulfill Kimura-Davison condition as $m'+p+r\geq n+1$. □

2.2.2 Sliding mode controller synthesis

The output-dependent sliding vector is designed as

$$s(t)=Fy(t) \tag{2.20}$$

where $F=F_2[K \quad I_m]T^T$ and $F_2\in\mathbb{R}^{m\times m}$ is invertible and designed later. Define the fourth transformation matrix as

$$\bar{T}=\begin{bmatrix} I_{n-m} & 0 \\ KC_1 & I_m \end{bmatrix} \tag{2.21}$$

and hence the triple $(\bar{A},\bar{B},F\bar{C})$ via $x\mapsto\bar{T}x$ can be obtained as

$$\bar{A}=\begin{bmatrix} \bar{A}_{11} & \bar{A}_{12} \\ \bar{A}_{21} & \bar{A}_{22} \end{bmatrix},\quad \bar{B}=\begin{bmatrix} 0 \\ B_2 \end{bmatrix},\text{ and }\ F\bar{C}=\begin{bmatrix} 0 & F_2 \end{bmatrix} \tag{2.22}$$

where $\bar{A}_{11}=A_{11}-A_{12}KC_1$. According to Lemma 2.3, there exists K_1 such that $\tilde{A}_{11}-\tilde{B}_1K_1\tilde{C}_1$ is stable and the stability of $\bar{A}_{11}$ can be guaranteed by Lemmas 2.1 and 2.2 as for the system is minimum system.

Along with system (2.22), design a positive definite matrix P as

$$P=\begin{bmatrix} P_1 & 0 \\ 0 & P_2 \end{bmatrix}>0 \tag{2.23}$$

where $P_1\in\mathbb{R}^{(n-m)\times(n-m)}$ and $P_2\in\mathbb{R}^{m\times m}$ are both positive definite. Since $\bar{A}_{11}$ is stable, P_1 satisfies the following Lyapunov equation,

$$P_1\bar{A}_{11}+\bar{A}_{11}^TP_1=-Q_1 \tag{2.24}$$

where $\boldsymbol{Q}_1 \in \mathbb{R}^{(n-m)\times(n-m)}$ is a positive definite matrix. If matrix $\boldsymbol{P}_2$ is chosen such that

$$\boldsymbol{F} \triangleq \boldsymbol{B}_2^T \boldsymbol{P}_2 \tag{2.25}$$

then $\boldsymbol{P}$ satisfies the following structural constraint

$$\boldsymbol{P}\overline{\boldsymbol{B}} = \overline{\boldsymbol{C}}^T \boldsymbol{F}^T . \tag{2.26}$$

Define the following matrices,

$$\boldsymbol{Q}_2 \triangleq \boldsymbol{P}_1 \overline{\boldsymbol{A}}_{12} + \overline{\boldsymbol{A}}_{21}^T \boldsymbol{P}_2 \tag{2.27}$$

$$\boldsymbol{Q}_3 \triangleq \boldsymbol{P}_2 \overline{\boldsymbol{A}}_{22} + \overline{\boldsymbol{A}}_{22}^T \boldsymbol{P}_2 \tag{2.28}$$

and a scalar as

$$\gamma_0 \triangleq \frac{1}{2}\lambda_{\max}\left(\left(\boldsymbol{F}_2^{-1}\right)^T \left(\boldsymbol{Q}_3 + \boldsymbol{Q}_2^T \boldsymbol{Q}_1^{-1} \boldsymbol{Q}_2\right) \boldsymbol{F}_2^{-1}\right). \tag{2.29}$$

Notice that γ_0 is a real number due to the symmetry of matrix on the right in (2.29). Moreover, design the sliding mode control input as

$$\begin{aligned} \boldsymbol{u}(t) &= -\gamma \boldsymbol{F}\boldsymbol{y}(t) - v(t) \\ v(t) &= \begin{cases} \rho(\boldsymbol{y},t)\dfrac{\boldsymbol{s}(t)}{\left\|\boldsymbol{s}(t)\right\|} & \text{if } \boldsymbol{s}(t) \neq \boldsymbol{0} \\ \boldsymbol{0} & \text{otherwise} \end{cases} \end{aligned} \tag{2.30}$$

where $\gamma > \gamma_0$ and $\rho(\boldsymbol{y},t) = \dfrac{1}{1-k_1}\left(k_1\gamma\left\|\boldsymbol{s}(t)\right\| + \eta(\boldsymbol{y},t) + \gamma_1\right)$ based on Assumption 2.1. The positive scalar γ_1 will be designed later. Lemma 2.4 below will assist to prove the stability of the closed-loop system.

Lemma 2.4 [2] The symmetric matrix $\boldsymbol{L}(\gamma) = \boldsymbol{P}\boldsymbol{A}_0 + \boldsymbol{A}_0^T \boldsymbol{P}$ where $\boldsymbol{A}_0 = \overline{\boldsymbol{A}} - \gamma \overline{\boldsymbol{B}}\boldsymbol{F}\overline{\boldsymbol{C}}$ is negative definite if and only if $\gamma > \gamma_0$. □

Based on (2.22), the controlled system (2.1) can be rewritten as

$$\dot{\overline{\boldsymbol{x}}}(t) = \overline{\boldsymbol{A}}\overline{\boldsymbol{x}}(t) + \overline{\boldsymbol{B}}\left(\boldsymbol{u}(t) + \boldsymbol{f}(\boldsymbol{x},\boldsymbol{u},t)\right). \tag{2.31}$$

Choose a Lyapunov function as the following,

$$V(\bar{\boldsymbol{x}}) = \bar{\boldsymbol{x}}^T \boldsymbol{P}\bar{\boldsymbol{x}} > 0 . \tag{2.32}$$

Provided the structural constraint (2.26) and controller (2.30), the derivative of $V(\bar{\boldsymbol{x}})$ is given by

$$\begin{aligned}
\dot{V} &= \bar{\boldsymbol{x}}^T \left(\bar{\boldsymbol{A}}^T \boldsymbol{P} + \boldsymbol{P}\bar{\boldsymbol{A}} - 2\gamma\bar{\boldsymbol{C}}^T \boldsymbol{F}^T \boldsymbol{F}\bar{\boldsymbol{C}}\right)\bar{\boldsymbol{x}} + 2\bar{\boldsymbol{x}}^T \boldsymbol{P}\bar{\boldsymbol{B}}(\boldsymbol{f} - \boldsymbol{v}) \\
&= \bar{\boldsymbol{x}}^T \boldsymbol{L}(\gamma)\bar{\boldsymbol{x}} + 2\boldsymbol{y}^T \boldsymbol{F}^T (\boldsymbol{f} - \boldsymbol{v}) \\
&\le \bar{\boldsymbol{x}}^T \boldsymbol{L}(\gamma)\bar{\boldsymbol{x}} - 2\boldsymbol{y}^T \boldsymbol{F}^T \boldsymbol{v} + 2\|\boldsymbol{s}\|\|\boldsymbol{f}\| \\
&= \bar{\boldsymbol{x}}^T \boldsymbol{L}(\gamma)\bar{\boldsymbol{x}} - 2\rho(\boldsymbol{y},t)\|\boldsymbol{s}\| + 2\|\boldsymbol{s}\|\|\boldsymbol{f}\| \\
&< \bar{\boldsymbol{x}}^T \boldsymbol{L}(\gamma)\bar{\boldsymbol{x}} - 2\|\boldsymbol{s}\|\left(\rho(\boldsymbol{y},t) - k_1\|\boldsymbol{u}\| - \eta(\boldsymbol{y},t)\right).
\end{aligned} \tag{2.33}$$

Through some operation, it follows that

$$\begin{aligned}
\rho(\boldsymbol{y},t) &= k_1\rho(\boldsymbol{y},t) + k_1\gamma\|\boldsymbol{s}\| + \eta(\boldsymbol{y},t) + \gamma_1 \\
&\ge k_1\left(\|\boldsymbol{v}\| + \gamma\|\boldsymbol{s}\|\right) + \eta(\boldsymbol{y},t) + \gamma_1 \\
&\ge k_1\|\boldsymbol{u}\| + \eta(\boldsymbol{y},t) + \gamma_1.
\end{aligned} \tag{2.34}$$

According to Lemma 2.4 and (2.34), the negative derivative of $V(\bar{\boldsymbol{x}})$ can be proved by $\dot{V} < \bar{\boldsymbol{x}}^T \boldsymbol{L}(\gamma)\bar{\boldsymbol{x}} - 2\gamma_1\|\boldsymbol{s}\| < 0$ and conclude that the system is quadratically stable.

For assuring that an ideal sliding motion takes place on the vector $\boldsymbol{s}(t) = \boldsymbol{0}$, from (2.31) the dynamics of $\boldsymbol{s}(\bar{\boldsymbol{x}}) = \boldsymbol{F}\bar{\boldsymbol{C}}\bar{\boldsymbol{x}}$ is expressed as

$$\dot{\boldsymbol{s}} = \boldsymbol{F}\bar{\boldsymbol{C}}\boldsymbol{A}_0\bar{\boldsymbol{x}} + \boldsymbol{F}\boldsymbol{B}_2(\boldsymbol{f} - \boldsymbol{v}). \tag{2.35}$$

From (2.25), it follows that $\left(\boldsymbol{F}^{-1}\right)^T \boldsymbol{P}_2\boldsymbol{F}^{-1}\boldsymbol{F}\bar{\boldsymbol{C}}\boldsymbol{A}_0 = \boldsymbol{B}_2^{-1}\boldsymbol{A}_{0L}$ which $\boldsymbol{A}_{0L}$ is the last m rows of $\boldsymbol{A}_0$. Using this relationship, define a Lyapunov function $V_c(\boldsymbol{s}) = 2\boldsymbol{s}^T\left(\boldsymbol{F}^{-1}\right)^T \boldsymbol{P}_2\boldsymbol{F}^{-1}\boldsymbol{s}$ and its derivative is shown as

$$\begin{aligned}
\dot{V}_c &= 2\boldsymbol{s}^T \boldsymbol{B}_2^{-1}\boldsymbol{A}_{0L}\bar{\boldsymbol{x}} + 2\boldsymbol{s}^T(\boldsymbol{f} - \boldsymbol{v}) \\
&\le 2\|\boldsymbol{s}\|\left\|\boldsymbol{B}_2^{-1}\boldsymbol{A}_{0L}\bar{\boldsymbol{x}}\right\| - 2\gamma_1\|\boldsymbol{s}\|.
\end{aligned} \tag{2.36}$$

If $\bar{\boldsymbol{x}} \in \Omega$ where $\Omega = \left\{\bar{\boldsymbol{x}} \in \mathbb{R}^n : \left\|\boldsymbol{B}_2^{-1}\boldsymbol{A}_{0L}\bar{\boldsymbol{x}}\right\| < \gamma_1 - \sigma\right\}$ and $0 < \sigma < \gamma_1$, it follows that

$\dot{V}_c < -2\sigma\|\boldsymbol{s}\|$. Since the system is quadratically stable, there exists a finite time t_0 that $\bar{\boldsymbol{x}}(t) \in \Omega$ for all $t > t_0$. Therefore it can be concluded that the ideal sliding motion will take place in a finite time. The simulation results are used to verify the feasibility of the proposed sliding mode controller in the example below.

Example 2.1 Consider the system with the matched disturbance as

$$\dot{\boldsymbol{x}}(t) = \begin{bmatrix} 0 & 1 & 0 \\ 0 & 0 & 1 \\ -1 & \frac{1}{3} & -1 \end{bmatrix} \boldsymbol{x}(t) + \begin{bmatrix} 0 \\ 1 \\ 1 \end{bmatrix} \left(u(t) + d(t)\right)$$

$$\boldsymbol{y}(t) = \begin{bmatrix} 1 & \frac{8}{3} & 1 \\ 4 & \frac{2}{3} & -2 \end{bmatrix} \boldsymbol{x}(t).$$

The demonstrated system is controllable and observable, having no finite zero and $r = 0$. Therefore the system satisfies Assumptions 2.2-2.4. Set the matched disturbance as $d(t) = 0.1(\sin t - 1 + \sin 2t \cos 3t + \cos 2t \sin 3t \cos t)$. Transform the system into the form of (2.6), and the transformed matrices are given by

$$\boldsymbol{A} = \begin{bmatrix} -1.5816 & 0.0192 & 0.1457 \\ 1.4071 & 0.3845 & -1.708 \\ 0.2953 & 0.34 & 0.1971 \end{bmatrix},\ \boldsymbol{B} = \begin{bmatrix} 0 \\ 0 \\ -3.9016 \end{bmatrix}, \text{ and } \boldsymbol{C} = \begin{bmatrix} 0 & 0.3417 & -0.9398 \\ 0 & 0.9398 & 0.3417 \end{bmatrix}.$$

Hence matrices B_2 and $\boldsymbol{T}$ can be obtained as $B_2 = -3.9016$ and $\boldsymbol{T} = \begin{bmatrix} 0.3417 & -0.9398 \\ 0.9398 & 0.3417 \end{bmatrix}$.

Further the triple $(\tilde{\boldsymbol{A}}_{11}, \tilde{\boldsymbol{B}}_1, \tilde{\boldsymbol{C}}_1)$ from (2.17) and (2.18) can be determined as

$$\tilde{\boldsymbol{A}}_{11} = \begin{bmatrix} -1.5816 & 0.0192 \\ 1.4071 & 0.3845 \end{bmatrix},\ \tilde{\boldsymbol{B}}_1 = \begin{bmatrix} 0.1457 \\ -1.708 \end{bmatrix}, \text{ and } \tilde{\boldsymbol{C}}_1 = \begin{bmatrix} 0 & 1 \end{bmatrix}.$$

Referring to [59], the gain matrix is designed as $K = K_1 = -1.0556$ locating eigenvalues of $\tilde{\boldsymbol{A}}_{11} - \tilde{\boldsymbol{B}}_1 K \tilde{\boldsymbol{C}}_1$ on the stable nodes -1 and -2. Based on the transformation in (2.21), matrix

$\bar{\boldsymbol{A}}_{11}$ is given by

$$\bar{\boldsymbol{A}}_{11} = \begin{bmatrix} -1.5816 & 0.1729 \\ 1.4071 & -1.4184 \end{bmatrix}$$

which eigenvalues are also -1 and -2. Design $\boldsymbol{P}_1 = \begin{bmatrix} 0.3368 & 0.1891 \\ 0.1891 & 0.5401 \end{bmatrix} > 0$ and $P_2 = 1$ such that $\boldsymbol{Q}_1 = \begin{bmatrix} -0.5332 & 0.2509 \\ 0.2509 & -1.4668 \end{bmatrix} < 0$ fulfilling (2.24) and $F_2 = -3.9016$. Consequently the parameter γ_0 is 0.2452 and matrix $\boldsymbol{F}$ is determined as

$$\begin{aligned} \boldsymbol{F} &= F_2 \left[K \quad 1 \right] \boldsymbol{T}^T \\ &= F_2 \left[-1.3005 \quad -0.6503 \right] \\ &= \left[5.0741 \quad 2.537 \right]. \end{aligned}$$

Design the output-dependent sliding vector as $s(t) = \boldsymbol{F}\boldsymbol{y}(t) = \left[5.0741 \quad 2.537 \right] \boldsymbol{y}(t)$. Using the structure of control input (2.30), design the related parameters as $\gamma = 0.25$, $k_1 = 0.7$, $\eta = 0.2$, and $\gamma_1 = 0.01$.

For avoiding the chattering phenomenon, the switching term $v(t)$ in the control input is modified as $v(t) = \rho(\boldsymbol{y},t)\,\mathrm{sat}\left(\boldsymbol{s}(t),\varepsilon\right)$, where $\varepsilon = 0.05$ is the thickness of the so-called sliding layer. Since the initial condition is set as $\boldsymbol{x}(0) = \left[1 \quad 0 \quad 0\right]^T$, the simulation results are depicted in Fig. 2.1-2.4. The state and output responses are shown in Figs. 2.1 and 2.2 respectively, converging around zero successfully. Since (2.26) holds, all trajectories of system states in Fig. 2.1 converge to zero quadratically as the analysis of (2.33). Figure 2.3 showed the sliding vector and verified that the system entered into the sliding layer in a finite time. Matching the derivation of (2.36), the approaching behavior occurs after the sliding vector entering the local region around zero in Fig. 2.3. According to the control input shape in Fig. 2.4, the sliding mode controller has avoided the chattering phenomenon indeed due to the replacement of saturation function in the control input.

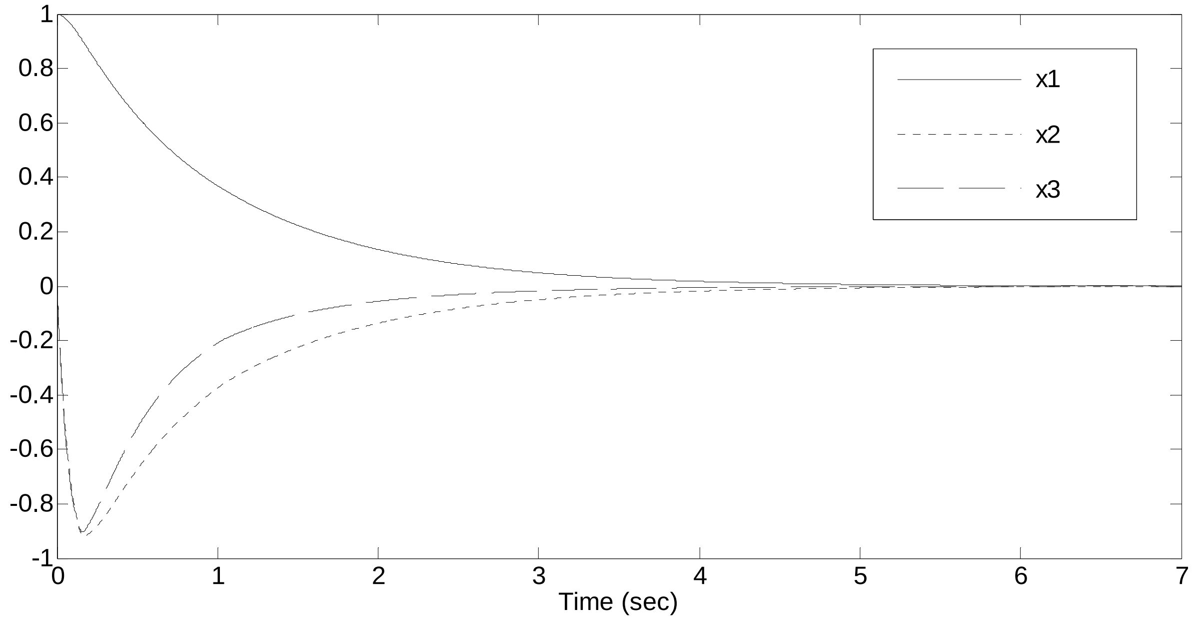

Fig. 2.1. System state responses in Example 2.1.

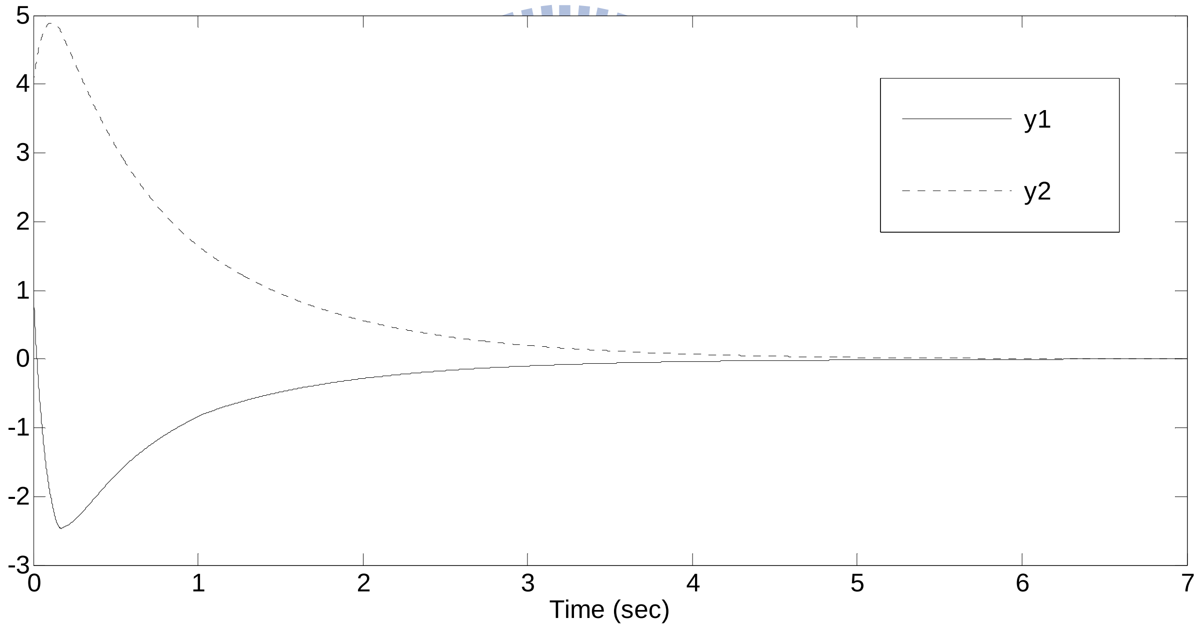

Fig. 2.2. System output responses in Example 2.1.

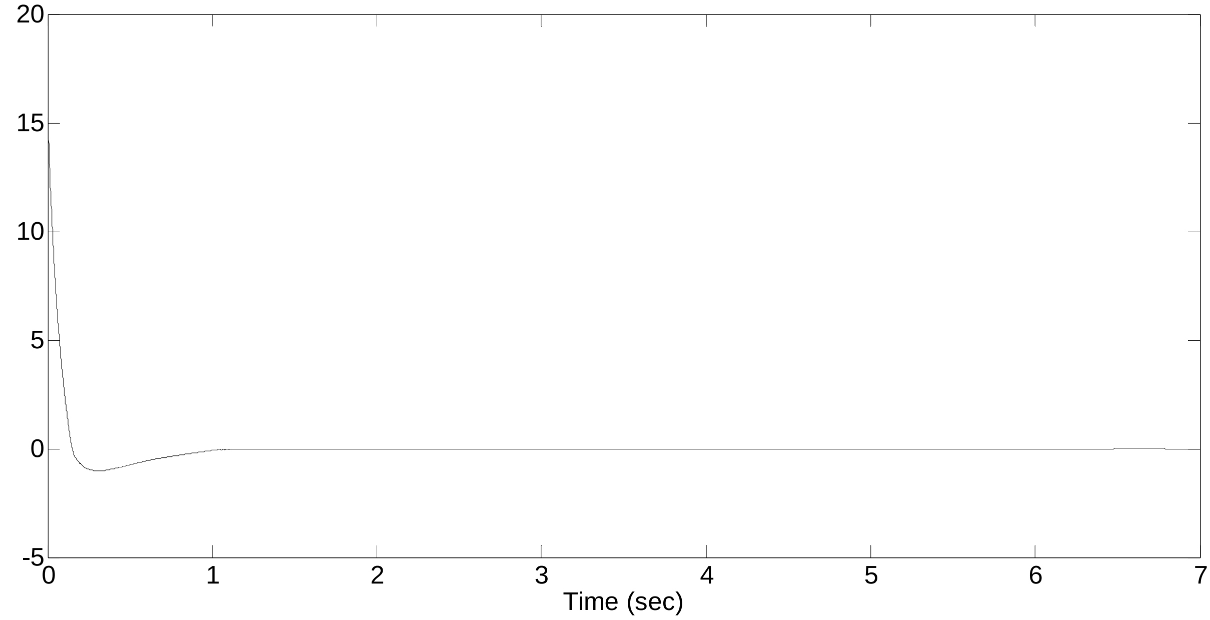

Fig. 2.3. Sliding vector in Example 2.1.

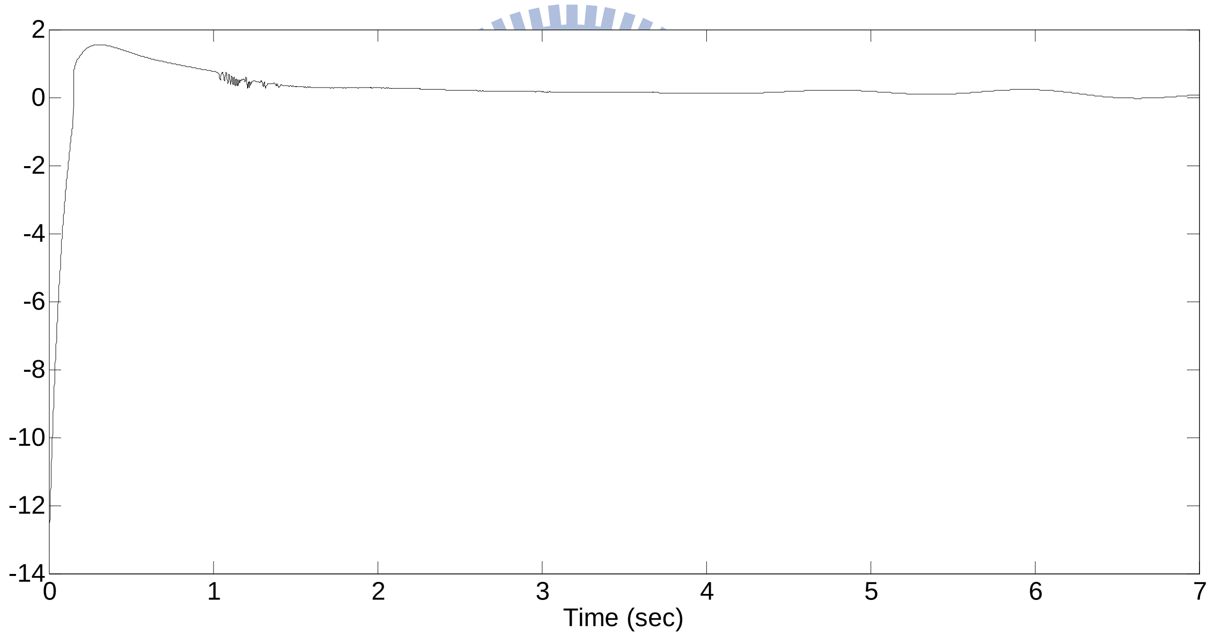

Fig. 2.4. System input response in Example 2.1.

2.3 Summary

This chapter has introduced a series of coordinate transformations, the sliding vector design method, and the sliding mode controller design, demonstrating the feasibility by the numerical example. Output feedback sliding mode control method still possesses the robustness against matched disturbances as the state feedback sliding mode controller. The designed controller can satisfy the approaching condition simply and improve the chattering phenomenon by the replacement of saturation function. Nevertheless, the static output feedback sliding vector has no ability locating eigenvalues of the system in the sliding mode arbitrary even though the system is controllable and observable. Besides the difficulty of designing the sliding vector, the output feedback sliding mode controller design suffered a structural constraint as a synthesis problem. Even though the synthesis constraint was satisfied, the designed controller guaranteed the local stability quadratically only rather than the global one.

For improving drawbacks of the static output feedback sliding mode controller mentioned above, next chapter will propose a dynamic output feedback sliding mode controller based on an integral sliding surface. The dynamic controller design can avoid the synthesis problem and assure the global stability using an adaptive law to estimate one of the controller parameters. The integral sliding surface and controller parameters will be offered by solutions to an algebraic Riccati equation.

III OUTPUT FEEDBACK INTEGRAL SLIDING MODE CONTROL

This chapter addresses the problem of designing an output feedback integral sliding mode control algorithm for linear MIMO systems with mismatched parameter uncertainties along with disturbances and matched nonlinear perturbations. Once the system is in the sliding mode, the proposed method of output-dependent integral sliding surface can robustly stabilize the closed-loop system and obtain the desired system performance. Two types of mismatched disturbances are considered and their effects in the sliding mode are explored. By introducing an additional dynamics into the controller design, the developed control law can guarantee that the system globally reaches to the stable sliding surface in a finite time. Finally, the feasibility of the proposed method is illustrated by numerical examples.

The system and the problem formulation are described in section 3.1. Section 3.2 presents the design of output-dependent integral sliding surface using the static output feedback technique and develops the controller design. The effectiveness of the proposed controller is illustrated in section 3.3 with numerical examples. A concluding summary is given in section 3.4.

3.1 Problem Formulation

Consider a continuous-time uncertain system described in the state space form as

$$\begin{aligned} \dot{\boldsymbol{x}}(t) &= \left(\boldsymbol{A} + \boldsymbol{D}\Phi(t)\boldsymbol{H}\right)\boldsymbol{x}(t) + \boldsymbol{B}\left(\boldsymbol{u}(t) + \boldsymbol{f}\left(\boldsymbol{x},\boldsymbol{u},t\right)\right) + \boldsymbol{E}\boldsymbol{d}(t) \\ \boldsymbol{y}(t) &= \boldsymbol{C}\boldsymbol{x}(t) \end{aligned} \tag{3.1}$$

where $\boldsymbol{x}(t) \in \mathbb{R}^n$ is the system state vector, $\boldsymbol{y}(t) \in \mathbb{R}^l$ is the system output vector, $\boldsymbol{u}(t) \in \mathbb{R}^m$ is the control input vector, and $\boldsymbol{d}(t) \in \mathbb{R}^p$ is the mismatched disturbance vector. The system matrices $\boldsymbol{A}$, $\boldsymbol{B}$, $\boldsymbol{C}$, $\boldsymbol{D}$, $\boldsymbol{E}$ and $\boldsymbol{H}$ are known matrices and have appropriate dimensions with $l \geq m$. Notice that $\boldsymbol{E}$ belongs to the columns of $\boldsymbol{B}^{\perp} \in \mathbb{R}^{n\times(n-m)}$ which span the null space of $\boldsymbol{B}^T$ [10]. The function $\boldsymbol{f}(\boldsymbol{x},\boldsymbol{u},t)\in\mathbb{R}^m$ is a time-varying vector in which it represents the lump sum of matched nonlinearities and/or uncertainties. In addition, $\Phi(t)$ is an unknown matrix satisfying $\Phi^T(t)\Phi(t)\le\boldsymbol{I}$. Although system (3.1) contains the mismatched disturbance, we design in this chapter an output-dependent integral sliding surface so that the proposed method can guarantee robust stability [55] of the closed-loop system once the system is in the sliding mode. A control law using output information and an additional dynamics is then designed to make the system globally satisfy the reaching and sliding condition [2]. Before introducing the proposed method, the following five assumptions are made throughout this chapter.

Assumption 3.1 The matched uncertain term is norm-bounded as

$$\left\|\boldsymbol{f}(\boldsymbol{x},\boldsymbol{u},t)\right\|\le a_1+a_2\left\|\boldsymbol{x}(t)\right\|+\chi\left\|\boldsymbol{u}(t)\right\| \tag{3.2}$$

where $0\le\chi<1$, a_1 and a_2 are known positive constants.

Assumption 3.2 The mismatched disturbance is bounded as

$$\left\|\boldsymbol{d}(t)\right\|\le\bar{d} \tag{3.3}$$

where $\bar{d}>0$ is a known constant.

Assumption 3.3 The pairs of $(\boldsymbol{A},\boldsymbol{B})$ and $(\boldsymbol{C},\boldsymbol{A})$ are stabilizable and detectable, respectively.

Assumption 3.4 The triple $(\boldsymbol{C},\boldsymbol{A},\boldsymbol{B})$ is of minimum phase.

Assumption 3.5 Matrices $\boldsymbol{B}$ and $\boldsymbol{C}$ have full rank, and $\operatorname{rank}(\boldsymbol{CB})=\operatorname{rank}(\boldsymbol{B})=m$.

As for Assumption 3.1, it is different from that in other papers [2, 7-8, 15-17, 21] in which the matched uncertainty $\boldsymbol{f}(\boldsymbol{x},\boldsymbol{u},t)$ is bounded by a function of the system outputs. Yan *et al*. [60] have shown that the condition is quite restrictive. Our proposed control scheme can eliminate the limitation. Assumptions 3.2-3.5 are generally developed from the conventional output feedback sliding mode control methods [2, 7-9, 15-21, 29].

3.2 Dynamic Output Feedback Sliding Mode Control

In this section, a design method of using the output-dependent integral sliding surface is proposed, in which robust stability of the closed-loop system can be guaranteed once the system is in the sliding mode. Seeking next to design the integral-type sliding surface for both matched and mismatched uncertain systems, Cao and Xu [22] developed a state-dependent integral sliding surface design in which the system is maintained on the sliding surface from the initial moment. However, the main problem related to the implementation of their method [22] is the requirement of the system states and their corresponding initial condition. In this work, we extend Cao and Xu's method to the uncertain system with regard to which only the output information is obtainable. Applying H_∞ control analyzing technique, the existence condition of the sliding surface is determined by solving an algebraic Riccati equation which is involved with the original system parameters. In comparison with the other output feedback sliding mode controllers [15-18, 21, 23-26, 60], our proposed control law can obtain global robust stability and avoid the high gain phenomenon in the transient time. Moreover, our control algorithm does not need any observer structure to estimate the system states.

3.2.1 Integral sliding surface design

Design the output-dependent integral sliding surface as

$$\boldsymbol{s}(t) = (\boldsymbol{CB})^{+} \boldsymbol{y}(t) - \int_{0}^{t} \boldsymbol{v}(\tau)\, d\tau \tag{3.4}$$

where $(\boldsymbol{CB})^{+} = \left((\boldsymbol{CB})^{T} \boldsymbol{CB}\right)^{-1} (\boldsymbol{CB})^{T} \in \mathbb{R}^{m\times l}$, $\boldsymbol{s} \in \mathbb{R}^{m}$, and the vector $\boldsymbol{v} \in \mathbb{R}^{m}$ is designed later. Taking the derivative of $\boldsymbol{s}(t)$ with respect to time and substituting (3.1) into it, we can obtain

$$\dot{\boldsymbol{s}}(t) = (\boldsymbol{CB})^{+} \boldsymbol{C}\left(\boldsymbol{A} + \boldsymbol{D}\Phi(t)\boldsymbol{H}\right)\boldsymbol{x}(t) - \boldsymbol{v}(t) + \boldsymbol{u}(t) + \boldsymbol{f}(\boldsymbol{x},\boldsymbol{u},t) + (\boldsymbol{CB})^{+} \boldsymbol{CEd}(t). \tag{3.5}$$

From (3.5), the control input is written as

$$\boldsymbol{u}(t)+\boldsymbol{f}(\boldsymbol{x},\boldsymbol{u},t)=\dot{\boldsymbol{s}}(t)+\boldsymbol{v}(t)-(\boldsymbol{CB})^{+}\boldsymbol{C}\left(\boldsymbol{A}+\boldsymbol{D}\Phi(t)\boldsymbol{H}\right)\boldsymbol{x}(t)-(\boldsymbol{CB})^{+}\boldsymbol{CEd}(t) \tag{3.6}$$

and then substitute it into (3.1) to obtain

$$\begin{aligned}\dot{\boldsymbol{x}}(t)&=\left(\boldsymbol{I}_n-\boldsymbol{B}(\boldsymbol{CB})^{+}\boldsymbol{C}\right)\left(\boldsymbol{A}+\boldsymbol{D}\Phi(t)\boldsymbol{H}\right)\boldsymbol{x}(t)+\left(\boldsymbol{I}_n-\boldsymbol{B}(\boldsymbol{CB})^{+}\boldsymbol{C}\right)\boldsymbol{Ed}(t)\\&\quad+\boldsymbol{Bv}(t)+\boldsymbol{B}\dot{\boldsymbol{s}}(t)\\&=\left(\boldsymbol{A}_1+\boldsymbol{D}_1\Phi(t)\boldsymbol{H}\right)\boldsymbol{x}(t)+\boldsymbol{E}_1\boldsymbol{d}(t)+\boldsymbol{Bv}(t)+\boldsymbol{B}\dot{\boldsymbol{s}}(t)\end{aligned} \tag{3.7}$$

where $\boldsymbol{A}_1=\left(\boldsymbol{I}_n-\boldsymbol{B}(\boldsymbol{CB})^{+}\boldsymbol{C}\right)\boldsymbol{A}$, $\boldsymbol{D}_1=\left(\boldsymbol{I}_n-\boldsymbol{B}(\boldsymbol{CB})^{+}\boldsymbol{C}\right)\boldsymbol{D}$, and $\boldsymbol{E}_1=\left(\boldsymbol{I}_n-\boldsymbol{B}(\boldsymbol{CB})^{+}\boldsymbol{C}\right)\boldsymbol{E}$.

Suppose that the system is in the sliding mode, $\boldsymbol{s}(t)=\boldsymbol{0}$ for $t\geq t_1$ where $t_1>0$ is a finite time. Then from (3.7) we obtain the system dynamics as

$$\dot{\boldsymbol{x}}(t)=\left(\boldsymbol{A}_1+\boldsymbol{D}_1\Phi(t)\boldsymbol{H}\right)\boldsymbol{x}(t)+\boldsymbol{E}_1\boldsymbol{d}(t)+\boldsymbol{Bv}(t)\quad \text{for } t\geq t_1. \tag{3.8}$$

Once the system is in the sliding mode, it follows from (3.8) that the robust stability problem of the closed-loop system becomes a standard output feedback controller design. As a result, the vector $\boldsymbol{v}(t)$ is a variable in the designed integral sliding surface, playing a role to affect the behavior of the system in the sliding mode. For system (3.8), a robust static output feedback controller is to be designed with the control algorithm in the form [17, 53-54, 56]

$$\boldsymbol{v}(t)=-\boldsymbol{FCx}(t)=-\boldsymbol{Fy}(t) \tag{3.9}$$

so that the closed-loop system $\dot{\boldsymbol{x}}(t)=\left(\boldsymbol{A}_1-\boldsymbol{BFC}+\boldsymbol{D}_1\Phi(t)\boldsymbol{H}\right)\boldsymbol{x}(t)$ is stable for all admissible uncertainties. Before introducing the main result, we have the following lemmas.

Lemma 3.1 If Assumptions 3.3 to 3.5 hold, then the pairs $(\boldsymbol{A}_1,\boldsymbol{B})$ and $(\boldsymbol{C},\boldsymbol{A}_1)$ are stabilizable and detectable, respectively.

Proof: Since state feedback control methods cannot change the controllability, from $\boldsymbol{A}_1=\boldsymbol{A}-\boldsymbol{B}(\boldsymbol{CB})^{+}\boldsymbol{CA}$, we can conclude that the pair $(\boldsymbol{A}_1,\boldsymbol{B})$ is stabilizable. From

$$\begin{bmatrix}s\boldsymbol{I}_n-\boldsymbol{A} & \boldsymbol{B}\\ \boldsymbol{C} & \boldsymbol{0}\end{bmatrix}\begin{bmatrix}\boldsymbol{I}_n & \boldsymbol{0}\\ (\boldsymbol{CB})^{+}\boldsymbol{CA} & \boldsymbol{I}_m\end{bmatrix}=\begin{bmatrix}s\boldsymbol{I}_n-\boldsymbol{A}_1 & \boldsymbol{B}\\ \boldsymbol{C} & \boldsymbol{0}\end{bmatrix},$$ one can obtain

$$\operatorname{rank}\left(\begin{bmatrix} s\boldsymbol{I}_n - \boldsymbol{A} & \boldsymbol{B} \\ \boldsymbol{C} & \boldsymbol{0} \end{bmatrix}\right) = \operatorname{rank}\left(\begin{bmatrix} s\boldsymbol{I}_n - \boldsymbol{A}_1 & \boldsymbol{B} \\ \boldsymbol{C} & \boldsymbol{0} \end{bmatrix}\right). \tag{3.10}$$

From Assumption 3.4 and the above equation, we know that the triple $(\boldsymbol{C}, \boldsymbol{A}_1, \boldsymbol{B})$ is of minimum phase. Since $\operatorname{rank}(\boldsymbol{CB}) = m$, the realization $(\boldsymbol{C}, \boldsymbol{A}_1, \boldsymbol{B})$ can be written in a special form [2] as

$$\boldsymbol{A}_1 = \begin{bmatrix} \boldsymbol{A}_{11} & \boldsymbol{A}_{12} \\ \boldsymbol{A}_{21} & \boldsymbol{A}_{22} \end{bmatrix}, \quad \boldsymbol{B} = \begin{bmatrix} \boldsymbol{B}_1 \\ \boldsymbol{0} \end{bmatrix}, \text{ and } \boldsymbol{C} = \begin{bmatrix} \boldsymbol{C}_1 & \boldsymbol{C}_2 \end{bmatrix} \tag{3.11}$$

where the matrix $\boldsymbol{B}_1 \in \mathbb{R}^{m\times m}$ is invertible and the matrix $\boldsymbol{C}_1 \in \mathbb{R}^{l\times m}$ has full rank. From Assumption 3.4 and

$$\begin{aligned} \operatorname{rank}\left(\begin{bmatrix} s\boldsymbol{I}_n - \boldsymbol{A}_1 & \boldsymbol{B} \\ \boldsymbol{C} & \boldsymbol{0} \end{bmatrix}\right) &= \operatorname{rank}\left(\begin{bmatrix} s\boldsymbol{I}_m - \boldsymbol{A}_{11} & -\boldsymbol{A}_{12} & \boldsymbol{B}_1 \\ -\boldsymbol{A}_{21} & s\boldsymbol{I}_{n-m} - \boldsymbol{A}_{22} & \boldsymbol{0} \\ \boldsymbol{C}_1 & \boldsymbol{C}_2 & \boldsymbol{0} \end{bmatrix}\right) \\ &= \operatorname{rank}\left(\begin{bmatrix} -\boldsymbol{A}_{21} & s\boldsymbol{I}_{n-m} - \boldsymbol{A}_{22} \\ \boldsymbol{C}_1 & \boldsymbol{C}_2 \end{bmatrix}\right) + m \end{aligned} \tag{3.12}$$

it follows that

$$\operatorname{rank}\left(\begin{bmatrix} -\boldsymbol{A}_{21} & s\boldsymbol{I}_{n-m} - \boldsymbol{A}_{22} \\ \boldsymbol{C}_1 & \boldsymbol{C}_2 \end{bmatrix}\right) = n \quad \forall \operatorname{Re}(s) > 0 . \tag{3.13}$$

Because the dimension of the matrix $\begin{bmatrix} s\boldsymbol{I}_n - \boldsymbol{A}_1 \\ \boldsymbol{C} \end{bmatrix}$ is $(n+l)\times n$, from the linear algebraic theory and the above rank condition, we can obtain

$$\operatorname{rank}\left(\begin{bmatrix} s\boldsymbol{I}_n - \boldsymbol{A}_1 \\ \boldsymbol{C} \end{bmatrix}\right) = \operatorname{rank}\left(\begin{bmatrix} s\boldsymbol{I}_m - \boldsymbol{A}_{11} & -\boldsymbol{A}_{12} \\ -\boldsymbol{A}_{21} & s\boldsymbol{I}_{n-m} - \boldsymbol{A}_{22} \\ \boldsymbol{C}_1 & \boldsymbol{C}_2 \end{bmatrix}\right) = n \quad \forall \operatorname{Re}(s) > 0 . \tag{3.14}$$

As a result, the pair $(\boldsymbol{C}, \boldsymbol{A}_1)$ is detectable. We complete the proof of the lemma. □

Lemma 3.2 [17] Consider the following uncertain system

$$\dot{\boldsymbol{x}}(t) = \left(\boldsymbol{A} + \boldsymbol{D}\Phi(t)\boldsymbol{H}\right)\boldsymbol{x}(t), \tag{3.15}$$

where $\boldsymbol{A}$, $\boldsymbol{D}$ and $\boldsymbol{H}$ are constant matrices of appropriate dimensions, and $\Phi^T(t)\Phi(t) \le \boldsymbol{I}$. The above system is asymptotically stable if and only if there exists a symmetric positive definite matrix $\boldsymbol{P}$ and a positive constant β such that

$$\boldsymbol{A}^T\boldsymbol{P} + \boldsymbol{P}\boldsymbol{A} + \frac{1}{\beta}\boldsymbol{P}\boldsymbol{D}\boldsymbol{D}^T\boldsymbol{P} + \beta\boldsymbol{H}^T\boldsymbol{H} < 0 . \qquad \square$$

Since the pair $(\boldsymbol{A}_1, \boldsymbol{B})$ is stabilizable and the pair $(\boldsymbol{C}, \boldsymbol{A}_1)$ is detectable, we can use the static output feedback technique to design

$$\boldsymbol{v}(t) = -\boldsymbol{F}\boldsymbol{y}(t) = -\boldsymbol{F}\boldsymbol{C}\boldsymbol{x}(t) = -\boldsymbol{R}^{-1}\left(\boldsymbol{B}^T\boldsymbol{P} + \boldsymbol{L}\right)\boldsymbol{x}(t) \tag{3.16}$$

where $\boldsymbol{R} > 0$ and $\boldsymbol{Q} > 0$ are the weighting matrices, and the matrices $\boldsymbol{L}$ and $\boldsymbol{P} > 0$ satisfy the following algebraic Riccati equation

$$\boldsymbol{A}_1^T\boldsymbol{P} + \boldsymbol{P}\boldsymbol{A}_1 - \boldsymbol{P}\boldsymbol{B}\boldsymbol{R}^{-1}\boldsymbol{B}^T\boldsymbol{P} + \boldsymbol{L}^T\boldsymbol{R}^{-1}\boldsymbol{L} + \frac{1}{\beta}\boldsymbol{P}\boldsymbol{D}_1\boldsymbol{D}_1^T\boldsymbol{P} + \beta\boldsymbol{H}^T\boldsymbol{H} + \boldsymbol{Q} = \boldsymbol{0} . \tag{3.17}$$

Hence the system states are bounded once the system is in the sliding mode, as the following theorem.

Theorem 3.1 Consider system (3.1) satisfying Assumptions 3.1 to 3.5 with the output-dependent integral sliding surface (3.4). Suppose that the system is in the sliding mode, and its behavior has been described as (3.8). If the mismatched disturbance is bounded and the matrix $\boldsymbol{A}_1 + \boldsymbol{D}_1\Phi(t)\boldsymbol{H} - \boldsymbol{B}\boldsymbol{F}\boldsymbol{C} = \boldsymbol{A}_1 + \boldsymbol{D}_1\Phi(t)\boldsymbol{H} - \boldsymbol{B}\boldsymbol{R}^{-1}\left(\boldsymbol{B}^T\boldsymbol{P} + \boldsymbol{L}\right)$ is Hurwitz, then all states of system (3.8) are bounded as

$$\left\|\boldsymbol{x}(t)\right\| \le \frac{2\left\|\boldsymbol{P}\boldsymbol{E}_1\right\|\bar{d}}{\rho\lambda_{\min}\left(\boldsymbol{Q} + \boldsymbol{C}^T\boldsymbol{F}^T\boldsymbol{R}\boldsymbol{F}\boldsymbol{C}\right)}\sqrt{\frac{\lambda_{\max}(\boldsymbol{P})}{\lambda_{\min}(\boldsymbol{P})}} \tag{3.18}$$

where $0 < \rho < 1$ is a constant.

Proof: Substitute (3.16) into (3.8) to obtain the closed-loop system dynamics in the sliding mode as

$$\begin{aligned}\dot{\boldsymbol{x}}(t) &= \left(\boldsymbol{A}_1 - \boldsymbol{B}\boldsymbol{R}^{-1}\left(\boldsymbol{B}^T\boldsymbol{P} + \boldsymbol{L}\right) + \boldsymbol{D}_1\Phi(t)\boldsymbol{H}\right)\boldsymbol{x}(t) + \boldsymbol{E}_1\boldsymbol{d}(t) \\ &= \left(\boldsymbol{A}_s + \boldsymbol{D}_1\Phi(t)\boldsymbol{H}\right)\boldsymbol{x}(t) + \boldsymbol{E}_1\boldsymbol{d}(t)\end{aligned} \tag{3.19}$$

where $\boldsymbol{A}_s = \boldsymbol{A}_1 - \boldsymbol{B}\boldsymbol{R}^{-1}\left(\boldsymbol{B}^T\boldsymbol{P} + \boldsymbol{L}\right)$. First we need to show that the matrix $\boldsymbol{A}_s + \boldsymbol{D}_1\Phi(t)\boldsymbol{H}$ is Hurwitz. Without considering the mismatched disturbance term in system (3.19), we rewrite the dynamic equation of $\boldsymbol{x}(t)$ as

$$\dot{\boldsymbol{x}}(t) = \left(\boldsymbol{A}_1 - \boldsymbol{B}\boldsymbol{R}^{-1}\left(\boldsymbol{B}^T\boldsymbol{P} + \boldsymbol{L}\right) + \boldsymbol{D}_1\Phi(t)\boldsymbol{H}\right)\boldsymbol{x}(t) = \left(\boldsymbol{A}_s + \boldsymbol{D}_1\Phi(t)\boldsymbol{H}\right)\boldsymbol{x}(t). \tag{3.20}$$

Rearranging the algebraic Riccati equation (3.17) yields

$$\boldsymbol{A}_s^T\boldsymbol{P} + \boldsymbol{P}\boldsymbol{A}_s + \frac{1}{\beta}\boldsymbol{P}\boldsymbol{D}_1\boldsymbol{D}_1^T\boldsymbol{P} + \beta\boldsymbol{H}^T\boldsymbol{H} = -\boldsymbol{Q} - \boldsymbol{C}^T\boldsymbol{F}^T\boldsymbol{R}\boldsymbol{F}\boldsymbol{C} < 0. \tag{3.21}$$

From Lemma 3.2, the above equation implies that the matrix $\boldsymbol{A}_s + \boldsymbol{D}_1\Phi(t)\boldsymbol{H}$ is asymptotically stable. Then choose a Lyapunov function $V_1(t) = \boldsymbol{x}^T(t)\boldsymbol{P}\boldsymbol{x}(t)$ where the positive definite matrix $\boldsymbol{P}$ satisfies (3.17), and take the time derivative of $V_1(t)$ to obtain

$$\begin{aligned}\dot{V}_1(t) &= -\boldsymbol{x}^T(t)\left(\boldsymbol{Q} + \boldsymbol{C}^T\boldsymbol{F}^T\boldsymbol{R}\boldsymbol{F}\boldsymbol{C} + \frac{1}{\beta}\boldsymbol{P}\boldsymbol{D}_1\boldsymbol{D}_1^T\boldsymbol{P} + \beta\boldsymbol{H}^T\boldsymbol{H}\right)\boldsymbol{x}(t) \\ &\quad + 2\boldsymbol{x}^T(t)\boldsymbol{P}\boldsymbol{D}_1\Phi(t)\boldsymbol{H}\boldsymbol{x}(t) + 2\boldsymbol{x}^T(t)\boldsymbol{P}\boldsymbol{E}_1\boldsymbol{d}(t) \\ &\le -\boldsymbol{x}^T(t)\left(\boldsymbol{Q} + \boldsymbol{C}^T\boldsymbol{F}^T\boldsymbol{R}\boldsymbol{F}\boldsymbol{C}\right)\boldsymbol{x}(t) + 2\boldsymbol{x}^T(t)\boldsymbol{P}\boldsymbol{E}_1\boldsymbol{d}(t) \\ &\le -\lambda_{\min}\left(\boldsymbol{Q} + \boldsymbol{C}^T\boldsymbol{F}^T\boldsymbol{R}\boldsymbol{F}\boldsymbol{C}\right)\left\|\boldsymbol{x}(t)\right\|^2 + 2\bar{d}\left\|\boldsymbol{P}\boldsymbol{E}_1\right\|\left\|\boldsymbol{x}(t)\right\| \\ &= -(1-\rho)\lambda_{\min}(\boldsymbol{Y})\left\|\boldsymbol{x}(t)\right\|^2 - \left\|\boldsymbol{x}(t)\right\|\left(\rho\lambda_{\min}(\boldsymbol{Y})\left\|\boldsymbol{x}(t)\right\| - 2\bar{d}\left\|\boldsymbol{P}\boldsymbol{E}_1\right\|\right)\end{aligned} \tag{3.22}$$

where $0 < \rho < 1$ is a constant and $\boldsymbol{Y} = \boldsymbol{Q} + \boldsymbol{C}^T\boldsymbol{F}^T\boldsymbol{R}\boldsymbol{F}\boldsymbol{C} > 0$. If $\left\|\boldsymbol{x}(t)\right\| \ge \dfrac{2\bar{d}\left\|\boldsymbol{P}\boldsymbol{E}_1\right\|}{\rho\lambda_{\min}(\boldsymbol{Y})}$, then the above equation becomes

$$\dot{V}_1(t) \le -(1-\rho)\lambda_{\min}(\boldsymbol{Y})\left\|\boldsymbol{x}(t)\right\|^2 \quad \text{for} \quad \left\|\boldsymbol{x}(t)\right\| \ge \frac{2\bar{d}\left\|\boldsymbol{P}\boldsymbol{E}_1\right\|}{\rho\lambda_{\min}(\boldsymbol{Y})}. \tag{3.23}$$

Since $\lambda_{\min}(\boldsymbol{P})\left\|\boldsymbol{x}(t)\right\|^2 \le \boldsymbol{x}^T(t)\boldsymbol{P}\boldsymbol{x}(t) \le \lambda_{\max}(\boldsymbol{P})\left\|\boldsymbol{x}(t)\right\|^2$, we can conclude from [61] that the system states are finally ultimately bounded

$$\|x(t)\| \le \frac{2\|PE_1\|\bar{d}}{\rho\lambda_{\min}\left(Q + C^T F^T RFC\right)}\sqrt{\frac{\lambda_{\max}(P)}{\lambda_{\min}(P)}}. \tag{3.24}$$

From $y(t) = Cx(t)$, we have that the system outputs are also bounded in a known region. Hence, the proof of the theorem is completed. □

Remark 3.1 Since $\operatorname{rank}(B) = m$, there exists a matrix $U \in \mathbb{R}^{(n-m)\times n}$ such that $UB = 0$. According to the linear algebraic theory, we know from $UB = 0$ and $(CB)^+ CB = I_m$ that the matrix $\begin{bmatrix} U \\ (CB)^+ C \end{bmatrix}$ is invertible. Let $\begin{bmatrix} U \\ (CB)^+ C \end{bmatrix}^{-1} = \begin{bmatrix} U_g & B \end{bmatrix}$ where the matrix $U_g \in \mathbb{R}^{n\times(n-m)}$ satisfies $UU_g = I_{n-m}$ and $CU_g = 0$. Define a system transformation as follows

$$\begin{bmatrix} w_1(t) \\ w_2(t) \end{bmatrix} = \begin{bmatrix} U \\ (CB)^+ C \end{bmatrix} x(t) \text{ and } x(t) = \begin{bmatrix} U_g & B \end{bmatrix}\begin{bmatrix} w_1(t) \\ w_2(t) \end{bmatrix} \tag{3.25}$$

where $w_1(t) \in \mathbb{R}^{n-m}$ and $w_2(t) \in \mathbb{R}^m$. From (3.19) and the above transformation, the state equations of $w_1(t)$ and $w_2(t)$ can be written as

$$\begin{bmatrix} \dot{w}_1(t) \\ \dot{w}_2(t) \end{bmatrix} = \Phi_A \begin{bmatrix} w_1(t) \\ w_2(t) \end{bmatrix} + \begin{bmatrix} UE_1 \\ (CB)^+ CE_1 \end{bmatrix} d(t) \tag{3.26}$$

where $\Phi_A = \begin{bmatrix} U \\ (CB)^+ C \end{bmatrix}\left(A_1 - BFC + D_1\Phi(t)H\right)\begin{bmatrix} U_g & B \end{bmatrix}$ is a stable matrix. Since the system is in the sliding mode, using direct calculations can yield

$$w_2(t) = (CB)^+ y(t) = s(t) - \int_0^t Fy(\tau)d\tau = -\int_0^t Fy(\tau)d\tau. \tag{3.27}$$

If $l = m$ and the mismatched disturbance varies slowly, it follows from Barbalat's lemma [61] and the above equation that $y(t) \to 0$ as $t \to \infty$. As a result, introducing the integral action into the sliding surface can yield a good system performance. □

3.2.2 Integral sliding surface design for $\boldsymbol{d}(t) \in L_2$

More specifically, when the mismatched disturbance is defined in L_2-norm space, i.e. $\boldsymbol{d}(t) \in L_2$, we can use the property of robust disturbance attenuation to design the controller. The problem of ensuring robust disturbance attenuation is to design a controller such that the closed-loop system is stable and there exists a constant $0 \le \gamma < \infty$ with respect to which the performance bound [56]

$$\int_0^t \left(\boldsymbol{y}^T(\tau)\boldsymbol{y}(\tau) + \boldsymbol{u}^T(\tau)\boldsymbol{R}\boldsymbol{u}(\tau) \right) d\tau \le \gamma^2 \int_0^t \left(\boldsymbol{d}^T(\tau)\boldsymbol{d}(\tau) \right) d\tau \quad \forall \ t \ge 0 \tag{3.28}$$

is satisfied for all $\boldsymbol{d}(t) \in L_2$. The disturbance attenuation problem encountered is to design an output feedback control law which can ensure that the effect of the disturbance acting on a system is reduced to an accepted level. As a whole, H_∞ optimization technique [53-54, 56] is an effective method to be used for solving this problem of which the design objective is to minimize the gain from disturbance input to the controlled output covering all frequencies. For system (3.8), it is required to find a static output feedback gain matrix $\boldsymbol{F}$ such that the closed-loop system is stable and its L_2 gain is bounded by a prescribed value γ.

Theorem 3.2 Consider system (3.1) with the output-dependent integral sliding surface (3.4), satisfying these Assumptions 3.1 to 3.5. Suppose that the system is in the sliding mode for $t > t_1$ and its behavior of the reduced-order system has described as equation (3.8). If the mismatched disturbance is of $\boldsymbol{d}(t) \in L_2$ and the vector $\boldsymbol{v}(t)$ is designed as

$$\boldsymbol{v}(t) = -\boldsymbol{F}\boldsymbol{C}\boldsymbol{x}(t) = -\boldsymbol{R}^{-1}\left(\boldsymbol{B}^T\boldsymbol{P} + \boldsymbol{L}\right)\boldsymbol{x}(t) \tag{3.29}$$

where the matrices $\boldsymbol{L}$ and $\boldsymbol{P} > 0$ satisfy the following algebraic Riccati equation

$$\boldsymbol{A}^T\boldsymbol{P} + \boldsymbol{P}\boldsymbol{A} + \boldsymbol{C}^T\boldsymbol{C} + \frac{1}{\gamma^2}\boldsymbol{P}\boldsymbol{E}_1\boldsymbol{E}_1^T\boldsymbol{P} - \boldsymbol{P}\boldsymbol{B}\boldsymbol{R}^{-1}\boldsymbol{B}^T\boldsymbol{P} + \boldsymbol{L}^T\boldsymbol{R}^{-1}\boldsymbol{L} + \frac{1}{\beta}\boldsymbol{P}\boldsymbol{D}_1\boldsymbol{D}_1^T\boldsymbol{P} + \beta\boldsymbol{H}^T\boldsymbol{H} = \boldsymbol{0} \tag{3.30}$$

then the matrix $\boldsymbol{A}_1 - \boldsymbol{B}\boldsymbol{F}\boldsymbol{C} = \boldsymbol{A}_1 - \boldsymbol{B}\boldsymbol{R}^{-1}\left(\boldsymbol{B}^T\boldsymbol{P} + \boldsymbol{L}\right)$ is Hurwitz and the system performance satisfies

$$\int_{t_1}^{t}\left(\boldsymbol{y}^T(\tau)\boldsymbol{y}(\tau)+\boldsymbol{v}^T(\tau)\boldsymbol{R}\boldsymbol{v}(\tau)\right)d\tau \le \gamma^2\int_{t_1}^{t}\left(\boldsymbol{d}^T(\tau)\boldsymbol{d}(\tau)\right)d\tau+\boldsymbol{x}^T(t_1)\boldsymbol{P}\boldsymbol{x}(t_1) \tag{3.31}$$

for $t \ge t_1$. Hence, the robust stability of the closed-loop system and the robust disturbance attenuation can be guaranteed.

Proof: The main approach employed here is the standard Hamilton-Jacobi-Isaac method [56]. First, we define a quadratic energy function

$$E(\boldsymbol{x}) = \boldsymbol{x}^T\boldsymbol{P}\boldsymbol{x} \tag{3.32}$$

where $\boldsymbol{P} > 0$ satisfies the algebraic Riccati equation (3.30). Then the Hamiltonian function is given by

$$H(\boldsymbol{v},\boldsymbol{d}) = \boldsymbol{y}^T\boldsymbol{y}+\boldsymbol{v}^T\boldsymbol{R}\boldsymbol{v}-\gamma^2\boldsymbol{d}^T\boldsymbol{d}+\frac{dE}{dt}. \tag{3.33}$$

A sufficient condition for assuring the robust disturbance attenuation is that [56]

$$H(\boldsymbol{v},\boldsymbol{d}) \le 0 \quad \text{for all } \boldsymbol{d}\in L_2. \tag{3.34}$$

From $E(\boldsymbol{x}) = \boldsymbol{x}^T\boldsymbol{P}\boldsymbol{x}$ and $\boldsymbol{y} = \boldsymbol{C}\boldsymbol{x}$, one can obtain

$$\begin{aligned} H(\boldsymbol{v},\boldsymbol{d}) &= \boldsymbol{x}^T\boldsymbol{C}^T\boldsymbol{C}\boldsymbol{x}+\boldsymbol{v}^T\boldsymbol{R}\boldsymbol{v}+\boldsymbol{x}^T\left[\left(\boldsymbol{A}_1+\boldsymbol{D}_1\Phi(t)\boldsymbol{H}\right)^T\boldsymbol{P}+\boldsymbol{P}\left(\boldsymbol{A}_1+\boldsymbol{D}_1\Phi(t)\boldsymbol{H}\right)\right]\boldsymbol{x} \\ &\quad +2\boldsymbol{x}^T\boldsymbol{P}\boldsymbol{B}\boldsymbol{v}-\gamma^2\boldsymbol{d}^T\boldsymbol{d}+2\boldsymbol{x}^T\boldsymbol{P}\boldsymbol{E}_1\boldsymbol{d}. \end{aligned} \tag{3.35}$$

From the H_∞ control theory [56] and the above equation, the worst case $\sup_{\boldsymbol{d}\in L_2} H(\boldsymbol{v},\boldsymbol{d})$ occurs when $\boldsymbol{d}(t) = \frac{1}{\gamma^2}\boldsymbol{E}_1^T\boldsymbol{P}\boldsymbol{x}(t)$ and then yields

$$\begin{aligned} H_1(\boldsymbol{v}) &\equiv \sup_{\boldsymbol{d}\in L_2} H(\boldsymbol{v},\boldsymbol{d}) \\ &= g(\boldsymbol{x})+\boldsymbol{v}^T\boldsymbol{R}\boldsymbol{v}+\boldsymbol{x}^T\left[\left(\boldsymbol{D}_1\Phi(t)\boldsymbol{H}\right)^T\boldsymbol{P}+\boldsymbol{P}\left(\boldsymbol{D}_1\Phi(t)\boldsymbol{H}\right)\right]\boldsymbol{x}+2\boldsymbol{x}^T\boldsymbol{P}\boldsymbol{B}\boldsymbol{v} \end{aligned} \tag{3.36}$$

where $g(\boldsymbol{x}) = \boldsymbol{x}^T\left(\boldsymbol{C}^T\boldsymbol{C}+\boldsymbol{A}_1^T\boldsymbol{P}+\boldsymbol{P}\boldsymbol{A}_1+\frac{1}{\gamma^2}\boldsymbol{P}\boldsymbol{E}_1\boldsymbol{E}_1^T\boldsymbol{P}\right)\boldsymbol{x}$. Since $\Phi^T(t)\Phi(t) \le \boldsymbol{I}$, the following inequality can be obtained

$$\boldsymbol{x}^T\left[\left(\boldsymbol{D}_1\Phi(t)\boldsymbol{H}\right)^T\boldsymbol{P}+\boldsymbol{P}\left(\boldsymbol{D}_1\Phi(t)\boldsymbol{H}\right)\right]\boldsymbol{x}\le\boldsymbol{x}^T\left(\frac{1}{\beta}\boldsymbol{P}\boldsymbol{D}_1\boldsymbol{D}_1^T\boldsymbol{P}+\beta\boldsymbol{H}^T\boldsymbol{H}\right)\boldsymbol{x} \tag{3.37}$$

and then $H(\boldsymbol{v},\boldsymbol{d})$ satisfies the following inequalities

$$H(\boldsymbol{v},\boldsymbol{d})\le H_1(\boldsymbol{v})\le g(\boldsymbol{x})+\boldsymbol{v}^T\boldsymbol{R}\boldsymbol{v}+2\boldsymbol{x}^T\boldsymbol{P}\boldsymbol{B}\boldsymbol{v}+\boldsymbol{x}^T\left(\frac{1}{\beta}\boldsymbol{P}\boldsymbol{D}_1\boldsymbol{D}_1^T\boldsymbol{P}+\beta\boldsymbol{H}^T\boldsymbol{H}\right)\boldsymbol{x}. \tag{3.38}$$

If the vector $\boldsymbol{v}(t)$ is chosen as

$$\boldsymbol{v}(t)=-\boldsymbol{F}\boldsymbol{C}\boldsymbol{x}(t)=-\boldsymbol{R}^{-1}\left(\boldsymbol{B}^T\boldsymbol{P}+\boldsymbol{L}\right)\boldsymbol{x}(t) \tag{3.39}$$

where the matrices $\boldsymbol{L}$ and $\boldsymbol{P}>0$ satisfy the following algebraic Riccati equation

$$\boldsymbol{A}_1^T\boldsymbol{P}+\boldsymbol{P}\boldsymbol{A}_1+\boldsymbol{C}^T\boldsymbol{C}+\boldsymbol{P}\left(\frac{1}{\gamma^2}\boldsymbol{E}_1\boldsymbol{E}_1^T+\frac{1}{\beta}\boldsymbol{D}_1\boldsymbol{D}_1^T-\boldsymbol{B}\boldsymbol{R}^{-1}\boldsymbol{B}^T\right)\boldsymbol{P}+\boldsymbol{L}^T\boldsymbol{R}^{-1}\boldsymbol{L}+\beta\boldsymbol{H}^T\boldsymbol{H}=\boldsymbol{0} \tag{3.40}$$

then it follows that

$$H(\boldsymbol{v},\boldsymbol{d})=\boldsymbol{y}^T\boldsymbol{y}+\boldsymbol{v}^T\boldsymbol{R}\boldsymbol{v}-\gamma^2\boldsymbol{d}^T\boldsymbol{d}+\frac{dE}{dt}\le 0 \quad \text{for all } \boldsymbol{d}\in L_2. \tag{3.41}$$

Integrating this equation yields

$$E(\boldsymbol{x}(t))-E(\boldsymbol{x}(t_1))+\int_{t_1}^{t}\left(\boldsymbol{y}^T\boldsymbol{y}+\boldsymbol{v}^T\boldsymbol{R}\boldsymbol{v}\right)d\tau\le\gamma^2\int_{t_1}^{t}\left(\boldsymbol{d}^T\boldsymbol{d}\right)d\tau \quad \text{for } t\ge t_1. \tag{3.42}$$

Rearranging the above inequality and noting $E(\boldsymbol{z}(t))\ge 0$, we can obtain

$$\int_{t_1}^{t}\left(\boldsymbol{y}^T\boldsymbol{y}+\boldsymbol{v}^T\boldsymbol{R}\boldsymbol{v}\right)d\tau\le\gamma^2\int_{t_1}^{t}\left(\boldsymbol{d}^T\boldsymbol{d}\right)d\tau+\boldsymbol{x}^T(t_1)\boldsymbol{P}\boldsymbol{x}(t_1) \quad \text{for } t\ge t_1. \tag{3.43}$$

Hence we know that the property of robust disturbance attenuation is guaranteed and complete the proof of this theorem. □

Remark 3.2 Gadewadikar *et al*. [53-54] have developed the search algorithm to solve the coupled design equations (3.16), (3.17), and (3.30). Using well-developed techniques for solving available algebraic Riccati equations is the main advantage of their method. We summarize their proposed method as follows.

1) Initialize: set $n=0$ and $\boldsymbol{L}_0=\boldsymbol{0}$, and select β, $\boldsymbol{Q}$, and $\boldsymbol{R}$.

2) At the nth iteration, solve for $\boldsymbol{P}_n$ in algebraic Riccati equations (3.17) or (3.30). Evaluate gain $\boldsymbol{F}$ and update $\boldsymbol{L}$

$$\boldsymbol{F}_{n+1} = -\boldsymbol{R}^{-1}\left(\boldsymbol{B}^T\boldsymbol{P}_n + \boldsymbol{L}_n\right)\boldsymbol{C}^T\left(\boldsymbol{C}\boldsymbol{C}^T\right)^{-1} \tag{3.44}$$

$$\boldsymbol{L}_{n+1} = -\boldsymbol{R}\boldsymbol{F}_{n+1}\boldsymbol{C} - \boldsymbol{B}^T\boldsymbol{P}_n . \tag{3.45}$$

Check the convergence condition $\left\|\boldsymbol{F}_{n+1} - \boldsymbol{F}_n\right\| < \kappa$ where $\kappa > 0$ is a given small number. If the convergence condition is satisfied, then go to Step 3. Otherwise, set $n = n+1$ and go to Step 2.

3) Terminate: set $\boldsymbol{F} = \boldsymbol{F}_{n+1}$. □

3.2.3 Control law synthesis

Having analyzed the system performance in the sliding mode, we focus on the synthesis of a control algorithm to induce the sliding mode within a finite time. Define a new state vector

$$\boldsymbol{z}(t) = \boldsymbol{x}(t) - \boldsymbol{B}\boldsymbol{s}(t) \tag{3.46}$$

and from (3.7) obtain its dynamic equation as

$$\dot{\boldsymbol{z}}(t) = \left(\boldsymbol{A}_1 + \boldsymbol{D}_1\Phi(t)\boldsymbol{H}\right)\boldsymbol{z}(t) + \boldsymbol{E}_1\boldsymbol{d}(t) + \boldsymbol{B}\boldsymbol{v}(t) + \left(\boldsymbol{A}_1 + \boldsymbol{D}_1\Phi(t)\boldsymbol{H}\right)\boldsymbol{B}\boldsymbol{s}(t). \tag{3.47}$$

Substitute $\boldsymbol{v} = -\boldsymbol{F}\boldsymbol{C}\boldsymbol{x} = -\boldsymbol{F}\boldsymbol{C}(\boldsymbol{z} + \boldsymbol{B}\boldsymbol{s})$ into (3.47) to obtain

$$\begin{aligned}\dot{\boldsymbol{z}}(t) &= \left(\boldsymbol{A}_1 - \boldsymbol{B}\boldsymbol{F}\boldsymbol{C} + \boldsymbol{D}_1\Phi(t)\boldsymbol{H}\right)\boldsymbol{z}(t) + \boldsymbol{E}_1\boldsymbol{d}(t) + \left(\boldsymbol{A}_1 + \boldsymbol{D}_1\Phi(t)\boldsymbol{H} - \boldsymbol{B}\boldsymbol{F}\boldsymbol{C}\right)\boldsymbol{B}\boldsymbol{s}(t) \\ &= \left(\boldsymbol{A}_s + \boldsymbol{D}_1\Phi(t)\boldsymbol{H}\right)\boldsymbol{z}(t) + \boldsymbol{E}_1\boldsymbol{d}(t) + \left(\boldsymbol{A}_s + \boldsymbol{D}_1\Phi(t)\boldsymbol{H}\right)\boldsymbol{B}\boldsymbol{s}(t)\end{aligned} \tag{3.48}$$

where $\boldsymbol{A}_s = \boldsymbol{A}_1 - \boldsymbol{B}\boldsymbol{F}\boldsymbol{C} = \boldsymbol{A}_1 - \boldsymbol{B}\boldsymbol{R}^{-1}\left(\boldsymbol{B}^T\boldsymbol{P} + \boldsymbol{L}\right)$ is a stable matrix. Moreover, the algebraic Riccati equation (3.17) can be rewritten as

$$\boldsymbol{A}_s^T\boldsymbol{P} + \boldsymbol{P}\boldsymbol{A}_s + \boldsymbol{C}^T\boldsymbol{F}^T\boldsymbol{R}\boldsymbol{F}\boldsymbol{C} + \frac{1}{\beta}\boldsymbol{P}\boldsymbol{D}_1\boldsymbol{D}_1^T\boldsymbol{P} + \beta\boldsymbol{H}^T\boldsymbol{H} = -\boldsymbol{Q} . \tag{3.49}$$

Since $\boldsymbol{P} > 0$, there exists a symmetric and nonsingular matrix $\boldsymbol{M} \in \mathbb{R}^{n\times n}$ such that

$\boldsymbol{P} = \boldsymbol{M}^T \boldsymbol{M}$. Now choose a Lyapunov function as

$$V_2(t) = \sqrt{\boldsymbol{z}^T(t)\boldsymbol{P}\boldsymbol{z}(t)} = \frac{\boldsymbol{z}^T(t)\boldsymbol{P}\boldsymbol{z}(t)}{\sqrt{\boldsymbol{z}^T(t)\boldsymbol{P}\boldsymbol{z}(t)}} = \|\boldsymbol{M}\boldsymbol{z}(t)\| \tag{3.50}$$

where the positive definite matrix $\boldsymbol{P}$ satisfies (3.49). Let $\boldsymbol{X} = \frac{1}{2}\left(\boldsymbol{Q} + \boldsymbol{C}^T\boldsymbol{F}^T\boldsymbol{R}\boldsymbol{F}\boldsymbol{C}\right) > 0$.

Differentiating (3.50) with respect to time and using (3.48) and (3.49) yield

$$\begin{aligned}\dot{V}_2(t) &= \frac{1}{2\sqrt{\boldsymbol{z}^T(t)\boldsymbol{P}\boldsymbol{z}(t)}}\Big[-2\boldsymbol{z}^T(t)\boldsymbol{X}\boldsymbol{z}(t) + 2\boldsymbol{z}^T(t)\boldsymbol{P}\boldsymbol{E}_1\boldsymbol{d}(t) + 2\boldsymbol{z}^T(t)\boldsymbol{P}\boldsymbol{D}_1\Phi(t)\boldsymbol{H}\boldsymbol{z}(t)\\ &\quad +2\boldsymbol{z}^T(t)\boldsymbol{P}\left(\boldsymbol{A}_s + \boldsymbol{D}_1\Phi(t)\boldsymbol{H}\boldsymbol{B}\right)\boldsymbol{s}(t) - \boldsymbol{z}^T(t)\left(\frac{1}{\beta}\boldsymbol{P}\boldsymbol{D}_1\boldsymbol{D}_1^T\boldsymbol{P} + \beta\boldsymbol{H}^T\boldsymbol{H}\right)\boldsymbol{z}(t)\Big]\\ &\le \frac{1}{\sqrt{\boldsymbol{z}^T(t)\boldsymbol{P}\boldsymbol{z}(t)}}\Big(-\boldsymbol{z}^T(t)\boldsymbol{X}\boldsymbol{z}(t) + \boldsymbol{z}^T(t)\boldsymbol{P}\boldsymbol{E}_1\boldsymbol{d}(t)\\ &\quad +\boldsymbol{z}^T(t)\boldsymbol{P}\left(\boldsymbol{A}_s + \boldsymbol{D}_1\Phi(t)\boldsymbol{H}\right)\boldsymbol{B}\boldsymbol{s}(t)\Big).\end{aligned} \tag{3.51}$$

From $\boldsymbol{P} = \boldsymbol{M}^T\boldsymbol{M}$ and $\boldsymbol{P} > 0$, the following inequalities can be attained

$$\boldsymbol{z}^T(t)\boldsymbol{P}\boldsymbol{E}_1\boldsymbol{d}(t) = \boldsymbol{z}^T(t)\boldsymbol{M}^T\boldsymbol{M}\boldsymbol{E}_1\boldsymbol{d}(t) \le \|\boldsymbol{M}\boldsymbol{z}(t)\|\|\boldsymbol{M}\boldsymbol{E}_1\|\bar{d} \tag{3.52}$$

and

$$\begin{aligned}\boldsymbol{z}^T(t)\boldsymbol{P}\left(\boldsymbol{A}_s + \boldsymbol{D}_1\Phi(t)\boldsymbol{H}\right)\boldsymbol{B}\boldsymbol{s}(t) &= \boldsymbol{z}^T(t)\boldsymbol{M}^T\boldsymbol{M}\left(\boldsymbol{A}_s + \boldsymbol{D}_1\Phi(t)\boldsymbol{H}\right)\boldsymbol{B}\boldsymbol{s}(t)\\ &\le \|\boldsymbol{M}\boldsymbol{z}(t)\|\left(\|\boldsymbol{M}\boldsymbol{A}_s\boldsymbol{B}\| + \|\boldsymbol{M}\boldsymbol{D}_1\|\|\boldsymbol{H}\boldsymbol{B}\|\right)\|\boldsymbol{s}(t)\|.\end{aligned} \tag{3.53}$$

Moreover, we have $\boldsymbol{z}^T(t)\boldsymbol{X}\boldsymbol{z}(t) \ge \lambda_{\min}\left(\boldsymbol{P}^{-1}\boldsymbol{X}\right)\boldsymbol{z}^T(t)\boldsymbol{P}\boldsymbol{z}(t)$. Substitute these inequalities into (3.51) to obtain

$$\begin{aligned}\dot{V}_2(t) &\le -\lambda_{\min}\left(\boldsymbol{P}^{-1}\boldsymbol{X}\right)\sqrt{\boldsymbol{z}^T(t)\boldsymbol{P}\boldsymbol{z}(t)} + \bar{d}\|\boldsymbol{M}\boldsymbol{E}_1\| + \left(\|\boldsymbol{M}\boldsymbol{A}_s\boldsymbol{B}\| + \|\boldsymbol{M}\boldsymbol{D}_1\|\|\boldsymbol{H}\boldsymbol{B}\|\right)\|\boldsymbol{s}(t)\|\\ &= -\lambda_{\min}\left(\boldsymbol{P}^{-1}\boldsymbol{X}\right)V_2(t) + b_1 + b_2\|\boldsymbol{s}(t)\|\end{aligned} \tag{3.54}$$

where $b_1 = \|\boldsymbol{M}\boldsymbol{E}_1\|\bar{d}$ and $b_2 = \|\boldsymbol{M}\boldsymbol{A}_s\boldsymbol{B}\| + \|\boldsymbol{M}\boldsymbol{D}_1\|\|\boldsymbol{H}\boldsymbol{B}\|$ are known constants. An auxiliary variable $\omega(t)$ is now introduced as

$$\dot{\omega}(t) = -\lambda_w\omega(t) + b_1 + b_2\|\boldsymbol{s}(t)\| \tag{3.55}$$

with $\omega(0) > 0$ and $0 < \lambda_w < \lambda_{\min}\left(\boldsymbol{P}^{-1}\boldsymbol{X}\right)$. Note that the three parameters λ_w, b_1, and b_2 are known. Comparing (3.54) and (3.55) indicates that there exists a finite time $t_2 > 0$ such that [9]

$$V_2(t) = \sqrt{\boldsymbol{z}^T(t)\boldsymbol{P}\boldsymbol{z}(t)} = \|\boldsymbol{M}\boldsymbol{z}(t)\| \le \omega(t) \quad \text{for} \quad t > t_2. \tag{3.56}$$

Substitute $\boldsymbol{x} = \boldsymbol{z} + \boldsymbol{B}\boldsymbol{s}$ and $\boldsymbol{v} = -\boldsymbol{F}\boldsymbol{y}$ into the derivative of $\boldsymbol{s}(t)$ to obtain

$$\begin{aligned}\dot{\boldsymbol{s}}(t) &= (\boldsymbol{CB})^{+}\boldsymbol{C}\left(\boldsymbol{A}+\boldsymbol{D}\Phi(t)\boldsymbol{H}\right)\left(\boldsymbol{z}(t)+\boldsymbol{B}\boldsymbol{s}(t)\right)+\boldsymbol{F}\boldsymbol{y}(t)+\boldsymbol{u}(t)\\ &\quad + \boldsymbol{f}(\boldsymbol{x},\boldsymbol{u},t)+(\boldsymbol{CB})^{+}\boldsymbol{CE}\boldsymbol{d}(t)\\ &= (\boldsymbol{CB})^{+}\boldsymbol{C}\left(\boldsymbol{A}+\boldsymbol{D}\Phi(t)\boldsymbol{H}\right)\boldsymbol{M}^{-1}\boldsymbol{M}\boldsymbol{z}(t)+(\boldsymbol{CB})^{+}\boldsymbol{C}\left(\boldsymbol{A}+\boldsymbol{D}\Phi(t)\boldsymbol{H}\right)\boldsymbol{B}\boldsymbol{s}(t)\\ &\quad + \boldsymbol{F}\boldsymbol{y}(t)+\boldsymbol{u}(t)+\boldsymbol{f}(\boldsymbol{x},\boldsymbol{u},t)+(\boldsymbol{CB})^{+}\boldsymbol{CE}\boldsymbol{d}(t).\end{aligned} \tag{3.57}$$

Although the system state vector $\boldsymbol{z}(t)$ cannot be measured, we can manage an upper bound of $\|\boldsymbol{M}\boldsymbol{z}(t)\|$ to drive the system into the sliding mode. Let

$$\boldsymbol{p}(t) = \boldsymbol{F}\boldsymbol{y}(t)+\left((\boldsymbol{CB})^{+}\boldsymbol{CAB}+b_3\boldsymbol{I}_m\right)\boldsymbol{s}(t) \tag{3.58}$$

where $b_3 = \left\|(\boldsymbol{CB})^{+}\boldsymbol{CD}\right\|\|\boldsymbol{HB}\|$. From the auxiliary variable $\omega(t)$ in (3.55), $\boldsymbol{x} = \boldsymbol{z} + \boldsymbol{B}\boldsymbol{s}$, and Assumption 3.1, we can obtain

$$\|\boldsymbol{x}(t)\| \le \|\boldsymbol{z}(t)\| + \|\boldsymbol{B}\boldsymbol{s}(t)\| \le \left\|\boldsymbol{M}^{-1}\right\|\|\boldsymbol{M}\boldsymbol{z}(t)\| + \|\boldsymbol{B}\boldsymbol{s}(t)\| \le \left\|\boldsymbol{M}^{-1}\right\|\omega(t) + \|\boldsymbol{B}\|\|\boldsymbol{s}(t)\| \tag{3.59}$$

and

$$\|\boldsymbol{f}(\boldsymbol{x},\boldsymbol{u},t)\| \le a_1 + a_2\|\boldsymbol{x}(t)\| + \chi\|\boldsymbol{u}(t)\| \le a_1 + a_2\left(\left\|\boldsymbol{M}^{-1}\right\|\omega(t) + \|\boldsymbol{B}\|\|\boldsymbol{s}(t)\|\right) + \chi\|\boldsymbol{u}(t)\|. \tag{3.60}$$

We design the control inputs $\boldsymbol{u}(t)$ as

$$\boldsymbol{u}(t) = -\boldsymbol{p}(t) - \eta(t)\frac{\boldsymbol{s}(t)}{\|\boldsymbol{s}(t)\|} \tag{3.61}$$

where $\eta(t) = \dfrac{1}{1-\chi}\left[\left(b_4 + a_2\left\|\boldsymbol{M}^{-1}\right\|\right)\omega(t) + \chi\|\boldsymbol{p}(t)\| + \bar{d}\left\|(\boldsymbol{CB})^{+}\boldsymbol{CE}\right\| + a_1 + a_2\|\boldsymbol{B}\|\|\boldsymbol{s}(t)\| + \delta\right]$,

$\delta > 0$ is a small constant, and $b_4 = \left\|(\boldsymbol{CB})^+ \boldsymbol{CAM}^{-1}\right\| + \left\|(\boldsymbol{CB})^+ \boldsymbol{CD}\right\| \left\|\boldsymbol{HM}^{-1}\right\|$. From (3.61), we have $\|\boldsymbol{u}(t)\| \le \|\boldsymbol{p}(t)\| + \eta(t)$ and then multiply both sides of $\eta(t)$ with $1-\chi$ to obtain

$$\begin{aligned}
\eta(t) &= \chi\eta(t) + \bar{d}\left\|(\boldsymbol{CB})^+ \boldsymbol{CE}\right\| + a_1 + a_2\|\boldsymbol{B}\|\|\boldsymbol{s}(t)\| \\
&\quad + \left(a_2\left\|\boldsymbol{M}^{-1}\right\| + b_4\right)\omega(t) + \chi\|\boldsymbol{p}(t)\| + \delta \\
&= \chi\left(\eta(t) + \|\boldsymbol{p}(t)\|\right) + \bar{d}\left\|(\boldsymbol{CB})^+ \boldsymbol{CE}\right\| + \left(a_2\left\|\boldsymbol{M}^{-1}\right\| + b_4\right)\omega(t) \\
&\quad + a_1 + a_2\|\boldsymbol{B}\|\|\boldsymbol{s}(t)\| + \delta \\
&\ge \chi\|\boldsymbol{u}(t)\| + \bar{d}\left\|(\boldsymbol{CB})^+ \boldsymbol{CE}\right\| + a_1 + a_2\|\boldsymbol{B}\|\|\boldsymbol{s}(t)\| + \left(a_2\left\|\boldsymbol{M}^{-1}\right\| + b_4\right)\omega(t) + \delta.
\end{aligned} \tag{3.62}$$

Substituting (3.61) into (3.57) and pre-multiplying both sides of (3.57) with $\boldsymbol{s}^T(t)$ can attain

$$\begin{aligned}
\boldsymbol{s}^T(t)\dot{\boldsymbol{s}}(t) &= \boldsymbol{s}^T(t)\Big((\boldsymbol{CB})^+ \boldsymbol{C}\left(\boldsymbol{A} + \boldsymbol{D}\Phi(t)\boldsymbol{H}\right)\boldsymbol{M}^{-1}\boldsymbol{Mz}(t) + (\boldsymbol{CB})^+ \boldsymbol{CD}\Phi(t)\boldsymbol{HBs}(t) \\
&\qquad + (\boldsymbol{CB})^+ \boldsymbol{CEd}(t) + \boldsymbol{f}(\boldsymbol{x},\boldsymbol{u},t)\Big) - \eta(t)\|\boldsymbol{s}(t)\| - b_3\|\boldsymbol{s}(t)\|^2 \\
&\le \left(b_4\|\boldsymbol{Mz}(t)\| + a_1 + a_2\|\boldsymbol{x}(t)\| + \chi\|\boldsymbol{u}(t)\| + \bar{d}\left\|(\boldsymbol{CB})^+ \boldsymbol{CE}\right\| - \eta(t)\right)\|\boldsymbol{s}(t)\| \\
&\le \Big(b_4\omega(t) + a_1 + a_2\left(\left\|\boldsymbol{M}^{-1}\right\|\omega(t) + \|\boldsymbol{B}\|\|\boldsymbol{s}(t)\|\right) + \chi\|\boldsymbol{u}(t)\| \\
&\qquad + \bar{d}\left\|(\boldsymbol{CB})^+ \boldsymbol{CE}\right\| - \eta(t)\Big)\|\boldsymbol{s}(t)\| \\
&\le -\delta\|\boldsymbol{s}(t)\|.
\end{aligned} \tag{3.63}$$

This aforementioned inequality proves that the reaching and sliding condition is satisfied. Therefore, the system will be driven to the sliding surface in a finite time and the sliding motion can be upheld. In past output feedback sliding mode researches, the controllers were designed to be stabilized the uncertain system locally and caused the high-gain control problem [15-17, 21]. For improving the existing problems and expanding the range of stability, we designed an adaptive variable, $\omega(t)$ in (3.55), to suppress a bound of unknown term in the controller. It can be adjusted following the variation of sliding surface and avoid the high-gain phenomenon in the transient time. Further it helps to complete the global stability of the closed-loop system. Consequently, avoiding the high-gain control force and assuring the robust global stability improve the effectiveness of proposed controller design.

Remark 3.3 If the vector $\boldsymbol{v}(t)$ is designed by Theorem 3.2, then the same procedure for the control law design should be obtained where the main difference is that the symmetric positive definite matrix $\boldsymbol{X}$ must be altered to $\boldsymbol{X}=\frac{1}{2}\left(\boldsymbol{C}^T\boldsymbol{C}+\frac{1}{\gamma^2}\boldsymbol{P}\boldsymbol{E}_1\boldsymbol{E}_1^T\boldsymbol{P}+\boldsymbol{C}^T\boldsymbol{F}^T\boldsymbol{R}\boldsymbol{F}\boldsymbol{C}\right)>0$.□

Remark 3.4 Since the dynamics of the sliding surface is always related to the unmeasured system states, Hu [26] used a variable structure observer to estimate the system states. Using the transformation matrix, Yan *et al*. [60] applied a dynamic observer to estimate the system states and then designed a sliding surface for the augmented space. For uncertain systems, adding the estimated states from the observer into the controller will undermine robust stability and thus deteriorate the worse performance. Without using any observer structure, our proposed formula is designed in a way that only original system matrices are involved. □

3.3 Numerical Examples

Example 3.1 Consider an unstable batch reactor from [25]. To demonstrate the effectiveness of the proposed method, the system uncertain matrix and the mismatched disturbance are introduced into the system and its state space form is given by

$$\dot{\boldsymbol{x}}(t)=\left(\begin{bmatrix}1.38 & -0.2077 & 6.715 & -5.676\\ -0.5814 & -4.29 & 0 & 0.675\\ 1.067 & 4.273 & -6.654 & 5.893\\ 0.048 & 4.273 & 1.343 & -2.104\end{bmatrix}+\Delta\boldsymbol{A}(t)\right)\boldsymbol{x}(t)$$
$$+\begin{bmatrix}0.2\\ -0.4\\ 0.5\\ 0.7\end{bmatrix}d(t)+\begin{bmatrix}0 & 0\\ 5.679 & 0\\ 1.136 & -3.146\\ 1.136 & 0\end{bmatrix}(\boldsymbol{u}(t)+\boldsymbol{f}(t))$$

$$\boldsymbol{y}(t)=\begin{bmatrix}1 & 0 & 1 & -1\\ 0 & 1 & 0 & 0\end{bmatrix}\boldsymbol{x}(t)$$

where $d(t)=4\cos\pi t+1$ and $\boldsymbol{f}(t)=\begin{bmatrix}0.5\sin{}^{\pi t}/_{2}\\ \cos 2t\end{bmatrix}$. The mismatched uncertainty is set as

$$\Delta \boldsymbol{A}(t)=\begin{bmatrix}0.15 & 0.1\\ 0.2 & -0.25\\ 0.2 & 0.3\\ 0.35 & -0.1\end{bmatrix}\begin{bmatrix}0 & \cos t & 0 & \cos 2t\\ \sin t & 0 & \sin 2t & 0\end{bmatrix}\begin{bmatrix}1 & 0 & 0 & 0\\ 0 & 1 & 0 & 0\\ 0 & 0 & 1 & 0\\ 0 & 0 & 0 & 1\end{bmatrix}.$$

It is easy to check that this system satisfies all assumptions proposed in section 3.1. Choosing $\bar{d}=5$, $a_1=1.12$, $a_2=0$, $\chi=0$, $\beta=0.2$, $\boldsymbol{Q}=0.2\boldsymbol{I}$, and $\boldsymbol{R}=\boldsymbol{I}$ and using the solution algorithm proposed by Gadewadikar *et al*. [53-54], we can obtain the solution to the algebraic Riccati equation (3.17) as

$$\boldsymbol{P}=\begin{bmatrix}0.2591 & -0.0112 & 0.2049 & -0.2013\\ -0.0112 & 0.1893 & 0.0255 & 0.0888\\ 0.2049 & 0.0255 & 0.2151 & -0.1342\\ -0.2013 & 0.0888 & -0.1342 & 0.2887\end{bmatrix} \text{ and } \boldsymbol{L}=\begin{bmatrix}-0.1078 & 0.0634\\ 0 & 0\\ -0.4042 & 0.0956\\ -0.5121 & 0.1590\end{bmatrix}^T.$$

The sliding surface is determined as

$$\boldsymbol{s}(t)=\begin{bmatrix}0 & 0.1761\\ -0.3179 & 0\end{bmatrix}\boldsymbol{y}(t)+\int_0^t\begin{bmatrix}-0.1676 & 1.2046\\ -0.5811 & -0.0802\end{bmatrix}\boldsymbol{y}(\tau)d\tau .$$

In order to avoid the chattering problem, the unit vector function $\boldsymbol{s}/\|\boldsymbol{s}\|$ in the control law should be replaced with the saturation function $\text{sat}(\boldsymbol{s},\varepsilon)$ where $\varepsilon>0$ is a small scalar. It can be visualized that as $\varepsilon\to 0$, the function $\text{sat}(\boldsymbol{s},\varepsilon)$ tends to the unit vector function. The variable ε can be used to trade off the requirement of maintaining ideal performance with that of ensuring a smooth control action. Therefore, we design the control input as

$$\dot{\omega}(t)=-1.52\omega(t)+0.1856\bar{d}+10.6401\|\boldsymbol{s}(t)\|$$
$$\boldsymbol{u}(t)=-\begin{bmatrix}-0.1676 & 1.2046\\ -0.5811 & -0.0802\end{bmatrix}\boldsymbol{y}(t)-\begin{bmatrix}3.6668 & 0.5271\\ -0.4554 & 1.5281\end{bmatrix}\boldsymbol{s}(t)-\eta(t)\text{sat}(\boldsymbol{s}(t),\varepsilon)$$

where $\eta(t)=11.7069\omega(t)+0.0704\bar{d}+1.8+\delta$, $\delta=0.1$, and $\varepsilon=0.01$. Figures 3.1-3.6 illustrate the simulation results using the initial conditions $\boldsymbol{x}(0)=[1 \;\; -2 \;\; 1 \;\; -1]^T$ and $\omega(0)=0.1$. Figure 3.1 shows trajectories of all system states and Fig. 3.2 shows the norm of states and its upper bound. In Fig. 3.2, the norm of states is indeed bounded by a certain value $\dfrac{2\|\boldsymbol{PE}_1\|\bar{d}}{\rho\lambda_{\min}\left(\boldsymbol{Q}+\boldsymbol{C}^T\boldsymbol{F}^T\boldsymbol{RFC}\right)}\sqrt{\dfrac{\lambda_{\max}(\boldsymbol{P})}{\lambda_{\min}(\boldsymbol{P})}}$ in (3.18), and Theorem 3.1 is guaranteed. The estimation result of (3.55) is depicted in Fig. 3.3; as it demonstrates the reality of (3.56) the adaptation law (3.55) can be applied to the controller design ensuring the global approaching condition. Figure 3.4 plots the evolution of the system outputs. Since this example is a square system (numbers of inputs and outputs are the same) and the mismatched disturbance varies slowly, the outputs in Fig. 3.4 converge to zero asymptotically based on Remark 3.1. Although the nominal system has the uncertain term and mismatched disturbance, our proposed control law involving the integral action can successfully restrain the effect of mismatched disturbance and obtain a good performance. Figure 3.5 depicts the control inputs without chattering phenomenon due to the replacement of saturation function. The response of $\|\boldsymbol{s}(t)\|$ is given in Fig. 3.6. The system trajectories enter the sliding mode globally in a finite time.

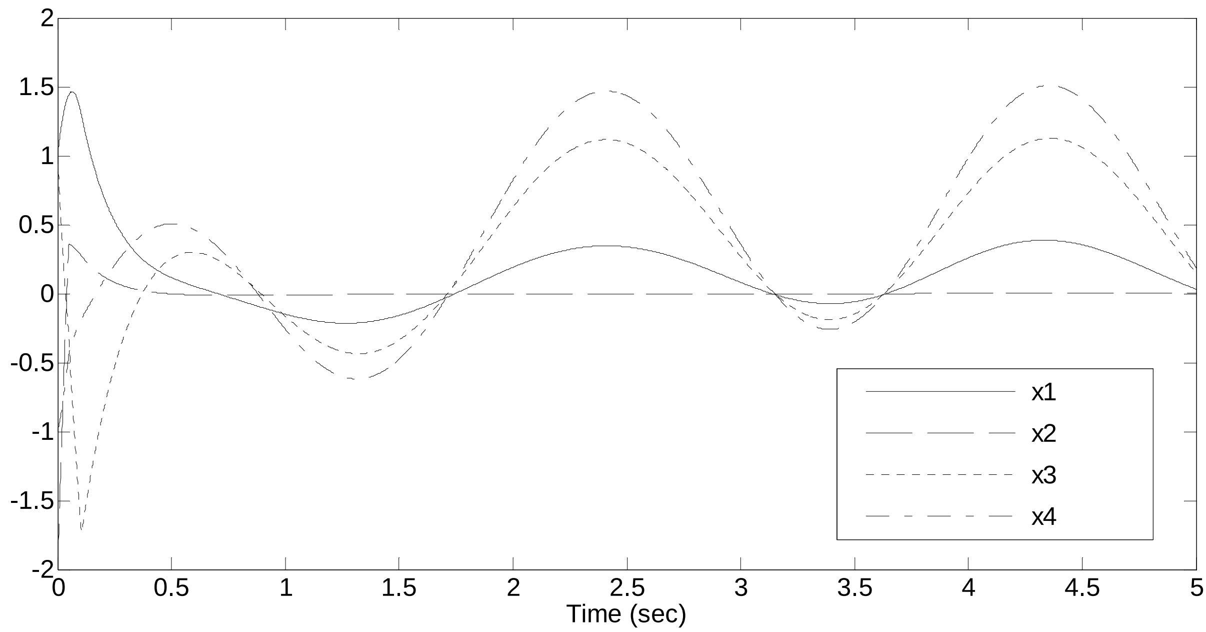

Fig. 3.1. System states in Example 3.1.

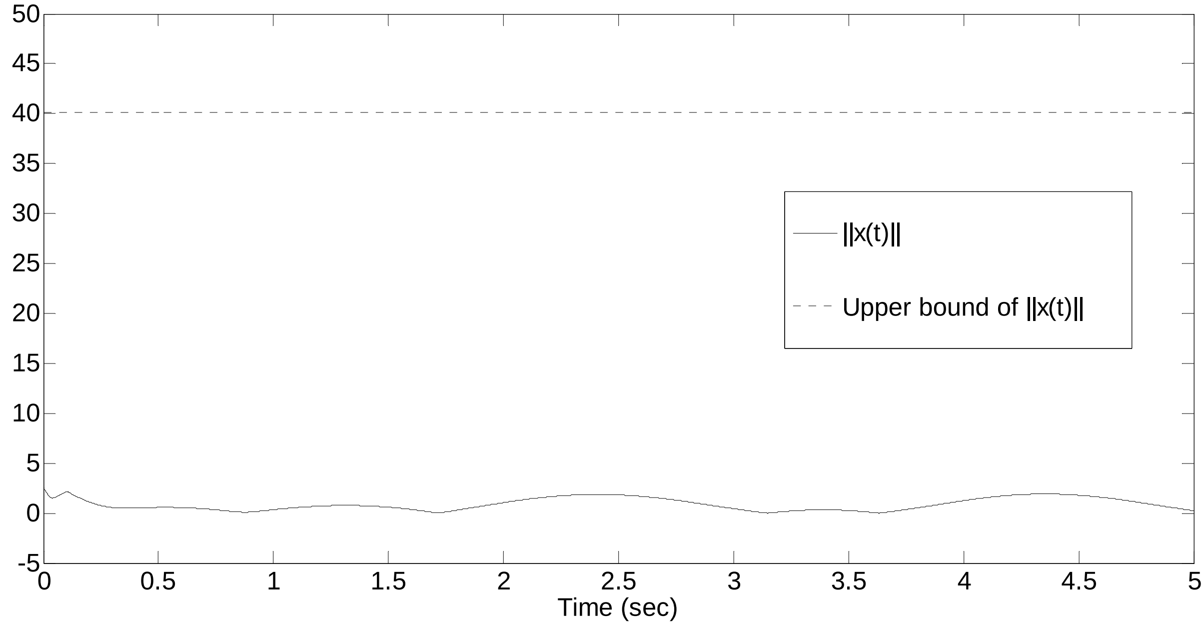

Fig. 3.2. Norm of states and its upper bound in Example 3.1.

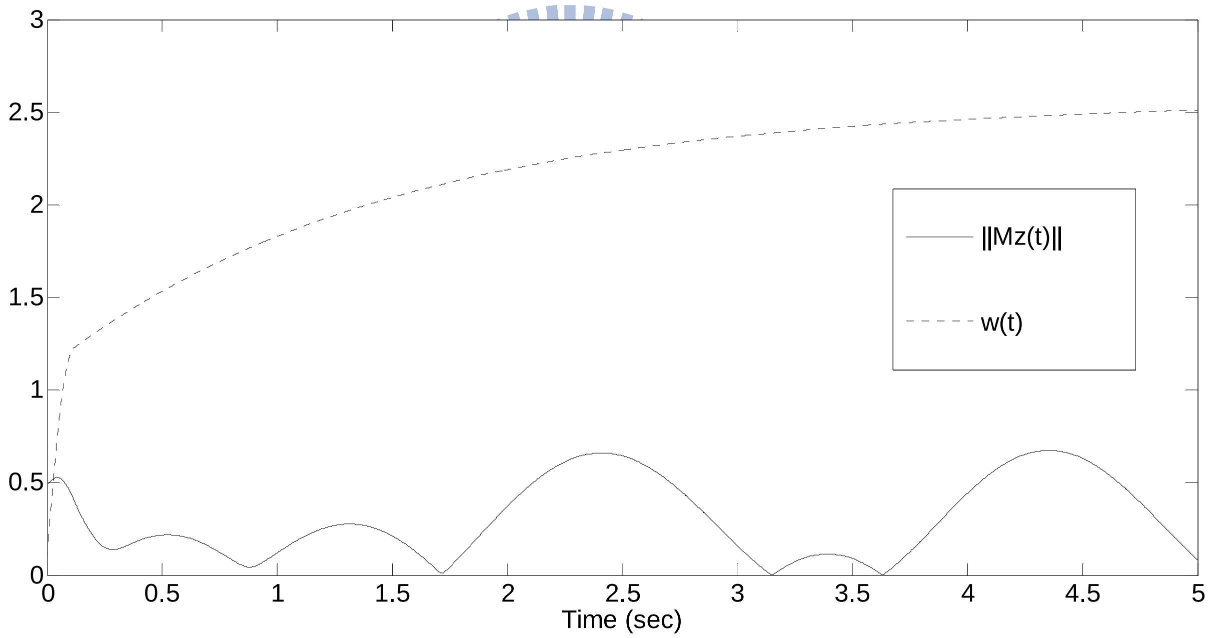

Fig. 3.3. Norm of $\boldsymbol{Mz}(t)$ and its upper bound $\omega(t)$ in Example 3.1.

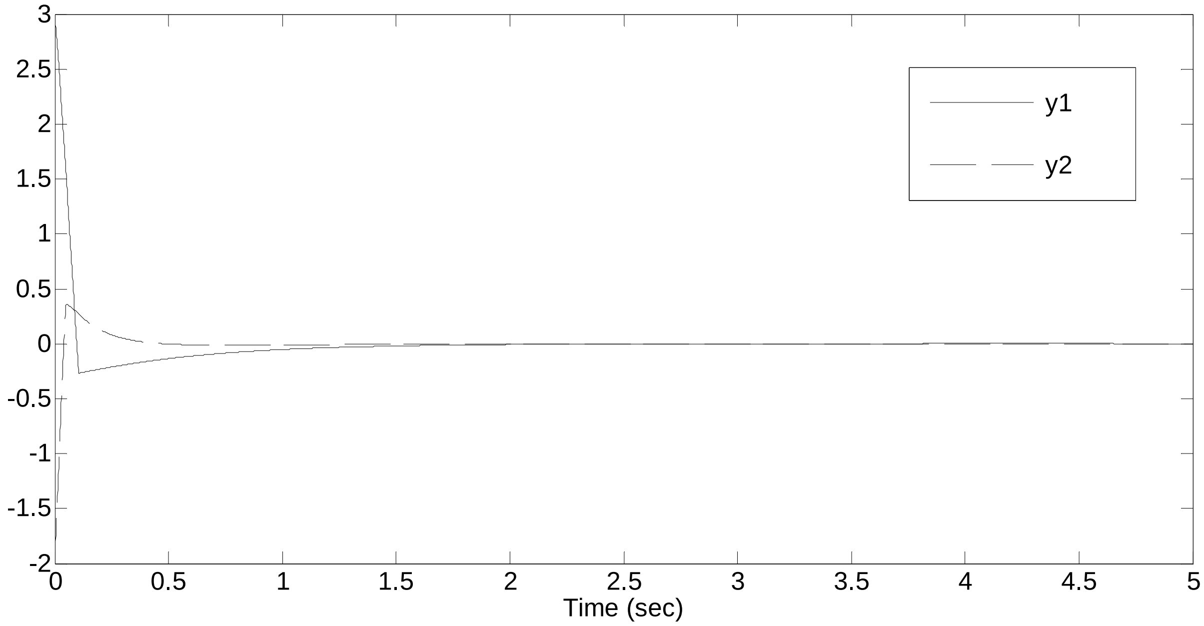

Fig. 3.4. System outputs in Example 3.1.

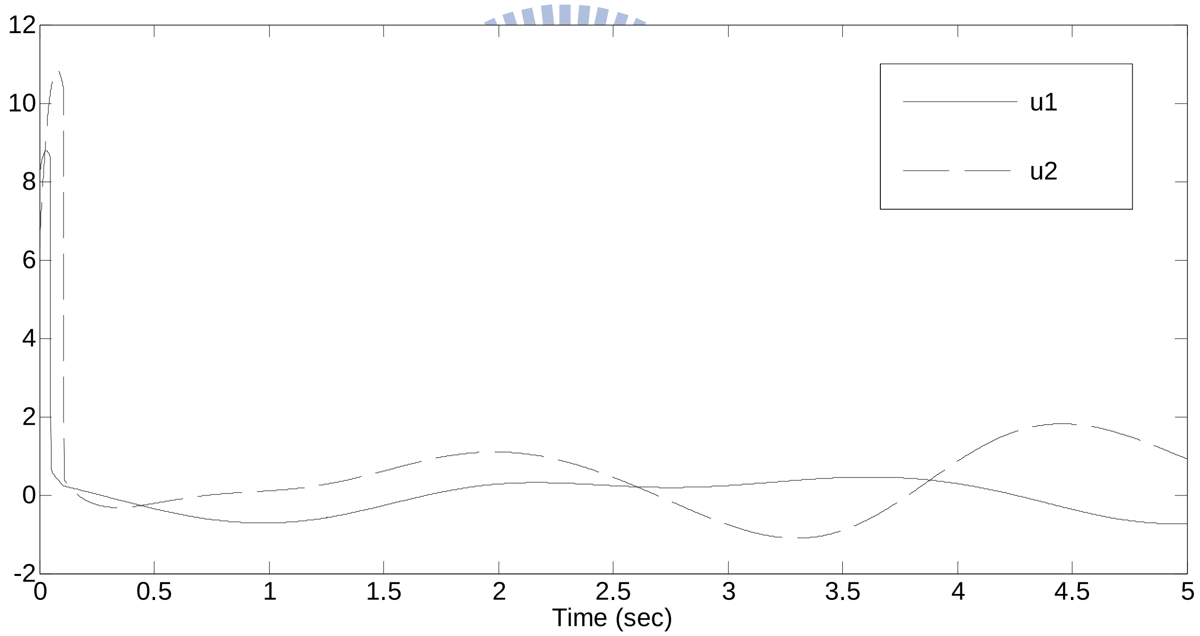

Fig. 3.5. System inputs in Example 3.1.

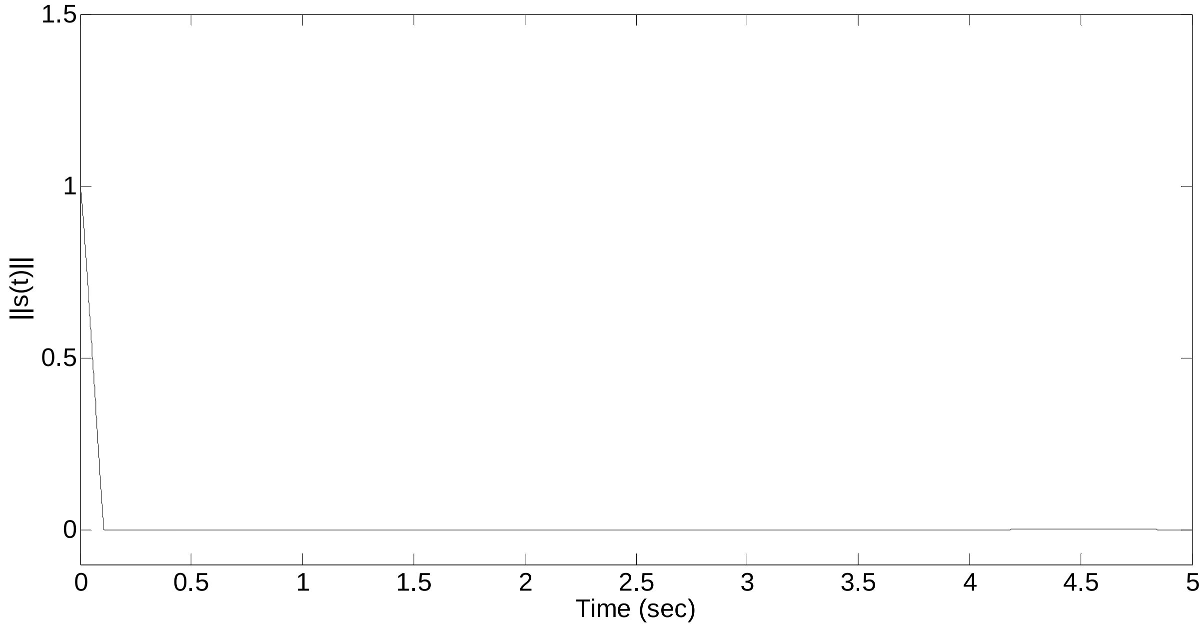

Fig. 3.6. Response of $\|\boldsymbol{s}(t)\|$ in Example 3.1.

Example 3.2 As for the case of $l > m$, a system presented by Xiang *et al*. [17] is considered as the following state space form

$$\dot{\boldsymbol{x}}(t) = \left(\begin{bmatrix} -2 & -2 & 0 \\ 1 & 2 & 1 \\ 0 & -3 & -4 \end{bmatrix} + \Delta\boldsymbol{A}(t)\right)\boldsymbol{x}(t) + \begin{bmatrix} 1 \\ 1 \\ 0 \end{bmatrix}\left(u(t) + \sin 2t\right) + \begin{bmatrix} 0.3 \\ -0.4 \\ 0.5 \end{bmatrix} e^{-0.001t}\cos\pi t$$

$$\boldsymbol{y}(t) = \begin{bmatrix} 0 & 1 & 0 \\ 1 & 1 & 0 \end{bmatrix}\boldsymbol{x}(t)$$

where the initial condition is altered as $\boldsymbol{x}(0) = \begin{bmatrix} 2 & -4 & 1 \end{bmatrix}^T$ to illustrate the high-gain phenomenon of Xiang's method [17]. Note that this example satisfies Assumptions 3.1-3.5 and the mismatched disturbance belongs to L_2 space. Choose $a_1 = \bar{d} = 1$, $a_2 = 0$, and $\chi = 0$. Moreover, the mismatched uncertainty is determined by

$$\Delta\boldsymbol{A}(t) = \begin{bmatrix} 1 & 0 \\ 0 & 0 \\ 0 & 1 \end{bmatrix}\begin{bmatrix} \sin t & 0 & \sin 2t \\ 0 & \sin 3t & 0 \end{bmatrix}\begin{bmatrix} 1 & 0 & 0 \\ 0 & 1 & 0 \\ 0 & 0 & 1 \end{bmatrix}.$$

Setting $\beta = 1$, $\gamma = 2$, $\boldsymbol{Q} = 2\boldsymbol{I}$, and $R = 1$ and then solving the algebraic Riccati equation (3.30), we can obtain its solution

$$\boldsymbol{P}=\begin{bmatrix}0.7841 & 0.5962 & 0.1875\\ 0.5962 & 1.8160 & 0.2411\\ 0.1875 & 0.2411 & 1.0717\end{bmatrix} \text{ and } \boldsymbol{L}=\begin{bmatrix}0 & 0 & -0.2410\end{bmatrix}.$$

In this case, we introduce the initial condition of the system outputs into the output-dependent integral sliding surface as

$$s(t)=\begin{bmatrix}0.5 & 0.5\end{bmatrix}\boldsymbol{y}(t)+\int_0^t\begin{bmatrix}1.3198 & 0.5962\end{bmatrix}\boldsymbol{y}(\tau)d\tau .$$

Then we design the control input including the dynamics of the auxiliary variable $\omega(t)$ as

$$\begin{aligned}\dot{\omega}(t)&=-1.7\omega(t)+0.5899\bar{d}+3.7204|s(t)|\\ u(t)&=-\begin{bmatrix}1.3198 & 0.5962\end{bmatrix}\boldsymbol{y}(t)-2.5s(t)-\left(2.7932\omega(t)+0.25\bar{d}+1+\delta\right)\text{sat}\left(s(t),\varepsilon\right)\end{aligned}$$

where $\delta=0.5$, $\varepsilon=0.05$, and $\omega(0)=3$. For comparison, the static sliding function $s(t)=\begin{bmatrix}4.4132 & 1.3153\end{bmatrix}\boldsymbol{y}(t)$ and the control law $u(t)=-2s(t)-1.5\text{sat}\left(s(t),\varepsilon\right)$ proposed by Xiang *et al*. [17] are simultaneously simulated. The time responses of the system states in the two cases are shown in Figs. 3.7 to 3.9, respectively. Figure 3.10 shows that the estimation function $\omega(t)$ is indeed larger than the norm of $\boldsymbol{Mz}(t)$ in our proposed method. Therefore, we can apply the linear combination of $\omega(t)$ to design the controller ensuring the global approaching condition. The time responses of the system outputs in the two cases are shown in Figs. 3.11 and 3.12, respectively. Figure 3.13 presents the controlled performance. The robust disturbance attenuation (3.31) is verified successfully in this figure. Figure 3.14 depicts the control inputs of two cases without chattering. By adjusting the parameter matrices $\boldsymbol{Q}$ and $\boldsymbol{R}$, from Fig. 3.14 the input gain in our method is smaller than the one in the method of Xiang *et al*. [17]. The response of sliding function in our method is given in Fig. 3.15. Although the dynamic output feedback control law raises the control complexity and incurs the additional software, our proposed control scheme can guarantee globally robust stability of the closed-loop system and effectively tackle the high gain control problem.

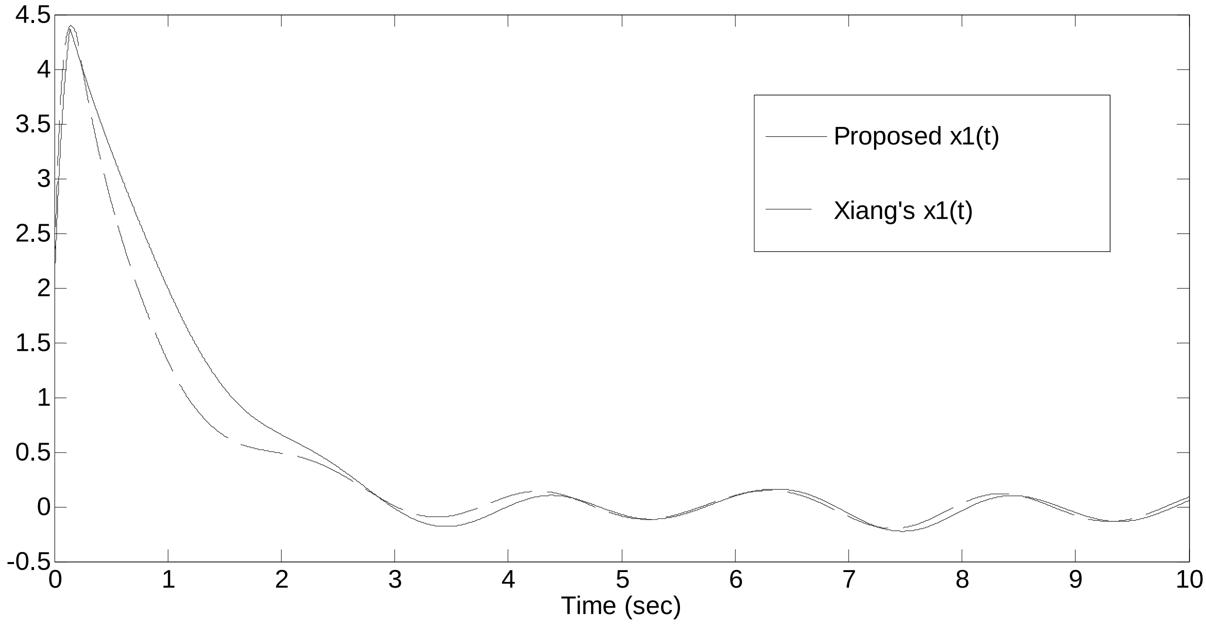

Fig. 3.7. System states $x_1(t)$ of two cases in Example 3.2.

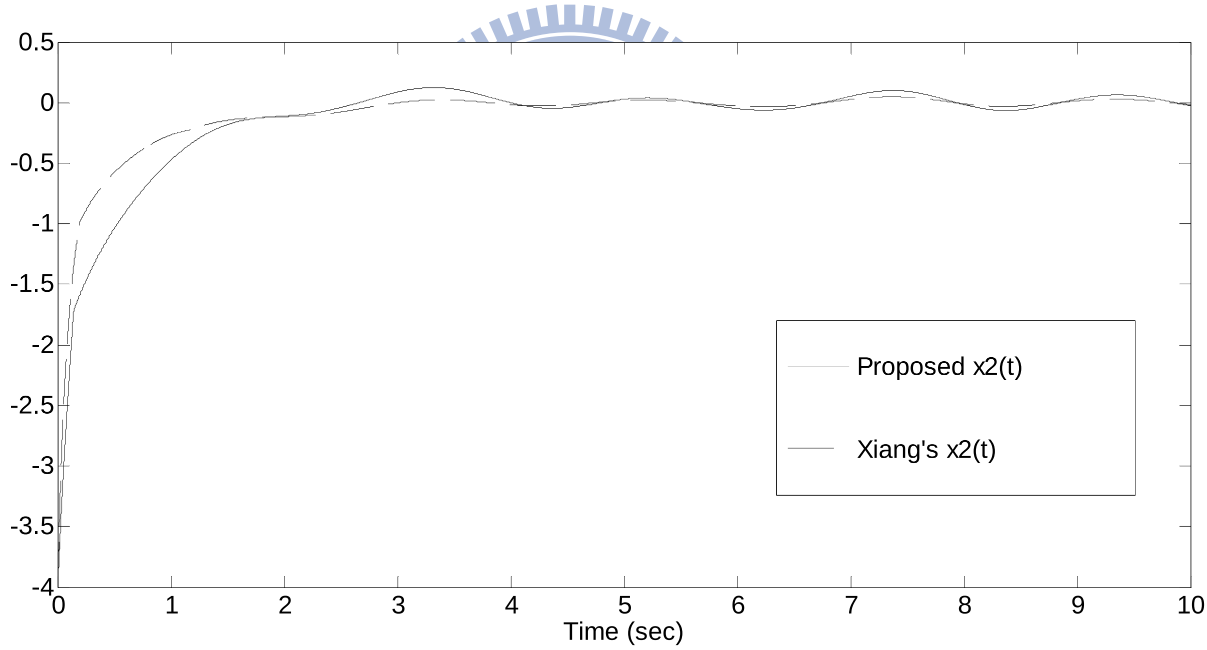

Fig. 3.8. System states $x_2(t)$ of two cases in Example 3.2.

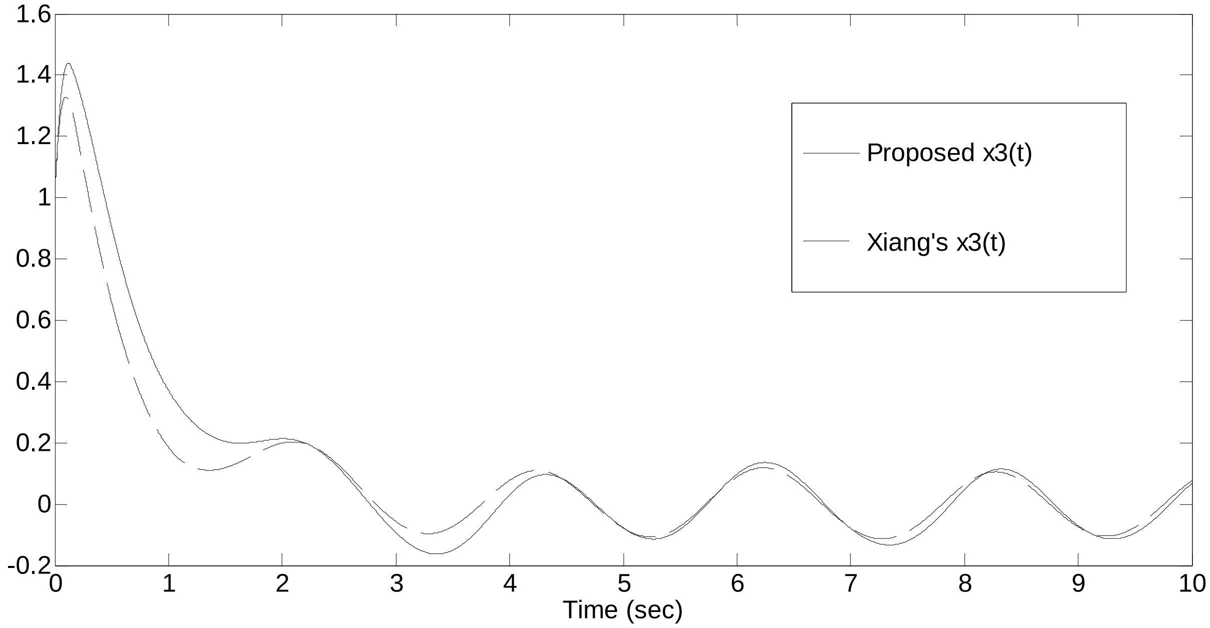

Fig. 3.9. System states $x_3(t)$ of two cases in Example 3.2.

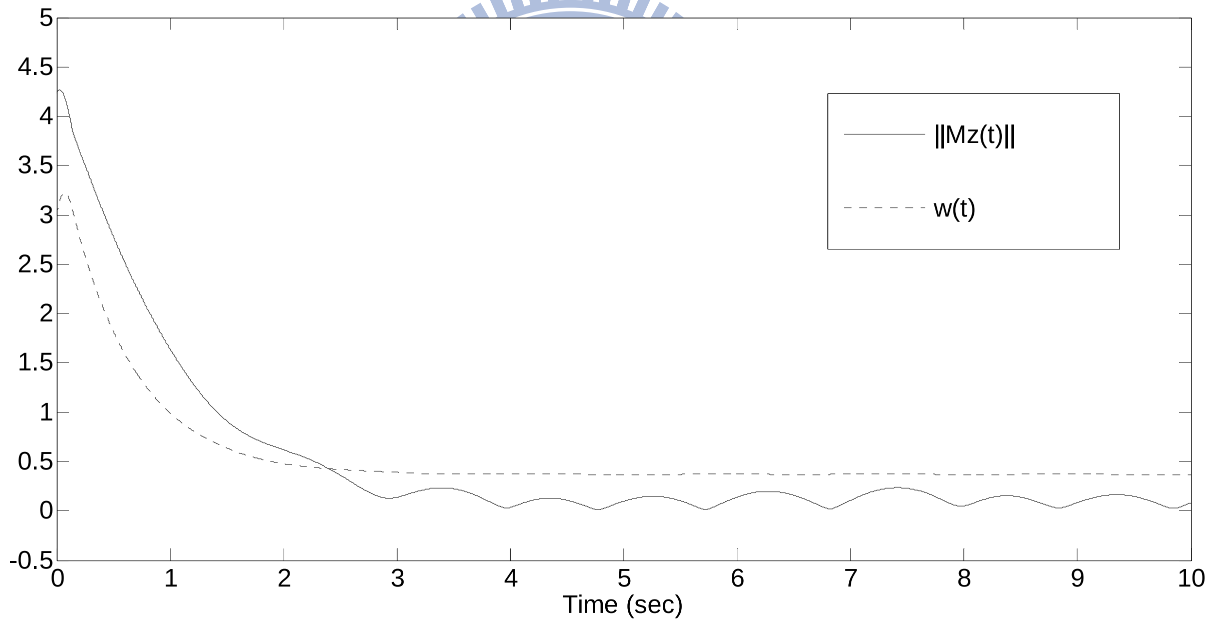

Fig. 3.10. Norm of $\boldsymbol{Mz}(t)$ and its upper bound $\omega(t)$ of our proposed method in Example 3.2.

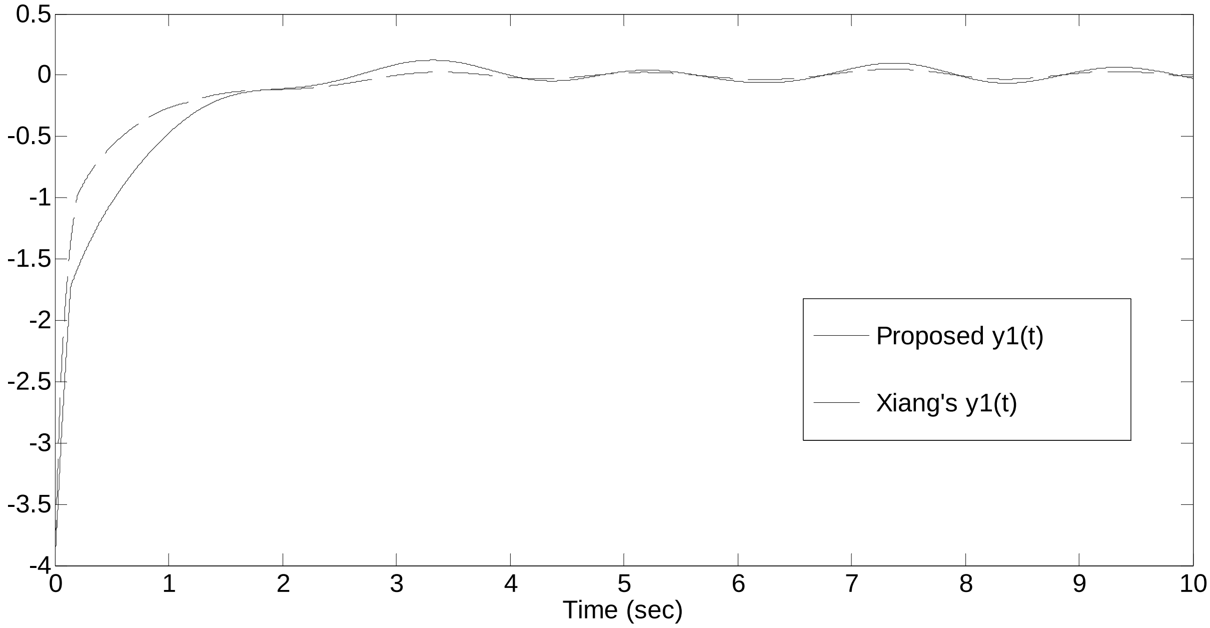

Fig. 3.11. System outputs $y_1(t)$ of two cases in Example 3.2.

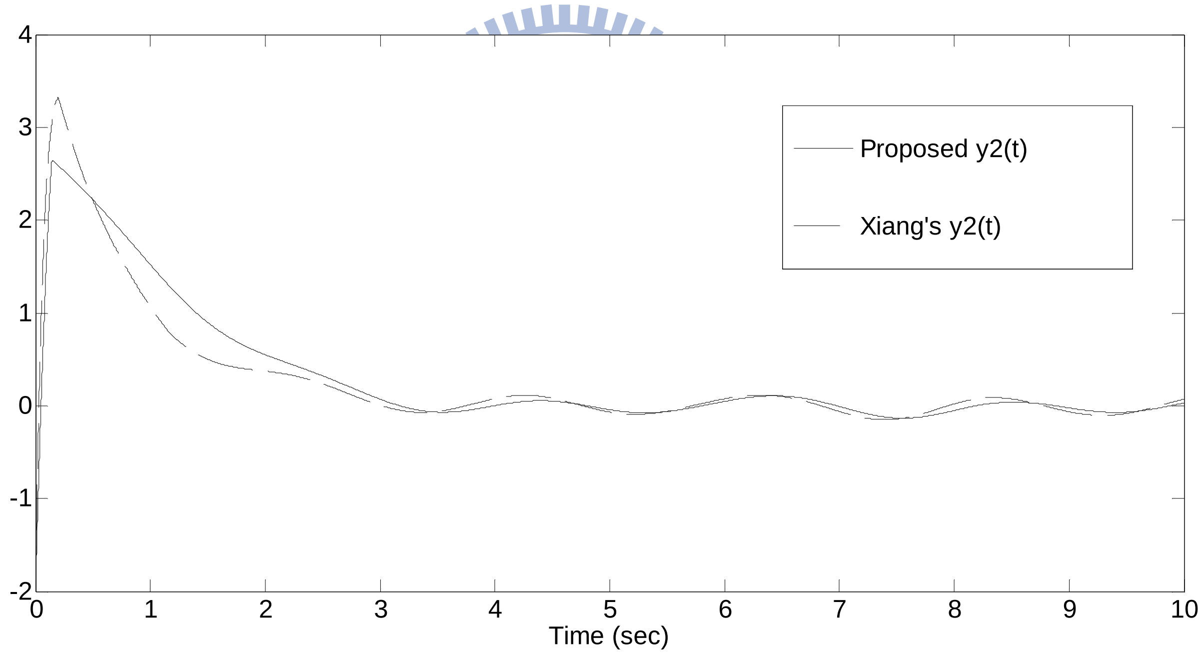

Fig. 3.12. System outputs $y_2(t)$ of two cases in Example 3.2.

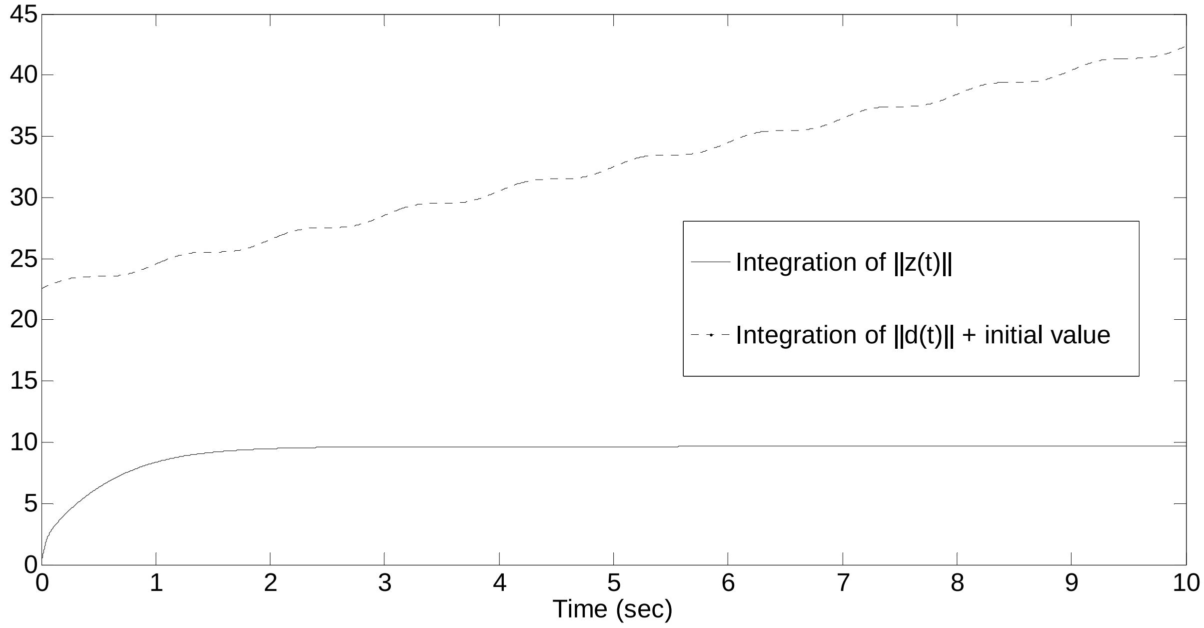

Fig. 3.13. Performance of robust disturbance attenuation of our proposed method in Example 3.2.

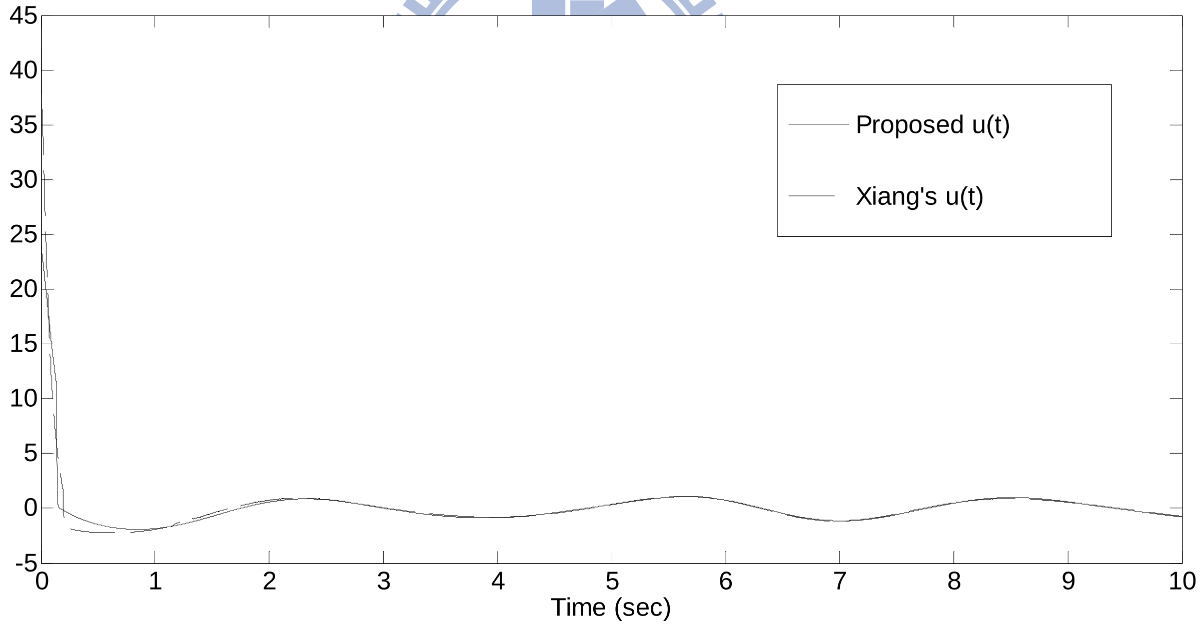

Fig. 3.14. System inputs $u(t)$ of two cases in Example 3.2.

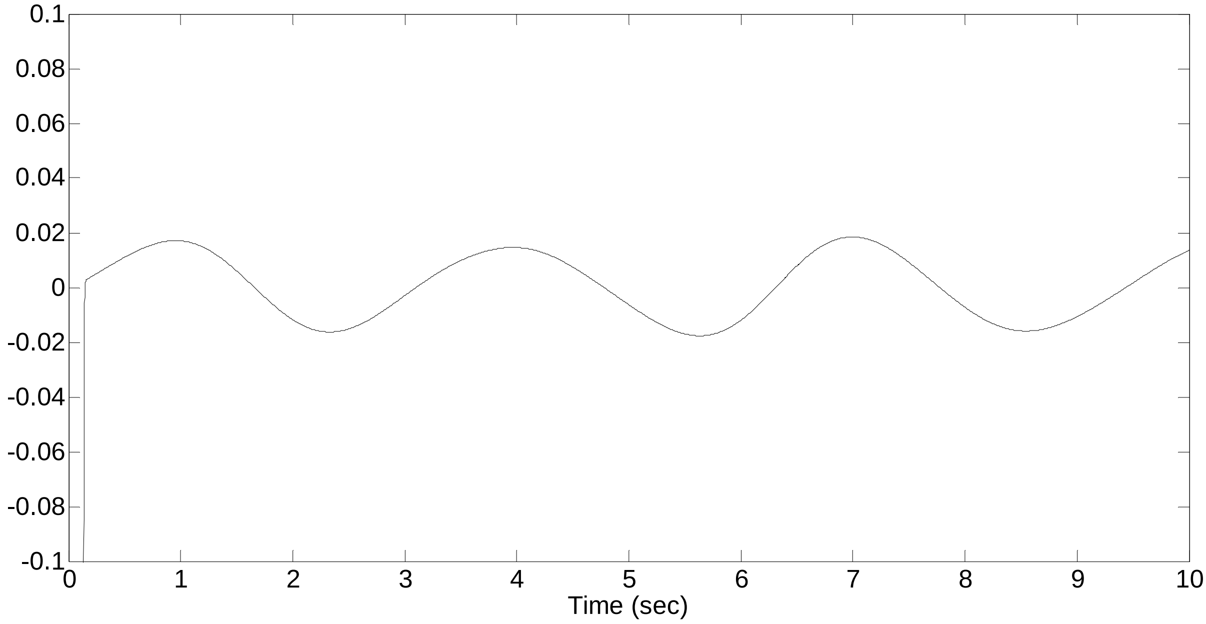

Fig. 3.15. Response of $s(t)$ in our proposed method in Example 3.2.

3.4 Summary

In this chapter, we have proposed a design method of the dynamic output feedback sliding mode control law for a linear MIMO uncertain system having the mismatched uncertainty and matched nonlinear perturbation. Once the system is in the sliding mode, the proposed output-dependent integral sliding surface design can obtain robust stability of the closed-loop system. Moreover, we discuss two types of mismatched disturbances and explore their effects on the sliding mode. The dynamic output feedback control law is then designed to guarantee that the system globally reaches and maintains in the sliding surface in a finite time. Our proposed method is simple in nature involving only its original system matrices and does not need any observer structure. The numerical examples also demonstrate that the proposed algorithm can be successfully implemented.

IV. OUTPUT FEEDBACK INTEGRAL SLIDING MODE CONTROL FOR TIME-DELAY SYSTEMS

For time-delay systems with mismatched disturbances and uncertainties, this chapter applies the output feedback integral sliding mode control algorithm developed in previous chapter to stabilize the system. The integral sliding surface is comprised of output signals and an auxiliary full-order compensator. The proposed output feedback sliding mode controller can satisfy the reaching and sliding condition and maintain the system on the sliding surface from the initial moment. Among the delay-independent condition, two types of analysis methods can assure the property of robust disturbance attenuation and determine the parameters of controller and compensator simultaneously. On the other hand, the stability analysis under delay-dependent condition is also considered. This condition is with less conservative and strengthens the complexity of controller design and difficulty analyzing the robust stability.

The first section of this chapter formulates the objective of problem. In section 4.2, a combination of an integral sliding surface and the related output feedback sliding mode controller is presented. Under the delay-independent condition, two types of robust stability conditions for the system in the sliding mode are given in section 4.3 with each corresponding compensator respectively. Section 4.4 proves the important sufficient condition of stability when the system is in the sliding mode and determines parameters of the controller and compensator as for the delay-dependent condition holds. A summary is given in the last section.

4.1 Problem Formulation

Consider a continuous-time time-delay system described by the state-space form as

$$\begin{aligned} \dot{\boldsymbol{x}}(t) &= \left(\boldsymbol{A}+\Delta\boldsymbol{A}(t)\right)\boldsymbol{x}(t)+\left(\boldsymbol{A}_d+\Delta\boldsymbol{A}_d(t)\right)\boldsymbol{x}(t-\tau)+\boldsymbol{B}\big(\boldsymbol{u}(t)+\boldsymbol{f}(\boldsymbol{x},\boldsymbol{u},t)\big)+\boldsymbol{E}\boldsymbol{d}(t) \\ \boldsymbol{y}(t) &= \boldsymbol{C}\boldsymbol{x}(t) \end{aligned} \tag{4.1}$$

$$x(t) = \phi(t),\ t \in [-\tau, 0] \tag{4.2}$$

where $x \in \mathbb{R}^n$ is the system state vector, $y \in \mathbb{R}^l$ is the system output vector, $u \in \mathbb{R}^m$ is the control input vector, $d \in \mathbb{R}^p$ is the mismatched disturbance vector. The function $f(x,u,t) \in \mathbb{R}^m$ represents the unknown matched uncertainty. The constant τ is an unknown delay time but bounded by a known constant $\bar{\tau}$, where $0 \le \tau \le \bar{\tau}$. The vector $\phi(t)$ is a continuous initial function. The real constant matrices $\boldsymbol{A}$, $\boldsymbol{A}_d$, $\boldsymbol{B}$, $\boldsymbol{E}$, and $\boldsymbol{C}$ are known and have appropriate dimensions with $l \ge m$. The structure uncertainties $\Delta\boldsymbol{A}(t)$ and $\Delta\boldsymbol{A}_d(t)$ satisfy $\Delta\boldsymbol{A} = \boldsymbol{D}\Phi(t)\boldsymbol{H}$ and $\Delta\boldsymbol{A}_d = \boldsymbol{D}_d\Phi_d(t)\boldsymbol{H}_d$, where $\boldsymbol{D}$, $\boldsymbol{D}_d$, $\boldsymbol{H}$, and $\boldsymbol{H}_d$ are non-unique known constant matrices with appropriate dimensions. Moreover, the matrices $\Phi(t)$ and $\Phi_d(t)$ are unknown, satisfying $\Phi^T(t)\Phi(t) \le \boldsymbol{I}$ and $\Phi_d^T(t)\Phi_d(t) \le \boldsymbol{I}$ for all *t*, respectively. As a result, the controlled plant (4.1) can be rewritten as

$$\begin{aligned} \dot{x}(t) &= (\boldsymbol{A} + \boldsymbol{D}\Phi(t)\boldsymbol{H})x(t) + (\boldsymbol{A}_d + \boldsymbol{D}_d\Phi_d(t)\boldsymbol{H}_d)x(t-\tau) + \boldsymbol{E}d(t) \\ &\quad + \boldsymbol{B}(u(t) + f(x,u,t)) \\ y(t) &= \boldsymbol{C}x(t). \end{aligned} \tag{4.3}$$

Suppose that the triple $(\boldsymbol{A},\boldsymbol{B},\boldsymbol{C})$ is completely controllable and observable. Edwards and Spurgeon [2] have shown that there exists a stable static output feedback sliding mode controller if

(C1) $\text{rank}(\boldsymbol{CB}) = \text{rank}(\boldsymbol{B}) = m$,

(C2) The triple $(\boldsymbol{A},\boldsymbol{B},\boldsymbol{C})$ is minimum phase.

In the case of time-delay systems satisfying conditions (C1) and (C2), Castanos and Fridman [10] mentioned the state-dependent integral sliding surface design for linear systems with mismatched disturbances to ensure the robust disturbance attenuation. Niu *et al.* [12] proposed the observer-based sliding mode controller involving a synthesis condition to stabilize uncertain time-delay systems. Since the output is the only available signal, next section will present the output-dependent integral sliding surface and the corresponding sliding mode controller. The control algorithm including the information of integral sliding surface without any synthesis condition is designed to satisfy the approaching condition and force the system trajectories to enter the sliding mode. Before introducing main results, the following three assumptions are fulfilled throughout this chapter.

Assumption 4.1 The matched term $\boldsymbol{f}(\boldsymbol{x},\boldsymbol{u},t)$ and mismatched disturbance $\boldsymbol{d}(t)$ are norm-bounded as

$$\left\|\boldsymbol{f}(\boldsymbol{x},\boldsymbol{u},t)\right\| \le \eta(t,\boldsymbol{y}) + \chi\left\|\boldsymbol{u}(t)\right\| \text{ and } \left\|\boldsymbol{d}(t)\right\| \le \bar{d} \tag{4.4}$$

where $0 \le \chi < 1$, $\eta(t,\boldsymbol{y})$, and $\bar{d}$ are all known positive constants.

Assumption 4.2 The triple $(\boldsymbol{A},\boldsymbol{B},\boldsymbol{C})$ is minimum phase.

Assumption 4.3: $\operatorname{rank}(\boldsymbol{CB}) = \operatorname{rank}(\boldsymbol{B}) = m$.

4.2 Integral Sliding Surface and Sliding Mode Controller

Since Assumption 4.3 holds, we design the output-dependant integral sliding surface as

$$\boldsymbol{s}(t) = (\boldsymbol{GCB})^{-1}\boldsymbol{G}\big(\boldsymbol{y}(t) - \boldsymbol{y}(0)\big) - \int_0^t \boldsymbol{v}(q)\,dq \tag{4.5}$$

where $\boldsymbol{G} \in \mathbb{R}^{m\times l}$ is chosen such that $\boldsymbol{GCB}$ is invertible. The integral term $\boldsymbol{v} \in \mathbb{R}^m$ will be designed later. Substituting system (4.3) into the derivative of $\boldsymbol{s}(t)$ with respect to time can obtain

$$\begin{aligned}\dot{\boldsymbol{s}}(t) &= \bar{\boldsymbol{G}}\Big(\big(\boldsymbol{A} + \boldsymbol{D}\Phi(t)\boldsymbol{H}\big)\boldsymbol{x}(t) + \big(\boldsymbol{A}_d + \boldsymbol{D}_d\Phi_d(t)\boldsymbol{H}_d\big)\boldsymbol{x}(t-\tau) \\ &\quad + \boldsymbol{B}\big(\boldsymbol{u}(t) + \boldsymbol{f}(\boldsymbol{x},\boldsymbol{u},t)\big) + \boldsymbol{Ed}(t)\Big) - \boldsymbol{v}(t) \\ &= \bar{\boldsymbol{G}}\Big(\big(\boldsymbol{A} + \boldsymbol{D}\Phi(t)\boldsymbol{H}\big)\boldsymbol{x}(t) + \big(\boldsymbol{A}_d + \boldsymbol{D}_d\Phi_d(t)\boldsymbol{H}_d\big)\boldsymbol{x}(t-\tau) + \boldsymbol{Ed}(t)\Big) \\ &\quad + \boldsymbol{u}(t) + \boldsymbol{f}(\boldsymbol{x},\boldsymbol{u},t) - \boldsymbol{v}(t)\end{aligned} \tag{4.6}$$

where $\bar{\boldsymbol{G}} = (\boldsymbol{GCB})^{-1}\boldsymbol{GC}$. Referring to [14], define two regions Ω_1 and Ω_2 as

$$\Omega_1 = \left\{ \boldsymbol{x}(t) \,|\, \left\| \bar{\boldsymbol{G}}\left(\boldsymbol{A} + \boldsymbol{D}\Phi(t)\boldsymbol{H} \right)\boldsymbol{x}(t) \right\| \le \sigma_1 \right\} \subset \Omega \tag{4.7}$$

$$\Omega_2 = \left\{ \boldsymbol{x}(t-\tau) \,|\, \left\| \bar{\boldsymbol{G}}\left(\boldsymbol{A}_d + \boldsymbol{D}_d\Phi_d(t)\boldsymbol{H}_d \right)\boldsymbol{x}(t-\tau) \right\| \le \sigma_2 \right\} \subset \Omega \tag{4.8}$$

where $\sigma_1 > 0$ and $\sigma_2 > 0$ are known and bounded constants. The region $\Omega \subset \mathbb{R}^n$ is a neighborhood of the origin. Consider system (4.3) in $\Omega_1 \times \Omega_2$ and design the control input as

$$\boldsymbol{u}(t) = \boldsymbol{v}(t) - \kappa(t)\frac{\boldsymbol{s}(t)}{\left\| \boldsymbol{s}(t) \right\|} \tag{4.9}$$

$$\kappa(t) = \frac{1}{1-\chi}\left(\sigma_1 + \sigma_2 + \eta(t,\boldsymbol{y}) + \chi\left\| \boldsymbol{v}(t) \right\| + \psi\bar{d} + \mu \right). \tag{4.10}$$

The remaining control parameters $\psi = \left\| \bar{\boldsymbol{G}}\boldsymbol{E} \right\|$ and μ are also positive constants. Through straightforward calculations, we know that

$$\begin{aligned} \kappa(t) &= \chi\kappa(t) + \chi\left\| \boldsymbol{v}(t) \right\| + \sigma_1 + \sigma_2 + \eta(t,\boldsymbol{y}) + \psi\bar{d} + \mu \\ &\ge \chi\left\| \boldsymbol{u}(t) \right\| + \sigma_1 + \sigma_2 + \eta(t,\boldsymbol{y}) + \psi\bar{d} + \mu. \end{aligned} \tag{4.11}$$

Substituting (4.9) into (4.6) can attain the following approaching and sliding condition

$$\begin{aligned} \boldsymbol{s}^T(t)\dot{\boldsymbol{s}}(t) &= \boldsymbol{s}^T(t)\Big(\bar{\boldsymbol{G}}\big(\left(\boldsymbol{A} + \boldsymbol{D}\Phi(t)\boldsymbol{H} \right)\boldsymbol{x}(t) + \left(\boldsymbol{A}_d + \boldsymbol{D}_d\Phi_d(t)\boldsymbol{H}_d \right)\boldsymbol{x}(t-\tau) + \boldsymbol{E}\boldsymbol{d}(t) \big) \\ &\quad + \boldsymbol{f}(\boldsymbol{x},\boldsymbol{u},t) \Big) - \kappa(t)\left\| \boldsymbol{s}(t) \right\| \\ &\le \left\| \boldsymbol{s}(t) \right\| \Big(\bar{\boldsymbol{G}}\big(\left(\boldsymbol{A} + \boldsymbol{D}\Phi(t)\boldsymbol{H} \right)\boldsymbol{x}(t) + \left(\boldsymbol{A}_d + \boldsymbol{D}_d\Phi_d(t)\boldsymbol{H}_d \right)\boldsymbol{x}(t-\tau) + \boldsymbol{E}\boldsymbol{d}(t) \big) \\ &\quad + \boldsymbol{f}(\boldsymbol{x},\boldsymbol{u},t) - \kappa(t) \Big) \\ &\le \left(\alpha(t) + \beta(t) + \eta(t,y) + \chi\left\| \boldsymbol{u}(t) \right\| + \psi\bar{d} - \kappa(t) \right)\left\| \boldsymbol{s}(t) \right\| \\ &\le \left(\alpha(t) + \beta(t) - \sigma_1 - \sigma_2 - \mu \right)\left\| \boldsymbol{s}(t) \right\| \\ &\le -\mu\left\| \boldsymbol{s}(t) \right\| \end{aligned} \tag{4.12}$$

where $\alpha(t,\boldsymbol{x}) = \left\| \bar{\boldsymbol{G}}\left(\boldsymbol{A} + \boldsymbol{D}\Phi(t)\boldsymbol{H} \right)\boldsymbol{x}(t) \right\|$ and $\beta(t,\boldsymbol{x}) = \left\| \bar{\boldsymbol{G}}\left(\boldsymbol{A}_d + \boldsymbol{D}_d\Phi_d(t)\boldsymbol{H}_d \right)\boldsymbol{x}(t-\tau) \right\|$.

Since $\boldsymbol{s}(0) = \boldsymbol{0}$, the control input (4.9) can guarantee the following identities

$$\boldsymbol{s}(t) = \dot{\boldsymbol{s}}(t) = \boldsymbol{0} \quad \forall \quad t \ge 0. \tag{4.13}$$

Therefore, the design of integral sliding surface (4.5) can shorten the transient time that the system entered the sliding mode efficiently. Subsequently, this chapter focuses on the stability analysis when the system is in the sliding mode.

4.3 Robust Stability in the Sliding Mode for Delay-Independent Condition

From (4.6), once the system is in the sliding mode, $\boldsymbol{s}(t)=\dot{\boldsymbol{s}}(t)=\boldsymbol{0}$, the corresponding equivalent control [2] is given by

$$\begin{aligned}\boldsymbol{u}_{eq}(t)+\boldsymbol{f}\left(\boldsymbol{x},\boldsymbol{u}_{eq},t\right)=-\bar{\boldsymbol{G}}\big(&(\boldsymbol{A}+\boldsymbol{D}\Phi(t)\boldsymbol{H})\boldsymbol{x}(t)+(\boldsymbol{A}_d+\boldsymbol{D}_d\Phi_d(t)\boldsymbol{H}_d)\boldsymbol{x}(t-\tau)\\&+\boldsymbol{Ed}(t)\big)+\boldsymbol{v}(t).\end{aligned}\tag{4.14}$$

Deriving the closed-loop system dynamics in the sliding mode from substituting (4.14) into system (4.3) can obtain

$$\begin{aligned}\dot{\boldsymbol{x}}(t)&=(\boldsymbol{A}+\boldsymbol{D}\Phi(t)\boldsymbol{H})\boldsymbol{x}(t)+(\boldsymbol{A}_d+\boldsymbol{D}_d\Phi_d(t)\boldsymbol{H}_d)\boldsymbol{x}(t-\tau)+\boldsymbol{Bf}\left(\boldsymbol{x},\boldsymbol{u}_{eq},t\right)\\&\quad-\boldsymbol{B}\bar{\boldsymbol{G}}\big((\boldsymbol{A}+\boldsymbol{D}\Phi(t)\boldsymbol{H})\boldsymbol{x}(t)+(\boldsymbol{A}_d+\boldsymbol{D}_d\Phi_d(t)\boldsymbol{H}_d)\boldsymbol{x}(t-\tau)+\boldsymbol{Ed}(t)\big)\\&\quad-\boldsymbol{Bf}\left(\boldsymbol{x},\boldsymbol{u}_{eq},t\right)+\boldsymbol{Bv}(t)+\boldsymbol{Ed}(t)\\&=(\boldsymbol{I}_n-\boldsymbol{B}\bar{\boldsymbol{G}})\big((\boldsymbol{A}+\boldsymbol{D}\Phi(t)\boldsymbol{H})\boldsymbol{x}(t)+(\boldsymbol{A}_d+\boldsymbol{D}_d\Phi_d(t)\boldsymbol{H}_d)\boldsymbol{x}(t-\tau)+\boldsymbol{Ed}(t)\big)\\&\quad+\boldsymbol{Bv}(t)\\&=\boldsymbol{N}(\boldsymbol{A}+\boldsymbol{D}\Phi(t)\boldsymbol{H})\boldsymbol{x}(t)+\boldsymbol{N}(\boldsymbol{A}_d+\boldsymbol{D}_d\Phi_d(t)\boldsymbol{H}_d)\boldsymbol{x}(t-\tau)\\&\quad+\boldsymbol{NEd}(t)+\boldsymbol{Bv}(t)\end{aligned}\tag{4.15}$$

where $\boldsymbol{N}=\boldsymbol{I}_n-\boldsymbol{B}\bar{\boldsymbol{G}}$. Since $\boldsymbol{NA}=\boldsymbol{A}-\boldsymbol{B}\bar{\boldsymbol{G}}\boldsymbol{A}$, we have the following relationship

$$\begin{bmatrix}s\boldsymbol{I}_n-\boldsymbol{NA} & \boldsymbol{B}\end{bmatrix}=\begin{bmatrix}s\boldsymbol{I}_n-\boldsymbol{A}+\boldsymbol{B}\bar{\boldsymbol{G}}\boldsymbol{A} & \boldsymbol{B}\end{bmatrix}=\begin{bmatrix}s\boldsymbol{I}_n-\boldsymbol{A} & \boldsymbol{B}\end{bmatrix}\begin{bmatrix}\boldsymbol{I}_n & \boldsymbol{0}\\ \bar{\boldsymbol{G}}\boldsymbol{A} & \boldsymbol{I}_n\end{bmatrix}.\tag{4.16}$$

Since the pair $(\boldsymbol{A},\boldsymbol{B})$ is controllable, $\operatorname{rank}\left(\begin{bmatrix}s\boldsymbol{I}_n-\boldsymbol{A} & \boldsymbol{B}\end{bmatrix}\right)=n$ for $s\in\mathbb{C}$, the controllability of $(\boldsymbol{NA},\boldsymbol{B})$ can be guaranteed by

$$\operatorname{rank}\left(\begin{bmatrix}s\boldsymbol{I}_n-\boldsymbol{NA} & \boldsymbol{B}\end{bmatrix}\right)=\operatorname{rank}\left(\begin{bmatrix}s\boldsymbol{I}_n-\boldsymbol{A} & \boldsymbol{B}\end{bmatrix}\begin{bmatrix}\boldsymbol{I}_n & \boldsymbol{0}\\ \bar{\boldsymbol{G}}\boldsymbol{A} & \boldsymbol{I}_n\end{bmatrix}\right)=n,\quad s\in\mathbb{C}.\tag{4.17}$$

It implies that the pair $(\boldsymbol{NA},\boldsymbol{B})$ is also controllable. Referring to [55-57], the robust disturbance attenuation for system (4.15) is to design an auxiliary input function $\boldsymbol{v}(t)$ such that the system is stable and satisfies the following inequality:

$$\int_0^t \left(\boldsymbol{y}^T\boldsymbol{y}+\boldsymbol{v}^T\boldsymbol{R}\boldsymbol{v}\right)dq \le \gamma^2\int_0^t \left(\boldsymbol{d}^T\boldsymbol{d}\right)dq \quad \forall \quad t \ge 0 \tag{4.18}$$

where $0 \le \gamma < \infty$ and $\boldsymbol{R} > 0$ is a weighting matrix. By using two similar full-order compensators, we will derive two sufficient conditions to complete the design of $\boldsymbol{v}(t)$ fulfilling the robust disturbance attenuation in the following subsections. Before designing compensators, define several matrices as

$$\boldsymbol{U} = -\boldsymbol{B}(\boldsymbol{CB})^+ + \boldsymbol{Y}\left(\boldsymbol{I}_l - \boldsymbol{CB}(\boldsymbol{CB})^+\right) \tag{4.19}$$

$$\boldsymbol{M} = \boldsymbol{I}_n + \boldsymbol{UC} \tag{4.20}$$

$$\Gamma = \boldsymbol{L}(\boldsymbol{I}_l + \boldsymbol{CU}) - \boldsymbol{MAU} \tag{4.21}$$

where $(\boldsymbol{CB})^+ = \left((\boldsymbol{CB})^T \boldsymbol{CB}\right)^{-1}(\boldsymbol{CB})^T$, $\boldsymbol{Y} \in \mathbb{R}^{n\times l}$ is an arbitrary matrix, and $\boldsymbol{L}$ is a gain matrix designed later. Notice that the product of $\boldsymbol{MB}$ is given by

$$\boldsymbol{MB} = \boldsymbol{B} + \boldsymbol{UCB} = \boldsymbol{B} - \boldsymbol{B}(\boldsymbol{CB})^+\boldsymbol{CB} + \boldsymbol{Y}\left(\boldsymbol{CB} - \boldsymbol{CB}(\boldsymbol{CB})^+\boldsymbol{CB}\right) = \boldsymbol{0} \tag{4.22}$$

and $\operatorname{rank}(\boldsymbol{M}) = n - m$ from Assumption 4.3.

Remark 4.1 In [10], the integration term in the sliding manifold can be thought as a trajectory of the system in the absence of perturbations and in the presence of the nominal control, that is, as a nominal trajectory for a given initial condition. In this chapter, adding the integration term $\boldsymbol{v}(t)$ into the sliding surface (4.5) can compensate the degree of freedom to attenuate the effects of disturbances and uncertainties in the closed-loop system. Involving the integrator is also helpful to analyze the stability and robustness of the closed-loop system. □

4.3.1 Robust disturbance attenuation by LMI

The input function $\boldsymbol{v}(t)$ in this section is generated from the following full-order dynamic compensator

$$\dot{\xi}(t) = (\boldsymbol{MA} - \boldsymbol{LC})\xi(t) + \Gamma \boldsymbol{y}(t) \tag{4.23}$$

$$\boldsymbol{v}(t) = -\boldsymbol{K}(\xi(t) - \boldsymbol{Uy}(t)) \tag{4.24}$$

where the auxiliary state vector $\xi \in \mathbb{R}^n$ is available. The feedback gain matrix $\boldsymbol{K} \in \mathbb{R}^{m\times n}$ is designed later. According to (4.23) and $\boldsymbol{MB} = \boldsymbol{0}$, the dynamics of error vector $\boldsymbol{e} = \boldsymbol{Mx} - \xi$ can be given by

$$\begin{aligned}\dot{\boldsymbol{e}}(t) &= -\Gamma \boldsymbol{y}(t) + \boldsymbol{M}\left((\boldsymbol{A} + \boldsymbol{D}\Phi(t)\boldsymbol{H})\boldsymbol{x}(t) + \boldsymbol{Ed}(t) + (\boldsymbol{A}_d + \boldsymbol{D}_d\Phi_d(t)\boldsymbol{H}_d)\boldsymbol{x}(t-\tau)\right) \\ &\quad -(\boldsymbol{MA} - \boldsymbol{LC})\xi(t) \\ &= \boldsymbol{MD}\Phi(t)\boldsymbol{Hx}(t) + (\boldsymbol{MA} - \boldsymbol{LC})\boldsymbol{e}(t) + \boldsymbol{M}(\boldsymbol{A}_d + \boldsymbol{D}_d\Phi_d(t)\boldsymbol{H}_d)\boldsymbol{x}(t-\tau) \\ &\quad + \boldsymbol{MEd}(t).\end{aligned} \tag{4.25}$$

On the other hand, $\boldsymbol{v}(t)$ can be rewritten as

$$\boldsymbol{v}(t) = -\boldsymbol{Kx}(t) + \boldsymbol{Ke}(t). \tag{4.26}$$

Substituting (4.26) into (4.15) can obtain the system dynamics in the sliding mode as

$$\begin{aligned}\dot{\boldsymbol{x}}(t) &= \left(\boldsymbol{N}(\boldsymbol{A} + \boldsymbol{D}\Phi(t)\boldsymbol{H}) - \boldsymbol{BK}\right)\boldsymbol{x}(t) + \boldsymbol{N}(\boldsymbol{A}_d + \boldsymbol{D}_d\Phi_d(t)\boldsymbol{H}_d)\boldsymbol{x}(t-\tau) + \boldsymbol{BKe}(t) \\ &\quad + \boldsymbol{NEd}(t).\end{aligned} \tag{4.27}$$

Combining (4.25) with (4.27), the overall closed-loop system is shown as below

$$\begin{aligned}\begin{bmatrix}\dot{\boldsymbol{x}}(t) \\ \dot{\boldsymbol{e}}(t)\end{bmatrix} &= \begin{bmatrix}\boldsymbol{NA} - \boldsymbol{BK} + \boldsymbol{ND}\Phi(t)\boldsymbol{H} & \boldsymbol{BK} \\ \boldsymbol{MD}\Phi(t)\boldsymbol{H} & \boldsymbol{MA} - \boldsymbol{LC}\end{bmatrix}\begin{bmatrix}\boldsymbol{x}(t) \\ \boldsymbol{e}(t)\end{bmatrix} + \begin{bmatrix}\boldsymbol{NE} \\ \boldsymbol{ME}\end{bmatrix}\boldsymbol{d}(t) \\ &\quad + \begin{bmatrix}\boldsymbol{NA}_d + \boldsymbol{ND}_d\Phi_d(t)\boldsymbol{H}_d & \boldsymbol{0} \\ \boldsymbol{MA}_d + \boldsymbol{MD}_d\Phi_d(t)\boldsymbol{H}_d & \boldsymbol{0}\end{bmatrix}\begin{bmatrix}\boldsymbol{x}(t-\tau) \\ \boldsymbol{e}(t-\tau)\end{bmatrix} \\ &= \boldsymbol{A}_w\begin{bmatrix}\boldsymbol{x}(t) \\ \boldsymbol{e}(t)\end{bmatrix} + \boldsymbol{B}_w\begin{bmatrix}\boldsymbol{x}(t-\tau) \\ \boldsymbol{e}(t-\tau)\end{bmatrix} + \boldsymbol{G}_w\boldsymbol{d}(t)\end{aligned} \tag{4.28}$$

where $\boldsymbol{A}_w = \begin{bmatrix}\boldsymbol{NA} - \boldsymbol{BK} + \boldsymbol{ND}\Phi(t)\boldsymbol{H} & \boldsymbol{BK} \\ \boldsymbol{MD}\Phi(t)\boldsymbol{H} & \boldsymbol{MA} - \boldsymbol{LC}\end{bmatrix}$, $\boldsymbol{B}_w = \begin{bmatrix}\boldsymbol{NA}_d + \boldsymbol{ND}_d\Phi_d(t)\boldsymbol{H}_d & \boldsymbol{0} \\ \boldsymbol{MA}_d + \boldsymbol{MD}_d\Phi_d(t)\boldsymbol{H}_d & \boldsymbol{0}\end{bmatrix}$, and $\boldsymbol{G}_w = \begin{bmatrix}\boldsymbol{NE} \\ \boldsymbol{ME}\end{bmatrix}$. Moreover, to represent the term $\boldsymbol{y}^T\boldsymbol{y} + \boldsymbol{v}^T\boldsymbol{Rv}$ in (4.18), we define the controlled output $\boldsymbol{z} \in \mathbb{R}^{l+m}$ as

$$\begin{aligned} \boldsymbol{z}(t) &= \begin{bmatrix} \boldsymbol{C} \\ \boldsymbol{0} \end{bmatrix} \boldsymbol{x}(t) + \begin{bmatrix} \boldsymbol{0} \\ \boldsymbol{C}_v \end{bmatrix} \boldsymbol{v}(t) = \begin{bmatrix} \boldsymbol{C} \\ -\boldsymbol{C}_v \boldsymbol{K} \end{bmatrix} \boldsymbol{x}(t) + \begin{bmatrix} \boldsymbol{0} \\ \boldsymbol{C}_v \boldsymbol{K} \end{bmatrix} \boldsymbol{e}(t) \\ &= \bar{\boldsymbol{C}} \boldsymbol{x}(t) + \bar{\boldsymbol{C}}_v \boldsymbol{e}(t) = \boldsymbol{C}_w \begin{bmatrix} \boldsymbol{x}(t) \\ \boldsymbol{e}(t) \end{bmatrix} \end{aligned} \tag{4.29}$$

where $\boldsymbol{C}_v^T \boldsymbol{C}_v = \boldsymbol{R}$ and $\boldsymbol{C}_w = \begin{bmatrix} \bar{\boldsymbol{C}} & \bar{\boldsymbol{C}}_v \end{bmatrix} = \begin{bmatrix} \boldsymbol{C} & \boldsymbol{0} \\ -\boldsymbol{C}_v \boldsymbol{K} & \boldsymbol{C}_v \boldsymbol{K} \end{bmatrix}$. The auxiliary matrix $\boldsymbol{C}_v$ is implicit and does not appear in the controller, but $\boldsymbol{C}_v^T \boldsymbol{C}_v$ is defined as the matrix $\boldsymbol{R}$ which is the weighting gain of input $\boldsymbol{v}(t)$. The next step is to design the matrices $\boldsymbol{K}$ and $\boldsymbol{L}$, and analyze the robust stability of the closed-loop system (4.28) by the following lemma and Theorem 4.1.

Lemma 4.1 Given real matrices $\boldsymbol{D}$, $\Phi(t)$, and $\boldsymbol{H}$ of appropriate dimensions, suppose $\Phi^T(t)\Phi(t) \le \boldsymbol{I}$, for any positive scalar ρ, then

(i) [42] $\boldsymbol{D}\Phi(t)\boldsymbol{H} + \boldsymbol{H}^T \Phi^T(t) \boldsymbol{D}^T \le \rho \boldsymbol{D}\boldsymbol{D}^T + \rho^{-1} \boldsymbol{H}^T \boldsymbol{H}$;

(ii) [11] $\begin{bmatrix} \boldsymbol{0} & \boldsymbol{H}^T \Phi^T(t) \boldsymbol{D}^T \\ \boldsymbol{D}\Phi(t)\boldsymbol{H} & \boldsymbol{0} \end{bmatrix} \le \begin{bmatrix} \rho \boldsymbol{H}^T \boldsymbol{H} & \boldsymbol{0} \\ \boldsymbol{0} & \rho^{-1} \boldsymbol{D}\boldsymbol{D}^T \end{bmatrix}$. □

Theorem 4.1 Consider system (4.15) with the full-order compensator (4.23). Given λ, $\rho_i > 0$, $i = 1, 2, \cdots, 10$, and a positive definite matrix $\boldsymbol{R}$, if there exists $\boldsymbol{P} = \begin{bmatrix} \boldsymbol{P}_{11} & \boldsymbol{P}_{12} \\ \boldsymbol{P}_{12}^T & \boldsymbol{P}_{22} \end{bmatrix} > 0$, $\boldsymbol{Q} = \begin{bmatrix} \boldsymbol{Q}_{11} & \boldsymbol{Q}_{12} \\ \boldsymbol{Q}_{12}^{\mathrm{T}} & \boldsymbol{Q}_{22} \end{bmatrix} > 0$, $\boldsymbol{P}_{22} \ge \boldsymbol{I}$, $\boldsymbol{Q}_{11} > \left(\rho_6^{-1} + \rho_7^{-1} + \rho_8^{-1} + \rho_9^{-1}\right) \boldsymbol{H}_d^T \boldsymbol{H}_d$, and a scalar $\gamma > 0$, satisfying the following LMI

$$\begin{bmatrix} \Pi_{11} & \Pi_{12} & \Pi_{13} & \boldsymbol{0} & \Pi_{15} & \Pi_{16} & \Pi_{17} & \boldsymbol{0} \\ * & \Pi_{22} & \Pi_{23} & \boldsymbol{0} & \Pi_{25} & \Pi_{26} & \boldsymbol{0} & \Pi_{28} \\ * & * & \Pi_{33} & \Pi_{34} & \boldsymbol{0} & \boldsymbol{0} & \boldsymbol{0} & \boldsymbol{0} \\ * & * & * & \Pi_{44} & \boldsymbol{0} & \boldsymbol{0} & \boldsymbol{0} & \boldsymbol{0} \\ * & * & * & * & \Pi_{55} & \boldsymbol{0} & \boldsymbol{0} & \boldsymbol{0} \\ * & * & * & * & * & \Pi_{66} & \boldsymbol{0} & \boldsymbol{0} \\ * & * & * & * & * & * & \Pi_{77} & \boldsymbol{0} \\ * & * & * & * & * & * & * & \Pi_{88} \end{bmatrix} < 0 \tag{4.30}$$

where $*$ symbols the transpose of the corresponding symmetric element and

$$\Pi_{11} = (\boldsymbol{NA})^T \boldsymbol{P}_{11} + \boldsymbol{P}_{11}\boldsymbol{NA} + \left(\rho_1^{-1} + \rho_2 + \rho_3 + \rho_4^{-1}\right)\boldsymbol{H}^T\boldsymbol{H} + \boldsymbol{C}^T\boldsymbol{C} + \boldsymbol{Q}_{11}$$

$$\Pi_{12} = (\boldsymbol{NA})^T \boldsymbol{P}_{12} + \boldsymbol{P}_{12}\boldsymbol{MA} + \boldsymbol{Q}_{12}$$

$$\Pi_{13} = \boldsymbol{P}_{11}\boldsymbol{NA}_d + \boldsymbol{P}_{12}\boldsymbol{MA}_d$$

$$\Pi_{22} = \boldsymbol{P}_{22}\boldsymbol{MA} + (\boldsymbol{MA})^T \boldsymbol{P}_{22} + \boldsymbol{Q}_{22} - \lambda\boldsymbol{C}^T\boldsymbol{C} + \frac{\lambda}{2}\rho_{10}^{-1}\boldsymbol{C}^T\boldsymbol{C}\boldsymbol{C}^T\boldsymbol{C}$$

$$\Pi_{23} = \boldsymbol{P}_{12}^T\boldsymbol{NA}_d + \boldsymbol{P}_{22}\boldsymbol{MA}_d$$

$$\Pi_{33} = -\left(\boldsymbol{Q}_{11} - \left(\rho_6^{-1} + \rho_7^{-1} + \rho_8^{-1} + \rho_9^{-1}\right)\boldsymbol{H}_d^T\boldsymbol{H}_d\right)$$

$$\Pi_{34} = -\boldsymbol{Q}_{12}$$

$$\Pi_{44} = -\boldsymbol{Q}_{22}$$

$$\Pi_{15} = \boldsymbol{P}_{11}\boldsymbol{NE} + \boldsymbol{P}_{12}\boldsymbol{ME}$$

$$\Pi_{16} = -\boldsymbol{P}_{11}\boldsymbol{B}$$

$$\Pi_{17} = \begin{bmatrix} \boldsymbol{P}_{12}\boldsymbol{MD} & \boldsymbol{P}_{11}\boldsymbol{ND} & \boldsymbol{P}_{11}\boldsymbol{ND}_d & \boldsymbol{P}_{12}\boldsymbol{MD}_d & \boldsymbol{P}_{12} \end{bmatrix}$$

$$\Pi_{25} = \boldsymbol{P}_{12}^T\boldsymbol{NE} + \boldsymbol{P}_{22}\boldsymbol{ME}$$

$$\Pi_{26} = \boldsymbol{P}_{12}^T\boldsymbol{B}$$

$$\Pi_{28} = \begin{bmatrix} \boldsymbol{P}_{12}^T\boldsymbol{ND} & \boldsymbol{P}_{22}\boldsymbol{MD} & \boldsymbol{P}_{11}\boldsymbol{BR}^{-1}\boldsymbol{B}^T & \boldsymbol{P}_{12}^T & \boldsymbol{P}_{11}\boldsymbol{B} & \boldsymbol{P}_{12}^T\boldsymbol{ND}_d & \boldsymbol{P}_{22}\boldsymbol{MD}_d \end{bmatrix}$$

$$\Pi_{55} = -\gamma^2\boldsymbol{I}$$

$$\Pi_{66} = -\boldsymbol{R}$$

$$\Pi_{77} = -\mathrm{diag}\left(\rho_1^{-1}\boldsymbol{I}, \rho_4^{-1}\boldsymbol{I}, \rho_6^{-1}\boldsymbol{I}, \rho_7^{-1}\boldsymbol{I}, 2\lambda^{-1}\rho_{10}^{-1}\boldsymbol{I}\right)$$

$$\Pi_{88} = -\mathrm{diag}\left(\rho_2\boldsymbol{I}, \rho_3\boldsymbol{I}, \rho_5^{-1}\boldsymbol{I}, \rho_5\boldsymbol{I}, \boldsymbol{R}, \rho_8^{-1}\boldsymbol{I}, \rho_9^{-1}\boldsymbol{I}\right)$$

then robust disturbance attenuation (4.18) can be guaranteed. Furthermore, matrices $\boldsymbol{K}$ and $\boldsymbol{L}$ are given by

$$K = R^{-1}B^T P_{11} \text{ and } L = \frac{\lambda}{2} P_{22}^{-1} C^T. \tag{4.31}$$

Proof: The detail is in Appendix 1. □

Remark 4.2 For determining the parameter matrices P_{11} and P_{22}, we recommend to follow the flowchart in Fig. 4.1. Adjusting λ, R, and $\rho_i > 0$, $i = 1, 2, \cdots, 10$ can solve different P and Q. If solutions satisfy requirements of Theorem 4.1 and the performance index γ is acceptable, substituting P_{11} and P_{22} into K and L can complete the controller design. □

The following numerical example demonstrates the proposed controller design in this section.

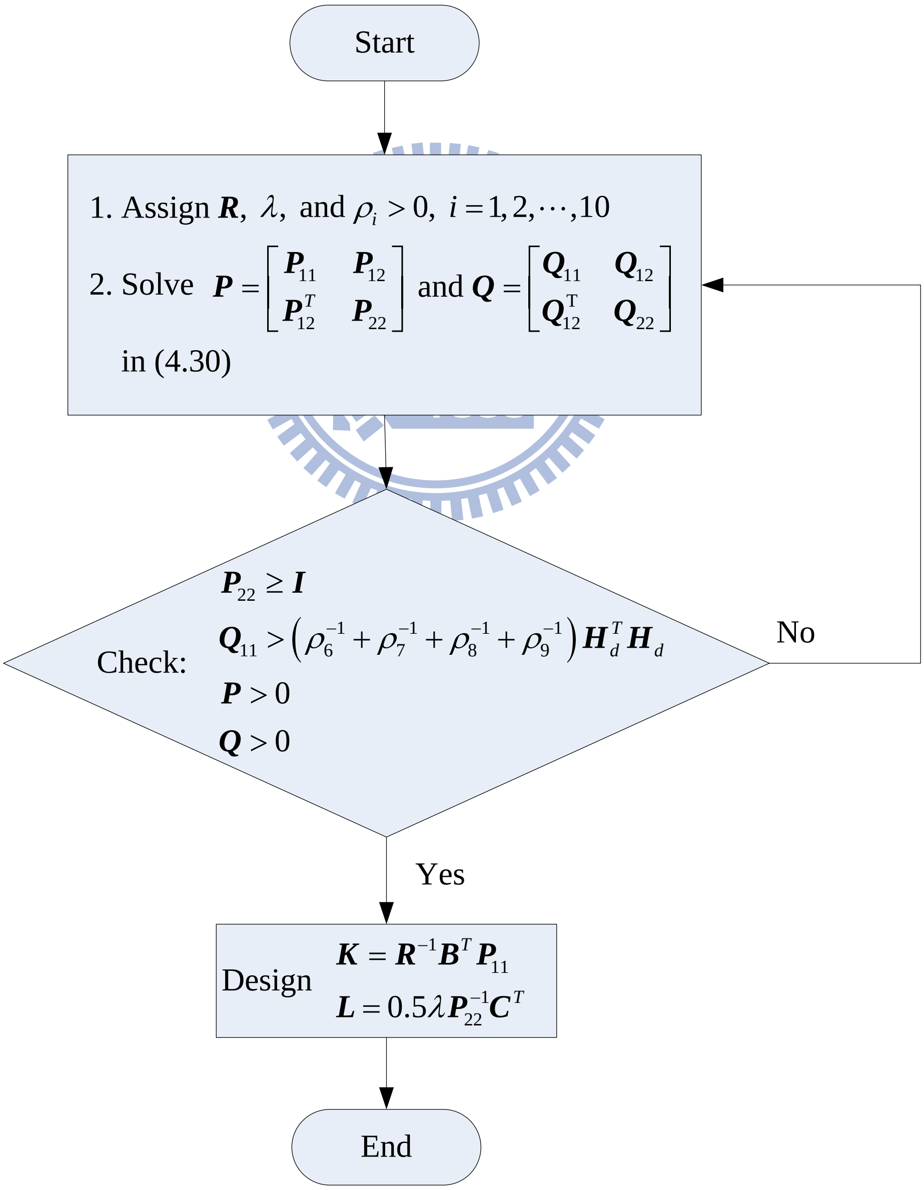

Fig. 4.1. Flowchart for solving parameters K and L by an LMI of controller and compensator.

Example 4.1 Consider the real example of chemical reactor system [32] within the corresponding form of system (4.3) with delay time $\tau = 1$ as

$$\boldsymbol{A} = \begin{bmatrix} -4.93 & -1.01 & 0 & 0 \\ -3.20 & -5.30 & -12.8 & 0 \\ -6.40 & 0.347 & -32.5 & -1.04 \\ 0 & 0.833 & 11.0 & -3.96 \end{bmatrix}, \quad \boldsymbol{B} = \begin{bmatrix} 1 & 0 \\ 0 & 1 \\ 0 & 0 \\ 0 & 0 \end{bmatrix}, \quad \boldsymbol{C} = \begin{bmatrix} 1 & 0 \\ 0 & 1 \\ -0.2 & 0 \\ 0 & 0.1 \end{bmatrix}^T, \quad \boldsymbol{E} = \begin{bmatrix} 1 \\ 0 \\ 1 \\ 0 \end{bmatrix},$$

and $\boldsymbol{A}_d = \operatorname{diag}(1.92, 1.92, 1.87, 0.724)$. The known parts of uncertainties in the system are given by

$$\boldsymbol{D} = \begin{bmatrix} -0.47 & 1.01 & 0 & 0 \\ -0.22 & -0.17 & 1.21 & 0 \\ 0.63 & 0.347 & 0.91 & -1.04 \\ 0 & 0 & 0.14 & -0.96 \end{bmatrix}, \quad \boldsymbol{H} = \begin{bmatrix} -0.55 & -0.02 & 0 & 0 \\ 0.78 & -0.35 & 0 & 0 \\ 0 & -0.72 & -0.49 & 0 \\ 0 & 0.33 & -0.54 & -0.39 \end{bmatrix},$$

$\boldsymbol{D}_d = \operatorname{diag}(0.47, 0.26, -0.85, 1.53)$, and $\boldsymbol{H}_d = \operatorname{diag}(-1.11, -0.21, 1.26, 0.47)$. The external disturbances and unknown parts of uncertainties for system (4.3) are set as $\Phi(t) = r_1(t)\boldsymbol{I}_4$, $\Phi_d(t) = r_2(t)\boldsymbol{I}_4$, $d(t) = e^{-0.001t}\sin 2t$, and

$$\boldsymbol{f}(\boldsymbol{x}, \boldsymbol{u}, t) = \begin{bmatrix} 0.12u_1 \sin t + 0.08u_2 \cos 1.3t + 0.2\sin x_1 \\ 0.07u_1 \cos 3t + 0.03u_2 \sin 5t + 0.3\cos x_2 \end{bmatrix}$$

where $\boldsymbol{u} = \begin{bmatrix} u_1^T & u_2^T \end{bmatrix}$, $r_1(t)$ and $r_2(t)$ are different random functions with values between -1 and 1. Notice that the triple $(\boldsymbol{A}, \boldsymbol{B}, \boldsymbol{C})$ has invariant zeros -4.4463 and -33.377, and $\operatorname{rank}(\boldsymbol{CB}) = 2$, satisfying Assumptions 4.2 and 4.3. For solving the LMI (4.30) of this example, select the parameters as $\lambda = 1000$, $\boldsymbol{R} = 0.002\boldsymbol{I}_2$, $\rho_1 = \rho_4 = 2$, $\rho_2 = \rho_3 = 0.1$, $\rho_6 = \rho_7 = \rho_8 = \rho_9 = 3$, and $\rho_5 = \rho_{10} = 1$. Then the solutions to (4.30) are given by

$$\boldsymbol{P}_{11} = \begin{bmatrix} 0.0139 & -0.0013 & 0.0668 & -0.0046 \\ -0.0013 & 0.0012 & -0.0127 & 0.0005 \\ 0.0668 & -0.0127 & 0.6492 & -0.1044 \\ -0.0046 & 0.0005 & -0.1044 & 0.1945 \end{bmatrix}$$

$$P_{12} = \begin{bmatrix} 0.0030 & -0.0001 & -0.0028 & -0.0072 \\ -0.0019 & -0.0005 & 0.0003 & 0.0094 \\ -0.0012 & -0.0011 & -0.0841 & -0.0242 \\ 0.0128 & 0.0044 & 0.0080 & -0.0734 \end{bmatrix}$$

$$P_{22} = \begin{bmatrix} 38.6114 & -0.0364 & -4.8448 & 0.4358 \\ -0.0364 & 38.9961 & -0.0304 & 3.4802 \\ -4.8448 & -0.0304 & 17.5268 & 0.4054 \\ 0.4358 & 3.4802 & 0.4054 & 6.0693 \end{bmatrix}$$

$$Q_{12} = \begin{bmatrix} 0.1010 & 0.0014 & 0.3402 & -0.1593 \\ -0.0501 & -0.0023 & -0.1692 & 0.0971 \\ -0.0227 & 0.0090 & -0.1059 & -0.1096 \\ -0.0121 & 0.0338 & -0.0276 & -0.4093 \end{bmatrix}$$

$$Q_{22} = \begin{bmatrix} 38.7504 & -0.0190 & 0.0192 & 0.1867 \\ -0.0190 & 38.5812 & 0.1953 & 2.6922 \\ 0.0192 & 0.1953 & 38.7613 & -2.5084 \\ 0.1867 & 2.6922 & -2.5084 & 14.4394 \end{bmatrix}$$

and $Q_{11} = 3I_4$. The performance index γ computed via the LMI is 0.9233. Notice that the solutions of (4.30) above fulfill the conditions of Theorem 4.1. Hence, we construct the full-order compensator as

$$\dot{\xi}(t) = -\begin{bmatrix} 13.9652 & -0.0678 & 3.9630 & 0.2082 \\ 0.0827 & 12.8218 & 1.0835 & 0.8778 \\ 4.2199 & -0.3461 & 32.9360 & 1.0401 \\ -0.8127 & 0.1007 & -10.8375 & 4.0534 \end{bmatrix}\xi(t) + \begin{bmatrix} -1.28 & 0.0694 \\ 0 & -0.0833 \\ -6.4 & 0.3470 \\ 0 & 0.8330 \end{bmatrix} y(t)$$

and design the sliding surface as

$$s(t) = y(t) - y(0) - \int_0^t \begin{bmatrix} -6.9387 & 0.6675 \\ 0.6675 & -0.6178 \end{bmatrix} y(q)\,dq - \int_0^t \begin{bmatrix} -6.9387 & 0.6675 & -33.4124 & 2.2778 \\ 0.6675 & -0.6178 & 6.3451 & -0.2742 \end{bmatrix} \xi(q)\,dq.$$

Moreover, in order to avoid the chattering problem, the term $\dfrac{s(t)}{\|s(t)\|}$ in the controller (4.9) is replaced with the saturation function [11], and the new version of the controller is given by

$$\boldsymbol{u}(t)=\begin{bmatrix}-6.9387 & 0.6675 & -33.4124 & 2.2778\\ 0.6675 & -0.6178 & 6.3451 & -0.2742\end{bmatrix}\xi(t)+\begin{bmatrix}-6.9387 & 0.6675\\ 0.6675 & -0.6178\end{bmatrix}\boldsymbol{y}(t)$$
$$-\frac{1}{1-\chi}\left(\sigma_1+\sigma_2+\eta(t,\boldsymbol{y})+\chi\|\boldsymbol{v}(t)\|+\psi\bar{d}+\mu\right)\mathrm{sat}\left(\boldsymbol{s}(t),\varepsilon\right)$$

where $\sigma_1=\sigma_2=5$, $\eta(t,\boldsymbol{y})=2$, $\chi=\psi=0.8$, $\bar{d}=1$, $\mu=2.5$, and $\varepsilon=0.002$. Figures 4.2-4.8 chart the simulation results using the initial state $\boldsymbol{x}(0)=\begin{bmatrix}2 & 3 & 4 & 1\end{bmatrix}^T$ and $\xi(0)=\begin{bmatrix}0 & 0 & 0 & 0\end{bmatrix}^T$. Figure 4.2 presents the system states which are bounded around zero. The time responses of the system outputs are shown in Fig. 4.3. The property (4.18) of robust disturbance attenuation is shown in Fig. 4.4. The integration of quadratic form of controlled output $\boldsymbol{z}(t)$ is indeed smaller than one of mismatched disturbance $d(t)$ and hence the proposed controller has assured the robust disturbance attenuation. Figures 4.5 and 4.6 show $\boldsymbol{s}(t)$ and $\|\boldsymbol{s}(t)\|$, respectively. In Fig. 4.6, the trajectory representing the controlled system can maintain in the sliding layer in the whole time. It fits in with the design of integral sliding surface (4.5). Figure 4.7 shows that the trajectories of $\boldsymbol{e}(t)$ are bounded around zero as system states. The responses of the control inputs $\boldsymbol{u}(t)$ are given in Fig. 4.8. The replacement of the saturation function eliminates the chattering phenomenon. From Fig. 4.3, although the nominal system contains the state delay term and the mismatched disturbance, the system outputs $\boldsymbol{y}(t)$ are finally bounded around zero. The simulation results demonstrate that the proposed controller design can guarantee the robust disturbance attenuation to outputs $\boldsymbol{y}(t)$ once the system is in the sliding mode.

4.3.2 Robust disturbance attenuation by algebraic Riccati inequalities

This section will alter the LMI (4.30) to algebraic Riccati inequalities as an equivalent sufficient condition assuring the property of robust disturbance attenuation. The full-order dynamic compensator is modified as

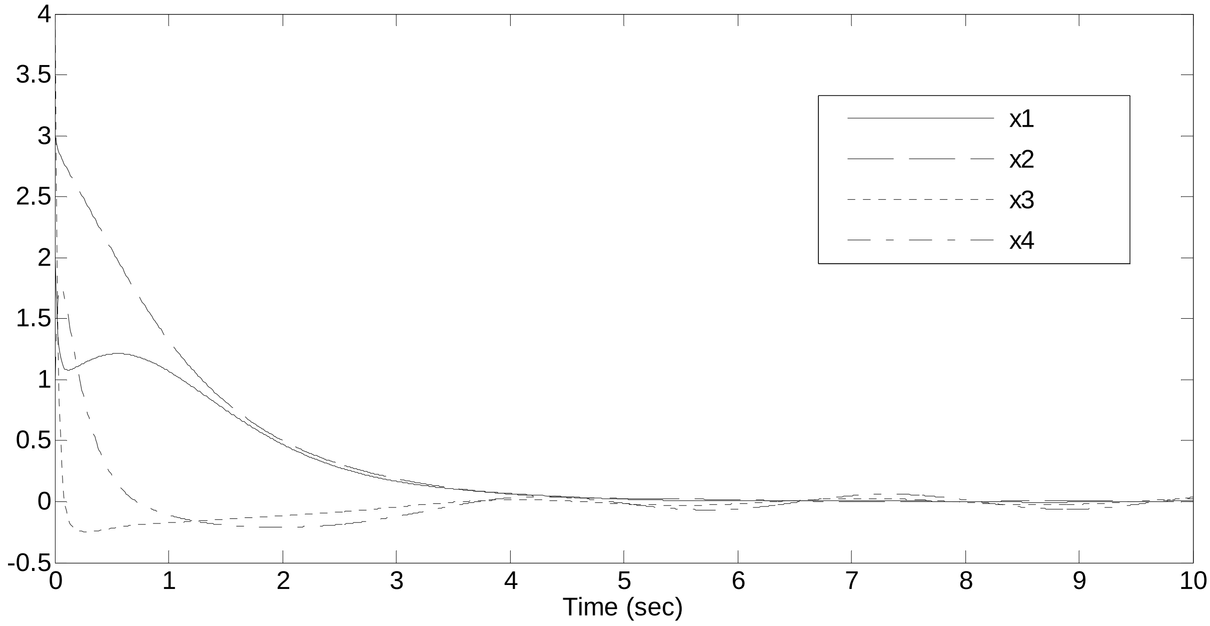

Fig. 4.2. System states in Example 4.1.

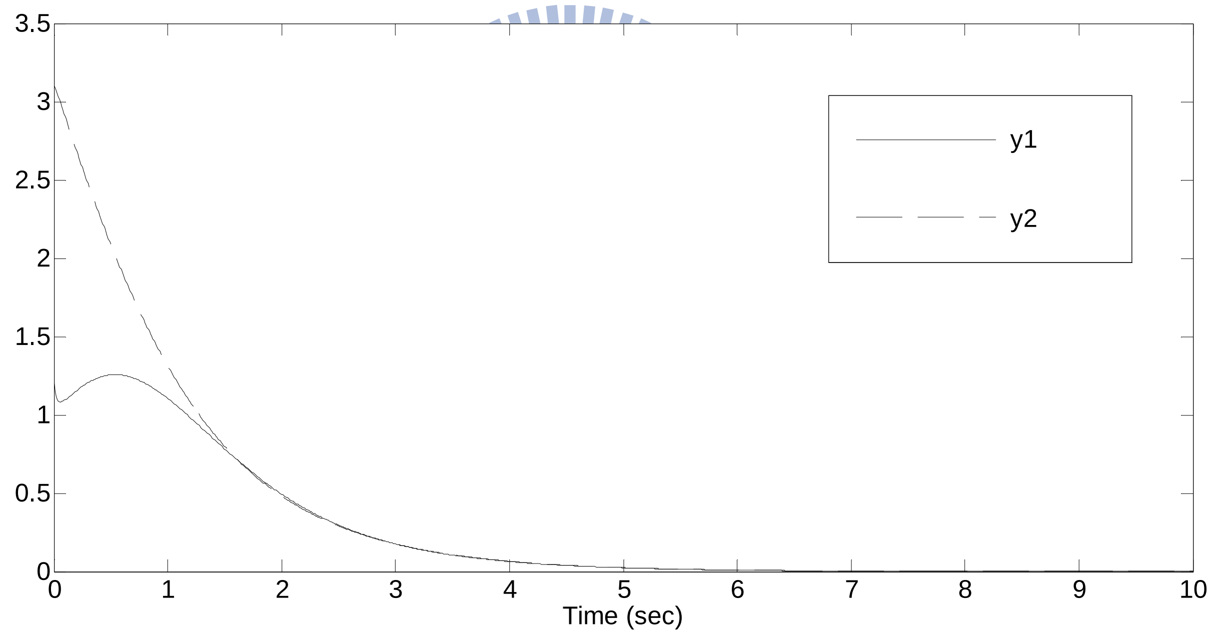

Fig. 4.3. System outputs in Example 4.1.

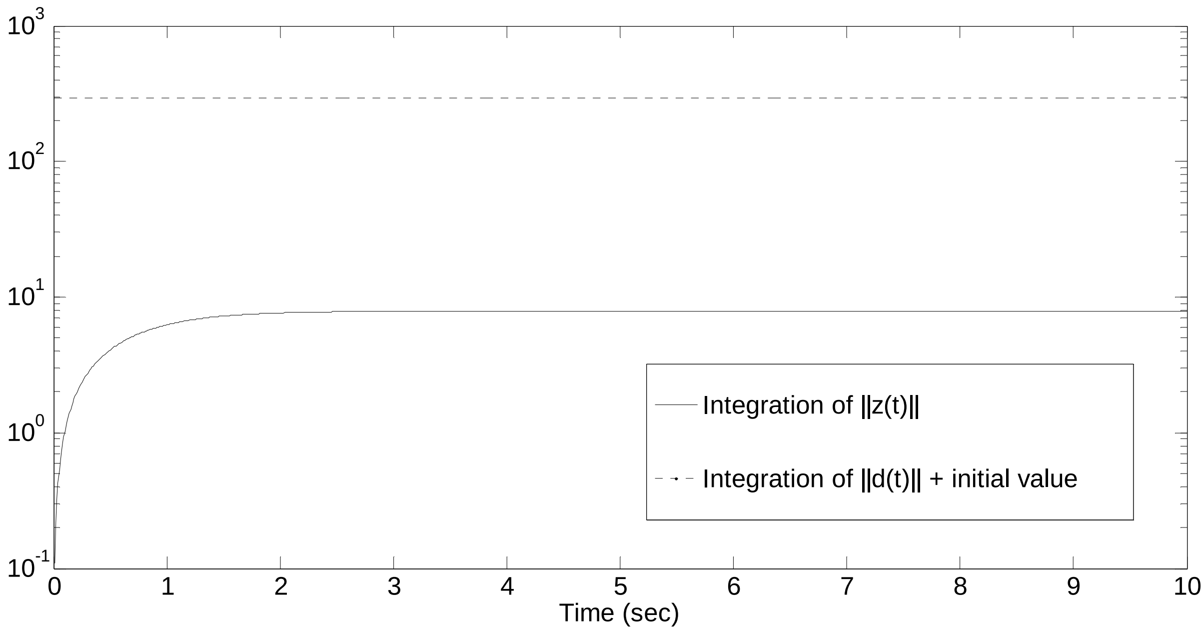

Fig. 4.4. Performance of robust disturbance attenuation in Example 4.1.

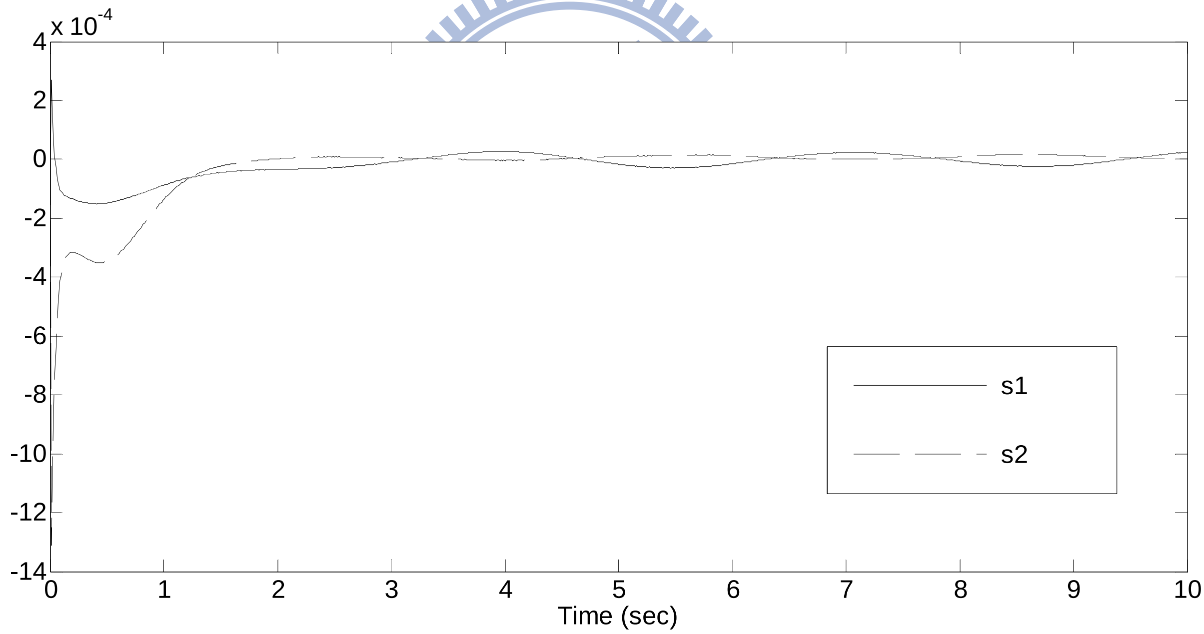

Fig. 4.5. Sliding functions in Example 4.1.

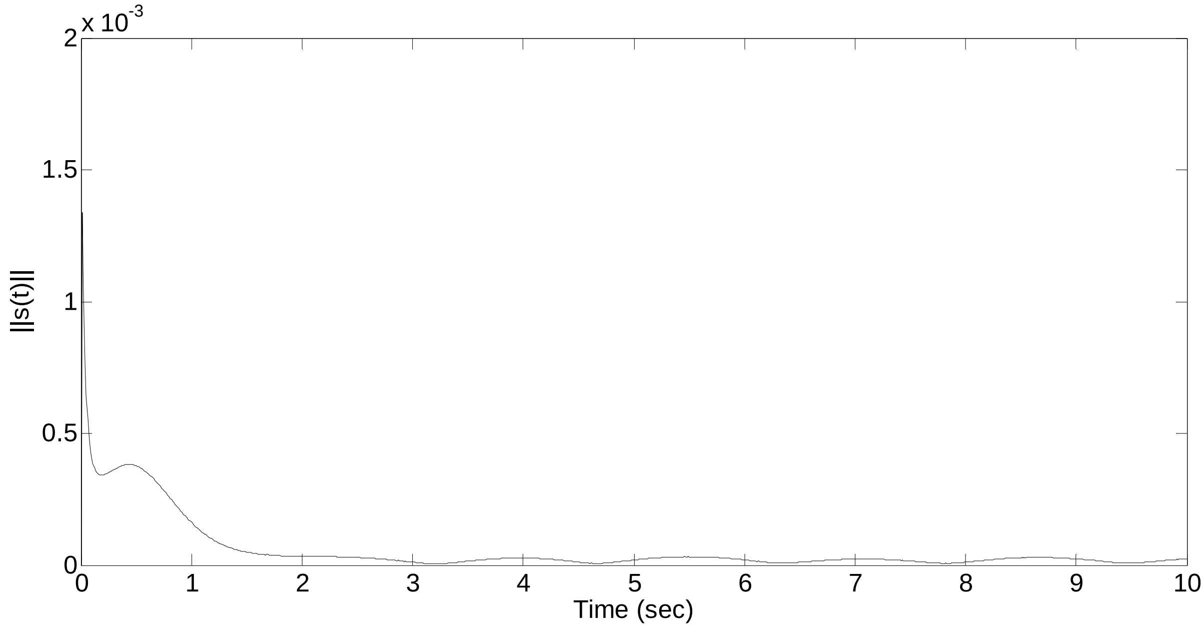

Fig. 4.6. Response of $\|s(t)\|$ in Example 4.1.

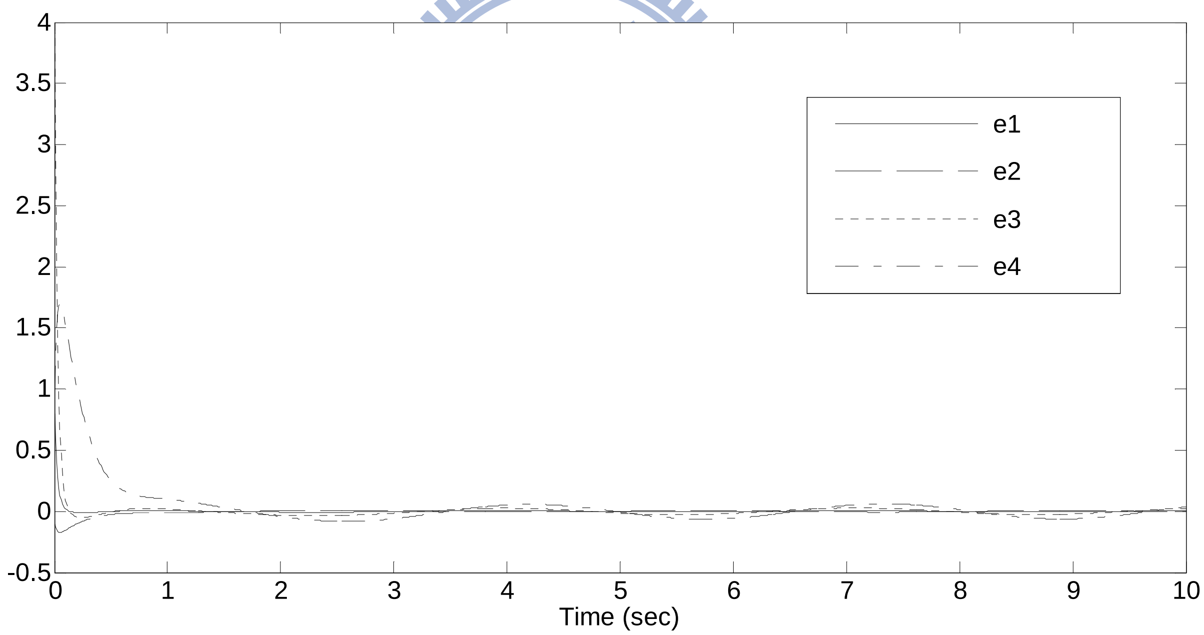

Fig. 4.7. Trajectories of $e(t)$ in Example 4.1.

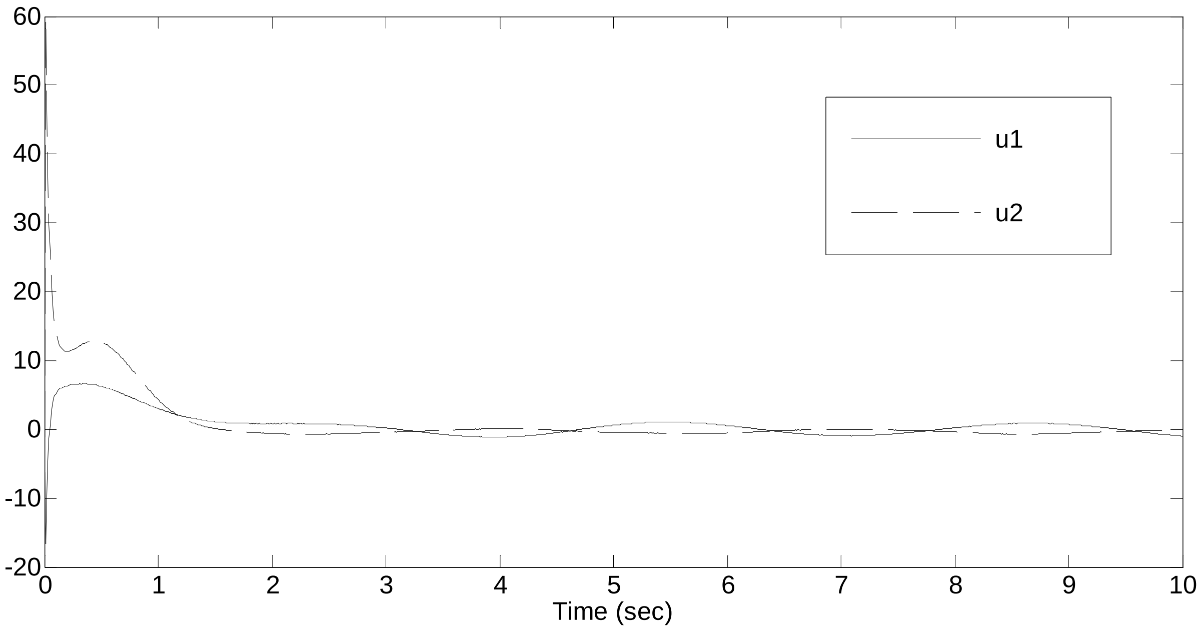

Fig. 4.8. System inputs in Example 4.1.

$$\dot{\xi}(t) = (\boldsymbol{MA} - \boldsymbol{LC} + \boldsymbol{F})\xi(t) + (\Gamma - \boldsymbol{FU})\boldsymbol{y}(t) \tag{4.32}$$

$$\boldsymbol{v}(t) = -\boldsymbol{K}(\xi(t) - \boldsymbol{Uy}(t)) \tag{4.33}$$

where $\boldsymbol{K}$ and $\boldsymbol{F} \in \mathbb{R}^{n \times n}$ are gain matrices determined later. According to (4.32) and $\boldsymbol{MB} = \boldsymbol{0}$, the dynamics of error vector $\boldsymbol{e}(t)$ can be given by

$$\begin{aligned}
\dot{\boldsymbol{e}}(t) &= \boldsymbol{M}\big((\boldsymbol{A} + \boldsymbol{D}\Phi(t)\boldsymbol{H})\boldsymbol{x}(t) + (\boldsymbol{A}_d + \boldsymbol{D}_d\Phi_d(t)\boldsymbol{H}_d)\boldsymbol{x}(t-\tau) + \boldsymbol{Ed}(t)\big) \\
&\quad -(\Gamma - \boldsymbol{FU})\boldsymbol{y}(t) - (\boldsymbol{MA} - \boldsymbol{LC} + \boldsymbol{F})\xi(t) \\
&= (\boldsymbol{MA} - \boldsymbol{LC})\boldsymbol{Mx}(t) + \boldsymbol{MEd}(t) - (\boldsymbol{MA} - \boldsymbol{LC})\xi(t) - \boldsymbol{Fx}(t) + \boldsymbol{Fe}(t) \\
&\quad + \boldsymbol{MD}\Phi(t)\boldsymbol{Hx}(t) + \boldsymbol{M}(\boldsymbol{A}_d + \boldsymbol{D}_d\Phi_d(t)\boldsymbol{H}_d)\boldsymbol{x}(t-\tau) \\
&= (\boldsymbol{MD}\Phi(t)\boldsymbol{H} - \boldsymbol{F})\boldsymbol{x}(t) + \boldsymbol{M}(\boldsymbol{A}_d + \boldsymbol{D}_d\Phi_d(t)\boldsymbol{H}_d)\boldsymbol{x}(t-\tau) \\
&\quad + (\boldsymbol{MA} - \boldsymbol{LC} + \boldsymbol{F})\boldsymbol{e}(t) + \boldsymbol{MEd}(t).
\end{aligned} \tag{4.34}$$

Combining (4.27) with (4.34), the integrated closed-loop system can be expressed as

$$\begin{aligned}
\begin{bmatrix} \dot{\boldsymbol{x}}(t) \\ \dot{\boldsymbol{e}}(t) \end{bmatrix} &= \begin{bmatrix} \boldsymbol{NA} - \boldsymbol{BK} + \boldsymbol{ND}\Phi(t)\boldsymbol{H} & \boldsymbol{BK} \\ -\boldsymbol{F} + \boldsymbol{MD}\Phi(t)\boldsymbol{H} & \boldsymbol{MA} - \boldsymbol{LC} + \boldsymbol{F} \end{bmatrix} \begin{bmatrix} \boldsymbol{x}(t) \\ \boldsymbol{e}(t) \end{bmatrix} + \begin{bmatrix} \boldsymbol{NE} \\ \boldsymbol{ME} \end{bmatrix} \boldsymbol{d}(t) \\
&\quad + \begin{bmatrix} \boldsymbol{NA}_d + \boldsymbol{ND}_d\Phi_d(t)\boldsymbol{H}_d & \boldsymbol{0} \\ \boldsymbol{MA}_d + \boldsymbol{MD}_d\Phi_d(t)\boldsymbol{H}_d & \boldsymbol{0} \end{bmatrix} \begin{bmatrix} \boldsymbol{x}(t-\tau) \\ \boldsymbol{e}(t-\tau) \end{bmatrix}.
\end{aligned} \tag{4.35}$$

The objective is transferred to design matrices $\boldsymbol{K}$, $\boldsymbol{L}$, and $\boldsymbol{F}$, and analyze the robust stability of the closed-loop system (4.35). Define a quadratic energy function as

$$E_n(\boldsymbol{x},\boldsymbol{e}) = \boldsymbol{x}^T \boldsymbol{P}_{11}\boldsymbol{x} + \boldsymbol{e}^T \boldsymbol{P}_{22}\boldsymbol{e} + \int_{t-\tau}^{t} \boldsymbol{x}^T(\alpha)\boldsymbol{Q}_{11}\boldsymbol{x}(\alpha)d\alpha + \int_{t-\tau}^{t} \boldsymbol{e}^T(\alpha)\boldsymbol{Q}_{22}\boldsymbol{e}(\alpha)d\alpha \tag{4.36}$$

where the positive definite matrices $\boldsymbol{P}_{11} > 0$, $\boldsymbol{P}_{22} > 0$, $\boldsymbol{Q}_{11} > 0$, and $\boldsymbol{Q}_{22} > 0$ are determined later. Choosing the same Hamiltonian function $H[\boldsymbol{d}] = \boldsymbol{z}^T\boldsymbol{z} - \gamma^2 \boldsymbol{d}^T\boldsymbol{d} + \frac{dE_n}{dt}$ and sufficient condition $H[\boldsymbol{d}] < 0$ for all $\boldsymbol{d} \in L_2$ as (A.2) and (A.3) respectively, the detail of the proposed Hamilton function is given by

$$\begin{aligned} H[\boldsymbol{d}] = {} & \boldsymbol{x}^T(t)\left(\boldsymbol{C}^T\boldsymbol{C} + \boldsymbol{K}^T\boldsymbol{R}\boldsymbol{K}\right)\boldsymbol{x}(t) - 2\boldsymbol{x}^T(t)\boldsymbol{K}^T\boldsymbol{R}\boldsymbol{K}\boldsymbol{e}(t) + \boldsymbol{e}^T(t)\boldsymbol{K}^T\boldsymbol{R}\boldsymbol{K}\boldsymbol{e}(t) \\ & + \left(\left(\boldsymbol{N}\boldsymbol{A} - \boldsymbol{B}\boldsymbol{K} + \boldsymbol{N}\boldsymbol{D}\Phi(t)\boldsymbol{H}\right)\boldsymbol{x}(t)\right)^T \boldsymbol{P}_{11}\boldsymbol{x}(t) + \boldsymbol{x}^T(t)\boldsymbol{Q}_{11}\boldsymbol{x}(t) \\ & + \left(\boldsymbol{N}\left(\boldsymbol{A}_d + \boldsymbol{D}_d\Phi_d(t)\boldsymbol{H}_d\right)\boldsymbol{x}(t-\tau)\right)^T \boldsymbol{P}_{11}\boldsymbol{x}(t) - \boldsymbol{x}^T(t-\tau)\boldsymbol{Q}_{11}\boldsymbol{x}(t-\tau) \\ & + \boldsymbol{x}^T(t)\boldsymbol{P}_{11}\left(\boldsymbol{N}\boldsymbol{A} - \boldsymbol{B}\boldsymbol{K} + \boldsymbol{N}\boldsymbol{D}\Phi(t)\boldsymbol{H}\right)\boldsymbol{x}(t) - \boldsymbol{e}^T(t-\tau)\boldsymbol{Q}_{22}\boldsymbol{e}(t-\tau) \\ & + \boldsymbol{x}^T(t)\boldsymbol{P}_{11}\boldsymbol{N}\left(\boldsymbol{A}_d + \boldsymbol{D}_d\Phi_d(t)\boldsymbol{H}_d\right)\boldsymbol{x}(t-\tau) + 2\boldsymbol{x}^T(t)\boldsymbol{P}_{11}\boldsymbol{N}\boldsymbol{E}\boldsymbol{d}(t) \\ & + 2\boldsymbol{x}^T(t)\boldsymbol{P}_{11}\boldsymbol{B}\boldsymbol{K}\boldsymbol{e}(t) + 2\boldsymbol{e}^T(t)\boldsymbol{P}_{22}\boldsymbol{M}\boldsymbol{E}\boldsymbol{d}(t) + \boldsymbol{e}^T(t)\boldsymbol{Q}_{22}\boldsymbol{e}(t) - \gamma^2\boldsymbol{d}^T(t)\boldsymbol{d}(t) \\ & + 2\left(\left(\boldsymbol{M}\boldsymbol{D}\Phi(t)\boldsymbol{H} - \boldsymbol{F}\right)\boldsymbol{x}(t) + \boldsymbol{M}\left(\boldsymbol{A}_d + \boldsymbol{D}_d\Phi_d(t)\boldsymbol{H}_d\right)\boldsymbol{x}(t-\tau)\right)^T \boldsymbol{P}_{22}\boldsymbol{e}(t) \\ & + \boldsymbol{e}^T(t)\boldsymbol{P}_{22}\left(\boldsymbol{M}\boldsymbol{A} - \boldsymbol{L}\boldsymbol{C} + \boldsymbol{F}\right)\boldsymbol{e}(t) + \boldsymbol{e}^T(t)\left(\boldsymbol{M}\boldsymbol{A} - \boldsymbol{L}\boldsymbol{C} + \boldsymbol{F}\right)^T \boldsymbol{P}_{22}\boldsymbol{e}(t). \end{aligned} \tag{4.37}$$

Based on the above equation, the worst case $\sup_{\boldsymbol{d}\in L_2} H[\boldsymbol{d}]$ occurs when $\boldsymbol{d}(t) = \gamma^{-2}\boldsymbol{E}^T\left(\boldsymbol{N}^T\boldsymbol{P}_{11}\boldsymbol{x}(t) + \boldsymbol{M}^T\boldsymbol{P}_{22}\boldsymbol{e}(t)\right)$, and it follows that

$$\begin{aligned} H[\boldsymbol{d}] \le {} & \boldsymbol{x}^T(t)\left(\boldsymbol{C}^T\boldsymbol{C} + \boldsymbol{K}^T\boldsymbol{R}\boldsymbol{K}\right)\boldsymbol{x}(t) - 2\boldsymbol{x}^T(t)\boldsymbol{K}^T\boldsymbol{R}\boldsymbol{K}\boldsymbol{e}(t) - \boldsymbol{e}^T(t-\tau)\boldsymbol{Q}_{22}\boldsymbol{e}(t-\tau) \\ & + \left(\left(\boldsymbol{N}\boldsymbol{A} - \boldsymbol{B}\boldsymbol{K} + \boldsymbol{N}\boldsymbol{D}\Phi(t)\boldsymbol{H}\right)\boldsymbol{x}(t)\right)^T \boldsymbol{P}_{11}\boldsymbol{x}(t) + \boldsymbol{x}^T(t)\boldsymbol{Q}_{11}\boldsymbol{x}(t) + \boldsymbol{e}^T(t)\boldsymbol{Q}_{22}\boldsymbol{e}(t) \\ & + \boldsymbol{x}^T(t)\boldsymbol{P}_{11}\left(\boldsymbol{N}\boldsymbol{A} - \boldsymbol{B}\boldsymbol{K} + \boldsymbol{N}\boldsymbol{D}\Phi(t)\boldsymbol{H}\right)\boldsymbol{x}(t) - \boldsymbol{x}^T(t-\tau)\boldsymbol{Q}_{11}\boldsymbol{x}(t-\tau) \\ & + 2\boldsymbol{x}^T(t)\boldsymbol{P}_{11}\left(\boldsymbol{B}\boldsymbol{K}\boldsymbol{e}(t) + \boldsymbol{N}\left(\boldsymbol{A}_d + \boldsymbol{D}_d\Phi_d(t)\boldsymbol{H}_d\right)\boldsymbol{x}(t-\tau)\right) + \boldsymbol{e}^T(t)\boldsymbol{K}^T\boldsymbol{R}\boldsymbol{K}\boldsymbol{e}(t) \\ & + \left(\left(\boldsymbol{M}\boldsymbol{A} - \boldsymbol{L}\boldsymbol{C} + \boldsymbol{F}\right)\boldsymbol{e}(t)\right)^T \boldsymbol{P}_{22}\boldsymbol{e}(t) + \boldsymbol{e}^T(t)\boldsymbol{P}_{22}\left(\left(\boldsymbol{M}\boldsymbol{A} - \boldsymbol{L}\boldsymbol{C} + \boldsymbol{F}\right)\boldsymbol{e}(t)\right) \\ & + 2\boldsymbol{e}^T(t)\boldsymbol{P}_{22}\left(\left(\boldsymbol{M}\boldsymbol{D}\Phi(t)\boldsymbol{H} - \boldsymbol{F}\right)\boldsymbol{x}(t) + \boldsymbol{M}\left(\boldsymbol{A}_d + \boldsymbol{D}_d\Phi_d(t)\boldsymbol{H}_d\right)\boldsymbol{x}(t-\tau)\right) \\ & + \gamma^{-2}\boldsymbol{x}^T(t)\boldsymbol{P}_{11}\boldsymbol{N}\boldsymbol{E}\boldsymbol{E}^T\boldsymbol{N}^T\boldsymbol{P}_{11}\boldsymbol{x}(t) + \gamma^{-2}\boldsymbol{e}^T(t)\boldsymbol{P}_{22}\boldsymbol{M}\boldsymbol{E}\boldsymbol{E}^T\boldsymbol{N}^T\boldsymbol{P}_{11}\boldsymbol{x}(t) \\ & + \gamma^{-2}\boldsymbol{x}^T(t)\boldsymbol{P}_{11}\boldsymbol{N}\boldsymbol{E}\boldsymbol{E}^T\boldsymbol{M}^T\boldsymbol{P}_{22}\boldsymbol{e}(t) + \gamma^{-2}\boldsymbol{e}^T(t)\boldsymbol{P}_{22}\boldsymbol{M}\boldsymbol{E}\boldsymbol{E}^T\boldsymbol{M}^T\boldsymbol{P}_{22}\boldsymbol{e}(t). \end{aligned} \tag{4.38}$$

According to Lemma 4.1, inequality (4.38) can be rewritten as

$$H[\boldsymbol{d}] \le \begin{bmatrix} \boldsymbol{x}(t) \\ \boldsymbol{e}(t) \\ \boldsymbol{x}(t-\tau) \\ \boldsymbol{e}(t-\tau) \end{bmatrix}^T \begin{bmatrix} \Pi_{11} & \Pi_{12} & \boldsymbol{P}_{11}\boldsymbol{N}\boldsymbol{A}_d & \boldsymbol{0} \\ * & \Pi_{22} & \boldsymbol{P}_{22}\boldsymbol{M}\boldsymbol{A}_d & \boldsymbol{0} \\ * & * & \left(\rho_2^{-1}+\rho_4^{-1}\right)\boldsymbol{H}_d^T\boldsymbol{H}_d - \boldsymbol{Q}_{11} & \boldsymbol{0} \\ * & * & * & -\boldsymbol{Q}_{22} \end{bmatrix} \begin{bmatrix} \boldsymbol{x}(t) \\ \boldsymbol{e}(t) \\ \boldsymbol{x}(t-\tau) \\ \boldsymbol{e}(t-\tau) \end{bmatrix} \tag{4.39}$$

where

$$\begin{aligned} \Pi_{11} &= (\boldsymbol{NA}-\boldsymbol{BK})^T\boldsymbol{P}_{11} + \boldsymbol{P}_{11}(\boldsymbol{NA}-\boldsymbol{BK}) + \boldsymbol{C}^T\boldsymbol{C} + \boldsymbol{K}^T\boldsymbol{RK} + \boldsymbol{Q}_{11} \\ &\quad + \boldsymbol{P}_{11}\boldsymbol{N}\left(\gamma^{-2}\boldsymbol{EE}^T + \rho_1\boldsymbol{DD}^T + \rho_2\boldsymbol{D}_d\boldsymbol{D}_d^T\right)\boldsymbol{N}^T\boldsymbol{P}_{11} + \left(\rho_1^{-1}+\rho_3^{-1}\right)\boldsymbol{H}^T\boldsymbol{H} \end{aligned} \tag{4.40}$$

$$\begin{aligned} \Pi_{22} &= (\boldsymbol{MA}-\boldsymbol{LC}+\boldsymbol{F})^T\boldsymbol{P}_{22} + \boldsymbol{P}_{22}(\boldsymbol{MA}-\boldsymbol{LC}+\boldsymbol{F}) + \boldsymbol{K}^T\boldsymbol{RK} + \boldsymbol{Q}_{22} \\ &\quad + \boldsymbol{P}_{22}\boldsymbol{M}\left(\gamma^{-2}\boldsymbol{EE}^T + \rho_3\boldsymbol{DD}^T + \rho_4\boldsymbol{D}_d\boldsymbol{D}_d^T\right)\boldsymbol{M}^T\boldsymbol{P}_{22} \end{aligned} \tag{4.41}$$

$$\Pi_{12} = \boldsymbol{P}_{11}\boldsymbol{BK} - \boldsymbol{K}^T\boldsymbol{RK} - \boldsymbol{F}^T\boldsymbol{P}_{22} + \gamma^{-2}\boldsymbol{P}_{11}\boldsymbol{NEE}^T\boldsymbol{M}^T\boldsymbol{P}_{22}\,. \tag{4.42}$$

Notice that ρ_i are positive constants, $i=1,\cdots,4$. The sufficient condition satisfying the robust disturbance attenuation, $\sup_{\boldsymbol{d}\in L_2} H[\boldsymbol{d}]<0$, is altered to fulfill the following matrix inequality

$$\begin{bmatrix} \Pi_{11} & \Pi_{12} & \boldsymbol{P}_{11}\boldsymbol{NA}_d & \boldsymbol{0} \\ \Pi_{12}^T & \Pi_{22} & \boldsymbol{P}_{22}\boldsymbol{MA}_d & \boldsymbol{0} \\ \boldsymbol{A}_d^T\boldsymbol{N}^T\boldsymbol{P}_{11} & \boldsymbol{A}_d^T\boldsymbol{M}^T\boldsymbol{P}_{22} & -\left(\boldsymbol{Q}_{11} - \left(\rho_2^{-1}+\rho_4^{-1}\right)\boldsymbol{H}_d^T\boldsymbol{H}_d\right) & \boldsymbol{0} \\ \boldsymbol{0} & \boldsymbol{0} & \boldsymbol{0} & -\boldsymbol{Q}_{22} \end{bmatrix} < 0\,. \tag{4.43}$$

Moreover, the following theorem transfers (4.43) into two algebraic Riccati inequalities using Schur decomposition and develops the designs of $\boldsymbol{K}$, $\boldsymbol{L}$, and $\boldsymbol{F}$ which guarantee the robust disturbance attenuation.

Theorem 4.2 Consider the system (4.15) with the integral sliding surface (4.5) and full-order compensator (4.32). Given $\boldsymbol{R}>0$ $\boldsymbol{Q}_{11}>0$, $\boldsymbol{Q}_{22}>0$, $\gamma\ge 0$, and $\rho_i>0$, $i=1,2,\cdots,4$, if there exists matrices $\boldsymbol{P}_{11}>0$ and $\boldsymbol{P}_{22}>0$ satisfying the following algebraic Riccati inequalities

$$\begin{aligned}&(\boldsymbol{NA})^T \boldsymbol{P}_{11} + \boldsymbol{P}_{11}(\boldsymbol{NA}) - \boldsymbol{P}_{11}\boldsymbol{B}\boldsymbol{R}^{-1}\boldsymbol{B}^T\boldsymbol{P}_{11} + \boldsymbol{C}^T\boldsymbol{C} + \boldsymbol{Q}_{11} + \left(\rho_1^{-1}+\rho_3^{-1}\right)\boldsymbol{H}^T\boldsymbol{H} + \boldsymbol{P}_{11}\boldsymbol{N} \\ &\times\left(\gamma^{-2}\boldsymbol{E}\boldsymbol{E}^T + \rho_1\boldsymbol{D}\boldsymbol{D}^T + \rho_2\boldsymbol{D}_d\boldsymbol{D}_d^T - \boldsymbol{A}_d\left(\left(\rho_2^{-1}+\rho_4^{-1}\right)\boldsymbol{H}_d^T\boldsymbol{H}_d - \boldsymbol{Q}_{11}\right)^{-1}\boldsymbol{A}_d^T\right)\boldsymbol{N}^T\boldsymbol{P}_{11} < 0\end{aligned} \tag{4.44}$$

$$\begin{aligned}&(\boldsymbol{MA}+\boldsymbol{F})^T \boldsymbol{P}_{22} + \boldsymbol{P}_{22}(\boldsymbol{MA}+\boldsymbol{F}) + \boldsymbol{P}_{11}\boldsymbol{B}\boldsymbol{R}^{-1}\boldsymbol{B}^T\boldsymbol{P}_{11} - \lambda\boldsymbol{C}^T\boldsymbol{C} + \boldsymbol{Q}_{22} + \boldsymbol{P}_{22}\boldsymbol{M}\left(\gamma^{-2}\boldsymbol{E}\boldsymbol{E}^T\right. \\ &\left.+\rho_3\boldsymbol{D}\boldsymbol{D}^T + \rho_4\boldsymbol{D}_d\boldsymbol{D}_d^T - \boldsymbol{A}_d\left(\left(\rho_2^{-1}+\rho_4^{-1}\right)\boldsymbol{H}_d^T\boldsymbol{H}_d - \boldsymbol{Q}_{11}\right)^{-1}\boldsymbol{A}_d^T\right)\boldsymbol{M}^T\boldsymbol{P}_{22} < 0\end{aligned} \tag{4.45}$$

where $\rho_2 > 0$ and $\rho_4 > 0$ are designed such that $\boldsymbol{Q}_{11} - \left(\rho_2^{-1}+\rho_4^{-1}\right)\boldsymbol{H}_d^T\boldsymbol{H}_d > 0$, then robust disturbance attenuation (4.18) can be guaranteed. Furthermore, matrices $\boldsymbol{K}$, $\boldsymbol{L}$, and $\boldsymbol{F}$ are given by $\boldsymbol{K} = \boldsymbol{R}^{-1}\boldsymbol{B}^T\boldsymbol{P}_{11}$, $\boldsymbol{L} = \frac{\lambda}{2}\boldsymbol{P}_{22}^{-1}\boldsymbol{C}^T$, and

$$\boldsymbol{F} = \boldsymbol{M}\left(\gamma^{-2}\boldsymbol{E}\boldsymbol{E}^T - \boldsymbol{A}_d\left(\left(\rho_2^{-1}+\rho_4^{-1}\right)\boldsymbol{H}_d^T\boldsymbol{H}_d - \boldsymbol{Q}_{11}\right)^{-1}\boldsymbol{A}_d^T\right)\boldsymbol{N}^T\boldsymbol{P}_{11}. \tag{4.46}$$

Proof: Since the condition $\left(\rho_2^{-1}+\rho_4^{-1}\right)\boldsymbol{H}_d^T\boldsymbol{H}_d - \boldsymbol{Q}_{11} < 0$ holds, by Schur decomposition, inequality (4.43) is equivalent to

$$\begin{bmatrix}\boldsymbol{J}_{11} & \boldsymbol{J}_{12} \\ \boldsymbol{J}_{12}^T & \boldsymbol{J}_{22}\end{bmatrix} < 0 \tag{4.47}$$

where

$$\begin{aligned}\boldsymbol{J}_{11} &= (\boldsymbol{NA}-\boldsymbol{BK})^T\boldsymbol{P}_{11} + \boldsymbol{P}_{11}(\boldsymbol{NA}-\boldsymbol{BK}) + \left(\rho_1^{-1}+\rho_3^{-1}\right)\boldsymbol{H}^T\boldsymbol{H} + \boldsymbol{Q}_{11} \\ &\quad - \boldsymbol{P}_{11}\boldsymbol{N}\boldsymbol{A}_d\left(\left(\rho_2^{-1}+\rho_4^{-1}\right)\boldsymbol{H}_d^T\boldsymbol{H}_d - \boldsymbol{Q}_{11}\right)^{-1}\boldsymbol{A}_d^T\boldsymbol{N}^T\boldsymbol{P}_{11} + \boldsymbol{C}^T\boldsymbol{C} + \boldsymbol{K}^T\boldsymbol{R}\boldsymbol{K} \\ &\quad + \boldsymbol{P}_{11}\boldsymbol{N}\left(\gamma^{-2}\boldsymbol{E}\boldsymbol{E}^T + \rho_1\boldsymbol{D}\boldsymbol{D}^T + \rho_2\boldsymbol{D}_d\boldsymbol{D}_d^T\right)\boldsymbol{N}^T\boldsymbol{P}_{11}\end{aligned} \tag{4.48}$$

$$\begin{aligned}\boldsymbol{J}_{12} &= \boldsymbol{P}_{11}\boldsymbol{BK} - \boldsymbol{K}^T\boldsymbol{RK} - \boldsymbol{F}^T\boldsymbol{P}_{22} + \gamma^{-2}\boldsymbol{P}_{11}\boldsymbol{N}\boldsymbol{E}\boldsymbol{E}^T\boldsymbol{M}^T\boldsymbol{P}_{22} \\ &\quad - \boldsymbol{P}_{11}\boldsymbol{N}\boldsymbol{A}_d\left(\left(\rho_2^{-1}+\rho_4^{-1}\right)\boldsymbol{H}_d^T\boldsymbol{H}_d - \boldsymbol{Q}_{11}\right)^{-1}\boldsymbol{A}_d^T\boldsymbol{M}^T\boldsymbol{P}_{22}\end{aligned} \tag{4.49}$$

$$\begin{aligned}\boldsymbol{J}_{22} &= (\boldsymbol{MA}-\boldsymbol{LC}+\boldsymbol{F})^T\boldsymbol{P}_{22} + \boldsymbol{P}_{22}(\boldsymbol{MA}-\boldsymbol{LC}+\boldsymbol{F}) + \boldsymbol{K}^T\boldsymbol{RK} + \boldsymbol{Q}_{22} \\ &\quad + \boldsymbol{P}_{22}\boldsymbol{M}\left(\rho_3\boldsymbol{D}\boldsymbol{D}^T + \rho_4\boldsymbol{D}_d\boldsymbol{D}_d^T\right)\boldsymbol{M}^T\boldsymbol{P}_{22} + \gamma^{-2}\boldsymbol{P}_{22}\boldsymbol{M}\boldsymbol{E}\boldsymbol{E}^T\boldsymbol{M}^T\boldsymbol{P}_{22} \\ &\quad - \boldsymbol{P}_{22}\boldsymbol{M}\boldsymbol{A}_d\left(\left(\rho_2^{-1}+\rho_4^{-1}\right)\boldsymbol{H}_d^T\boldsymbol{H}_d - \boldsymbol{Q}_{11}\right)^{-1}\boldsymbol{A}_d^T\boldsymbol{M}^T\boldsymbol{P}_{22}.\end{aligned} \tag{4.50}$$

Design $\boldsymbol{F} = \boldsymbol{M}\left(\gamma^{-2}\boldsymbol{E}\boldsymbol{E}^T - \boldsymbol{A}_d\left(\left(\rho_2^{-1}+\rho_4^{-1}\right)\boldsymbol{H}_d^T\boldsymbol{H}_d - \boldsymbol{Q}_{11}\right)^{-1}\boldsymbol{A}_d^T\right)\boldsymbol{N}^T\boldsymbol{P}_{11}$, $\boldsymbol{K} = \boldsymbol{R}^{-1}\boldsymbol{B}^T\boldsymbol{P}_{11}$, and

$\boldsymbol{L} = \frac{\lambda}{2}\boldsymbol{P}_{22}^{-1}\boldsymbol{C}^T$. Then substituting them into (4.47) can attain

$$\begin{aligned}\boldsymbol{J}_{11} &= (\boldsymbol{NA})^T \boldsymbol{P}_{11} + \boldsymbol{P}_{11}(\boldsymbol{NA}) - \boldsymbol{P}_{11}\boldsymbol{BR}^{-1}\boldsymbol{B}^T\boldsymbol{P}_{11} + \boldsymbol{C}^T\boldsymbol{C} + \boldsymbol{Q}_{11} + \left(\rho_1^{-1} + \rho_3^{-1}\right)\boldsymbol{H}^T\boldsymbol{H} \\ &\quad + \boldsymbol{P}_{11}\boldsymbol{N}\left(\gamma^{-2}\boldsymbol{EE}^T + \rho_1\boldsymbol{DD}^T + \rho_2\boldsymbol{D}_d\boldsymbol{D}_d^T - \boldsymbol{A}_d\left(\left(\rho_2^{-1} + \rho_4^{-1}\right)\boldsymbol{H}_d^T\boldsymbol{H}_d - \boldsymbol{Q}_{11}\right)^{-1}\boldsymbol{A}_d^T\right) \\ &\quad \times \boldsymbol{N}^T\boldsymbol{P}_{11}\end{aligned} \tag{4.51}$$

$$\boldsymbol{J}_{12} = \boldsymbol{0} \tag{4.52}$$

$$\begin{aligned}\boldsymbol{J}_{22} &= (\boldsymbol{MA} + \boldsymbol{F})^T \boldsymbol{P}_{22} + \boldsymbol{P}_{22}(\boldsymbol{MA} + \boldsymbol{F}) + \boldsymbol{P}_{11}\boldsymbol{BR}^{-1}\boldsymbol{B}^T\boldsymbol{P}_{11} - \lambda\boldsymbol{C}^T\boldsymbol{C} + \boldsymbol{Q}_{22} \\ &\quad + \boldsymbol{P}_{22}\boldsymbol{M}\left(\gamma^{-2}\boldsymbol{EE}^T + \rho_3\boldsymbol{DD}^T + \rho_4\boldsymbol{D}_d\boldsymbol{D}_d^T - \boldsymbol{A}_d\left(\left(\rho_2^{-1} + \rho_4^{-1}\right)\boldsymbol{H}_d^T\boldsymbol{H}_d - \boldsymbol{Q}_{11}\right)^{-1}\boldsymbol{A}_d^T\right) \\ &\quad \times \boldsymbol{M}^T\boldsymbol{P}_{22}.\end{aligned} \tag{4.53}$$

Therefore, if there exists $\boldsymbol{P}_{11} > 0$ and $\boldsymbol{P}_{22} > 0$ such that $\boldsymbol{J}_{11} < 0$ and $\boldsymbol{J}_{22} < 0$, it implies to $\sup_{\boldsymbol{d} \in L_2} H[\boldsymbol{d}] < 0$, and to guarantee the robust disturbance attenuation. The proof of this theorem is completed. □

Remark 4.3 Figure 4.9 shows the flowchart to solve parameters of controller and compensator. First adjusting γ, $\boldsymbol{Q}_{11}$, and $\rho_i > 0$, $i = 1, 2, \cdots, 4$ can determine different $\boldsymbol{P}_{11}$. Substituting $\boldsymbol{P}_{11}$ into (4.46) can obtain matrix $\boldsymbol{F}$. Then choose λ to determine $\boldsymbol{P}_{22}$ from (4.45). Generally, for any γ that there exists a solution $\boldsymbol{P}_{11}$ to (4.44) (which is used for the state feedback gain), we can find a λ large enough such that there exists a solution $\boldsymbol{P}_{22}$ to the inequality (4.45). It means that a high gain compensator can be used to accomplish the work. Besides, LMI technique [3] can be used to solve the two inequalities (4.44) and (4.45). Finally, we summarize the output feedback integral sliding mode controller as

$$\begin{aligned}\dot{\xi}(t) &= (\boldsymbol{MA} - \boldsymbol{LC} + \boldsymbol{F})\xi(t) + (\Gamma - \boldsymbol{FU})\boldsymbol{y}(t) \\ \boldsymbol{s}(t) &= (\boldsymbol{GCB})^{-1}\boldsymbol{G}\big(\boldsymbol{y}(t) - \boldsymbol{y}(0)\big) + \int_0^t \boldsymbol{K}\big(\xi(q) - \boldsymbol{Uy}(q)\big)dq \\ \boldsymbol{u}(t) &= -\boldsymbol{K}\big(\xi(t) - \boldsymbol{Uy}(t)\big) - \kappa(t)\frac{\boldsymbol{s}(t)}{\|\boldsymbol{s}(t)\|}.\end{aligned}$$ □

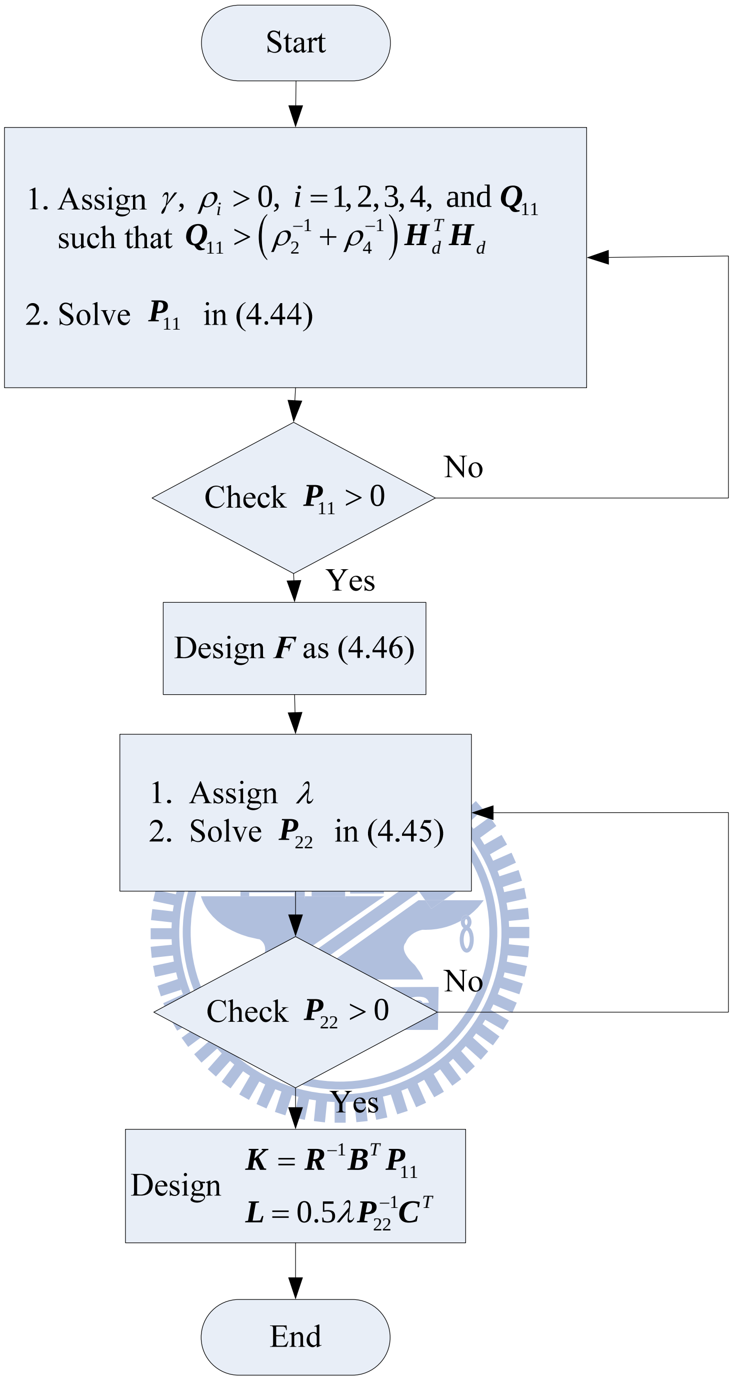

Fig. 4.9. Flowchart for solving parameters $\boldsymbol{K}$ and $\boldsymbol{L}$ by algebraic Riccati inequalities of controller and compensator.

The following examples are simulated to verify the proposed controller design in this section. The results of comparison with [28] are in Example 4.2. Further the proposed method is simulated for an unstable system to verify the feasibility in the last example.

Example 4.2 Consider a nonlinear uncertain state-delayed system [28] within the following form

$$\dot{\boldsymbol{x}}(t)=\left(\boldsymbol{A}+\Delta\boldsymbol{A}(t)\right)\boldsymbol{x}(t)+\left(\boldsymbol{A}_d+\Delta\boldsymbol{A}_d(t)\right)\boldsymbol{x}(t-\tau)+\left(\boldsymbol{B}+\Delta\boldsymbol{B}(t)\right)\boldsymbol{u}(t)+\boldsymbol{w}(\boldsymbol{x},t)$$
$$\boldsymbol{y}(t)=\boldsymbol{C}\boldsymbol{x}(t)$$

where

$$\boldsymbol{A}=\begin{bmatrix}-1.8 & 1 & 0\\ 0.6 & -1.5 & 0\\ 0 & 1 & -1\end{bmatrix},\ \boldsymbol{A}_d=\begin{bmatrix}0.2 & 0.1 & 0.1\\ 0.1 & 0.1 & 0\\ 0 & 0.1 & 0\end{bmatrix},\ \boldsymbol{B}=\begin{bmatrix}2 & 0\\ 0 & 1\\ 1 & 1\end{bmatrix},\ \boldsymbol{C}=\begin{bmatrix}1 & 3\\ 5 & 1\\ 2 & 0\end{bmatrix}^T,$$

and delay time $\tau=1$, $\Delta\boldsymbol{B}(t)$ is the input uncertainty. The external disturbances and unknown uncertainties are set as

$$\Delta\boldsymbol{A}(t)=\begin{bmatrix}0.4\sin 2t & 0.2\cos 2t & 0.3\cos t\\ 0.1\sin 2t & 0.2\cos 2t & 0.1\cos t\\ 0.3\sin 2t & 0.3\cos 2t & 0.25\cos t\end{bmatrix},\ \Delta\boldsymbol{A}_d(t)=\begin{bmatrix}0.2\sin t & 0.2\cos t & 0.4\sin 3t\\ 0.2\sin t & -0.2\cos t & -0.1\sin 3t\\ 0.3\sin t & -0.1\cos t & 0.1\sin 3t\end{bmatrix}$$

$$\Delta\boldsymbol{B}(t)=\begin{bmatrix}0.4\sin t & 0.3\cos 3t\\ 0.15\sin t & 0.1\cos 3t\\ 0.35\sin t & 0.25\cos 3t\end{bmatrix},\text{ and }\ \boldsymbol{w}(\boldsymbol{x},t)=\begin{bmatrix}0.4x_1\sin x_1\\ 0.3x_2\cos x_2\\ 0.2x_1\sin x_1+0.3x_2\cos x_2\end{bmatrix}.$$

Notice that the triple $(\boldsymbol{A},\boldsymbol{B},\boldsymbol{C})$ has an invariant zero -1.3368 and $\operatorname{rank}(\boldsymbol{CB})=2$ satisfying Assumptions 4.2 and 4.3. For solving algebraic Riccati inequalities (4.44) and (4.45) of this example, select the parameters as $\gamma=0.01$, $\lambda=10$, $\boldsymbol{R}=0.02\boldsymbol{I}_2$, $\boldsymbol{Q}_{11}=2\boldsymbol{I}_3$, $\boldsymbol{Q}_{22}=0.002\boldsymbol{I}_3$, $\rho_1=0.333$, $\rho_2=1$, $\rho_3=0.6$, and $\rho_4=5$. Then a set of solutions is

$$\boldsymbol{P}_{11}=\begin{bmatrix}0.3684 & 0.2725 & -0.2493\\ 0.2725 & 0.9441 & -0.2735\\ -0.2493 & -0.2735 & 0.5813\end{bmatrix}\ \text{and}\ \boldsymbol{P}_{22}=\begin{bmatrix}8.8627 & 3.0587 & 0.2814\\ 3.0587 & 14.4483 & 4.4264\\ 0.2814 & 4.4264 & 4.3339\end{bmatrix}.$$

The parameters designed above all satisfy the requirement of Theorem 4.2. Hence, we construct the full-order compensator as

$$\dot{\xi}(t)=\begin{bmatrix}-5.0534 & -1.6143 & -0.1594\\ -1.6742 & -8.0701 & -2.6512\\ -0.1452 & -2.3519 & -2.3132\end{bmatrix}\xi(t)+\begin{bmatrix}0.0177 & -0.0188\\ -0.0532 & 0.0565\\ 0.1241 & -0.1318\end{bmatrix}\boldsymbol{y}(t)$$

$$\boldsymbol{v}(t)=\begin{bmatrix}-24.3778 & -13.5769 & -4.1372\\ -1.1628 & -33.5294 & -15.3885\end{bmatrix}\xi(t)+\begin{bmatrix}-1.4050 & -7.8788\\ -7.2577 & 1.8861\end{bmatrix}\boldsymbol{y}(t)$$

and design the sliding surface as

$$\boldsymbol{s}_1(t)=\begin{bmatrix}-0.0263 & 0.1842\\ 0.1579 & -0.1053\end{bmatrix}\left(\boldsymbol{y}(t)-\boldsymbol{y}(0)\right)-\int_0^t \boldsymbol{v}(q)\,dq\,.$$

Moreover, in order to avoid the chattering problem, the term $\dfrac{\boldsymbol{s}_1(t)}{\left\|\boldsymbol{s}_1(t)\right\|}$ in the controller (4.9) is replaced with the saturation function [11], and the new version of the controller is given by

$$\boldsymbol{u}(t)=\boldsymbol{v}(t)-\frac{1}{1-\chi}\left(\sigma_1+\sigma_2+\eta(t,\boldsymbol{y})+\chi\left\|\boldsymbol{v}(t)\right\|+\mu\right)\text{sat}\left(\boldsymbol{s}_1(t),\varepsilon\right)$$

where $\sigma_1=\sigma_2=5$, $\eta(t,\boldsymbol{y})=2$, $\chi=0.8$, $\mu=2.5$, and $\varepsilon=0.1$.

On the other hand, the controller in [28] was designed as

$$\boldsymbol{u}(t)=\boldsymbol{K}\boldsymbol{x}_e(t)-(\boldsymbol{G}\boldsymbol{B})^{-1}(0.1+\hat{\eta})\text{sat}\left(\frac{\boldsymbol{s}_2(t)}{0.1}\right)$$

where $\boldsymbol{K}=\begin{bmatrix}-0.2796 & -0.2580 & -0.1676\\ -0.1152 & -0.3624 & -0.1952\end{bmatrix}$ and $\boldsymbol{G}=\begin{bmatrix}0.02 & 0.1 & 0.04\\ 0.15 & 0.05 & 0\end{bmatrix}$. The parameter $\hat{\eta}=\hat{g}_0+\hat{g}_1\left\|\boldsymbol{y}(t)\right\|$ is obtained by the adaptation laws $\hat{g}_0=\int_0^t\left\|\boldsymbol{s}_2\right\|dt$ and $\hat{g}_0=\int_0^t\left\|\boldsymbol{y}\right\|\left\|\boldsymbol{s}_2\right\|dt$. The estimated state $\boldsymbol{x}_e(t)$ and the switching function $\boldsymbol{s}_2(t)$ are given by the following structure

$$\dot{\boldsymbol{x}}_e(t)=\boldsymbol{A}\boldsymbol{x}_e(t)+\boldsymbol{A}_d\boldsymbol{x}_e(t-\tau)+\boldsymbol{L}\left(\boldsymbol{y}(t)-\boldsymbol{C}\boldsymbol{x}_e(t)\right)$$
$$\boldsymbol{s}_2(t)=\boldsymbol{N}\left(\boldsymbol{y}(t)-\boldsymbol{C}\boldsymbol{x}_e(t)\right)+\boldsymbol{G}\boldsymbol{x}_e(t)-\boldsymbol{G}\int_0^t(\boldsymbol{A}+\boldsymbol{B}\boldsymbol{K})\boldsymbol{x}_e(q)\,dq-\boldsymbol{G}\int_0^t\boldsymbol{A}_d\boldsymbol{x}_e(q-\tau)\,dq$$

where $\boldsymbol{L}=\begin{bmatrix}0.3094 & 1.0149 & 2.0751\\ 1.7152 & -0.0940 & 0.3489\end{bmatrix}^T$ and $\boldsymbol{N}=\begin{bmatrix}0.02 & 0\\ 0 & 0.05\end{bmatrix}$. Figures 4.10-4.18 chart the simulation results using the initial state $\boldsymbol{x}(0)=[1 \quad 1 \quad 1]^T$ and $\xi(0)=\boldsymbol{x}_e(0)=[0 \quad 0 \quad 0]^T$. Time responses of system states in two cases are shown in Figs. 4.10-4.12 respectively. All states in both cases converge around zero. The time responses of the system outputs are shown in Figs. 4.13 and 4.14. All system outputs underlying these two methods converge around zero quickly, and two outputs controlled by the proposed method have no overshooting. Figure 4.15 charts the property of robust disturbance attenuation and demonstrates that the inequality (4.18) is guaranteed. Figure 4.16 depicts the comparison of the responses of $\|\boldsymbol{s}(t)\|$ in detail, which both trajectories of $\|\boldsymbol{s}(t)\|$ indeed enter the bounded layer around zero in a finite time, and the proposed method keeps the response $\|\boldsymbol{s}(t)\|$ in the layer consistently from the initial moment. The responses of the control inputs $\boldsymbol{u}(t)$ are given in Figs 4.17 and 4.18. There exists no high gain in all inputs and the replacement of the saturation function eliminates the chattering. Although there exists the state delay term and uncertainties in the nominal system, the system outputs are finally bounded around zero. The simulation results demonstrate that the proposed controller design can guarantee the robust disturbance attenuation to outputs $\boldsymbol{y}(t)$ once the system is in the sliding mode.

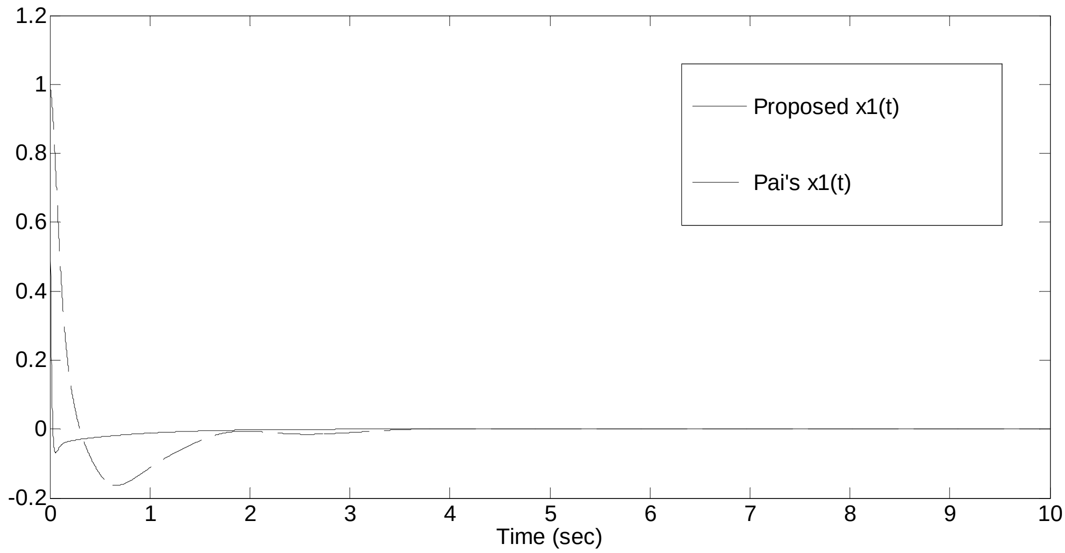

Fig. 4.10. System states $x_1(t)$ of two cases in Example 4.2.

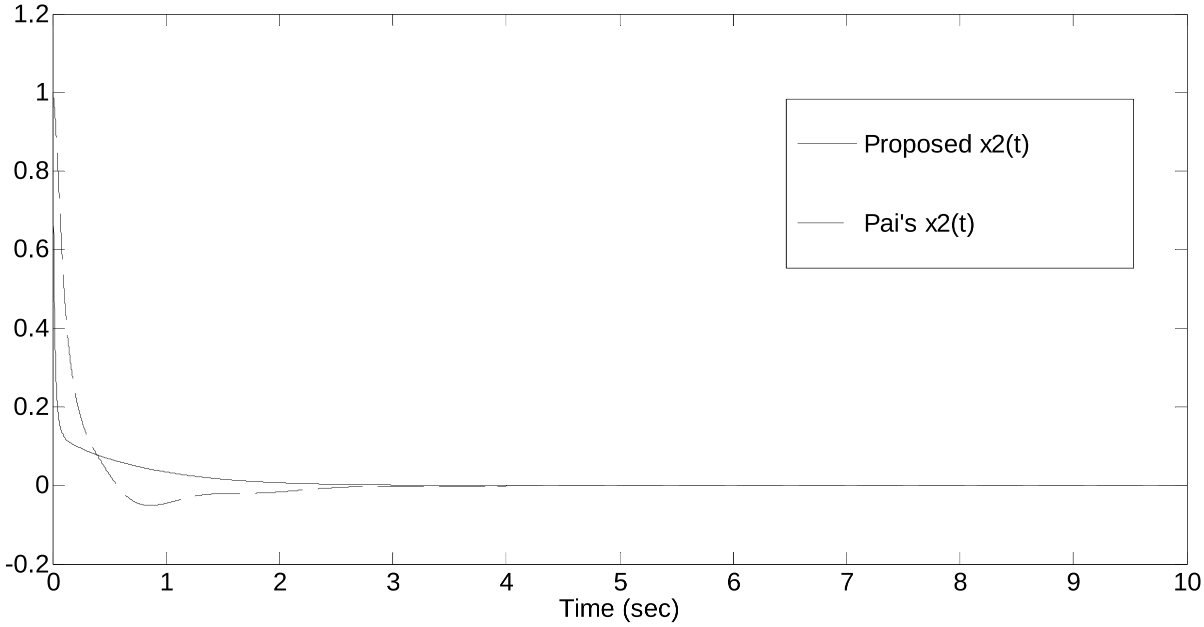

Fig. 4.11. System states $x_2(t)$ of two cases in Example 4.2.

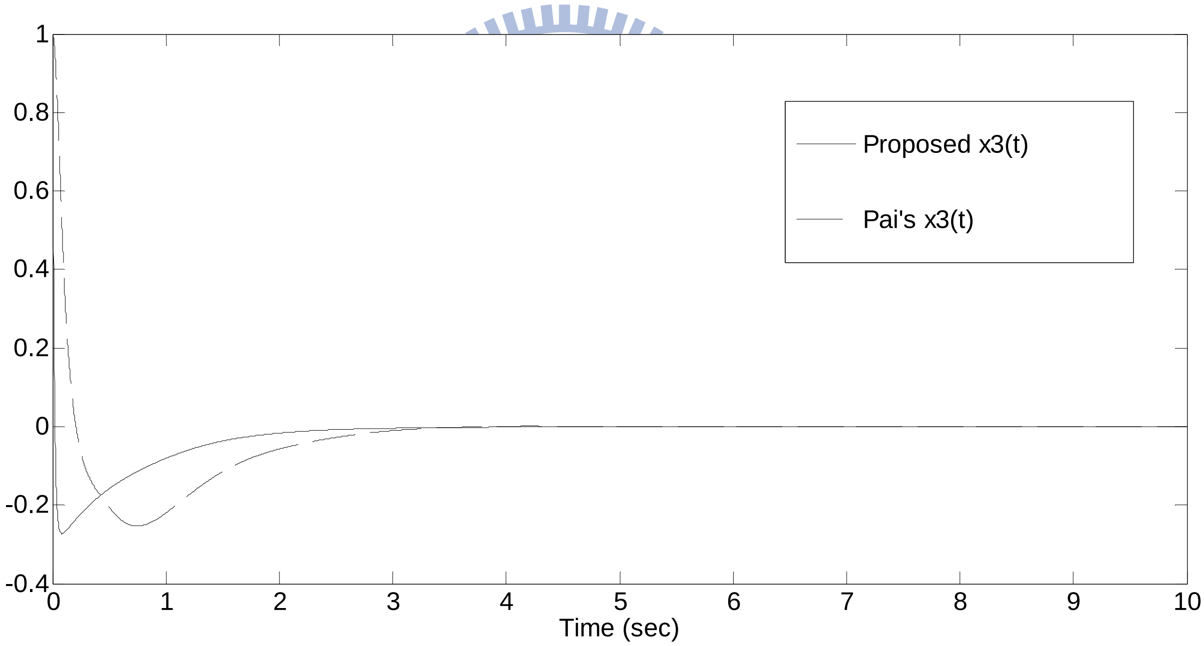

Fig. 4.12. System states $x_3(t)$ of two cases in Example 4.2.

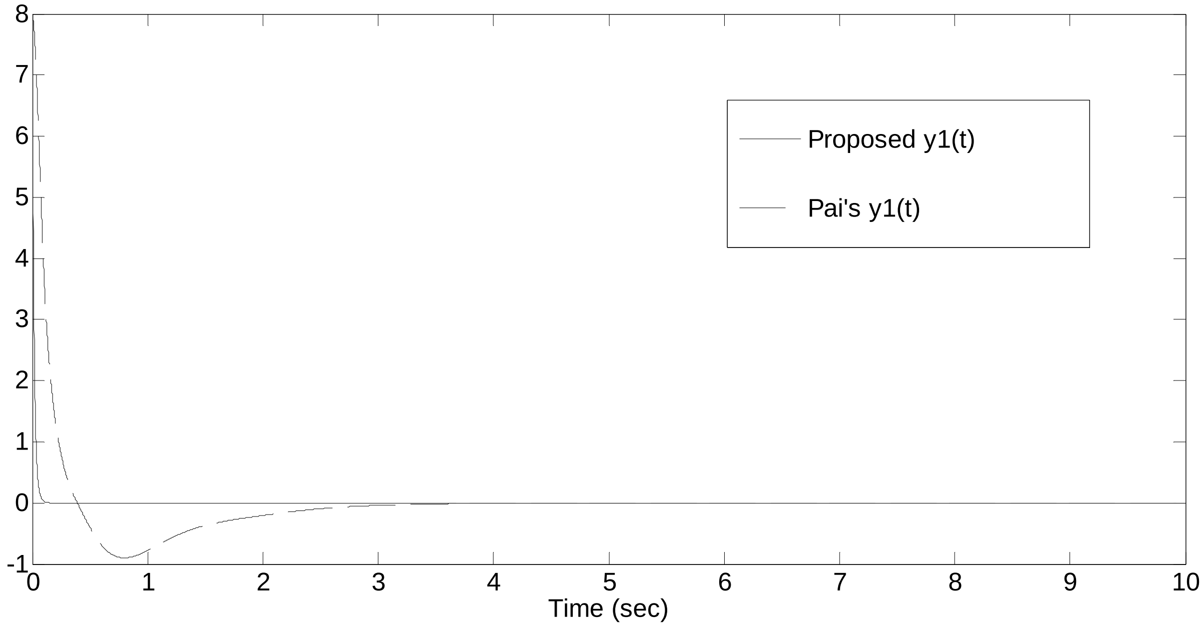

Fig. 4.13. System output $y_1(t)$ of two cases in Example 4.2.

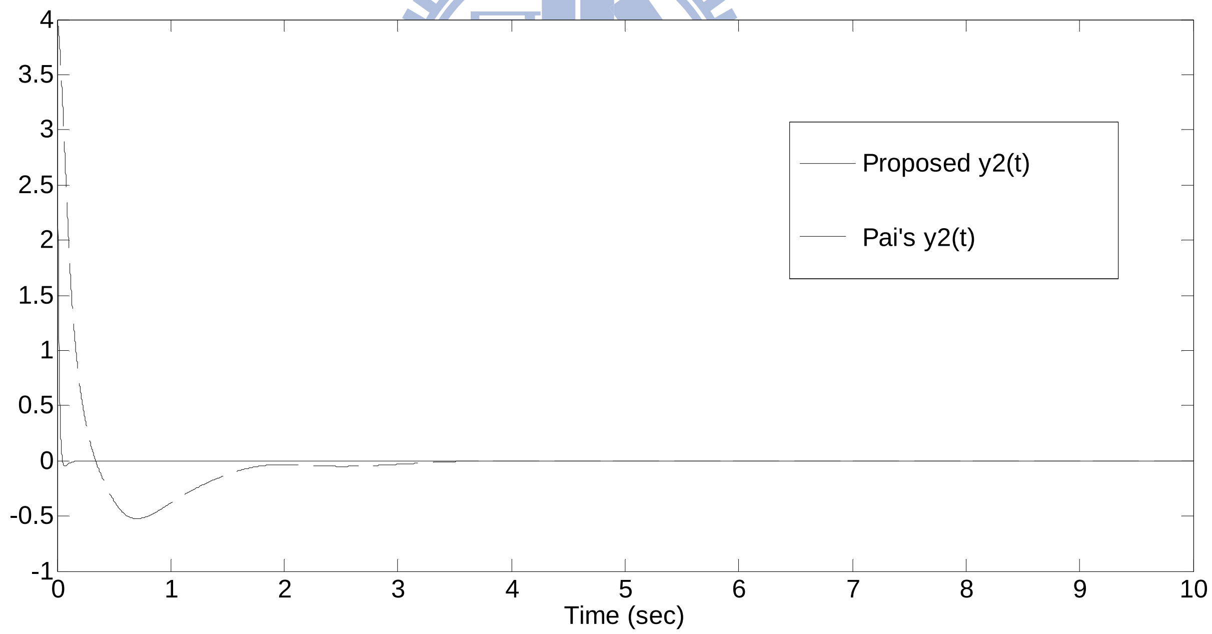

Fig. 4.14. System output $y_2(t)$ of two cases in Example 4.2.

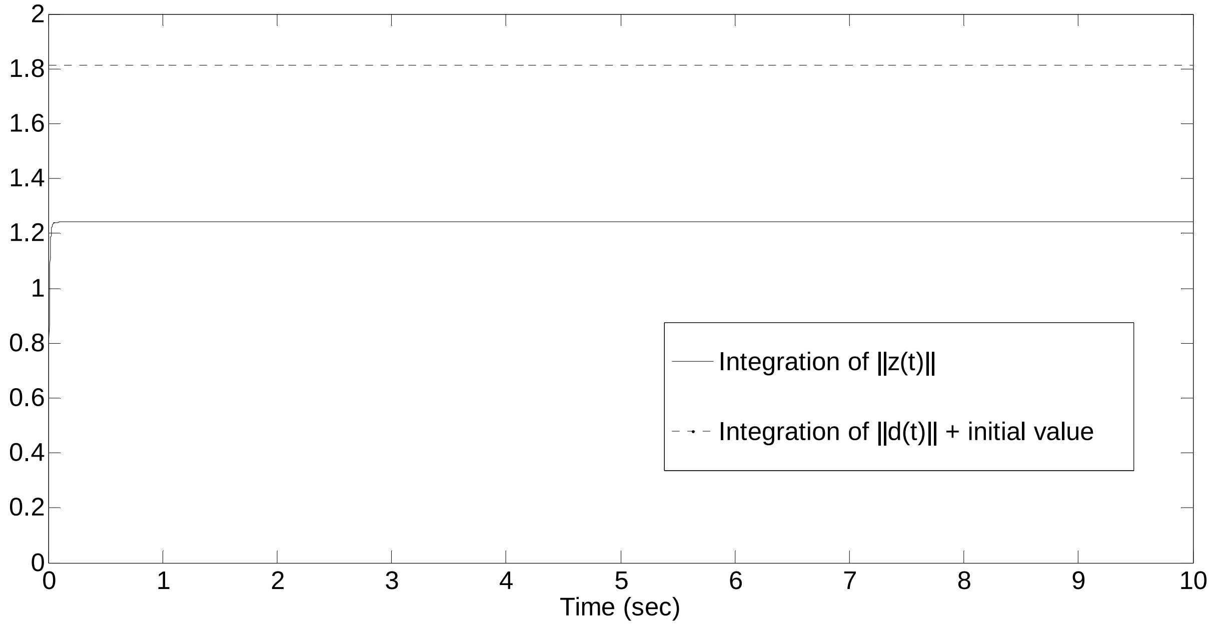

Fig. 4.15. Performance of robust disturbance attenuation of our proposed method in Example 4.2.

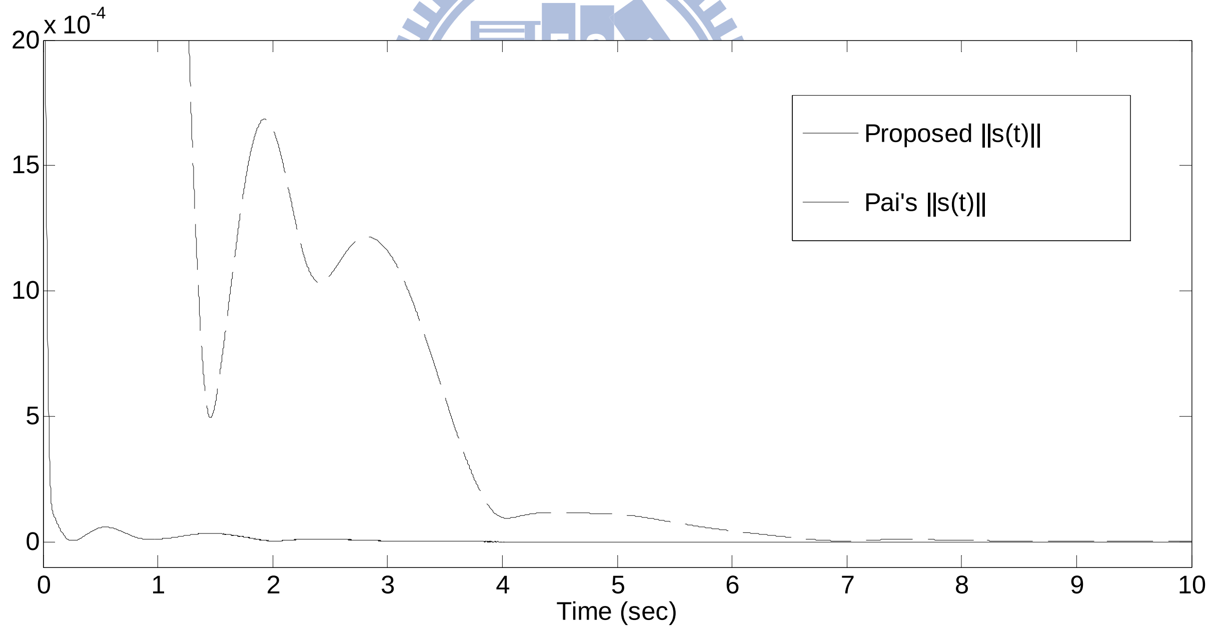

Fig. 4.16. Responses of $\|s(t)\|$ of two cases in Example 4.2.

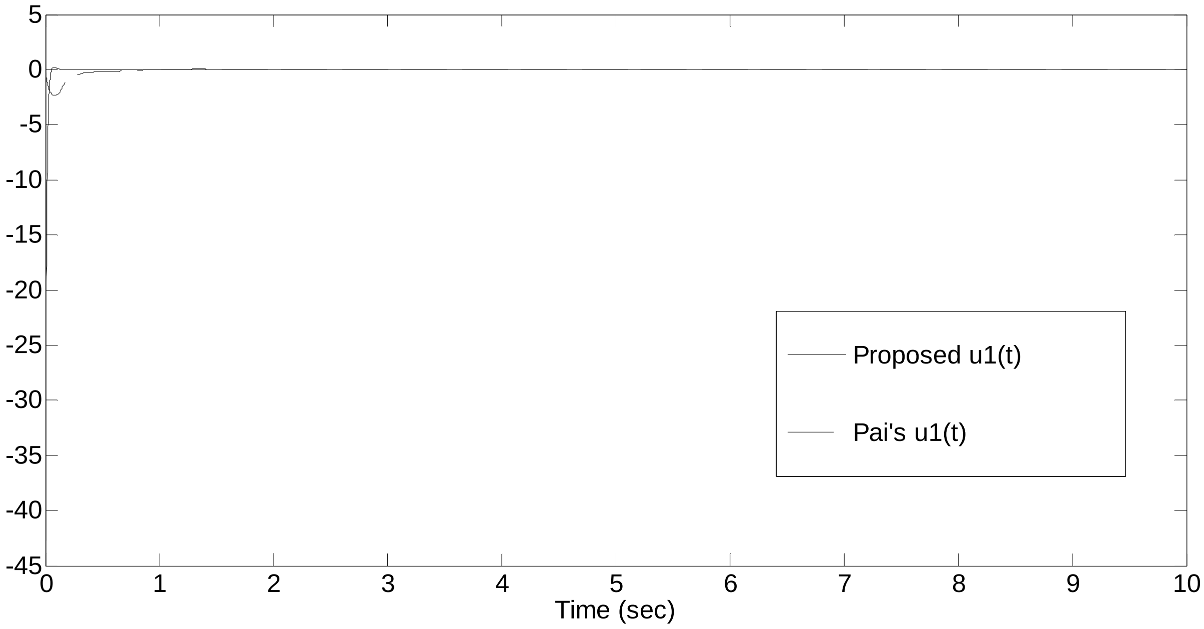

Fig. 4.17. Control inputs $u_1(t)$ of two cases in Example 4.2.

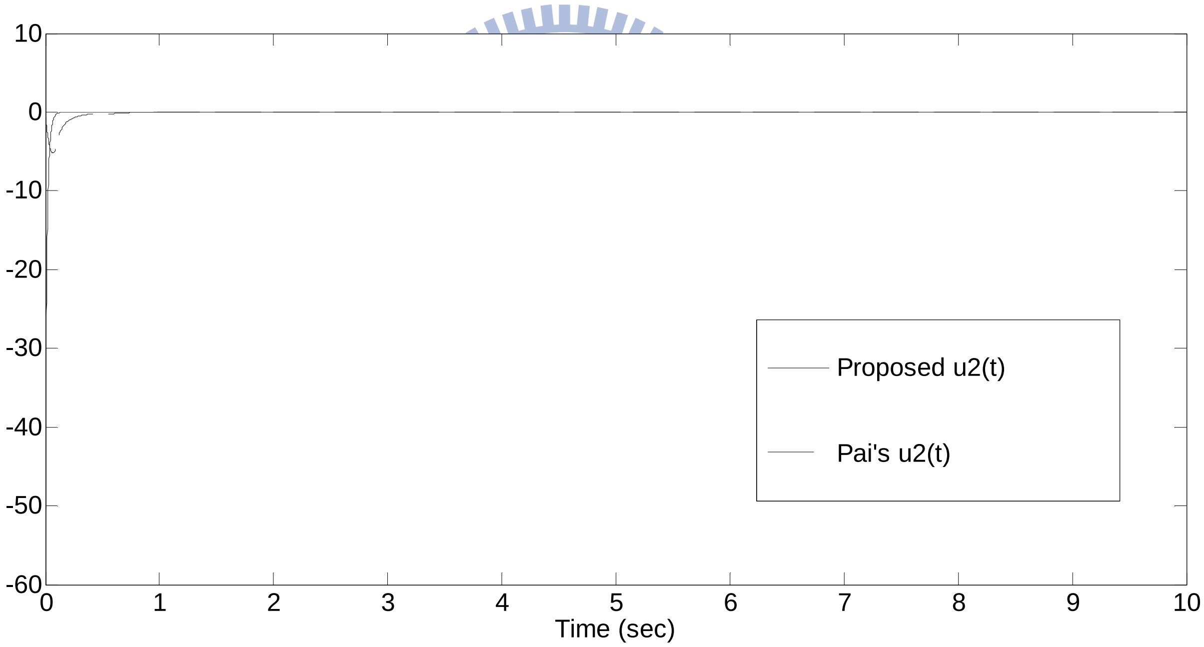

Fig. 4.18. Control inputs $u_2(t)$ of two cases in Example 4.2.

Example 4.3 Consider an unstable example modified from the real example of chemical reactor system [32] within the corresponding form of system (4.3) with delay time $\tau = 1$. The system structure and parameters are the same as Example 4.1, and matrix $\boldsymbol{A}$ is altered to

$$\boldsymbol{A} = \begin{bmatrix} -4.93 & -1.01 & 0 & 0 \\ -3.20 & 0.3 & -12.8 & 0 \\ -6.40 & 0.347 & -32.5 & -1.04 \\ 0 & 0.833 & 11.0 & -3.96 \end{bmatrix}$$

such that the open-loop system is unstable. For solving algebraic Riccati inequalities (4.44) and (4.45) of this example, select the parameters as $\gamma = 0.53$, $\lambda = 10$, $\boldsymbol{R} = 0.02\boldsymbol{I}_2$, $\boldsymbol{Q}_{11} = 2\boldsymbol{I}_4$, $\boldsymbol{Q}_{22} = 0.002\boldsymbol{I}_4$, $\rho_1 = 0.333$, $\rho_2 = 1$, $\rho_3 = 0.6$, and $\rho_4 = 5$ such that $\boldsymbol{Q}_{11} - \left(\rho_2^{-1} + \rho_4^{-1}\right)\boldsymbol{H}_d^T\boldsymbol{H}_d > 0$ and conditions in Theorem 4.2 are fulfilled. Then a set of solutions is

$$\boldsymbol{P}_{11} = \begin{bmatrix} 0.3493 & -0.0274 & -0.0731 & -0.0453 \\ -0.0274 & 0.3308 & 0.0096 & 0.0028 \\ -0.0731 & 0.0096 & 0.1228 & 0.1475 \\ -0.0453 & 0.0028 & 0.1475 & 0.3863 \end{bmatrix}$$

$$\boldsymbol{P}_{22} = \begin{bmatrix} 1.8870 & 0.0822 & 0.1077 & 0.4531 \\ 0.0822 & 2.0885 & -0.0778 & 0.2438 \\ 0.1077 & -0.0778 & 4.0664 & -0.3196 \\ 0.4531 & 0.2438 & -0.3196 & 0.3283 \end{bmatrix}.$$

Hence, we construct the full-order compensator as

$$\dot{\xi}(t) = \begin{bmatrix} -5.8010 & 0.1534 & -5.4216 & 0.0241 \\ -0.6640 & -2.4837 & -1.0249 & -0.0067 \\ -5.4708 & 0.3417 & -31.8148 & 0.0781 \\ 7.4909 & 0.8308 & 10.0792 & -2.3331 \end{bmatrix}\xi(t) + \begin{bmatrix} -1.2852 & 0.0760 \\ 0.0178 & -0.0706 \\ -6.4260 & 0.3802 \\ -0.1780 & 0.7062 \end{bmatrix}\boldsymbol{y}(t),$$

and design the sliding surface as

$$\boldsymbol{s}(t) = \boldsymbol{y}(t) - \boldsymbol{y}(0) - \int_0^t \begin{bmatrix} -17.4651 & 1.3691 & 3.6532 & 2.2646 \\ 1.3691 & -16.5404 & -0.4786 & -0.1376 \end{bmatrix}\xi(q)\,dq$$

$$-\int_0^t \begin{bmatrix} -17.4651 & 1.3691 \\ 1.3691 & -16.5404 \end{bmatrix} \boldsymbol{y}(q)\,dq.$$

For avoiding the chattering problem, the term $\boldsymbol{s}(t)/\|\boldsymbol{s}(t)\|$ in the controller is also replaced with the saturation function, and the new version of the controller is given by

$$\boldsymbol{u}(t) = \begin{bmatrix} -17.4651 & 1.3691 & 3.6532 & 2.2646 \\ 1.3691 & -16.5404 & -0.4786 & -0.1376 \end{bmatrix} \xi(t) + \begin{bmatrix} -17.4651 & 1.3691 \\ 1.3691 & -16.5404 \end{bmatrix} \boldsymbol{y}(t)$$
$$-\frac{1}{1-\chi}\left(\sigma_1 + \sigma_2 + \eta(t,\boldsymbol{y}) + \chi\|\boldsymbol{v}(t)\| + \psi\bar{d} + \mu\right)\mathrm{sat}\left(\boldsymbol{s}(t),\varepsilon\right)$$

where $\sigma_1 = \sigma_2 = 5$, $\eta(t,\boldsymbol{y}) = 2$, $\chi = \psi = 0.8$, $\bar{d} = 1$, $\mu = 2.5$, and $\varepsilon = 0.002$.

Figures 4.19-4.25 chart the simulation results of the new version of controller using the initial state $\boldsymbol{x}(0) = [2 \quad 3 \quad 4 \quad 1]^T$ and $\xi(0) = [0 \quad 0 \quad 0 \quad 0]^T$. Figure 4.19 depicts responses of system states. All trajectories of system states converge around zero. The time responses of the system outputs are shown in Fig. 4.20. The outputs also converge to zero quickly. The integrations of $\boldsymbol{z}^T(t)\boldsymbol{z}(t)$ and $d^2(t)$ are shown in Fig. 4.21. This figure verifies that robust disturbance attenuation (4.18) is guaranteed. Figures 4.22 and 4.23 illustrate $\boldsymbol{s}(t)$ and $\|\boldsymbol{s}(t)\|$, respectively. In Fig. 4.23, the controlled system can maintain in the sliding layer in the whole time. Figure 4.24 depicts that the trajectories of $\boldsymbol{e}(t)$ are bounded around zero and do not converge to zero as system states because of the mismatched disturbance. The responses of the control inputs $\boldsymbol{u}(t)$ are given in Fig. 4.25. The replacement of the saturation function eliminates the chattering. In Fig. 4.20, although the nominal system contains an unstable root, the state delay term, and the mismatched disturbance, the system outputs $\boldsymbol{y}(t)$ are finally bounded around zero. The simulation results demonstrated that the proposed controller design can guarantee the robust disturbance attenuation to outputs $\boldsymbol{y}(t)$ once the system is in the sliding mode.

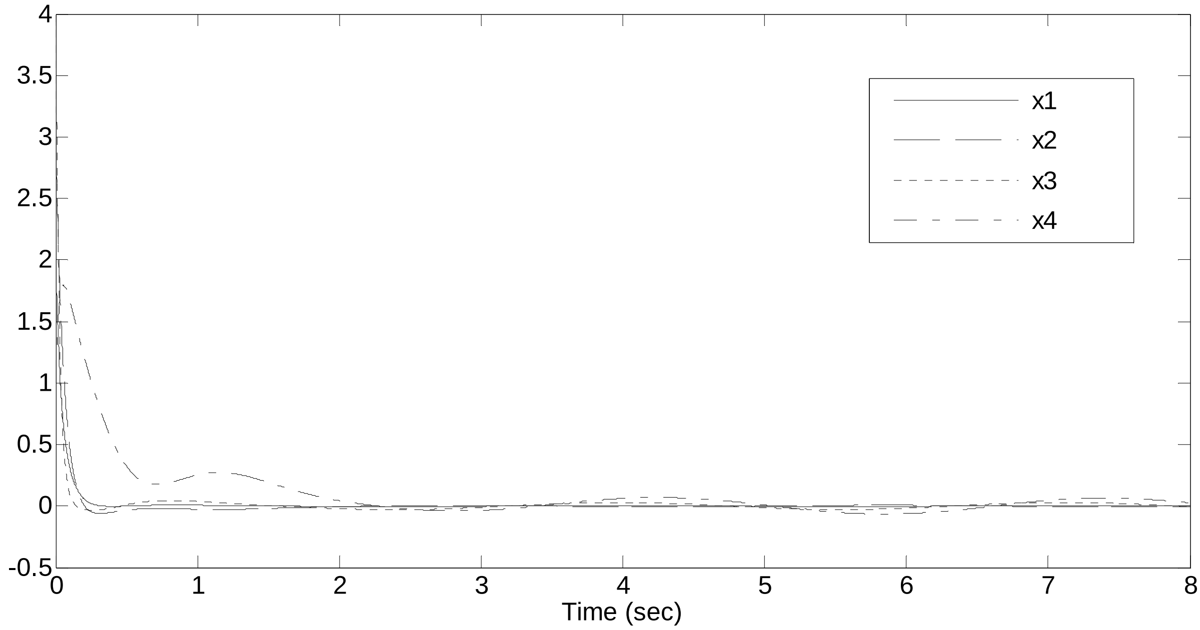

Fig. 4.19. System states in Example 4.3.

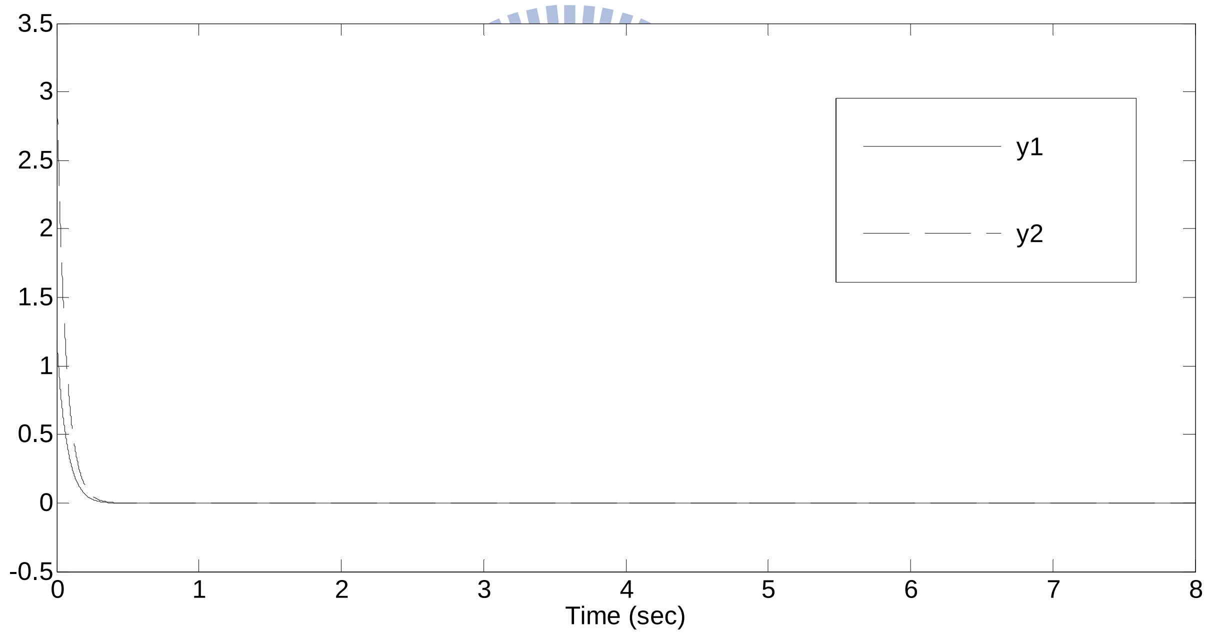

Fig. 4.20. System outputs in Example 4.3.

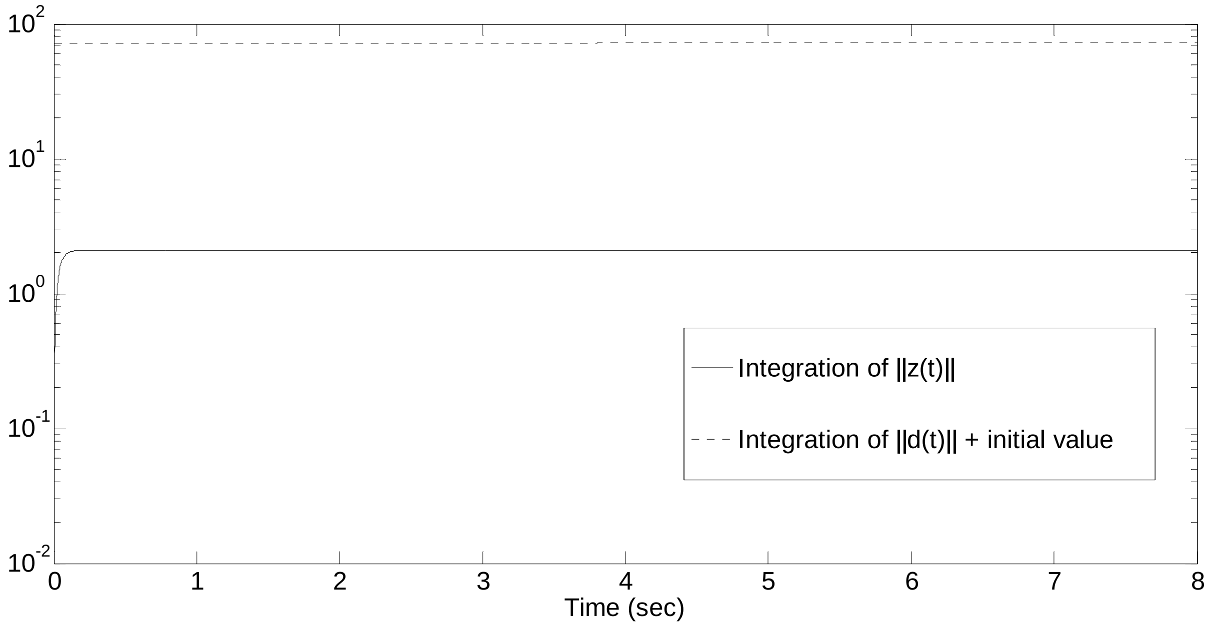

Fig. 4.21. Performance of robust disturbance attenuation in Example 4.3.

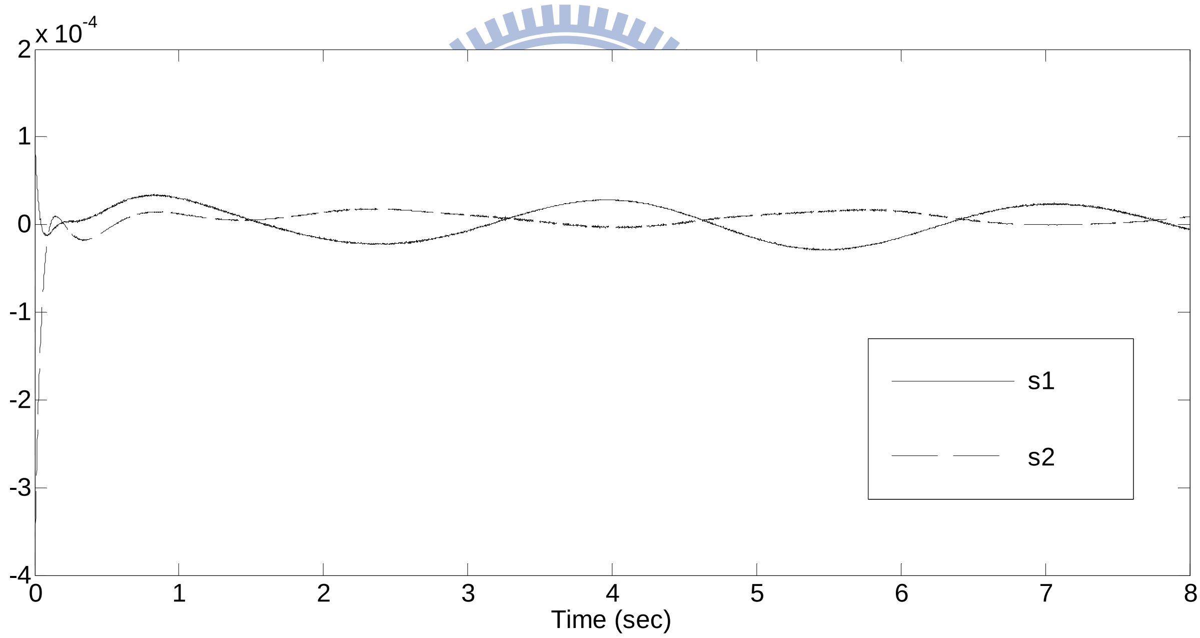

Fig. 4.22. Sliding functions in Example 4.3.

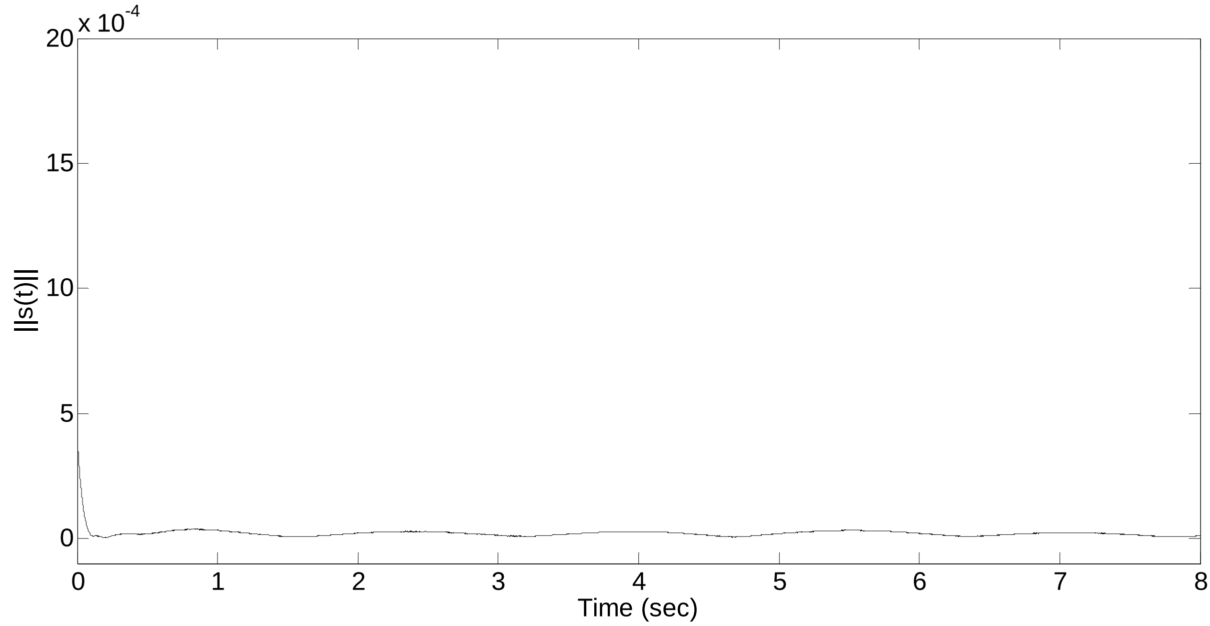

Fig. 4.23. Response of $\|\boldsymbol{s}(t)\|$ in Example 4.3.

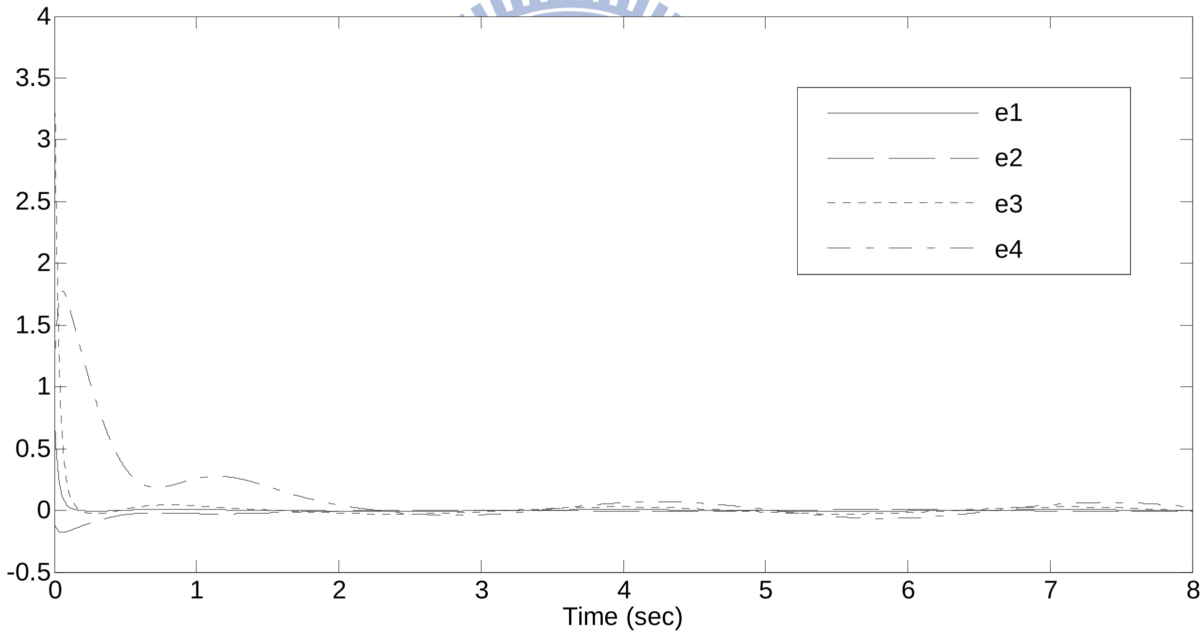

Fig. 4.24. Trajectories of $\boldsymbol{e}(t)$ in Example 4.3.

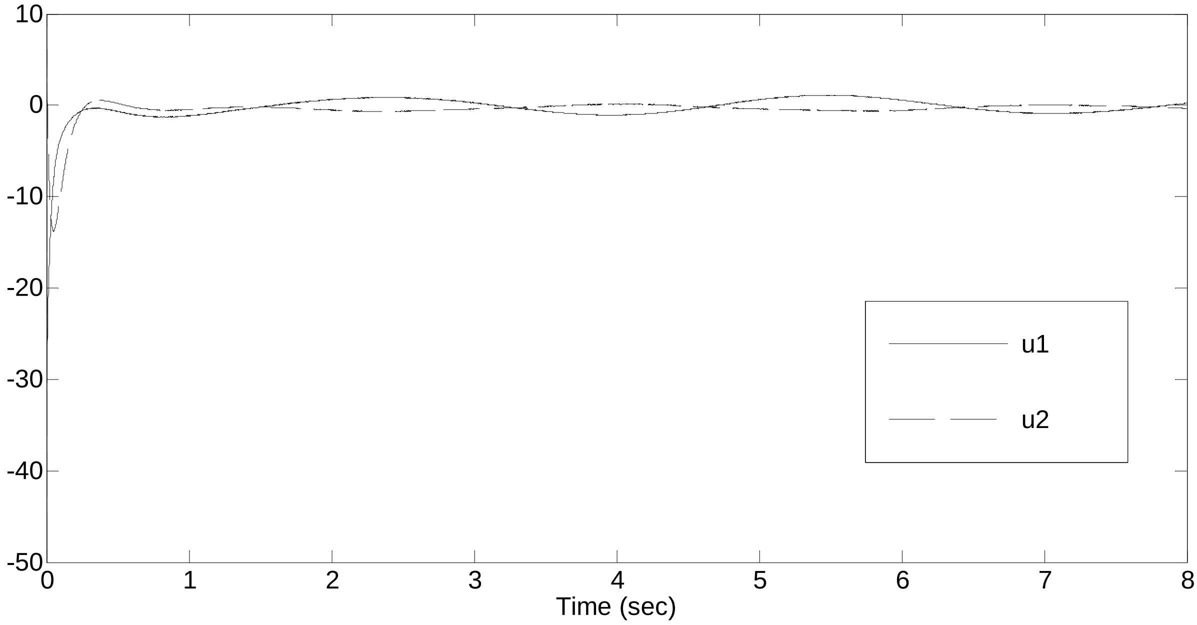

Fig. 4.25. System inputs in Example 4.3.

4.4 Robust Stability in the Sliding Mode for Delay-Dependent Condition

Define an unknown time-varying function $\tau(t) \in \mathbb{R}$ as the state delay time satisfying

$$0 < \tau(t) \le \bar{\tau} \quad \text{and} \quad \dot{\tau}(t) \le \tau^* \tag{4.54}$$

where $\bar{\tau}$ and τ^* are known bounds of the delay time and its derivative. Altering τ by $\tau(t)$, the system (4.3) can be rewritten as

$$\begin{aligned} \dot{\boldsymbol{x}}(t) &= \left(\boldsymbol{A} + \boldsymbol{D}\Phi(t)\boldsymbol{H}\right)\boldsymbol{x}(t) + \left(\boldsymbol{A}_d + \boldsymbol{D}_d\Phi_d(t)\boldsymbol{H}_d\right)\boldsymbol{x}\left(t - \tau(t)\right) \\ &\quad + \boldsymbol{B}\left(\boldsymbol{u}(t) + \boldsymbol{f}(\boldsymbol{x}, \boldsymbol{u}, t)\right) + \boldsymbol{Ed}(t) \\ \boldsymbol{y}(t) &= \boldsymbol{Cx}(t). \end{aligned} \tag{4.55}$$

Among the delay-dependent condition, the autonomous system $\dot{\boldsymbol{x}}(t) = \boldsymbol{Ax}(t) + \boldsymbol{A}_d\boldsymbol{x}\left(t - \tau(t)\right)$ is stable for some $\tau(t)$; otherwise, the system is unstable for the other delay time — the stability of system depends on the delay time. The integral sliding surface (4.5), controller (4.9), and full-order compensator (4.23) are continued using. The closed-loop system with time-varying delay in the sliding mode is modified as

$$\begin{bmatrix} \dot{\boldsymbol{x}}(t) \\ \dot{\boldsymbol{e}}(t) \end{bmatrix} = \begin{bmatrix} \boldsymbol{NA} - \boldsymbol{BK} + \boldsymbol{ND}\Phi(t)\boldsymbol{H} & \boldsymbol{BK} \\ \boldsymbol{MD}\Phi(t)\boldsymbol{H} & \boldsymbol{MA} - \boldsymbol{LC} \end{bmatrix} \begin{bmatrix} \boldsymbol{x}(t) \\ \boldsymbol{e}(t) \end{bmatrix} + \begin{bmatrix} \boldsymbol{NE} \\ \boldsymbol{ME} \end{bmatrix} \boldsymbol{d}(t) + \begin{bmatrix} \boldsymbol{NA}_d + \boldsymbol{ND}_d\Phi_d(t)\boldsymbol{H}_d & \boldsymbol{0} \\ \boldsymbol{MA}_d + \boldsymbol{MD}_d\Phi_d(t)\boldsymbol{H}_d & \boldsymbol{0} \end{bmatrix} \begin{bmatrix} \boldsymbol{x}(t-\tau(t)) \\ \boldsymbol{e}(t-\tau(t)) \end{bmatrix} \tag{4.56}$$

$$\boldsymbol{z}(t) = \boldsymbol{C}_w \begin{bmatrix} \boldsymbol{x}(t) \\ \boldsymbol{e}(t) \end{bmatrix}. \tag{4.57}$$

Before introducing main results, an extra assumption is introduced.

Assumption 4.4: The delay time and its derivative are bounded, $0 < \tau(t) \le \bar{\tau}$ and $\dot{\tau}(t) \le \tau^* < 1$ where $\bar{\tau}$ and τ^* are known constants.

Defining a new state vector $\boldsymbol{q}(t) = \begin{bmatrix} \boldsymbol{x}(t) \\ \boldsymbol{e}(t) \end{bmatrix}$, the dynamics (4.56) and (4.57) can be expressed as

$$\begin{aligned} \dot{\boldsymbol{q}}(t) &= \tilde{\boldsymbol{A}}\boldsymbol{q}(t) + \tilde{\boldsymbol{A}}_d\boldsymbol{q}(t-\tau(t)) + \tilde{\boldsymbol{D}}\boldsymbol{d}(t) \\ \boldsymbol{z}(t) &= \boldsymbol{C}_w\boldsymbol{q}(t) \end{aligned} \tag{4.58}$$

where $\tilde{\boldsymbol{A}} = \begin{bmatrix} \boldsymbol{NA} - \boldsymbol{BK} + \boldsymbol{ND}\Phi(t)\boldsymbol{H} & \boldsymbol{BK} \\ \boldsymbol{MD}\Phi(t)\boldsymbol{H} & \boldsymbol{MA} - \boldsymbol{LC} \end{bmatrix}$, $\tilde{\boldsymbol{A}}_d = \begin{bmatrix} \boldsymbol{NA}_d + \boldsymbol{ND}_d\Phi_d(t)\boldsymbol{H}_d & \boldsymbol{0} \\ \boldsymbol{MA}_d + \boldsymbol{MD}_d\Phi_d(t)\boldsymbol{H}_d & \boldsymbol{0} \end{bmatrix}$, and $\tilde{\boldsymbol{D}} = \begin{bmatrix} \boldsymbol{NE} \\ \boldsymbol{ME} \end{bmatrix}$. The following lemma is cited to complete the stability analysis in Theorem 4.3.

Lemma 4.2 (Jensen inequality) [62] For any constant matrix $\boldsymbol{M} \in \mathbb{R}^{m\times m}$, $\boldsymbol{M} = \boldsymbol{M}^T > 0$, scalar $\gamma > 0$, and vector function $\omega : [0, \gamma] \to \mathbb{R}^m$ such that the integrations concerned are well defined, then

$$\gamma \int_0^\gamma \omega^T(\beta)\boldsymbol{M}\omega(\beta)d\beta \ge \left(\int_0^\gamma \omega(\beta)d\beta\right)^T \boldsymbol{M} \left(\int_0^\gamma \omega(\beta)d\beta\right). \quad \square$$

For the closed-loop system (4.58), the following theorem presents the stability criterion and the design of matrices $\boldsymbol{K}$ and $\boldsymbol{L}$.

Theorem 4.3 Consider the system (4.58) in the sliding mode with the full-order compensator

(4.23). Given λ, $\rho_i > 0$, $i = 1, 2, \cdots, 11$, and a positive definite matrix $\boldsymbol{R}$, if there exists $\boldsymbol{P}_{11} > 0$, $\boldsymbol{P}_{22} \geq \boldsymbol{I}$, $\boldsymbol{Q}_{11} > 0$, $\boldsymbol{Q}_{11} + \dfrac{1}{\overline{\tau}}\boldsymbol{Z}_1 > \dfrac{\rho_3^{-1} + \rho_4^{-1} + \rho_7^{-1} + \rho_8^{-1}}{1 - \tau^*}\boldsymbol{H}_d^T\boldsymbol{H}_d$, $\boldsymbol{Q}_{22} > 0$, $\boldsymbol{Z}_1 > 0$, $\boldsymbol{Z}_2 > 0$, and a scalar $\gamma > 0$, satisfying the following LMI

$$
\begin{bmatrix}
\Psi_{11} & \mathbf{0} & \Psi_{13} & \mathbf{0} & \Psi_{15} & \Psi_{16} & \mathbf{0} & \Psi_{18} & \mathbf{0} & \mathbf{0} & \mathbf{0} \\
* & \Psi_{22} & \Psi_{23} & \Psi_{24} & \Psi_{25} & \mathbf{0} & \Psi_{27} & \mathbf{0} & \Psi_{29} & \mathbf{0} & \mathbf{0} \\
* & * & \Psi_{33} & \mathbf{0} & \mathbf{0} & \Psi_{36} & \Psi_{37} & \mathbf{0} & \mathbf{0} & \mathbf{0} & \mathbf{0} \\
* & * & * & \Psi_{44} & \mathbf{0} & \mathbf{0} & \mathbf{0} & \mathbf{0} & \mathbf{0} & \mathbf{0} & \mathbf{0} \\
* & * & * & * & \Psi_{55} & \Psi_{56} & \Psi_{57} & \mathbf{0} & \mathbf{0} & \mathbf{0} & \mathbf{0} \\
* & * & * & * & * & \Psi_{66} & \mathbf{0} & \mathbf{0} & \mathbf{0} & \Psi_{6a} & \mathbf{0} \\
* & * & * & * & * & * & \Psi_{77} & \mathbf{0} & \mathbf{0} & \mathbf{0} & \Psi_{7b} \\
* & * & * & * & * & * & * & \Psi_{88} & \mathbf{0} & \mathbf{0} & \mathbf{0} \\
* & * & * & * & * & * & * & * & \Psi_{99} & \mathbf{0} & \mathbf{0} \\
* & * & * & * & * & * & * & * & * & \Psi_{aa} & \mathbf{0} \\
* & * & * & * & * & * & * & * & * & * & \Psi_{bb}
\end{bmatrix} < 0 \qquad (4.59)
$$

where

$$\Psi_{11} = \boldsymbol{P}_{11}\boldsymbol{NA} + (\boldsymbol{NA})^T\boldsymbol{P}_{11} + \boldsymbol{C}^T\boldsymbol{C} + \left(\rho_1^{-1} + \rho_2^{-1} + \rho_5^{-1} + \rho_6^{-1}\right)\boldsymbol{H}^T\boldsymbol{H} - \overline{\tau}^{-1}\left(1 - \tau^*\right)\boldsymbol{Z}_1 + \boldsymbol{Q}_{11}$$

$$\Psi_{22} = \boldsymbol{P}_{22}\boldsymbol{MA} + (\boldsymbol{MA})^T\boldsymbol{P}_{22} - \lambda\boldsymbol{C}^T\boldsymbol{C} - \overline{\tau}^{-1}\left(1 - \tau^*\right)\boldsymbol{Z}_2 + \boldsymbol{Q}_{22} + \rho_{11}\frac{\lambda^2}{4}\boldsymbol{C}^T\boldsymbol{C}\boldsymbol{C}^T\boldsymbol{C}$$

$$\Psi_{13} = \boldsymbol{P}_{11}\boldsymbol{NA}_d - \overline{\tau}^{-1}\left(1 - \tau^*\right)\boldsymbol{Z}_1$$

$$\Psi_{23} = \boldsymbol{P}_{22}\boldsymbol{MA}_d$$

$$\Psi_{33} = \left(\rho_3^{-1} + \rho_4^{-1} + \rho_7^{-1} + \rho_8^{-1}\right)\boldsymbol{H}_d^T\boldsymbol{H}_d - \left(1 - \tau^*\right)\left(\boldsymbol{Q}_{11} + \overline{\tau}^{-1}\boldsymbol{Z}_1\right)$$

$$\Psi_{24} = -\overline{\tau}^{-1}\left(1 - \tau^*\right)\boldsymbol{Z}_2$$

$$\Psi_{44} = -\left(1 - \tau^*\right)\left(\boldsymbol{Q}_{22} + \overline{\tau}^{-1}\boldsymbol{Z}_2\right)$$

$$\Psi_{15} = \boldsymbol{P}_{11}\boldsymbol{NE}$$

$$\Psi_{25} = \boldsymbol{P}_{22}\boldsymbol{ME}$$

$$\Psi_{55} = -\gamma^2\boldsymbol{I}$$

$$\Psi_{16} = \bar{\tau}\left(\boldsymbol{NA}\right)^T \boldsymbol{Z}_1$$

$$\Psi_{36} = \bar{\tau}\left(\boldsymbol{NA}_d\right)^T \boldsymbol{Z}_1$$

$$\Psi_{56} = \bar{\tau}\left(\boldsymbol{NE}\right)^T \boldsymbol{Z}_1$$

$$\Psi_{66} = -\bar{\tau}\boldsymbol{Z}_1$$

$$\Psi_{27} = \bar{\tau}\left(\boldsymbol{MA}\right)^T \boldsymbol{Z}_2$$

$$\Psi_{37} = \bar{\tau}\left(\boldsymbol{MA}_d\right)^T \boldsymbol{Z}_2$$

$$\Psi_{57} = \bar{\tau}\left(\boldsymbol{ME}\right)^T \boldsymbol{Z}_2$$

$$\Psi_{77} = -\bar{\tau}\boldsymbol{Z}_2$$

$$\Psi_{18} = \left[\boldsymbol{P}_{11}\boldsymbol{ND} \quad \boldsymbol{P}_{11}\boldsymbol{ND}_d \quad \bar{\tau}\boldsymbol{P}_{11}\boldsymbol{B}\right]$$

$$\Psi_{88} = -\mathrm{diag}\left(\rho_1^{-1}\boldsymbol{I}, \rho_3^{-1}\boldsymbol{I}, \rho_9^{-1}\boldsymbol{I}\right)$$

$$\Psi_{29} = \left[\boldsymbol{P}_{11}\boldsymbol{B} \quad \boldsymbol{P}_{22}\boldsymbol{MD} \quad \boldsymbol{P}_{22}\boldsymbol{MD}_d \quad \bar{\tau}\boldsymbol{P}_{11}\boldsymbol{B}\right]$$

$$\Psi_{99} = -\mathrm{diag}\left(\boldsymbol{R}, \rho_2^{-1}\boldsymbol{I}, \rho_4^{-1}\boldsymbol{I}, \rho_{10}^{-1}\boldsymbol{I}\right)$$

$$\Psi_{6a} = \left[\bar{\tau}\boldsymbol{Z}_1\boldsymbol{ND} \quad \bar{\tau}\boldsymbol{Z}_1\boldsymbol{ND}_d \quad \boldsymbol{Z}_1\boldsymbol{BR}^{-1}\right]$$

$$\Psi_{aa} = -\mathrm{diag}\left(\rho_5^{-1}\boldsymbol{I}, \rho_7^{-1}\boldsymbol{I}, \left(\rho_9^{-1} + \rho_{10}^{-1}\right)^{-1}\boldsymbol{I}\right)$$

$$\Psi_{7b} = \left[\bar{\tau}\boldsymbol{Z}_2\boldsymbol{MD} \quad \bar{\tau}\boldsymbol{Z}_2\boldsymbol{MD}_d \quad \bar{\tau}\boldsymbol{Z}_2\right]$$

$$\Psi_{bb} = -\mathrm{diag}\left(\rho_6^{-1}\boldsymbol{I}, \rho_8^{-1}\boldsymbol{I}, \rho_{11}\boldsymbol{I}\right)$$

then robust disturbance attenuation (4.18) can be guaranteed. Furthermore, matrices $\boldsymbol{K}$ and $\boldsymbol{L}$ are given by

$$\boldsymbol{K} = \boldsymbol{R}^{-1}\boldsymbol{B}^T\boldsymbol{P}_{11} \quad \text{and} \quad \boldsymbol{L} = \frac{\lambda}{2}\boldsymbol{P}_{22}^{-1}\boldsymbol{C}^T. \tag{4.60}$$

Proof: The detail is in Appendix 2. □

The method determining matrices $\boldsymbol{K}$ and $\boldsymbol{L}$ is similar to Remark 4.2 by replacing (4.30) with (4.59). Choose suitable parameters λ, ρ_i for $i=1,2,\cdots,11$, and $\boldsymbol{R}$ to obtain $\boldsymbol{P}_{11}$ and $\boldsymbol{P}_{22}$ in (4.59). Of course all solutions to (4.59) must satisfy the requirement in Theorem 4.3. The following example demonstrates the proposed method.

Example 4.4 Refer to the real example of chemical reactor system [32] within the corresponding form of system (4.55) as

$$\boldsymbol{A}=\begin{bmatrix} -4.93 & -1.01 & 0 & 0 \\ -3.20 & -5.30 & -12.8 & 0 \\ -6.40 & 0.347 & -32.5 & -1.04 \\ 0 & 0.833 & 11.0 & -3.96 \end{bmatrix},\ \boldsymbol{B}=\begin{bmatrix} 1 & 0 \\ 0 & 1 \\ 0 & 0 \\ 0 & 0 \end{bmatrix},\ \boldsymbol{C}=\begin{bmatrix} 0.1 & 0 \\ 0 & 0.5 \\ -0.2 & 0 \\ 0 & 0.1 \end{bmatrix}^T,\ \boldsymbol{E}=\begin{bmatrix} 1 \\ 0 \\ 1 \\ 0 \end{bmatrix},$$

and $\boldsymbol{A}_d=\operatorname{diag}(1.92, 1.92, 1.87, 0.724)$. The known parts of uncertainties in the system are given by

$$\boldsymbol{D}=\begin{bmatrix} -0.47 & 1.01 & 0 & 0 \\ -0.22 & -0.17 & 1.21 & 0 \\ 0.63 & 0.347 & 0.91 & -1.04 \\ 0 & 0 & 0.14 & -0.96 \end{bmatrix},\ \boldsymbol{H}=\begin{bmatrix} -0.55 & -0.02 & 0 & 0 \\ 0.78 & -0.35 & 0 & 0 \\ 0 & -0.72 & -0.49 & 0 \\ 0 & 0.33 & -0.54 & -0.39 \end{bmatrix},$$

$\boldsymbol{D}_d=\operatorname{diag}(0.47, 0.26, -0.85, 1.53)$, and $\boldsymbol{H}_d=\operatorname{diag}(-1.11, -0.21, 1.26, 0.47)$. The external disturbances and unknown parts of uncertainties for system (4.55) are set as $\Phi(t)=r_1(t)\boldsymbol{I}_4$, $\Phi_d(t)=r_2(t)\boldsymbol{I}_4$, $d(t)=e^{-0.001t}\sin 2t$, and

$$\boldsymbol{f}(\boldsymbol{x},\boldsymbol{u},t)=\begin{bmatrix} 0.12u_1\sin t+0.08u_2\cos 1.3t+0.2\sin x_1 \\ 0.07u_1\cos 3t+0.03u_2\sin 5t+0.3\cos x_2 \end{bmatrix}$$

where $\boldsymbol{u}=\begin{bmatrix} u_1^T & u_2^T \end{bmatrix}$, $r_1(t)$ and $r_2(t)$ are different random functions with values between -1 and 1. The time-varying delay is set as $\tau(t)=0.4\cos t+0.5>0$ with $\bar{\tau}=1$ and $\tau^*=0.5$. Notice that the triple $(\boldsymbol{A},\boldsymbol{B},\boldsymbol{C})$ has invariant zeros -4.4252 and -45.0014, and $\operatorname{rank}(\boldsymbol{CB})=2$, satisfying Assumptions 4.2 and 4.3.

For solving the corresponding LMI (4.59) of this example, select the parameters as $\lambda = 1.5$, $\boldsymbol{R} = 0.01\boldsymbol{I}_2$, $\rho_i = 10$ for $i = 1, \cdots, 8$, $\rho_9 = \rho_{10} = 0.1$, and $\rho_{11} = 28$. Then the solutions are given by

$$\boldsymbol{P}_{11} = \begin{bmatrix} 5.0181 & -1.2310 & -5.4493 & 6.5153 \\ -1.2310 & 4.3124 & 1.2474 & -2.9403 \\ -5.4493 & 1.2474 & 22.3435 & -7.0087 \\ 6.5153 & -2.9403 & -7.0087 & 19.4398 \end{bmatrix}$$

$$\boldsymbol{P}_{22} = \begin{bmatrix} 6.8922 & -1.4873 & -8.9189 & 7.0708 \\ -1.4873 & 28.0807 & 1.5531 & 1.1411 \\ -8.9189 & 1.5531 & 28.5323 & -7.7643 \\ 7.0708 & 1.1411 & -7.7643 & 20.9222 \end{bmatrix}$$

$$\boldsymbol{Q}_{22} = \begin{bmatrix} 11.4726 & -2.8032 & 6.7521 & 11.8654 \\ -2.8032 & 5.3647 & 0.4501 & -5.6781 \\ 6.7521 & 0.4501 & 38.2936 & -2.5132 \\ 11.8654 & -5.6781 & -2.5132 & 26.8219 \end{bmatrix}$$

$$\boldsymbol{Z}_1 = \begin{bmatrix} 0.004 & 0 & -0.007 & -0.0007 \\ 0 & 0.0041 & 0 & 0.0009 \\ -0.007 & 0 & 1.0984 & 0.9233 \\ -0.0007 & 0.0009 & 0.9233 & 4.1742 \end{bmatrix}$$

$$\boldsymbol{Z}_2 = \begin{bmatrix} 0.022 & 0.0005 & -0.0005 & -0.0021 \\ 0.0005 & 0.0221 & 0 & 0.001 \\ -0.0005 & 0 & 0.0174 & 0.0001 \\ -0.0021 & 0.001 & 0.0001 & 0.0174 \end{bmatrix}$$

and $\boldsymbol{Q}_{11} = 5\boldsymbol{I}_4$ satisfying the sufficient condition in Theorem 4.3. Notice that the finite performance index γ is 0.9598 in this case. Hence, we construct the full-order compensator as

$$\dot{\xi}(t) = \begin{bmatrix} -12.8013 & 0.694 & -64.9973 & -2.08 \\ -0.0001 & -0.1733 & -2.1998 & 0.7907 \\ -6.3997 & 0.347 & -32.5005 & -1.04 \\ 0.0006 & 0.8315 & 10.9989 & -3.9603 \end{bmatrix} \xi(t) + \begin{bmatrix} -128 & 1.388 \\ 0 & -0.3332 \\ -64 & 0.694 \\ 0 & 1.666 \end{bmatrix} \boldsymbol{y}(t)$$

and design the sliding surface as

$$\boldsymbol{s}(t) = (\boldsymbol{GCB})^{-1}\boldsymbol{G}\left(\boldsymbol{y}(t) - \boldsymbol{y}(0)\right) - \int_0^t \begin{bmatrix} -5018.1 & 246.2 \\ 1231 & -862.5 \end{bmatrix} \boldsymbol{y}(q)\,dq$$
$$- \int_0^t \begin{bmatrix} -501.8113 & 123.0986 & 544.9341 & -651.5326 \\ 123.0986 & -431.2409 & -124.7431 & 294.0253 \end{bmatrix} \xi(q)\,dq$$

where $\boldsymbol{G} = \boldsymbol{I}_2$. Moreover, in order to avoid the chattering problem, the term $\dfrac{\boldsymbol{s}(t)}{\|\boldsymbol{s}(t)\|}$ in the controller (4.9) is replaced with the saturation function [11], and the new version of the controller is given by

$$\boldsymbol{u}(t) = \begin{bmatrix} -501.8113 & 123.0986 & 544.9341 & -651.5326 \\ 123.0986 & -431.2409 & -124.7431 & 294.0253 \end{bmatrix} \xi(t)$$
$$+ \begin{bmatrix} -5018.1 & 246.2 \\ 1231 & -862.5 \end{bmatrix} \boldsymbol{y}(t) - \frac{1}{1-\chi}\left(\sigma_1 + \sigma_2 + \eta(t,\boldsymbol{y}) + \chi\|\boldsymbol{v}(t)\| + \psi\bar{d} + \mu\right)$$
$$\times \mathrm{sat}\left(\boldsymbol{s}(t), \varepsilon\right)$$

where $\sigma_1 = \sigma_2 = 10$, $\eta(t,\boldsymbol{y}) = 2$, $\chi = 0.8$, $\psi = 1$, $\bar{d} = 1$, $\mu = 25$, and $\varepsilon = 0.002$. Figures 4.26-4.34 chart the simulation results using the initial state $\boldsymbol{x}(0) = [2 \quad 3 \quad 4 \quad 1]^T$ and $\xi(0) = [6 \quad -3.2 \quad 0 \quad 0]^T$. The first one in these figures depicts all system states which converge around zero. The time responses of the system outputs are shown in Fig. 4.27. Since $d(t) \in L_2$, the system and controller designed above satisfy Theorem 4.3 so that both system outputs converge to zero asymptotically. Although the control law design completely fulfilled Theorem 4.3, the dominant pole of the closed-loop system was very close to the origin such that the output responses converged toward zero slowly. The performance of robust disturbance attenuation is shown in Fig. 4.28. The robust disturbance attenuation (4.18) in this case is guaranteed. Figures 4.29-4.31 illustrate $s_1(t)$, $s_2(t)$, and $\|\boldsymbol{s}(t)\|$ respectively. In Fig. 4.31, the trajectory representing the controlled system can maintain in the sliding layer in the whole time. Figure 4.32 shows that the trajectories of $\boldsymbol{e}(t)$ affecting by the mismatched disturbance also converged toward zero slowly due to the dominant pole. The responses of the control inputs $\boldsymbol{u}(t)$ are given in Figs. 4.33-4.34. The replacement of the saturation function eliminates the chattering. The simulation results demonstrate that the proposed controller design can guarantee the robust disturbance attenuation to outputs $\boldsymbol{y}(t)$ once the system is in the sliding mode.

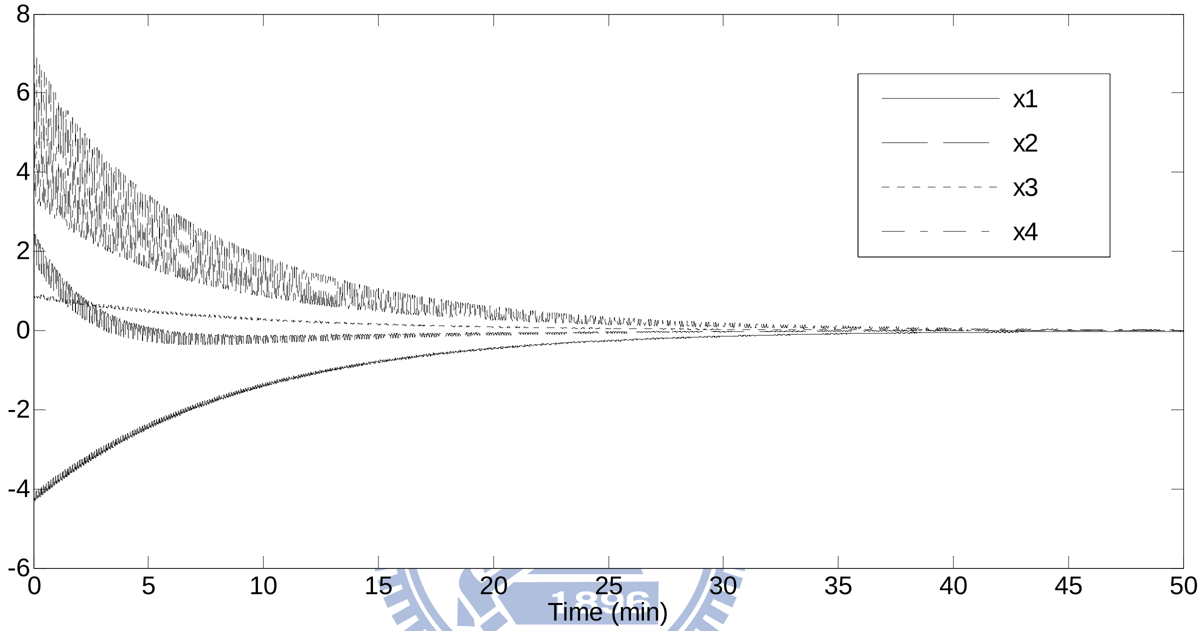

Fig. 4.26. System states in Example 4.4.

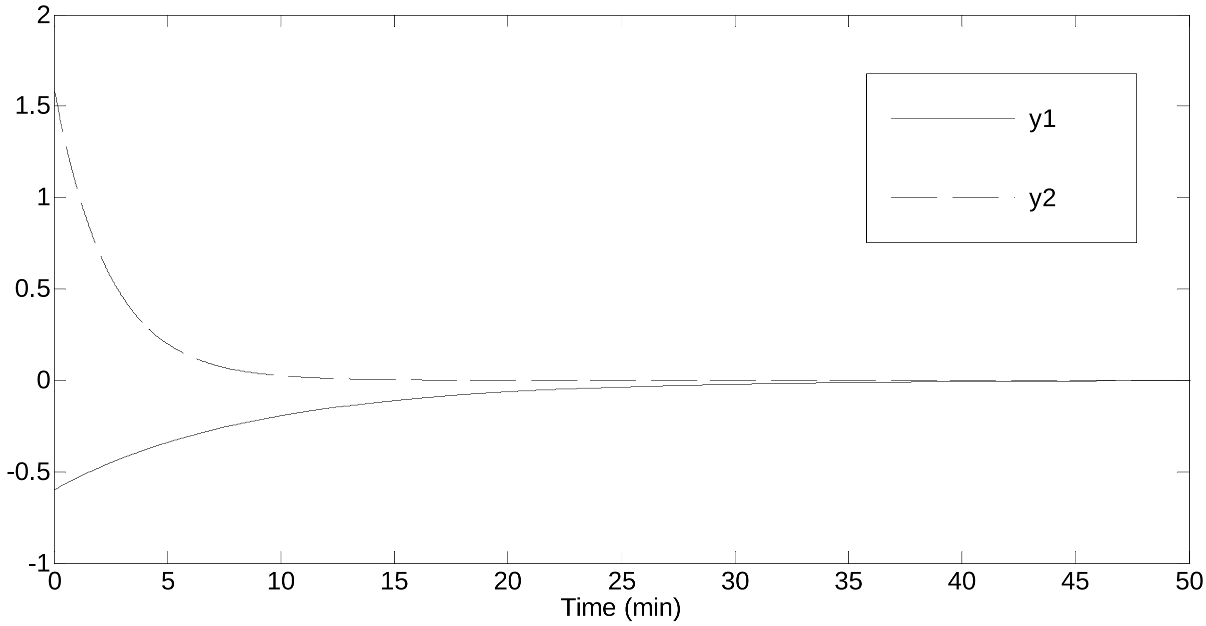

Fig. 4.27. System outputs in Example 4.4.

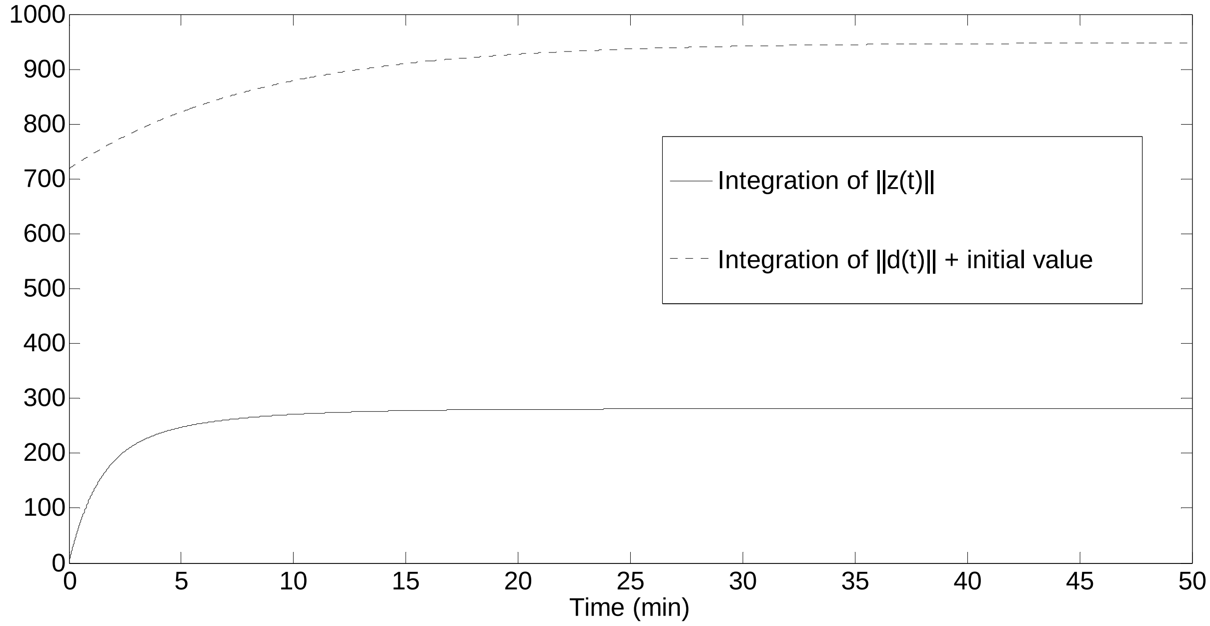

Fig. 4.28. Performance of robust disturbance attenuation in Example 4.4.

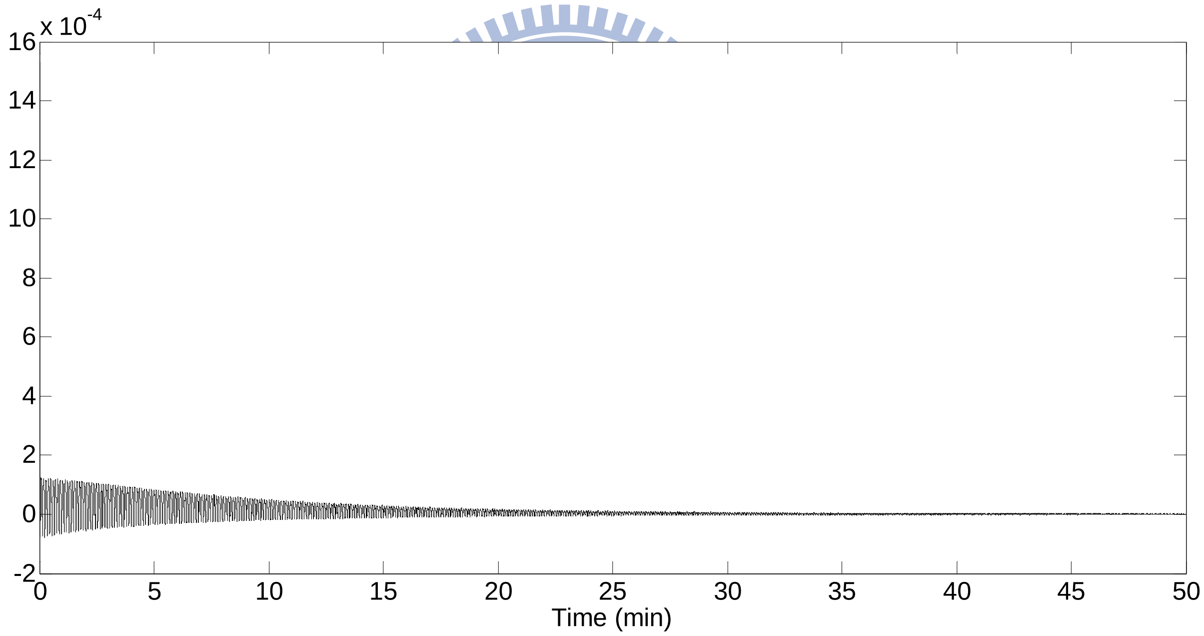

Fig. 4.29. Sliding function $s_1(t)$ in Example 4.4.

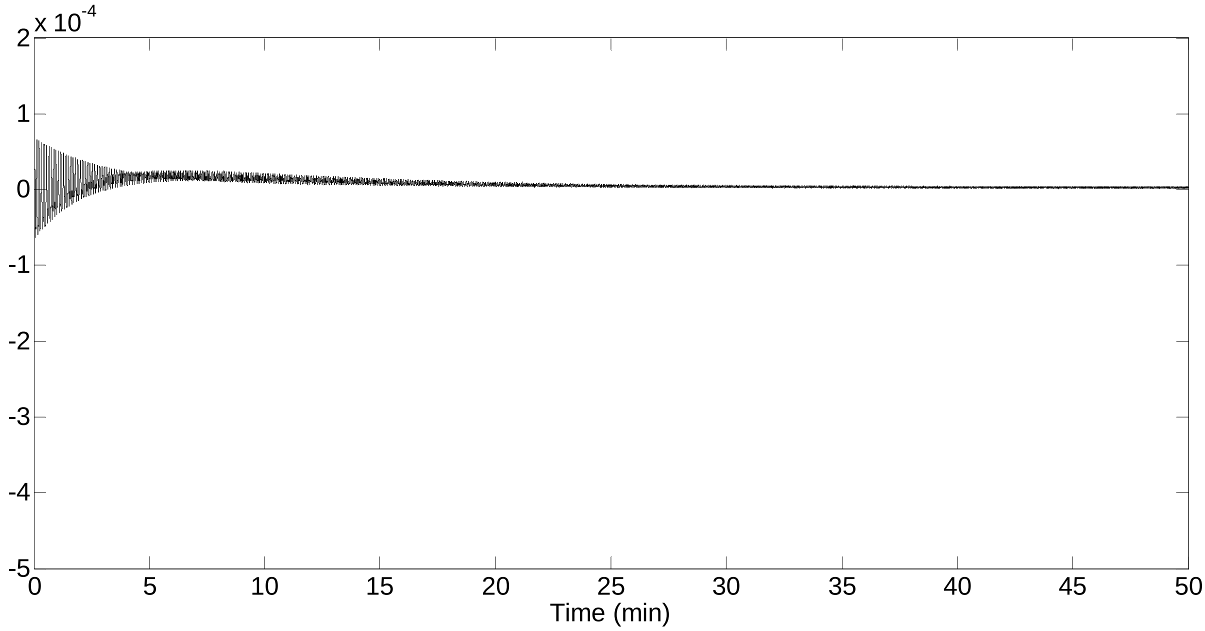

Fig. 4.30. Sliding function $s_2(t)$ in Example 4.4.

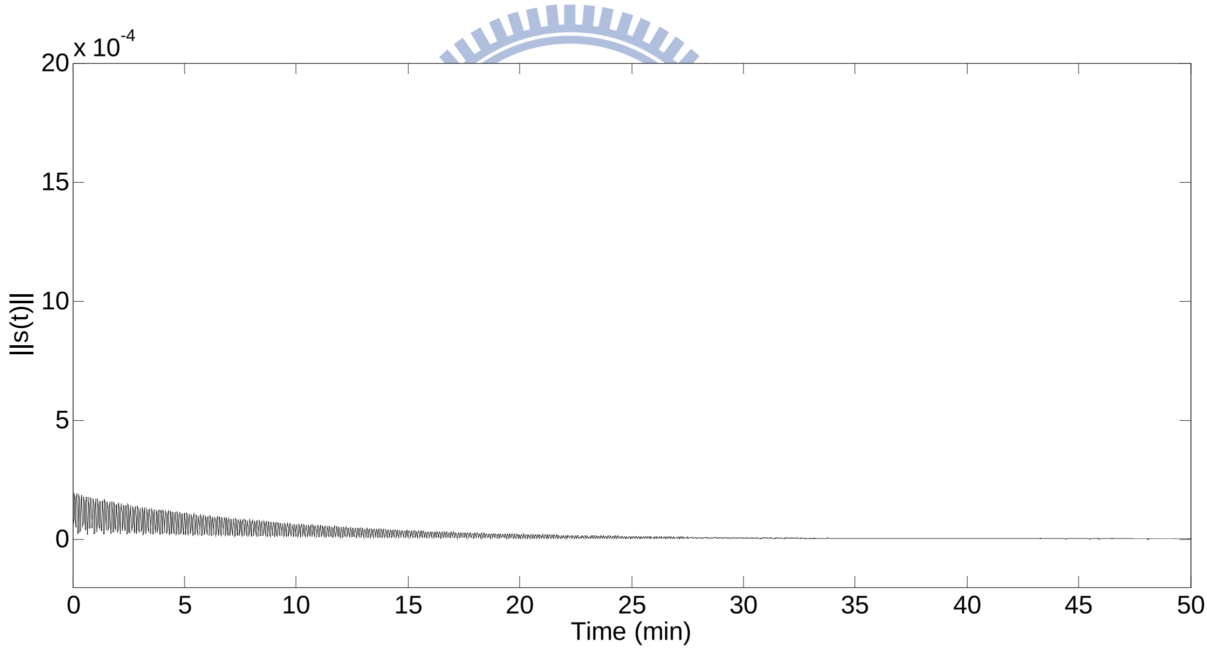

Fig. 4.31. Response of $\|\boldsymbol{s}(t)\|$ in Example 4.4.

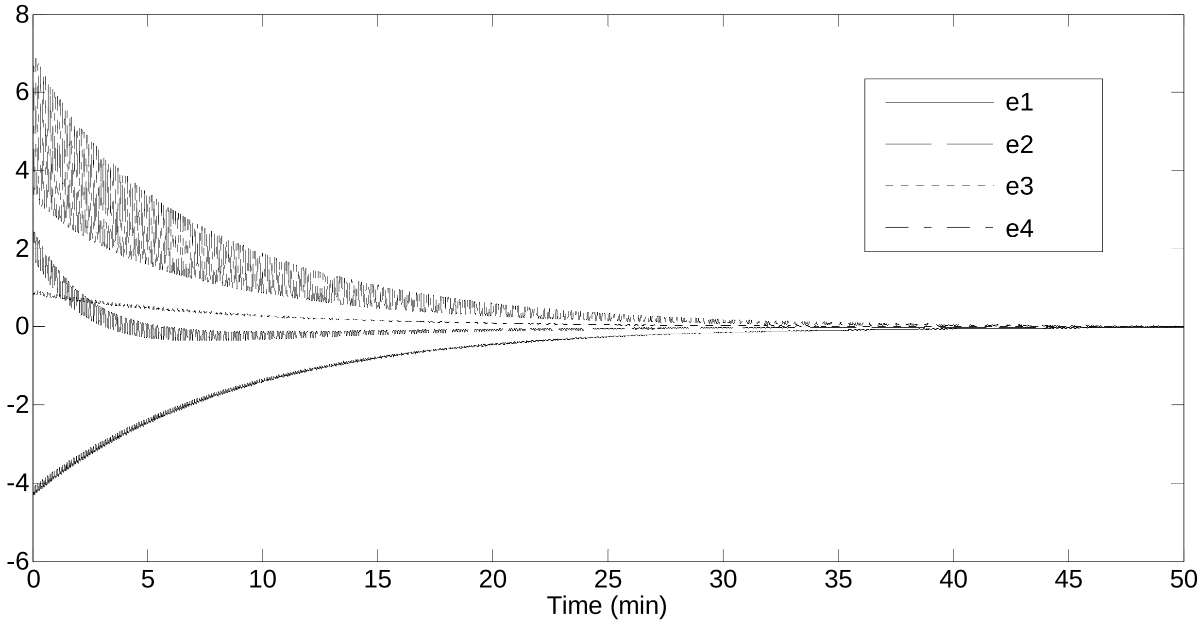

Fig. 4.32. Responses of $\boldsymbol{e}(t)$ in Example 4.4.

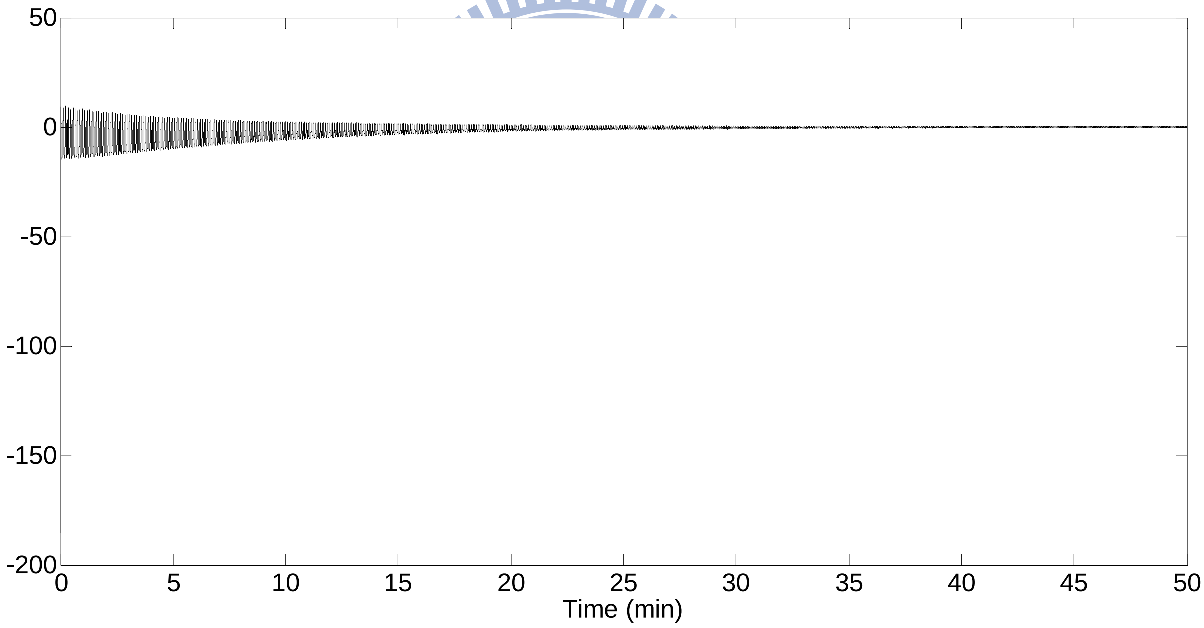

Fig. 4.33. Control input $u_1(t)$ in Example 4.4.

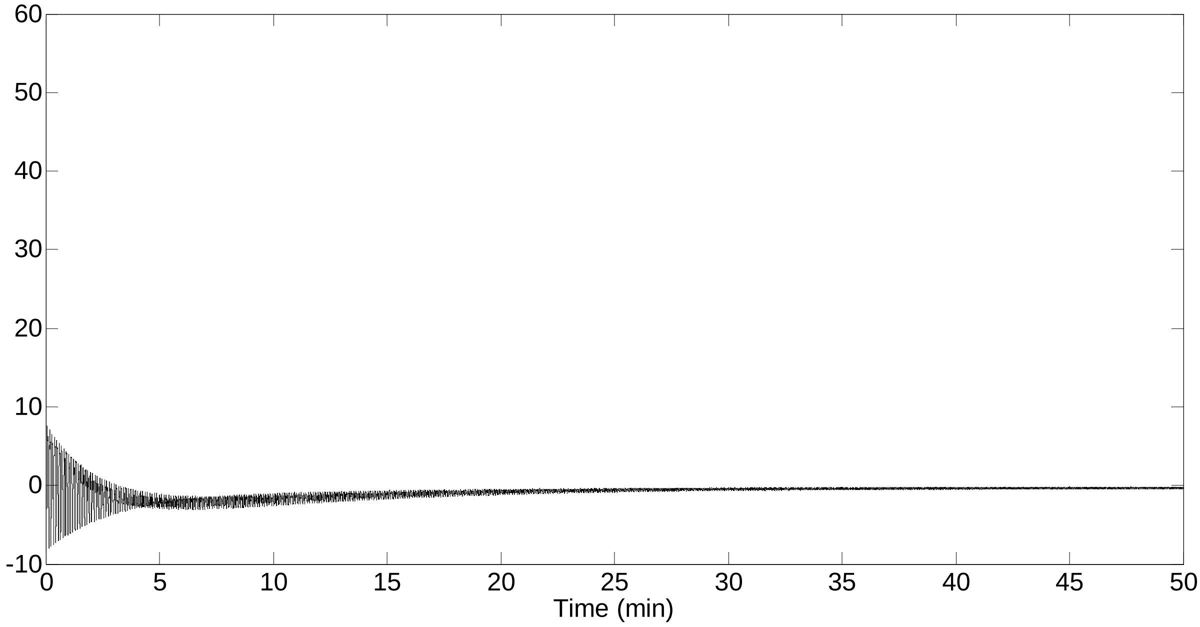

Fig. 4.34. Control input $u_2(t)$ in Example 4.4.

4.5 Summary

This chapter has presented the output feedback integral sliding mode controller for a class of time-delay systems with structure uncertainties and mismatched disturbances. The auxiliary full-order compensator added into the design of the integral sliding surface can improve the synthesis problem of static output feedback sliding mode control. For ensuring the property of robust disturbance attenuation in the delay-independent condition, two types of sufficient conditions are derived successfully for time-delay systems with uncertainties. In contrast with two conditions, the two control performances are similar. In the field of the computing time and complexity of solving procedure, solving algebraic Riccai inequalities is faster and simpler than solving the LMI. The enormous dimension of LMI caused the complexity of solution and increased the computing time. Adding a matrix $\boldsymbol{F}$ into the compensator and modifying the quadratic energy function can decompose the LMI to two algebraic Riccati inequalities and bring the simplicity for solving parameters of compensator and controller. When the LMI or two algebraic Riccati inequalities have solutions, both the stability of the closed-loop system and the condition of robust disturbance attenuation can be guaranteed. Moreover, the designed controller can maintain that the system is always in the sliding mode from the initial moment. The simulation results in examples demonstrated the feasibility of the propose control scheme successfully.

Provided the delay-dependent condition, this chapter has also completed the output feedback integral sliding mode controller design for the same time-varying delay systems. The proposed control method utilized the disturbance rejection condition in H_∞ theory to derive the LMI comprised of the parameters of the system, controller, and compensator. While the LMI has a set of solutions, both the stability of the closed-loop system and the property of robust disturbance attenuation have been proved. Finally, the simulation results of the real chemical reactor example also demonstrated the stable system trajectories by the proposed control scheme.

V. CONCLUSION

5.1 Concluding Remarks

Sliding mode control method has several advantages such as the robustness against matched disturbances, short transient time, simplicity in contrast with other nonlinear control schemes, etc. For linear MIMO systems which output signals are only available, this thesis reserved the original properties and developed the output feedback integral sliding mode control method. In many research reports, the design of sliding surface, synthesis of the controller, and local stability limited the development and applicability of the output feedback sliding mode control in practice. For improving these constraints, the integral term and adaption law were added into the sliding surface and controller, respectively. They released the synthesis problem and offered an extra degree of freedom for the system in the sliding mode, rather than depending on a stable matrix only. Solutions to an algebraic Riccati equation are used to determine the stability and robust disturbance attenuation against mismatched disturbances of the closed-loop system. Moreover, the adaption law in the controller played an important role to complete global stability and to avoid the high-gain problem.

The applications applied to time-delay systems have been developed by including the full-order compensator to perform the integral term in the sliding surface. Equally, the introduction of integral term in the sliding surface improved the synthesis problem. As for the stability problem of the system in the sliding mode, the LMI and a set of algebraic Riccati inequalities were derived respectively as a sufficient condition of the robust disturbance attenuation for the systems in the delay-independent condition. In contrast with two kinds of inequalities, algebraic Riccati inequality was with smaller space dimensions and spent less computing time, than LMI. For the delay-dependent condition, Chapter IV has also developed a sufficient condition as an LMI for ensuring the property of robust disturbance attenuation.

As the systems located in such severe conditions, disturbing by mismatched uncertainties and having time-varying delay feedback states, the primary LMI became very large for covering all disturbed terms to guarantee the stability and robust disturbance attenuation. Several examples in two kinds of delay conditions are simulated the feasibility of the proposed methods.

5.2 Future Works

For all output feedback controller designs in this thesis, two conditions are necessary to satisfy: the system must be minimum phase and with relative degree one. Position states are the only measurable variables in many mechanical systems whose relative degree in general is larger than one, e.g. inverted pendulum systems. Hence the development for the output feedback controller of systems with larger relative degree is necessary. How to compensate the relative degree problem and elaborate merits of sliding mode methods is essential.

In the field of output feedback controller design, an important topic is how to design a sliding mode controller assuring that the system approaches the sliding mode in a finite time globally. Present methods can complete it locally and cause high-gain control force due to the shortage of state information. Although Chapter III has offered a global stabilizing method, how to apply this stabilizing method to time-delay systems is still a challenge. On the other hand, solving an LMI with large dimensions is not easy in the delay-dependent condition. Finding out a simpler sufficient condition to ensure the stability and robust disturbance attenuation is also an important research topic in the future.

BIBLIOGRAPHIES

[1] V. I. Utkin, Sliding Modes in Control and Optimization, Springer Verlag, New York, 1992.

[2] C. Edwards and S. K. Spurgeon, Sliding Mode Control Theory and Application, Taylor & Francis, London, 1998.

[3] Y. Xia and Y. Jia, “Robust sliding-mode control for uncertain time-delay systems: an LMI approach,” IEEE Trans. Automatic Control, Vol. 48, No. 6, pp. 1086-1092, 2003.

[4] S. Qu and Y. Wang, “Robust control of uncertain time delay system: a novel sliding mode control design via LMI,” Journal of Systems Engineering and Electronics, Vol. 17, No. 3, pp. 624-628, 2006.

[5] T. S. Chiang and C. S. Chiu, “Sliding mode control of a class of uncertain nonlinear time-delay systems using LMI and TS recurrent fuzzy neural network,” IEICE Trans. Fundamentals, Vol. E92-A, No. 1, pp. 252-262, 2009.

[6] C. C. Kung, T. H. Chen, and L. H. Kung, “Modified adaptive fuzzy sliding mode controller for uncertain nonlinear systems,” IEICE Trans. Fundamentals, Vol. E88-A, No. 5, pp. 1328-1334, 2005.

[7] S. H. Zak and S. Hui, “Output feedback variable structure controllers and state estimators for uncertain/nonlinear dynamic systems,” IEE Proceedings D, Control Theory and Applications. Vol. 140, pp. 41-49, 1993.

[8] S. V. Yallapragada, B. S. Heck, and J. D. Finney, “Reaching condition for variable structure control with output feedback,” Journal of Guidance, Control and Dynamics, Vol. 19, pp. 848-853, 1996.

[9] C. M. Kwan, “On variable structure output feedback Controller,” IEEE Trans. Automatic Control, Vol. 41, pp. 1691-1693, 1996.

[10] F. Castanos and L. Fridman, “Analysis and design of integral sliding manifolds for

systems with unmatched perturbations," IEEE Trans. Automation Control, Vol. 51, No. 5, pp. 853-858, 2006.

[11] J. J. E. Slotine and S. S. Sastry, "Tracking control of nonlinear systems using sliding surfaces with application to robot manipulators," International Journal of Control, Vol. 38, No. 2, pp. 465-492, 1983.

[12] Y. Niu, et al., "Observer-based sliding mode control for nonlinear state-delayed systems," International Journal of Systems Science, Vol. 35, No. 2, pp. 139-150, 2004.

[13] X. R. Han, et al., "On the design of sliding mode static output feedback controllers for systems with time-varying delay," International Workshop of Variable Structure Systems, pp. 136-140, 2008.

[14] X. G. Yan, S. K. Spurgeon, and C. Edwards, "Static output feedback sliding mode control for time-varying delay systems with time-delayed nonlinear disturbances," International Journal of Robust Nonlinear Control, Vol. 20, No. 7, pp. 777-788, 2010.

[15] H. H. Choi, "Variable structure output feedback control design for a class of uncertain dynamic systems," Automatica, Vol. 38, pp. 335-341, 2002.

[16] P. Park, D. J. Choi, and S. G. Kong, "Output feedback variable structure control for linear systems with uncertainties and disturbances," Automatica, Vol. 43, pp. 72-79, 2007.

[17] J. Xiang, W. Wei, and H. Su, "An ILMI approach to robust static output feedback sliding mode control," International Journal of Control, Vol. 79, pp. 959-967, 2006.

[18] J. C. Juang and C. M. Lee, "Design of sliding mode controllers with bounded L_2 gain performance: an LMI approach," International Journal of Control, Vol. 78, pp. 647-661, 2005.

[19] A. S. Lewis, "Robust output feedback using sliding mode control," AIAA Journal of Guidance, Control and Dynamics, Vol. 24, pp. 873-878, 2001.

[20] M. C. Pai and A. Sinha, "Sliding mode output feedback control of vibration in a flexible structure," Journal of Dynamic Systems, Measurement, and Control, Vol. 129, pp. 851-855, 2007.

[21] J. M. Andrade-Da Silva, C. Edwards, and S. K. Spurgeon, "Sliding-mode output feedback control based on LMIs for plants with mismatched uncertainties," IEEE Trans. Industrial Electronics, Vol. 56, pp. 3675-3683, 2009.

[22] W. J. Cao and J. X. Xu, "Nonlinear integral-type sliding surface for both matched and unmatched uncertain systems," IEEE Trans. Automatic Control, Vol. 49, pp. 1355-1360, 2004.

[23] F. J. Bejarano, L. Firdman, and A. Poznyak, "Output integral sliding mode control based on algebraic hierarchical observer," International Journal of Control, Vol. 80, pp. 443-453, 2007.

[24] C. C. Cheng and I. M. Liu, "Design of MIMO integral variable structure controller," Journal of Franklin Institute, Vol. 336, pp. 1119-1134, 1999.

[25] J. L. Chang, "Design of a robust controller using only output feedback to solve the servomechanism problem," IEE Proceedings Control Theory Applications, Vol. 150, pp. 28-36, 2003.

[26] Q. Hu, "Robust integral variable structure controller and pulse-width pulse-frequency modulated input shaper design for flexible spacecraft with mismatched uncertainty/disturbance," ISA Transactions, Vol. 46, pp. 505-518, 2007.

[27] Y. Niu, B. Chen, and X. Wang, "Sliding mode control for a class of nonlinear stochastic systems with state and input delays," International Journal of Control, Automation, and Systems, Vol. 7, No. 3, pp. 365-370, 2009.

[28] M. C. Pai, "Observer-based adaptive sliding mode control for nonlinear uncertain state-delayed systems," International Journal of Control, Automation, and Systems, Vol.

7, No. 4, pp. 536-544, 2009.

[29] S. P. Boyd, et al., Linear Matrix Inequality, PA: SIAM, Philadelphia, 1994.

[30] C. C. Hua, Q. G. Wang, and X. P. Guan, "Memoryless state feedback controller design for time delay systems with matched uncertain nonlinearities," IEEE Trans. Automatic Control, Vol. 53, No. 3, pp. 801-807, 2003.

[31] J. H. Kim, "Delay-dependent robust and non-fragile guaranteed cost control for uncertain singular systems with time-varying state and input delays," International Journal of Control, Automation, and Systems, Vol. 7, No. 3, pp. 357-364, 2009.

[32] Y. S. Lee, S. H. Han, and W. H. Kwon, "Receding horizon H_∞ control for systems with a state-delay," Asian Journal of Control, Vol. 8, No. 1, pp. 63-71, 2006.

[33] O. Santos and S. Mondié, "Guaranteed cost control of linear systems with distributed delays: a complete type functional approach," International Journal of Control, Automation, and Systems, Vol. 8, No. 3, pp. 497-505, 2010.

[34] Z. Wang, et al., "H_∞ control for uncertain system with time-delay and nonlinear external disturbance via adaptive control method," International Journal of Control, Automation, and Systems, Vol. 8, No. 2, pp. 266-271, 2010.

[35] M. Chen and W. H. Chen, "Disturbance-observer-based robust control for time delay uncertain systems," International Journal of Control, Automation, and Systems, Vol. 8, No. 2, pp. 445-453, 2010.

[36] A. Fattouh, O. Sename, and J. M. Dion, "An unknown input observer design for linear time-delay systems," Proceeding 38th Conference of Decision and Control, Phoenix, Arizona, USA, pp. 4222-4227, 1999.

[37] Y. M. Fu, G. R. Duan, and S. M. Song, "Design of unknown input observer for linear time-delay systems," International Journal of Control, Automation, and Systems, Vol. 2, No. 4, pp. 530-535, 2004.

[38] A. G. Wu, J. Dong, and G. R. Duan, "Robust H-infinity estimation for linear time-delay systems: an improved LMI approach," International Journal of Control, Automation, and Systems, Vol. 7, No. 4, pp. 668-673, 2009.

[39] M. Darouach, "Full order unknown inputs observers design for delay systems," 2006 14th Mediterranean Conference of Control and Automation, Ancona, Italy, pp. 1-5, 2006.

[40] M. Darouach, "Unknown inputs observers design for delay systems," Asian Journal of Control, Vol. 9, No. 4, pp. 436-434, 2007.

[41] E. Fridman and U. Shaked, "A descriptor system approach to H_∞ control of linear time-delay systems," IEEE Trans. Automatic Control, Vol. 47, No. 2, pp. 253-270, 2002.

[42] S. C. Bengea, X. Li, and R. A. DeCarlo, "Combined controller-observer design for uncertain time delay systems with application to engine idle speed control," Journal of Dynamic Systems, Measurement, and Control, Vol. 126, pp. 772-780, 2004.

[43] J. W. Ko and P. G. Park, "Delay-dependet robust stabilization for systems with time-varying delays," International Journal of Control, Automation, and Systems, Vol. 7, No. 5, pp. 711-722, 2009.

[44] W. H. Chen and W. X. Zheng, "Delay-independent minimum dwell time for exponential stability of uncertain switched delay systems," IEEE Trans. Automation Control, Vol. 55, No. 10, pp. 2406-2413, 2010.

[45] L. Wu, et al., "A new approach to stability analysis and stabilization of discrete-time T-S fuzzy time-varying delay systems," IEEE Trans. Systems, Man, and Cybernetics B: Cybernetics, Vol. 41, No. 1, pp. 273-286, 2011.

[46] T. Co, "Relay-stabilization and bifurcations of unstable SISO processes with time delay," IEEE Trans. Automatic Control, Vol. 55, No. 5, pp. 1131-1141, 2010.

[47] F. Gouaisbaut and Y. Ariba, "Delay range stability of a class of distributed time delay

systems," Systems & Control Letters, Vol. 60, pp. 211-217, 2011.

[48] D. Meng, et al., "Robust iterative learning control design for uncertain time-delay systems based on a performance index," IET Control Theory Application, Vol. 4, No. 5, pp. 759-772, 2010.

[49] J. Na, et al., "Repetitive controller for time-delay systems based on disturbance observer," IET Control Theory Application, Vol. 4, No. 11, pp. 2391-2404, 2010.

[50] Y. Wen and X. Ren, "Observer-based fuzzy adaptive control for noon-linear time-varying delay systems with unknown control direction," IET Control Theory Application, Vol. 4, No. 12, pp. 2757-2769, 2010.

[51] S. Ibrir, "Observer-based control of a class of time-delay nonlinear systems having triangular structure," Automatica, Vol. 47, pp. 388-394, 2011.

[52] L. Hetel, et al., "Delay-dependent sampled-data control based on delay esimates," Systems & Control Letters, Vol. 60, pp. 146-150, 2011.

[53] J. Gadewadikar, F. L. Lewis, and M. Abu-Khalaf, "Necessary and sufficient conditions for H_∞ static output feedback control," Journal of Guidance, Control, and Dynamics, Vol. 43, pp. 915-920, 2006.

[54] J. Gadewadikar, et al., "Parameterization of all stabilized H_∞ static-feedback gains: application to output-feedback design," Automatica, Vol. 43, pp. 1597-1604, 2007.

[55] L. Y. Wang and W. Zhan, "Robust disturbance attenuation with stability for linear systems with norm-bounded nonlinear uncertainties," IEEE Trans. Automation Control, Vol. 41, No. 6, pp. 886-888, 1996.

[56] L. Zhou, J. C. Doyle, and K. Glover, Robust and Optimal Control, Prentice Hall, New Jersey, 1996.

[57] G. Zhai, et al., "Stability and H_∞ disturbance attenuation analysis for LTI control systems with controllers failures," Asian Journal of Control, Vol. 6, No. 1, pp. 104-111,

2004.

[58] C. T. Chen, Linear System Theory and Design, Holt, Rinehart & Winston, New York, 1984.

[59] K. Ogata, Modern Control Engineering, 3rd edition, Prentice Hall, Englewood Cliffs NJ, 1997.

[60] X. G. Yan, C. Edwards, and S. K. Spurgeon, “Dynamic sliding mode control for a class of systems with mismatched uncertainty,” European Journal of Control, Vol. 11, pp. 1-10, 2005.

[61] J. J. E. Slotine and W. Li, Applied Nonlinear Control, Prentice Hall, New Jersey, 1991.

[62] K. Gu, V. L. Kharitonov, and J. Chen, Stability of Time-Delay Systems, Birkhauser, Boston, Massachusetts, 2003.

Appendix 1

Proof of Theorem 4.1

Define $\boldsymbol{q}(t)=\begin{bmatrix}\boldsymbol{x}(t)\\ \boldsymbol{e}(t)\end{bmatrix}$ and a quadratic energy function as

$$E_n(\boldsymbol{q})=\boldsymbol{q}^T\boldsymbol{P}\boldsymbol{q}+\int_{t-\tau}^{t}\boldsymbol{q}^T(\alpha)\boldsymbol{Q}\boldsymbol{q}(\alpha)d\alpha \tag{A.1}$$

where the matrices $\boldsymbol{P}>0$ and $\boldsymbol{Q}>0$ are determined later. Then define the Hamiltonian function as

$$H[\boldsymbol{d}]=\boldsymbol{z}^T\boldsymbol{z}-\gamma^2\boldsymbol{d}^T\boldsymbol{d}+\frac{dE_n}{dt} \tag{A.2}$$

where $\frac{dE_n}{dt}$ is the derivative of E_n along the trajectory of the closed-loop system (4.28). A sufficient condition satisfying the robust disturbance attenuation is that

$$H[\boldsymbol{d}]<0 \quad \text{for all} \quad \boldsymbol{d}\in L_2 \tag{A.3}$$

where all functions $\boldsymbol{d}(s)$ fulfilled that $\int_0^\infty \text{trace}\left[\boldsymbol{d}^T(s)\boldsymbol{d}(s)\right]ds<\infty$ are bounded. Since (A.3) holds, $E_n(\boldsymbol{q})$ is a strict radially unbounded Lyapunov function of the closed-loop system (4.28), and hence the robust stability can be guaranteed [55]. Notice that (A.3) is equivalent to $\sup_{\boldsymbol{d}\in L_2}H[\boldsymbol{d}]<0$. As $\boldsymbol{z}(t)=\boldsymbol{C}_w\boldsymbol{q}(t)$, (A.2) can be rewritten as

$$\begin{aligned}H[\boldsymbol{d}]&=\boldsymbol{z}^T\boldsymbol{z}-\gamma^2\boldsymbol{d}^T\boldsymbol{d}+\frac{dE_n}{dt}\\&=\boldsymbol{q}^T(t)\left(\boldsymbol{A}_w^T\boldsymbol{P}+\boldsymbol{P}\boldsymbol{A}_w+\boldsymbol{Q}+\boldsymbol{C}_w^T\boldsymbol{C}_w\right)\boldsymbol{q}(t)-\gamma^2\boldsymbol{d}(t)^T\boldsymbol{d}(t)+\boldsymbol{q}^T(t)\boldsymbol{P}\boldsymbol{B}_w\boldsymbol{q}(t-\tau)\\&\quad-\boldsymbol{q}^T(t-\tau)\boldsymbol{Q}\boldsymbol{q}(t-\tau)+\boldsymbol{q}^T(t)\boldsymbol{P}\boldsymbol{G}_w\boldsymbol{d}(t)+\boldsymbol{q}^T(t-\tau)\boldsymbol{B}_w^T\boldsymbol{P}\boldsymbol{q}(t)+\boldsymbol{d}^T(t)\boldsymbol{G}_w^T\boldsymbol{P}\boldsymbol{q}(t).\end{aligned}$$

Based on the above equation, the worst case $\sup_{\boldsymbol{d}\in L_2}H[\boldsymbol{d}]$ occurs when $\boldsymbol{d}(t)=\gamma^{-2}\boldsymbol{G}_w^T\boldsymbol{P}\boldsymbol{q}(t)$, and it follows that

$$H[\boldsymbol{d}]\le\boldsymbol{q}^T(t)\left(\boldsymbol{A}_w^T\boldsymbol{P}+\boldsymbol{P}\boldsymbol{A}_w+\boldsymbol{Q}+\boldsymbol{C}_w^T\boldsymbol{C}_w+\gamma^{-2}\boldsymbol{P}\boldsymbol{G}_w\boldsymbol{G}_w^T\boldsymbol{P}\right)\boldsymbol{q}(t)$$

$$+q^T(t-\tau)B_w^T P q(t) + q^T(t) P B_w q(t-\tau) - q^T(t-\tau) Q q(t-\tau). \tag{A.4}$$

If there exists $P_{22} \geq I$, according to Lemma 4.1 (ii), the following inequality is established as

$$q^T(t)\begin{bmatrix} 0 & -P_{12}P_{22}^{-1}C^T C \\ -C^T C P_{22}^{-1} P_{12}^T & 0 \end{bmatrix} q(t) \leq q^T(t) \begin{bmatrix} \rho_{10} P_{12} P_{12}^T & 0 \\ 0 & \rho_{10}^{-1} C^T C C^T C \end{bmatrix} q(t)$$

where $\rho_{10} > 0$. Applying Lemma 4.1 and designing $K = R^{-1}B^T P_{11}$ and $L = \frac{\lambda}{2} P_{22}^{-1} C^T$, the upper bound of $H[d]$ can be expressed as $H[d] \leq \begin{bmatrix} q(t) \\ q(t-\tau) \end{bmatrix}^T \begin{bmatrix} \Xi_{11} & \Xi_{12} \\ \Xi_{12}^T & \Xi_{22} \end{bmatrix} \begin{bmatrix} q(t) \\ q(t-\tau) \end{bmatrix}$ where

$$\begin{aligned}
\Xi_{11} = & \begin{bmatrix} (NA)^T P_{11} + P_{11} NA + C^T C & 0 \\ P_{12}^T NA + (MA)^T P_{12}^T & P_{22} MA + (MA)^T P_{22} \end{bmatrix} \\
& + \begin{bmatrix} \frac{\lambda}{2}\rho_{10} P_{12} P_{12}^T & -P_{11} B R^{-1} B^T P_{12} \\ 0 & \frac{\lambda}{2}\rho_{10}^{-1} C^T C C^T C + P_{12}^T B R^{-1} B^T P_{12} \end{bmatrix} \\
& + \begin{bmatrix} P_{11} B R^{-1} B^T P_{11} + \rho_1 P_{12} M D D^T M^T P_{12}^T + \rho_1^{-1} H^T H & 0 \\ -P_{12}^T B R^{-1} B^T P_{11} & 0 \end{bmatrix} \\
& + \begin{bmatrix} \rho_2 H^T H + \rho_3 H^T H & 0 \\ 0 & \rho_2^{-1} P_{12}^T N D D^T N^T P_{12} + \rho_5^{-1} P_{12}^T P_{12} \end{bmatrix} \\
& + \begin{bmatrix} \rho_4 P_{11} N D D^T N^T P_{11} + \rho_4^{-1} H^T H & 0 \\ 0 & P_{11} B R^{-1} B^T P_{11} \end{bmatrix} \\
& + \begin{bmatrix} 0 & (NA)^T P_{12} + P_{12} MA \\ 0 & \rho_5 P_{11} B R^{-1} B^T B R^{-1} B^T P_{11} + \rho_3^{-1} P_{22} M D D^T M^T P_{22} \end{bmatrix} \\
& + \begin{bmatrix} \rho_6 P_{11} N D_d D_d^T N^T P_{11} + \rho_7 P_{12} M D_d D_d^T M^T P_{12}^T & 0 \\ 0 & -\lambda C^T C \end{bmatrix} \\
& + \begin{bmatrix} 0 & 0 \\ 0 & \rho_8 P_{12}^T N D_d D_d^T N^T P_{12} + \rho_9 P_{22} M D_d D_d^T M^T P_{22} \end{bmatrix} + \gamma^{-2} P G_w G_w^T P + Q,
\end{aligned}$$

$\Xi_{22} = \begin{bmatrix} (\rho_6^{-1} + \rho_7^{-1} + \rho_8^{-1} + \rho_9^{-1}) H_d^T H_d & 0 \\ 0 & 0 \end{bmatrix} - Q$, and $\Xi_{12} = \begin{bmatrix} P_{11} N A_d + P_{12} M A_d & 0 \\ P_{12}^T N A_d + P_{22} M A_d & 0 \end{bmatrix}$. Notice that $P = \begin{bmatrix} P_{11} & P_{12} \\ P_{12}^T & P_{22} \end{bmatrix} > 0$, $Q = \begin{bmatrix} Q_{11} & Q_{12} \\ Q_{12}^T & Q_{22} \end{bmatrix} > 0$, and $\rho_i > 0$, $i = 1, 2, \cdots, 9$. Provided

$\begin{bmatrix} \Xi_{11} & \Xi_{12} \\ \Xi_{12}^T & \Xi_{22} \end{bmatrix} < 0$, then $H[\boldsymbol{d}] < 0$ and the property of robust disturbance attenuation (4.18) is also satisfied. Through Schur decomposition, if there exists $\boldsymbol{Q}_{11} - \left(\rho_7^{-1} + \rho_8^{-1} + \rho_9^{-1} + \rho_{10}^{-1}\right)\boldsymbol{H}_d^T \boldsymbol{H}_d > 0$, inequality $\begin{bmatrix} \Xi_{11} & \Xi_{12} \\ \Xi_{12}^T & \Xi_{22} \end{bmatrix} < 0$ is equivalent to the LMI (4.30). If there exists γ, $\boldsymbol{P}_{11}$, $\boldsymbol{P}_{12}$, $\boldsymbol{P}_{22}$, $\boldsymbol{Q}_{11}$, $\boldsymbol{Q}_{12}$, and $\boldsymbol{Q}_{22}$ satisfying the LMI, it implies to $\sup_{\boldsymbol{d} \in L_2} H[\boldsymbol{d}] < 0$ and to guarantee the robust disturbance attenuation. The proof of this theorem is completed.

Appendix 2

Proof of Theorem 4.3

Among the delay-dependent condition, choose three quadratic energy functions as

$$E_1(\boldsymbol{x},\boldsymbol{e}) = \boldsymbol{x}^T\boldsymbol{P}_{11}\boldsymbol{x} + \boldsymbol{e}^T\boldsymbol{P}_{22}\boldsymbol{e} = \boldsymbol{q}^T\begin{bmatrix}\boldsymbol{P}_{11} & \boldsymbol{0}\\ \boldsymbol{0} & \boldsymbol{P}_{22}\end{bmatrix}\boldsymbol{q} = \boldsymbol{q}^T\boldsymbol{P}\boldsymbol{q} \tag{B.1}$$

$$\begin{aligned} E_2(\boldsymbol{x},\boldsymbol{e}) &= \int_{t-\tau(t)}^{t}\boldsymbol{x}^T(\alpha)\boldsymbol{Q}_{11}\boldsymbol{x}(\alpha)d\alpha + \int_{t-\tau(t)}^{t}\boldsymbol{e}^T(\alpha)\boldsymbol{Q}_{22}\boldsymbol{e}(\alpha)d\alpha \\ &= \int_{t-\tau(t)}^{t}\boldsymbol{q}^T(\alpha)\begin{bmatrix}\boldsymbol{Q}_{11} & \boldsymbol{0}\\ \boldsymbol{0} & \boldsymbol{Q}_{22}\end{bmatrix}\boldsymbol{q}(\alpha)d\alpha = \int_{t-\tau(t)}^{t}\boldsymbol{q}^T(\alpha)\boldsymbol{Q}\boldsymbol{q}(\alpha)d\alpha \end{aligned} \tag{B.2}$$

$$\begin{aligned} E_3(\boldsymbol{x},\boldsymbol{e}) &= \int_{-\tau(t)}^{0}\int_{t+\beta}^{t}\dot{\boldsymbol{x}}^T(\alpha)\boldsymbol{Z}_1\dot{\boldsymbol{x}}(\alpha)d\alpha d\beta + \int_{-\tau(t)}^{0}\int_{t+\beta}^{t}\dot{\boldsymbol{e}}^T(\alpha)\boldsymbol{Z}_2\dot{\boldsymbol{e}}(\alpha)d\alpha d\beta \\ &= \int_{-\tau(t)}^{0}\int_{t+\beta}^{t}\dot{\boldsymbol{q}}^T(\alpha)\begin{bmatrix}\boldsymbol{Z}_1 & \boldsymbol{0}\\ \boldsymbol{0} & \boldsymbol{Z}_2\end{bmatrix}\dot{\boldsymbol{q}}(\alpha)d\alpha d\beta = \int_{-\tau(t)}^{0}\int_{t+\beta}^{t}\dot{\boldsymbol{q}}^T(\alpha)\boldsymbol{Z}\dot{\boldsymbol{q}}(\alpha)d\alpha d\beta \end{aligned} \tag{B.3}$$

where $\boldsymbol{P} = \begin{bmatrix}\boldsymbol{P}_{11} & \boldsymbol{0}\\ \boldsymbol{0} & \boldsymbol{P}_{22}\end{bmatrix}$, $\boldsymbol{Q} = \begin{bmatrix}\boldsymbol{Q}_{11} & \boldsymbol{0}\\ \boldsymbol{0} & \boldsymbol{Q}_{22}\end{bmatrix}$, and $\boldsymbol{Z} = \begin{bmatrix}\boldsymbol{Z}_1 & \boldsymbol{0}\\ \boldsymbol{0} & \boldsymbol{Z}_2\end{bmatrix}$. The positive definite matrices $\boldsymbol{P}_{11} > 0$, $\boldsymbol{P}_{22} > 0$, $\boldsymbol{Q}_{11} > 0$, $\boldsymbol{Q}_{22} > 0$, $\boldsymbol{Z}_1 > 0$, and $\boldsymbol{Z}_2 > 0$ are determined later. Then define a Hamiltonian function as

$$H[\boldsymbol{d}] = \boldsymbol{z}^T\boldsymbol{z} - \gamma^2\boldsymbol{d}^T\boldsymbol{d} + \frac{dE_1}{dt} + \frac{dE_2}{dt} + \frac{dE_3}{dt} \tag{B.4}$$

where $\frac{dE_i}{dt}$ is the derivative of E_i along the trajectory of the closed-loop system (4.58), $i = 1,2,3$. A sufficient condition satisfying the robust disturbance attenuation (4.18), i.e. $\int_0^t\left(\boldsymbol{y}^T\boldsymbol{y} + \boldsymbol{v}^T\boldsymbol{R}\boldsymbol{v}\right)dq \le \gamma^2\int_0^t\left(\boldsymbol{d}^T\boldsymbol{d}\right)dq \quad \forall \quad t \ge 0$, is

$$H[\boldsymbol{d}] < 0, \text{ for all } \boldsymbol{d} \in L_2[0,\infty).$$

Along arbitrary trajectories of system (4.58), the derivative of E_1 with respect to time is

$$\frac{dE_1}{dt} = \boldsymbol{q}^T(t)\left(\boldsymbol{P}\tilde{\boldsymbol{A}} + \tilde{\boldsymbol{A}}^T\boldsymbol{P}\right)\boldsymbol{q}(t) + 2\boldsymbol{q}^T(t)\boldsymbol{P}\tilde{\boldsymbol{A}}_d\boldsymbol{q}\left(t-\tau(t)\right) + 2\boldsymbol{q}^T(t)\boldsymbol{P}\tilde{\boldsymbol{D}}\boldsymbol{d}(t). \tag{B.5}$$

Similarly, the derivatives of E_2 and E_3 with respect to time are given by

$$\begin{aligned}\frac{dE_2}{dt} &= \boldsymbol{q}^T(t)\boldsymbol{Q}\boldsymbol{q}(t) - (1-\dot{\tau})\boldsymbol{q}^T(t-\tau(t))\boldsymbol{Q}\boldsymbol{q}(t-\tau(t)) \\ &\le \boldsymbol{q}^T(t)\boldsymbol{Q}\boldsymbol{q}(t) - (1-\tau^*)\boldsymbol{q}^T(t-\tau(t))\boldsymbol{Q}\boldsymbol{q}(t-\tau(t))\end{aligned}$$

and

$$\begin{aligned}\frac{dE_3}{dt} &= \tau(t)\dot{\boldsymbol{q}}^T(t)\boldsymbol{Z}\dot{\boldsymbol{q}}(t) - (1-\dot{\tau})\int_{t-\tau(t)}^{t}\dot{\boldsymbol{q}}^T(\alpha)\boldsymbol{Z}\dot{\boldsymbol{q}}(\alpha)\,d\alpha \\ &\le \bar{\tau}\dot{\boldsymbol{q}}^T(t)\boldsymbol{Z}\dot{\boldsymbol{q}}(t) - (1-\dot{\tau})\int_{t-\tau(t)}^{t}\dot{\boldsymbol{q}}^T(\alpha)\boldsymbol{Z}\dot{\boldsymbol{q}}(\alpha)\,d\alpha.\end{aligned}$$

Lemma 4.2 can assist to determine the bound of integral term of the derivative of E_3 as

$$\begin{aligned}\frac{dE_3}{dt} &\le \bar{\tau}\dot{\boldsymbol{q}}^T(t)\boldsymbol{Z}\dot{\boldsymbol{q}}(t) - \frac{1-\dot{\tau}}{\tau(t)}\left(\int_{t-\tau(t)}^{t}\dot{\boldsymbol{q}}(\alpha)\,d\alpha\right)^T\boldsymbol{Z}\left(\int_{t-\tau(t)}^{t}\dot{\boldsymbol{q}}(\alpha)\,d\alpha\right) \\ &\le \bar{\tau}\dot{\boldsymbol{q}}^T(t)\boldsymbol{Z}\dot{\boldsymbol{q}}(t) - \frac{1-\tau^*}{\bar{\tau}}\left(\int_{t-\tau(t)}^{t}\dot{\boldsymbol{q}}(\alpha)\,d\alpha\right)^T\boldsymbol{Z}\left(\int_{t-\tau(t)}^{t}\dot{\boldsymbol{q}}(\alpha)\,d\alpha\right) \\ &\le -\frac{1-\tau^*}{\bar{\tau}}\left(\boldsymbol{q}^T(t)\boldsymbol{Z}\boldsymbol{q}(t) - 2\boldsymbol{q}^T(t)\boldsymbol{Z}\boldsymbol{q}(t-\tau(t)) + \boldsymbol{q}^T(t-\tau(t))\boldsymbol{Z}\boldsymbol{q}(t-\tau(t))\right) \\ &\quad + \bar{\tau}\dot{\boldsymbol{q}}^T(t)\boldsymbol{Z}\dot{\boldsymbol{q}}(t)\end{aligned}$$

where $\int_{t-\tau(t)}^{t}\dot{\boldsymbol{q}}(\alpha)\,d\alpha = \boldsymbol{q}(t) - \boldsymbol{q}(t-\tau(t))$. Summing up $\frac{dE_1}{dt}$, $\frac{dE_2}{dt}$, and $\frac{dE_3}{dt}$, the Hamiltonian function is bounded by

$$\begin{aligned}H[\boldsymbol{d}] &\le \boldsymbol{q}^T(t)\boldsymbol{C}_w^T\boldsymbol{C}_w\boldsymbol{q}(t) - \gamma^2\boldsymbol{d}^T\boldsymbol{d} + \boldsymbol{q}^T(t)\left(\boldsymbol{P}\tilde{\boldsymbol{A}} + \tilde{\boldsymbol{A}}^T\boldsymbol{P}\right)\boldsymbol{q}(t) + 2\boldsymbol{q}^T(t)\boldsymbol{P}\tilde{\boldsymbol{A}}_d\boldsymbol{q}(t-\tau(t)) \\ &\quad + 2\boldsymbol{q}^T(t)\boldsymbol{P}\tilde{\boldsymbol{D}}\boldsymbol{d}(t) + \boldsymbol{q}^T(t)\boldsymbol{Q}\boldsymbol{q}(t) - (1-\tau^*)\boldsymbol{q}^T(t-\tau(t))\boldsymbol{Q}\boldsymbol{q}(t-\tau(t)) \\ &\quad - \frac{1-\tau^*}{\bar{\tau}}\left(\boldsymbol{q}^T(t)\boldsymbol{Z}\boldsymbol{q}(t) - 2\boldsymbol{q}^T(t)\boldsymbol{Z}\boldsymbol{q}(t-\tau(t)) + \boldsymbol{q}^T(t-\tau(t))\boldsymbol{Z}\boldsymbol{q}(t-\tau(t))\right) \\ &\quad + \bar{\tau}\dot{\boldsymbol{q}}^T(t)\boldsymbol{Z}\dot{\boldsymbol{q}}(t) \\ &= \boldsymbol{q}^T(t)\left(\boldsymbol{P}\tilde{\boldsymbol{A}} + \tilde{\boldsymbol{A}}^T\boldsymbol{P} + \boldsymbol{C}_w^T\boldsymbol{C}_w + \boldsymbol{Q} - \frac{1-\tau^*}{\bar{\tau}}\boldsymbol{Z}\right)\boldsymbol{q}(t) + \bar{\tau}\dot{\boldsymbol{q}}^T(t)\boldsymbol{Z}\dot{\boldsymbol{q}}(t) + 2\boldsymbol{q}^T(t)\boldsymbol{P}\tilde{\boldsymbol{D}}\boldsymbol{d}(t) \\ &\quad + 2\boldsymbol{q}^T(t)\left(\boldsymbol{P}\tilde{\boldsymbol{A}}_d - \frac{1-\tau^*}{\bar{\tau}}\boldsymbol{Z}\right)\boldsymbol{q}(t-\tau(t)) - \gamma^2\boldsymbol{d}^T\boldsymbol{d} \\ &\quad - (1-\tau^*)\boldsymbol{q}^T(t-\tau(t))\left(\boldsymbol{Q} + \frac{1}{\bar{\tau}}\boldsymbol{Z}\right)\boldsymbol{q}(t-\tau(t)).\end{aligned}$$

According to the Lemma 4.1, the bound of the uncertainty variations in the inequality above can be obtained by known quantities as

$$
\begin{aligned}
H[\boldsymbol{d}] \le\ & \boldsymbol{q}^T(t)\left(\boldsymbol{P}\bar{\boldsymbol{A}} + \bar{\boldsymbol{A}}^T\boldsymbol{P} + \boldsymbol{C}_w^T\boldsymbol{C}_w + \boldsymbol{Q} - \bar{\tau}^{-1}\left(1-\tau^*\right)\boldsymbol{Z} + \boldsymbol{P}\Gamma_1\boldsymbol{P} + \Gamma_2\right)\boldsymbol{q}(t) \\
& + 2\boldsymbol{q}^T(t)\left(\boldsymbol{P}\bar{\boldsymbol{A}}_d - \bar{\tau}^{-1}\left(1-\tau^*\right)\boldsymbol{Z}\right)\boldsymbol{q}\left(t-\tau(t)\right) + 2\boldsymbol{q}^T(t)\boldsymbol{P}\tilde{\boldsymbol{D}}\boldsymbol{d}(t) \\
& + \boldsymbol{q}^T\left(t-\tau(t)\right)\left(\Gamma_3 - \left(1-\tau^*\right)\left(\boldsymbol{Q} + \bar{\tau}^{-1}\boldsymbol{Z}\right)\right)\boldsymbol{q}\left(t-\tau(t)\right) \\
& + \bar{\tau}\dot{\boldsymbol{q}}^T(t)\boldsymbol{Z}\dot{\boldsymbol{q}}(t) - \gamma^2\boldsymbol{d}^T\boldsymbol{d}
\end{aligned}
\qquad \text{(B.6)}
$$

where

$$
\bar{\boldsymbol{A}} = \begin{bmatrix} \boldsymbol{NA}-\boldsymbol{BK} & \boldsymbol{BK} \\ \boldsymbol{0} & \boldsymbol{MA}-\boldsymbol{LC} \end{bmatrix},\quad \bar{\boldsymbol{A}}_d = \begin{bmatrix} \boldsymbol{NA}_d & \boldsymbol{0} \\ \boldsymbol{MA}_d & \boldsymbol{0} \end{bmatrix},
$$

$$
\Gamma_1 = \begin{bmatrix} \boldsymbol{N}\left(\rho_1\boldsymbol{DD}^T + \rho_3\boldsymbol{D}_d\boldsymbol{D}_d^T\right)\boldsymbol{N}^T & \boldsymbol{0} \\ \boldsymbol{0} & \boldsymbol{M}\left(\rho_2\boldsymbol{DD}^T + \rho_4\boldsymbol{D}_d\boldsymbol{D}_d^T\right)\boldsymbol{M}^T \end{bmatrix},
$$

$$
\Gamma_2 = \begin{bmatrix} \left(\rho_1^{-1}+\rho_2^{-1}\right)\boldsymbol{H}^T\boldsymbol{H} & \boldsymbol{0} \\ \boldsymbol{0} & \boldsymbol{0} \end{bmatrix}, \text{ and } \Gamma_3 = \begin{bmatrix} \left(\rho_3^{-1}+\rho_4^{-1}\right)\boldsymbol{H}_d^T\boldsymbol{H}_d & \boldsymbol{0} \\ \boldsymbol{0} & \boldsymbol{0} \end{bmatrix}.
$$

The constants $\rho_1 > 0$, $\rho_2 > 0$, $\rho_3 > 0$, and $\rho_4 > 0$ are designed such that $\Gamma_3 - \left(1-\tau^*\right)\left(\boldsymbol{Q} + \bar{\tau}^{-1}\boldsymbol{Z}\right) < 0$. The inequality (B.6) can be written as the matrix form

$$
\begin{aligned}
H[\boldsymbol{d}] \le & \begin{bmatrix} \boldsymbol{q}(t) \\ \boldsymbol{q}\left(t-\tau(t)\right) \\ \boldsymbol{d}(t) \end{bmatrix}^T \left(\begin{bmatrix} \Pi + \boldsymbol{P}\Gamma_1\boldsymbol{P} & \boldsymbol{P}\bar{\boldsymbol{A}}_d - \bar{\tau}^{-1}\left(1-\tau^*\right)\boldsymbol{Z} & \boldsymbol{P}\tilde{\boldsymbol{D}} \\ \left(\boldsymbol{P}\bar{\boldsymbol{A}}_d - \bar{\tau}^{-1}\left(1-\tau^*\right)\boldsymbol{Z}\right)^T & \Gamma_3 - \left(1-\tau^*\right)\left(\boldsymbol{Q}+\bar{\tau}^{-1}\boldsymbol{Z}\right) & \boldsymbol{0} \\ \left(\boldsymbol{P}\tilde{\boldsymbol{D}}\right)^T & \boldsymbol{0} & -\gamma^2\boldsymbol{I} \end{bmatrix} \right. \\
& \left. + \bar{\tau}\begin{bmatrix} \tilde{\boldsymbol{A}}^T \\ \tilde{\boldsymbol{A}}_d^T \\ \tilde{\boldsymbol{D}}^T \end{bmatrix} \boldsymbol{Z} \begin{bmatrix} \tilde{\boldsymbol{A}} & \tilde{\boldsymbol{A}}_d & \tilde{\boldsymbol{D}} \end{bmatrix} \right) \begin{bmatrix} \boldsymbol{q}(t) \\ \boldsymbol{q}\left(t-\tau(t)\right) \\ \boldsymbol{d}(t) \end{bmatrix}
\end{aligned}
\qquad \text{(B.7)}
$$

where $\Pi = \boldsymbol{P}\bar{\boldsymbol{A}} + \bar{\boldsymbol{A}}^T\boldsymbol{P} + \boldsymbol{C}_w^T\boldsymbol{C}_w + \boldsymbol{Q} - \bar{\tau}^{-1}\left(1-\tau^*\right)\boldsymbol{Z} + \Gamma_2$. Applying Schur decomposition to (B.7), if the following matrix inequality is satisfied,

$$\begin{bmatrix} \Pi + \boldsymbol{P}\Gamma_1\boldsymbol{P} & \boldsymbol{P}\bar{\boldsymbol{A}}_d - \bar{\tau}^{-1}(1-\tau^*)\boldsymbol{Z} & \boldsymbol{P}\tilde{\boldsymbol{D}} & \bar{\tau}\tilde{\boldsymbol{A}}^T\boldsymbol{Z} \\ (\boldsymbol{P}\bar{\boldsymbol{A}}_d - \bar{\tau}^{-1}(1-\tau^*)\boldsymbol{Z})^T & \Gamma_3 - (1-\tau^*)(\boldsymbol{Q} + \bar{\tau}^{-1}\boldsymbol{Z}) & \boldsymbol{0} & \bar{\tau}\tilde{\boldsymbol{A}}_d^T\boldsymbol{Z} \\ (\boldsymbol{P}\tilde{\boldsymbol{D}})^T & \boldsymbol{0} & -\gamma^2\boldsymbol{I} & \bar{\tau}\tilde{\boldsymbol{D}}^T\boldsymbol{Z} \\ \bar{\tau}\boldsymbol{Z}\tilde{\boldsymbol{A}} & \bar{\tau}\boldsymbol{Z}\tilde{\boldsymbol{A}}_d & \bar{\tau}\boldsymbol{Z}\tilde{\boldsymbol{D}} & -\bar{\tau}\boldsymbol{Z} \end{bmatrix} < 0, \tag{B.8}$$

then $H[\boldsymbol{d}] < 0$. Furthermore, matrices $\tilde{\boldsymbol{A}}$ and $\tilde{\boldsymbol{A}}_d$ in the nonlinear matrix inequality above involve uncertainties, hence applying Lemma 4.1 again can attain

$$\begin{bmatrix} \Pi + \boldsymbol{P}\Gamma_1\boldsymbol{P} + \Gamma_5 & \boldsymbol{P}\bar{\boldsymbol{A}}_d - \bar{\tau}^{-1}(1-\tau^*)\boldsymbol{Z} & \boldsymbol{P}\tilde{\boldsymbol{D}} & \bar{\tau}\bar{\boldsymbol{A}}^T\boldsymbol{Z} \\ (\boldsymbol{P}\bar{\boldsymbol{A}}_d - \bar{\tau}^{-1}(1-\tau^*)\boldsymbol{Z})^T & \Gamma_3 + \Gamma_6 - (1-\tau^*)(\boldsymbol{Q} + \bar{\tau}^{-1}\boldsymbol{Z}) & \boldsymbol{0} & \bar{\tau}\bar{\boldsymbol{A}}_d^T\boldsymbol{Z} \\ (\boldsymbol{P}\tilde{\boldsymbol{D}})^T & \boldsymbol{0} & -\gamma^2\boldsymbol{I} & \bar{\tau}\tilde{\boldsymbol{D}}^T\boldsymbol{Z} \\ \bar{\tau}\boldsymbol{Z}\bar{\boldsymbol{A}} & \bar{\tau}\boldsymbol{Z}\bar{\boldsymbol{A}}_d & \bar{\tau}\boldsymbol{Z}\tilde{\boldsymbol{D}} & \bar{\tau}^2\boldsymbol{Z}\Gamma_4\boldsymbol{Z} - \bar{\tau}\boldsymbol{Z} \end{bmatrix} < 0 \tag{B.9}$$

where

$$\Gamma_4 = \begin{bmatrix} \boldsymbol{N}(\rho_5\boldsymbol{D}\boldsymbol{D}^T + \rho_7\boldsymbol{D}_d\boldsymbol{D}_d^T)\boldsymbol{N}^T & \boldsymbol{0} \\ \boldsymbol{0} & \boldsymbol{M}(\rho_6\boldsymbol{D}\boldsymbol{D}^T + \rho_8\boldsymbol{D}_d\boldsymbol{D}_d^T)\boldsymbol{M}^T \end{bmatrix},$$

$$\Gamma_5 = \begin{bmatrix} (\rho_5^{-1} + \rho_6^{-1})\boldsymbol{H}^T\boldsymbol{H} & \boldsymbol{0} \\ \boldsymbol{0} & \boldsymbol{0} \end{bmatrix}, \text{ and } \Gamma_6 = \begin{bmatrix} (\rho_7^{-1} + \rho_8^{-1})\boldsymbol{H}_d^T\boldsymbol{H}_d & \boldsymbol{0} \\ \boldsymbol{0} & \boldsymbol{0} \end{bmatrix}.$$

Notice that positive scalars ρ_i, $i = 1, 2, \dots, 8$, must be chosen such that $\Gamma_3 + \Gamma_6 - (1-\tau^*)(\boldsymbol{Q} + \bar{\tau}^{-1}\boldsymbol{Z}) < 0$. Therefore, if there exists positive matrices ***P***, ***Q***, and ***Z*** satisfying (B.9), then the stability and robust disturbance attenuation of the system can be guaranteed.

Since designing $\boldsymbol{K} = \boldsymbol{R}^{-1}\boldsymbol{B}^T\boldsymbol{P}_{11}$ and $\boldsymbol{L} = \frac{\lambda}{2}\boldsymbol{P}_{22}^{-1}\boldsymbol{C}^T$, the matrix $\bar{\boldsymbol{A}}$ can be rewritten as

$$\bar{\boldsymbol{A}} = \begin{bmatrix} \boldsymbol{NA} - \boldsymbol{BK} & \boldsymbol{BK} \\ \boldsymbol{0} & \boldsymbol{MA} - \boldsymbol{LC} \end{bmatrix} = \begin{bmatrix} \boldsymbol{NA} - \boldsymbol{BR}^{-1}\boldsymbol{B}^T\boldsymbol{P}_{11} & \boldsymbol{BR}^{-1}\boldsymbol{B}^T\boldsymbol{P}_{11} \\ \boldsymbol{0} & \boldsymbol{MA} - \frac{\lambda}{2}\boldsymbol{P}_{22}^{-1}\boldsymbol{C}^T\boldsymbol{C} \end{bmatrix}. \tag{B.10}$$

Define a matrix ***W*** representing identity to the one of (B.9) as

$$W = \begin{bmatrix} W_{11} & W_{12} & W_{13} & W_{14} \\ * & W_{22} & 0 & W_{24} \\ * & * & W_{33} & W_{34} \\ * & * & * & W_{44} \end{bmatrix} < 0 .$$

Substituting (B.10) into W, the details of W are given by

$$W_{11} = \Pi + P\Gamma_1 P + \Gamma_5 = \begin{bmatrix} W_{1111} & 0 \\ 0 & W_{1122} \end{bmatrix},$$

$$W_{12} = P\bar{A}_d - \bar{\tau}^{-1}(1-\tau^*)Z = \begin{bmatrix} P_{11}NA_d - \bar{\tau}^{-1}(1-\tau^*)Z_1 & 0 \\ P_{22}MA_d & -\bar{\tau}^{-1}(1-\tau^*)Z_2 \end{bmatrix},$$

$$W_{22} = \Gamma_3 + \Gamma_6 - (1-\tau^*)(Q + \bar{\tau}^{-1}Z) = \begin{bmatrix} W_{2211} & 0 \\ 0 & -(1-\tau^*)(Q_{22} + \bar{\tau}^{-1}Z_2) \end{bmatrix},$$

$$W_{13} = P\tilde{D} = \begin{bmatrix} P_{11}NE \\ P_{22}ME \end{bmatrix}, \quad W_{33} = -\gamma^2 I ,$$

$$W_{14} = \bar{\tau}\bar{A}^T Z = \begin{bmatrix} \bar{\tau}(NA)^T Z_1 - \bar{\tau}P_{11}BR^{-1}B^T Z_1 & 0 \\ \bar{\tau}P_{11}BR^{-1}B^T Z_1 & \bar{\tau}(MA)^T Z_2 - \dfrac{\bar{\tau}\lambda}{2}C^T CP_{22}^{-1}Z_2 \end{bmatrix},$$

$$W_{24} = \bar{\tau}\bar{A}_d^T Z = \begin{bmatrix} \bar{\tau}(NA_d)^T Z_1 & \bar{\tau}(MA_d)^T Z_2 \\ 0 & 0 \end{bmatrix},$$

$$W_{34} = \bar{\tau}\tilde{D}^T Z = \begin{bmatrix} \bar{\tau}(NE)^T Z_1 & \bar{\tau}(ME)^T Z_2 \end{bmatrix}, \quad W_{44} = \bar{\tau}^2 Z\Gamma_4 Z - \bar{\tau}Z = \begin{bmatrix} W_{4411} & 0 \\ 0 & W_{4422} \end{bmatrix},$$

where

$$W_{1111} = P_{11}NA + (NA)^T P_{11} + C^T C + (\rho_1^{-1} + \rho_2^{-1} + \rho_5^{-1} + \rho_6^{-1})H^T H - \bar{\tau}^{-1}(1-\tau^*)Z_1 + Q_{11}$$
$$- P_{11}BR^{-1}B^T P_{11} + P_{11}N(\rho_1 DD^T + \rho_3 D_d D_d^T)N^T P_{11},$$

$$W_{1122} = P_{22}MA + (MA)^T P_{22} - \lambda C^T C - \bar{\tau}^{-1}(1-\tau^*)Z_2 + Q_{22} + P_{11}BR^{-1}B^T P_{11}$$
$$+ P_{22}M(\rho_2 DD^T + \rho_4 D_d D_d^T)M^T P_{22},$$

$$W_{2211} = (\rho_3^{-1} + \rho_4^{-1} + \rho_7^{-1} + \rho_8^{-1})H_d^T H_d - (1-\tau^*)(Q_{11} + \bar{\tau}^{-1}Z_1)$$

$$W_{4411} = \bar{\tau}^2 Z_1 N\left(\rho_5 DD^T + \rho_7 D_d D_d^T\right) N^T Z_1 - \bar{\tau} Z_1$$

$$W_{4422} = \bar{\tau}^2 Z_2 M\left(\rho_6 DD^T + \rho_8 D_d D_d^T\right) M^T Z_2 - \bar{\tau} Z_2 .$$

After decomposing nonlinear terms in the upper triangular area except the diagonal line by Lemma 4.1, an upper bound of W is obtained as

$$W \le \bar{W} = \begin{bmatrix} \bar{W}_{11} & W_{12} & W_{13} & \bar{W}_{14} \\ * & W_{22} & 0 & W_{24} \\ * & * & W_{33} & W_{34} \\ * & * & * & \bar{W}_{44} \end{bmatrix} < 0$$

where $\bar{W}_{11} = \begin{bmatrix} \bar{W}_{1111} & 0 \\ 0 & \bar{W}_{1122} \end{bmatrix}$, $\bar{W}_{14} = \begin{bmatrix} \bar{\tau}(NA)^T Z_1 & 0 \\ 0 & \bar{\tau}(MA)^T Z_2 \end{bmatrix}$, $\bar{W}_{44} = \begin{bmatrix} \bar{W}_{4411} & 0 \\ 0 & \bar{W}_{4422} \end{bmatrix}$, and

$$\begin{aligned} \bar{W}_{1111} = {} & P_{11} NA + (NA)^T P_{11} + C^T C + \left(\rho_1^{-1} + \rho_2^{-1} + \rho_5^{-1} + \rho_6^{-1}\right) H^T H - \bar{\tau}^{-1}\left(1-\tau^*\right) Z_1 + Q_{11} \\ & + P_{11} N\left(\rho_1 DD^T + \rho_3 D_d D_d^T\right) N^T P_{11} + \rho_9 \bar{\tau}^2 P_{11} BB^T P_{11}, \end{aligned}$$

$$\begin{aligned} \bar{W}_{1122} = {} & P_{22} MA + (MA)^T P_{22} - \lambda C^T C - \bar{\tau}^{-1}\left(1-\tau^*\right) Z_2 + Q_{22} + P_{11} BR^{-1} B^T P_{11} \\ & + P_{22} M\left(\rho_2 DD^T + \rho_4 D_d D_d^T\right) M^T P_{22} + \rho_{10} \bar{\tau}^2 P_{11} BB^T P_{11} + \rho_{11} \frac{\lambda^2}{4} C^T C C^T C, \end{aligned}$$

$$\begin{aligned} \bar{W}_{4411} = {} & \bar{\tau}^2 Z_1 N\left(\rho_5 DD^T + \rho_7 D_d D_d^T\right) N^T Z_1 - \bar{\tau} Z_1 + \rho_9^{-1} Z_1 BR^{-1} R^{-1} B^T Z_1 \\ & + \rho_{10}^{-1} Z_1 BR^{-1} R^{-1} B^T Z_1, \end{aligned}$$

$$\bar{W}_{4422} = \bar{\tau}^2 Z_2 M\left(\rho_6 DD^T + \rho_8 D_d D_d^T\right) M^T Z_2 - \bar{\tau} Z_2 + \rho_{11}^{-1} \bar{\tau}^2 Z_2 Z_2 .$$

Finally, using Schur decomposition can transfer $\bar{W}$ to the LMI (4.59). If there exists solutions of LMI (4.59), the negative Hamiltonian function $H[d] < 0$ is guaranteed to maintain the property of robust disturbance attenuation (4.18). The proof of theorem 4.3 is completed.

VITA

博 士 候 選 人 學 經 歷 資 料

姓名：丁桓展

性別：男

生日：民國 70 年 4 月 28 日

出生地：台灣省新北市

論文題目：

中文：應用於時滯系統之輸出回授積分型順滑模態控制

英文：Output Feedback Integral Sliding Mode Control Applied to Time-Delay Systems

學歷：

1. 民國 85 年 9 月~90 年 6 月國立台北工業專科學校電機工程科
2. 民國 90 年 9 月~92 年 6 月國立台北科技大學電機工程系
3. 民國 92 年 9 月~93 年 6 月國立交通大學電控工程研究所碩士班
4. 民國 93 年 9 月~ 國立交通大學電控工程研究所博士班(逕讀)

榮譽：

1. 參加 2007 第一屆富士通微電子盃 8FX 系列 MCU 競賽(以 8FX 系列晶片實現之通用序列埠檔案傳輸裝置)榮獲優異獎

著作目錄：

國際期刊論文

[1] Ting, H. C., Chang, J. L., and Chen, Y. P., "Applying output feedback integral sliding mode controller of time-delay systems," *IEICE Trans. Fundamentals*, Vol. E94-A, No. 4, pp. 1051-1058, 2011.

[2] Ting, H. C., Chang, J. L., and Chen, Y. P., "Combining sliding mode and descriptor system observers to simultaneously estimate states and unknown inputs," *Advances in Differential Equations and Control Processes*, Vol. 7, No. 1, pp. 41-55, 2011.

[3] Chang, J. L. and Ting, H. C., "Output feedback integral sliding mode control for uncertain systems with bounded L_2 performance," *Journal of System Design Dynamics*, Vol. 3, No. 3, pp. 318-329, 2009.

[4] Chang, J. L., Ting, H. C., and Chen, Y. P., "Robust discrete-time output tracking controller design for nonminimum phase systems," *Journal of System Design Dynamics*, Vol. 2, No. 4, pp. 950-961, 2008.

[5] Ting, H. C., Chang, J. L., Yeh, C. H., and Chen, Y. P., "Discrete time sliding-mode control design with grey predictor," *International Journal of Fuzzy Systems*, Vol. 9, No. 3, pp. 179-185, 2007.

[6] Ting, H. C., Chang, J. L., and Chen, Y. P., "Output feedback integral sliding mode controller of time-delay systems with mismatch disturbances," *Asian Journal of Control*, accepted.

[7] Ting, H. C., Chang, J. L., and Chen, Y. P., "Applying output feedback integral sliding

mode controller to uncertain time-delay systems with mismatched disturbances," *International Journal of Control, Automation, and Systems*, re-revised.

[8] Ting, H. C., Chang, J. L., Chen, Y. P., "Unknown input observer design using descriptor system approach," *International Journal of Control, Automation, and Systems*, revised.

研討會論文：

國際研討會

[1] Ting, H. C., Chang, J. L., and Chen, Y. P., "Unknown input observer design using descriptor system approach," *SICE 2010*, pp. 2207-2213, Taipei, Taiwan, 2010.

[2] Ting, H. C., Chang, J. L., and Chen, Y. P., "Observer-based output tracking controller design for high relative degree SISO systems," *Proceedings of 2009 CACS International Automatic Control Conference*, Taipei, Taiwan, 2009.

[3] Ting, H. C., Chang, J. L., and Chen, Y. P., "Output feedback sliding mode controller of uncertain time delay systems," *The 7th Asian Control Conference*, pp. 535-540, Hong Kong, 2009.

[4] Chang, J. L. and Ting, H. C., "Output feedback integral sliding mode control for uncertain systems with bounded L_2 performance," *The 7th Asian Control Conference*, pp. 630-635, Hong Kong, 2009.

[5] Ting, H. C., Chang, J. L., and Chan, Y. P., "Output sliding mode control for time-delay systems with mismatch disturbance," *Proceedings of 2008 CACS International Automatic*

Control Conference, Tainan, Taiwan, 2008.

[6] Ting, H. C., Chang, J. L., Yeh, C. H., and Chen, Y. P., "Discrete time sliding-mode control design with grey predictor," *Proceedings of 2007 CACS International Automatic Control Conference*, Taichung, Taiwan, 2007.

[7] Ting, H. C., Chang, J. L., and Chan, Y. P., "Output sliding-mode control of discrete-time nonminimum phase systems," *9th International Conference on Control, Automation, Robotics and Vision*, Singapore, 2006.

國內研討會

[1] 曾國雄、蔡宏福、王士豪、丁桓展、鐘文成，"電腦輔助複數短路容量法分析電弧爐閃爍電壓之研究"，中華民國第 24 屆電力工程研討會，第 1076-1080 頁，台灣台南，2003 年。